

# **The Transformations and Fate of Nanoplastic and Microplastics in the Aquatic Environment.**

Olubukola S. Alimi

Doctor of Philosophy

Department of Chemical Engineering

McGill University

Montreal, Canada

August 2021

A thesis submitted to McGill University in partial fulfilment of the requirements of the degree of Doctor of Philosophy.

## **Acknowledgement**

During my research projects, I was privileged to have pleasant interactions with numerous people who together helped in making this project a reality. First, I would like to thank my supervisor, Prof. Nathalie Tufenkji for the guidance, support, encouragement, mentorship and confidence placed in me throughout my PhD journey. I learnt so much from working with you.

I would also like to thank all members of the Biocolloids and Surfaces laboratory for their support and the opportunity of having useful discussions about my work and wellbeing. I specially appreciate the useful interactions and feedback I got during my group meeting presentations. I would like to thank all my collaborators and importantly Dr. Jeffrey Farner, Dr. Dominique Claveau-Mallet, Dr. Laura Roweczyk and Think Biu for the critical discussions and great teamwork which was instrumental to the success of this thesis. I am also extremely grateful to Professor Kevin Wilkinson for the useful guidance, comments and feedback on my project. Thank you, Sara Mathews for helping with sampling at the start of the COVID-19 pandemic. Thank you, Shawn, Laura, Nick, Brian and Rafael, for useful discussions.

Special thanks to Dr. Joseph Kangmennaang who took up multiple roles professionally and personally in contributing to my wellbeing and sanity in the last few years of my PhD program. Your editorial assistance is also appreciated.

I would like to thank my family, the Alimis' and my friends for their care. To my parents and siblings, thank you for the unending support and prayers throughout the course of this program. I do not take your care and support for granted. To my friends who helped me in keeping my sanity, even the geographical distance could not hamper your support.

I am indebted to these funding agencies for supporting my research, without which this work would not have been possible: National Universities Commission, Nigeria (NUC), Petroleum Technology Development Fund of Nigeria (PTDF), PURE-CREATE network, McGill Engineering doctoral award program (MEDA), Fonds de recherche du Quebec-Nature et technologies (FRQNT), EcotoQ, Natural Sciences and Engineering Research Council of Canada, the Canada Foundation for Innovation and the Canada Research Chairs program

## **Dedication**

This thesis is dedicated to my parents, Bolanle Alimi and Adegboyega Alimi. Thank you for everything.

## Abstract

The risks posed by plastic debris to the environment and human health, depend on several factors, including their 1) tendency to remain colloidally stable in the aquatic environment, 2) transport potential in natural aquatic environments, including the subsurface, and 3) potential to act as vectors for other pollutants in ecosystems. An improved understanding of the key processes and factors that govern the behaviour of plastic debris under realistic environmental conditions will contribute towards providing mitigating strategies for plastic pollution as well as improved risk assessment.

In the first part of this thesis, the scientific literature was critically reviewed and used to determine an estimate of plastic loads and pathways in different environmental compartments. The key factors controlling the aggregation, deposition and contaminant cotransport of microplastics in the aquatic environment were identified and critically analyzed. From the critical data synthesis, it was shown that the rubbery polymer, polyethylene, generally has a higher contaminant sorption capacity than other synthetic plastic types. Important gaps in the literature that preclude our understanding of the risks associated with nanoplastics and microplastics in the aquatic environment were identified.

To address some of these knowledge gaps, the next part of this thesis investigated the role of climate and temperature cycling on nanoplastic transport. It is shown that by ignoring the effect of freeze-thaw, a key component of cold climate regions, previous conclusions on nanoplastic mobility might have been overestimated. Controlled laboratory experiments were used to show that exposure of nanoplastics to repeated freeze-thaw cycles, such as those experienced in cold climates will lead to aggregation and reduced transport in soils and subsurface environments. These experiments also provided insight into the strength of the freeze-thaw induced aggregates, showing that they are not prone to disaggregation even after applying a high shear force to disaggregate them. Although the presence of natural organic matter (NOM) significantly increases nanoplastic mobility, it was not sufficient to counter the impact of freeze-thaw.

In another study, the factors and mechanisms by which different plastic sizes interact with NOM (humic acid, fulvic acid and alginate) in simple and complex artificial and natural environmental matrices were investigated and compared. By using environmentally realistic

plastic/natural organic matter ratio, it was shown that the different organic molecules will interact with the different plastics in a size-specific manner. In the absence of NOM, the minimum  $\text{CaCl}_2$  concentration needed to destabilize the particle suspension is insensitive to plastic size. Although the presence of the polysaccharide alginate enhanced aggregation in  $\text{CaCl}_2$ , it had no effect/stabilized nanoplastics in a complex ionic matrix. Overall, the effect of all three NOM types was more pronounced for the larger nanoplastics than the smaller ones. While there were no significant differences in the attachment efficiencies of both bare nanoplastics at the CCC ( $\text{CaCl}_2$ ) and in artificial seawater, the larger nanoplastics were more stable than the smaller ones in a natural seawater matrix.

A critical literature review reveals that only ten percent of laboratory studies investigating the effects of microplastic pollution in ecosystems have used environmentally relevant (aged) particles. Amongst these few studies, there is huge variability and disparity in weathering protocols used across effect studies which may overestimate/trivialize the true environmental risks posed by microplastics. An extensive synthesis of laboratory effect studies in the context of environmentally relevant protocols for weathered microplastics, nanoplastics and leachates is presented which also provides a framework for method harmonization. In addition, the appropriateness of current microplastic weathering protocols is compared with international standard protocols.

Hence, in a final experimental study, the impact of environmental weathering on the physicochemical properties of microplastics originating from real plastic debris (single use plastic) is investigated using a range of spectroscopy, microscopy and profilometry techniques. The impacts of these physicochemical changes on microplastic transport and contaminant facilitated transport are examined. Changes to the surface chemistry, polarity, morphology, and density all impacted the fate of the microplastics. The experimental results show that aging reduced the sorption of a hydrophobic contaminant, triclosan, to the microplastics while both pristine and aged plastics partially desorb this contaminant. Measurements of microplastic settling velocity show that aging significantly increased the mobility of the microplastics. The combined experimental findings and transport simulations imply that pristine plastics will undergo long range transport and may facilitate the mobility of hydrophobic contaminants in surface waters.

Overall, these results advance our knowledge of how different environmental conditions will influence nanoplastic fate and transport, provide fundamental and mechanistic understanding

of factors affecting nanoplastics stability in aquatic environments as well as improved understanding on the risks associated with microplastics with environmental relevance.

## **Resume**

Les risques que représentent les débris plastiques pour l'environnement et la santé humaine dépendent de plusieurs facteurs, dont leur tendance à rester colloïdalement stables, leur potentiel de transport et leur capacité à agir comme vecteurs d'autres polluants dans l'environnement aquatique. Une meilleure compréhension des processus et facteurs clés qui régissent le comportement des débris plastiques dans des conditions environnementales réalistes contribuera à l'élaboration de stratégies d'atténuation de la pollution plastique et à une évaluation précise des risques.

La littérature scientifique a fait l'objet d'un examen critique et a été utilisée pour estimer les charges et les voies de pénétration des plastiques dans différents compartiments de l'environnement. Les facteurs clés contrôlant l'agrégation, le dépôt et le transport des contaminants des microplastiques (MPs) dans l'environnement aquatique ont été identifiés et analysés de manière critique. Il a été démontré que le polyéthylène a une plus grande capacité de sorption des contaminants que les autres types de plastique synthétique. Des lacunes importantes dans la littérature qui empêchent notre compréhension des risques associés aux MPs dans l'environnement aquatique ont été identifiées.

La partie suivante de cette thèse a étudié le rôle du climat et des cycles de température sur le transport des nanoplastiques (NPs). Il est démontré qu'en ignorant l'effet du gel-dégel, les conclusions précédentes sur la mobilité des NPs dans les climats froids pourraient avoir été surestimées. Des expériences de laboratoire contrôlées ont été utilisées pour montrer que l'exposition des NP à des cycles répétés de gel-dégel, tels que ceux que l'on rencontre dans les climats froids, entraîne une agrégation et une réduction du transport dans les sols et les environnements souterrains. Bien que la présence de matière organique naturelle (NOM) augmente significativement la mobilité des NP, elle n'est pas suffisante pour contrer l'impact du gel-dégel.

Les facteurs et mécanismes par lesquels différentes tailles de plastique interagissent avec la NOM dans des matrices environnementales artificielles et naturelles simples et complexes ont également été étudiés et comparés. En utilisant un rapport NP/NOM réaliste du point de vue environnemental, il a été démontré que les différentes molécules organiques interagissent avec les différentes NP d'une manière spécifique à leur taille. Dans l'ensemble, l'effet de trois NOM était plus prononcé pour les grands NP que pour les petits. Bien qu'il n'y ait pas eu de différences

significatives dans les efficacités d'attachement des deux NPs nus à la concentration critique de coagulation ( $\text{CaCl}_2$ ) et dans l'eau de mer artificielle, les NPs les plus grands étaient plus stables que les plus petits dans une matrice d'eau de mer naturelle.

Une analyse critique de la littérature révèle que seuls dix pour cent des études en laboratoire portant sur les effets de la pollution par les MPs dans les écosystèmes ont utilisé des particules pertinentes pour l'environnement. Une synthèse exhaustive des études de laboratoire sur les effets dans le contexte de protocoles pertinents pour l'environnement pour les MP vieilliss, les NPs et les lixivants est présentée et fournit également un cadre pour l'harmonisation des méthodes. En outre, l'adéquation des protocoles actuels d'altération des MPs est comparée aux protocoles standard internationaux.

Dans une dernière étude expérimentale, l'impact de l'altération environnementale sur les propriétés physico-chimiques des MPs provenant de débris plastiques réels a été étudié à l'aide d'une série de techniques. Les modifications de la chimie de surface, de la mouillabilité, de la morphologie, de la densité, etc. ont toutes eu un impact sur le devenir des MPs. Les résultats expérimentaux montrent que le vieillissement réduit la sorption d'un contaminant hydrophobe, le triclosan, sur les MPs, alors que les plastiques vierges et vieilliss désorbent partiellement ce contaminant. Les mesures de la vitesse de sédimentation des MPs montrent que le vieillissement augmente significativement la mobilité des MPs. Les résultats expérimentaux et les simulations de transport impliquent que les plastiques vierges subissent un transport à longue distance et peuvent faciliter la mobilité des contaminants hydrophobes dans les eaux de surface.

Dans l'ensemble, ces résultats font progresser nos connaissances sur la manière dont les différentes conditions environnementales influencent le devenir et le transport des plastiques. Ils permettent de comprendre de manière fondamentale et mécaniste les facteurs qui influencent leur stabilité dans les environnements aquatiques et les risques associés aux PM pertinents pour l'environnement.

# Table of Contents

Acknowledgement .....	i
Dedication .....	ii
Abstract .....	i
Resume.....	iv
Table of Contents .....	vi
List of Figures .....	xi
List of Tables .....	xvi
List of Abbreviations .....	xviii
Chapter 1: Introduction .....	1
1.1 Motivation .....	1
1.2 Research objectives .....	2
1.3 Thesis organisation.....	2
1.4 Contributions to knowledge .....	3
1.5 Contributions of the author .....	6
References .....	8
Preamble to Chapter 2.....	9
Chapter 2: Microplastics and Nanoplastics in Aquatic Environments: Aggregation, Deposition, and Enhanced Contaminant Transport.....	10
2.1 Introduction .....	11
2.1.1 From macro to micro to...nano? .....	13
2.2 Living in the Plasticene: Plastic in every corner of the earth.....	14
2.2.1 Freshwaters are key vectors for microplastic transport .....	14
2.2.2 Aquatic species are at high risk .....	16
2.2.3 Plastic loads in soils and sediments are less understood .....	16
2.2.4 Modeling with incomplete data .....	17
2.3 Current state of knowledge on micro- and nanoplastic aggregation and deposition .....	18
2.3.1 Laboratory studies investigating the aggregation of nanoplastics and microplastics... ..	19
2.3.2 Laboratory studies investigating the deposition of nanoplastics and microplastics. ....	24
2.4 Plastics may act as vectors for other contaminants .....	32
2.4.1 Plastics as contaminant source and sink .....	32

2.4.2 Nanoplastics and microplastics can facilitate the transport of contaminants .....	36
2.5 Regulatory policy .....	37
2.6 Environmental implications and outlook .....	38
References .....	40
Supporting information .....	53
Preamble to Chapter 3 .....	63
Chapter 3: Exposure of Nanoplastics to Freeze-Thaw Leads to Aggregation and Reduced Transport in Model Groundwater Environments .....	64
Abstract .....	64
3.1 Introduction .....	64
3.2 Materials and methods .....	66
3.2.1 Nanoplastic and natural organic matter suspension preparation .....	66
3.2.2 Temperature pre-treatments.....	67
3.2.3 Nanoplastic characterization.....	67
3.2.4 Nanoplastic transport studies.....	68
3.2.5 Interpreting transport experiments.....	69
3.3 Results and discussion.....	69
3.3.1 Physicochemical properties of nanoplastics exposed to freeze-thaw .....	69
3.3.2. Proposed mechanism of aggregation upon exposure to freeze-thaw .....	74
3.3.3 Nanoplastic transport in the absence of freeze-thaw .....	74
3.3.4. Nanoplastic transport after exposure to 10 FT cycles .....	76
3.3.5 Interpreting transport experiments.....	77
3.4 Conclusions .....	80
References .....	81
3.5 Supporting information .....	85
References .....	89
Preamble to Chapter 4.....	90
Chapter 4: Mechanistic Understanding of the Aggregation Kinetics of Nanoplastics in Marine Environments .....	91
Abstract .....	91
4.1 Introduction .....	92
4.2 Materials and methods .....	94
4.2.1 Preparation of water samples and aqueous suspensions of the plastics .....	94

4.2.2 Nanoplastic aggregation .....	95
4.2.3 Probing nanoplastic interactions with silica .....	96
4.3 Results and discussions .....	97
4.3.1 Aggregation kinetics in the absence of organic matter.....	97
4.3.2 Size dependent enhanced aggregation in the presence of Ca <sup>2+</sup> and alginate.....	100
4.3.3 Effect of fulvic acid in the presence of Ca <sup>2+</sup> differs with plastic size. ....	102
4.3.4 Enhanced aggregation in the presence of Ca <sup>2+</sup> and humic acid .....	103
4.3.5 Aggregation kinetics of the nanoplastics in artificial seawater with and without natural organic matter. ....	105
4.3.6 Aggregation kinetics of the nanoplastics in natural surface water .....	107
4.3.7 Interaction energies between nanoplastics and silica surfaces. ....	107
4.4 Conclusions .....	108
Acknowledgments .....	109
References .....	109
Supporting information .....	114
References .....	121
Preamble to Chapter 5.....	123
Chapter 5: Weathering Pathways and Protocols for Environmentally Relevant Microplastics and Nanoplastics: What Are We Missing?.....	124
Abstract .....	124
5.1 Introduction .....	124
5.2 Key weathering conditions and pathways encountered by plastics throughout their lifecycle .....	127
5.2.1 UV photooxidation .....	127
5.2.2 Biological weathering.....	128
5.2.3 Chemical oxidation and disinfection .....	129
5.2.4 Thermal effects .....	130
5.2.5 Other transformations .....	131
5.2.6 Weathering processes in major environmental compartments of the water cycle.....	132
5.3 Effects of weathering on microplastic fate in the environment .....	133
5.4 Current knowledge about weathering protocols used in microplastics effect studies.....	135
5.4.1 Weathering protocols used in microplastic effect studies. ....	135
5.4.2 Proportion of microplastic effect studies that use weathered plastics .....	140

5.4.3 Microplastics effect studies using environmental samples: comparison with laboratory weathered microplastics. ....	141
5.5 Standardized international weathering protocols in different applications.....	144
5.5.1 Outdoor exposure .....	144
5.5.2 Marine exposure .....	146
5.5.3 Solid waste conditions .....	146
5.5.4 Appropriateness of standard protocols for micro/nanoplastics research .....	147
5.6 Overview of the current state of research on environmentally relevant microplastics and proposed weathering guidelines for future research. ....	149
Acknowledgements .....	152
CRedit authorship contribution statement .....	153
References .....	154
5.7 Supporting information .....	160
Preamble to Chapter 6.....	174
Chapter 6: Effects of Weathering on the Properties and Fate of Secondary Microplastics from a Disposable Cup .....	175
Abstract .....	175
6.1 Introduction .....	175
6.2 Materials and methods .....	177
6.2.1 Plastic source and UV weathering treatment.....	177
6.2.2 Characterization of microplastics .....	178
6.2.3 Settling experiment.....	179
6.2.4 Adsorption kinetics and isotherm experiment .....	180
6.2.5 Desorption experiment .....	181
6.2.6 Analytical instrumentation .....	181
6.2.7 Transport distance simulation.....	181
6.2.8 Data and statistical analysis .....	182
6.3 Results and discussion.....	182
6.3.1 Changes to physical and chemical properties of microplastics after weathering .....	182
6.3.2 UV weathering increases the settling rate of polystyrene microplastics .....	187
6.3.3 Effect of weathering on adsorption capacity of triclosan on microplastics.....	190
6.3.4 Effect of weathering on desorption of triclosan from microplastics and potential for facilitated transport .....	193

6.4 Environmental implications .....	194
Acknowledgments .....	196
References .....	197
6.5 Supporting information .....	200
Chapter 7: Conclusions and Future Directions .....	209
7.1 Conclusion and implications .....	209
7.1 Future directions.....	211
7.1.1 What is the competitive interaction between microplastics and multiple contaminants and organic matter? .....	211
7.1.2 What is the behaviour of fragmented microplastics and different polymer types? ....	211

## List of Figures

**Figure 2.1.** Estimates of plastic loading and transport pathways in the environment aggregated from reports in the literature. Percentages indicate the fraction of plastics in a given compartment moving to a subsequent compartment, with wider arrows representing greater plastic transfer. Ranges of concentrations measured, either in number of particles per liter or per area, are given where reliable values were observed. Values indicated are for macro and microplastics.

\*corresponds to estimates for microplastics only. †corresponds to values divided between two compartments. ‡corresponds to best estimates in the absence of data in the literature. Data and references are summarized in Table S2.1. .... 12

**Figure 2.2.** Aggregation stability curves of selected PS NPs and MPs in (a) multivalent salts (b) monovalent salts without coating and (c) monovalent salts with coatings from studies summarized in Table 2.1.<sup>116-118, 129</sup> Here,  $\alpha_{pp}$  = particle-particle attachment efficiency and SMP, CMP and AMP = sulfate-, carboxyl- and amidine-modified plastics, respectively. Solid symbols indicate addition of polyelectrolyte to the background solution..... 23

**Figure 2.1.** Deposition stability curves of PS NPs and MPs from studies in Table 2.2.<sup>141, 157, 160, 161, 164, 167</sup> (a) SMP with and without SRHA and (b) SMP, AMP, and CMP with and without various types of NOM Here,  $\alpha_{pc}$  = particle-collector attachment efficiency and solid symbols indicate addition of NOM. PHA = peat humic acid, GFA = Georgetown fulvic acid, SRHA = Suwannee river humic acid and ChMP = chloromethyl-modified plastic..... 25

**Figure 2.4. (a)** Contaminants that have been found to associate with plastic debris in the environment.<sup>17, 57, 59, 62, 186-189</sup> Schematic adapted from<sup>185</sup> **(b)** Relative ranking of sorption capacity as a function of plastic type. In a given study, a score of 1 indicates the highest sorption capacity and increasing values indicate plastics that exhibit lower sorption capacities. HDPE = high-density polyethylene; LDPE = low-density polyethylene; POM = polyoxymethylene; PA = polyamide; PET = polyethylene terephthalate. \*Glass transition temperature from<sup>190</sup>..... 33

**Figure S2.1.** Molecular structures of some commonly detected plastics in the environment. (Adapted from Quinn and Crawford, 2016) ..... 53

**Figure 3.1.** Representative intensity particle size distribution of nanoplastics in 30 mM NaCl (a) without NOM and (b) in the presence of NOM for three replicate samples (A, B, C). Representative TEM images of nanoplastics kept at 10°C for 240 hours (c and d) and after 10 FT cycles (e and f) all in 30 mM NaCl (a), (c), and (e) are suspensions without NOM. (b), (d), and (f) are suspensions with NOM. .... 72

**Figure 3.2.** The stability of the nanoplastic suspension in 10 mM NaCl after exposure to (a) 1 FT cycle (b) 5 FT cycles and (c) 10 FT cycles. Sample stability was measured after FT exposure and named Post FT day 1 – 5. Samples that were vortexed Post FT from day 1 – 5 are collectively plotted as Post FT (vortexed). .... 73

**Figure 3.3.** Breakthrough curves of nanoplastics conducted at (a) 10°C without NOM, (b) 10°C in the presence of NOM, (c) after 10 FT cycles without NOM, (d) after 10 FT cycles in the presence of NOM. Error bars represent standard deviation between duplicate runs. .... 75

<b>Figure 3.4. (a)</b> Attachment efficiency as a function of IS calculated from $d_{h,z-avg}$ for different nanoplastics and microplastics across different studies. CNP = carboxyl-modified nanoplastic, CMP = carboxyl-modified microplastic, SNP = sulfate-modified nanoplastics. The shaded regions indicate standard deviation (from duplicate measurement) around the mean for this study. Note that values for 4°C and 10°C from Kim and Walker 2008 overlap. (b) Predicted travel distances as a function of ionic strength at both 10°C and FT conditions.....	78
<b>Figure S3.1.</b> Temperature profiles for 10 °C and FT pretreatments. ....	85
<b>Figure S3.2.</b> Representative intensity weighted particle size distribution of 20 nm PS before and after FT treatment (a) 3 mM (b) 10 mM (c) 30 mM (d) 100 mM (e) 30 mM + NOM (f) 100 mM + NOM. Plots indicate triplicate measurements of the same sample suspension. ....	86
<b>Figure S3.3.</b> Representative (a) intensity particle size distribution versus (b) volume particle size distribution in 10 mM IS at 10 °C highlighting the insignificance of large aggregates or artifacts above 2000 nm. Plots indicate triplicate measurements of the same sample suspension. ....	87
<b>Figure S3.4.</b> Breakthrough curve of the NPs in (a) 30 mM and (b) 100 mM NaCl highlighting the effect of FT in the presence of NOM. ....	88
<b>Figure S3.5.</b> Attachment efficiency as a function of ionic strength calculated using (a) DLS hydrodynamic Z-average, $d_{h, Z-avg}$ and (b) DLS hydrodynamic intensity mean, $d_{h, intensity}$ .....	88
<b>Figure 4.1.</b> Transmission electron micrographs of (a) NP <sub>28</sub> and (b) NP <sub>220</sub> in 10 mM CaCl <sub>2</sub> , representative aggregation profiles of (c) NP <sub>28</sub> and (d) NP <sub>220</sub> in CaCl <sub>2</sub> . (e) Attachment efficiency of nanoplastics in CaCl <sub>2</sub> .....	99
<b>Figure 4.2.</b> Electrophoretic mobilities of (a) NP <sub>28</sub> and (b) NP <sub>220</sub> as a function of electrolyte concentration in CaCl <sub>2</sub> and ASW. All experiments were carried out at a pH of 8 ± 0.5. ASW ionic strength is equivalent to 561 – 714 mM; (c) Electrophoretic mobilities of both plastic sizes in natural surface water (NW) samples. The box plots show mean, 25 <sup>th</sup> and 75 <sup>th</sup> percentiles, and outliers. * p < 0.05 when compared to each bare or NW1 sample using One-way ANOVA and Tukey mean comparison. ....	100
<b>Figure 4.3.</b> (top panels = NP <sub>28</sub> . bottom panels = NP <sub>220</sub> ) Representative aggregation profile in 10 mM CaCl <sub>2</sub> (CCC) in the presence and absence of 10 mg/L alginate (a & e), 10 mg/L humic acid (b & f) and 10 mg/L fulvic acid (c & g). Stability curves of NP <sub>28</sub> and NP <sub>220</sub> in the absence and presence of all three organic matters at 10 mg/L (d & h). Error bars represent standard deviation for 3 independent experiments. Using One-way ANOVA and Tukey mean comparison, in the diffusion limited regime, attachment efficiencies in AL and HA were statistically significant (p<0.05) compared to its absence (for NP <sub>220</sub> , panel d) while no significant difference for NP <sub>28</sub> , panel h. ....	102
<b>Figure 4.4.</b> (Top panel = NP <sub>28</sub> . Bottom panel = NP <sub>220</sub> ) Transmission electron micrographs of NP <sub>28</sub> and NP <sub>220</sub> in the presence of alginate (a & b), humic acid (c & d) and fulvic acid (e & h). Salt concentration = 10 mM CaCl <sub>2</sub> , NOM concentration = 10 mg/L. All experiments were carried out at a pH of 8 ± 0.5. ....	103

**Figure 4.5.** Schematic showing the proposed/possible mechanisms of interaction between NP<sub>28</sub> and NP<sub>220</sub> with alginate, humic acid and fulvic acid in CaCl<sub>2</sub> in the diffusion limited regime. Schematic is for illustration purposes and not drawn to scale ..... 105

**Figure 4.6:** (a) Representative aggregation profiles of the bare nanoplastics, NP<sub>28</sub> and NP<sub>220</sub> in ASW and (b) attachment efficiencies in ASW in the presence and absence of humic acid, fulvic acid and alginate, as compared with the attachment efficiency in 10 mM CaCl<sub>2</sub> (i.e CCC). (c) attachment efficiency in natural surface waters as compared with the attachment efficiency at in 10 mM CaCl<sub>2</sub>. Error bars represent standard deviations determined for 3 independent experiments. \* p < 0.05 when compared to 10 mM CaCl<sub>2</sub> or ASW (bare) using One-way ANOVA and Tukey mean comparison. .... 106

**Figure 4.7.** Interaction energy profiles for the interaction of NP<sub>220</sub> and a silica surface in the presence of 1 mg/L fulvic acid, humic acid and alginate and 0.5 mM CaCl<sub>2</sub>. Error bars indicate standard deviation for n = 3 independent experiments. Details of the fitting parameters are presented in Table S4.8. Note that curves for NP<sub>220</sub> + HA (green) and NP<sub>220</sub> + AL (yellow) largely overlap. .... 107

**Figure S4.1.** Representative aggregation profile showing the effect of ionic strength (1, 10, 30, 100 mM CaCl<sub>2</sub> and ASW) on the NP<sub>220</sub>. .... 115

**Figure S4.2.** Aggregation rates of NP<sub>28</sub> and NP<sub>220</sub> in CaCl<sub>2</sub> and ASW in the presence and absence of different organic matter. AL = Alginate, HA = humic acid, FA = fulvic acid and ASW = artificial seawater. Error bars represent standard deviation of at least 3 measurements. Additional experiments were carried out at 30 ppm HA only to better elucidate its interaction with the smaller NPs since the aggregation rate measured in the presence of 10 ppm HA was not significantly different from 1 ppm HA. .... 116

**Figure S4.3.** Comparison of CCC of nanoplastics and microplastics from literature to show the effect of particle size on CCC. .... 117

**Figure S4.4.** Transmission electron microscope images of (a) calcium alginate sheets formed in the absence of plastic particles. Close up images of plastic interaction with calcium alginate (b) NP<sub>28</sub> (c) NP<sub>220</sub> ..... 118

**Figure S4.5.** Representative aggregation profile of NP<sub>28</sub> showing the effect of humic acid at 10 mM CaCl<sub>2</sub> and 10 ppm HA. .... 120

**Figure S4.6.** Hydrodynamic diameter of NP<sub>28</sub> and NP<sub>220</sub> after 30 minutes in CaCl<sub>2</sub> and ASW in the presence and absence of different organic matter. AL = Alginate, HA = humic acid, FA = fulvic acid and ASW = artificial seawater. Error bars represent standard deviation of at least 3 measurements. .... 121

**Figure 5.1.** Major weathering pathways that plastic and its degradation products will encounter throughout its lifecycle before and after entering the environment. Percentages refer to estimated fraction of plastics released into a given compartment after manufacturing and use based on data from <sup>13</sup>. .... 133

**Figure 5.2.** Distribution of the various types of weathering treatments applied to microplastics and plastic leachates among controlled laboratory effects studies. First layer = plastic state,

second layer = study type/effect studied, third layer = weathering pathway/choice, fourth layer = weathering medium. WWTP – Wastewater treatment plant, N/A – Not available. Total of 93 studies identified from 63 articles. Articles reporting more than one weathering media are treated as separate studies. Data references provided in Table S5.2. .... 136

**Figure 5.3.** General trend in irradiance versus duration (hr) and plastic type across different laboratory effect studies reporting these parameters. Here, we see that the type of UV treatment and plastic type varies across studies. CO -chemical oxidation, PS - polystyrene, PE - polyethylene, PP – polypropylene, PVC – polyvinyl chloride, PET – polyethylene terephthalate, PA – polyamide, PC – polycarbonate, PMMA – polymethyl methacrylate, PLA – polylactic acid. References: a - <sup>93</sup>, b - <sup>94</sup>, c - <sup>95</sup>, d - <sup>96</sup>, e - <sup>11</sup>, f - <sup>97</sup>, g - <sup>44</sup>, h - <sup>98</sup>, i - <sup>99</sup>, j - <sup>92</sup>, k - <sup>83</sup>, l - <sup>100</sup>, m - <sup>101</sup>, n - <sup>102</sup>, o - <sup>103</sup>, p - <sup>104</sup>, q - <sup>105</sup> ..... 138

**Figure 5.4.** (a) The distribution of microplastic types used in effect studies highlighting the small proportion using weathered plastics in comparison to pristine ones; (b) The number of effects studies reporting types of polymer weathered in those studies. Dot pattern are polymer types reported in effects studies using microplastics sampled from the environment. Studies reporting both PE and HDPE/LDPE were counted as one PE; (c) A ranking of top 5 plastic types used in weathering effects studies in the present review versus those detected in the environment, produced or used in laboratory studies globally. Plastics rank 1 (most common) – 5 (least common) from left to right. PS - polystyrene, PE - polyethylene, PP – polypropylene, PVC – polyvinyl chloride, PET – polyethylene terephthalate, PA – polyamide, PC – polycarbonate, PMMA – polymethyl methacrylate, PU - polyurethane. .... 141

**Figure 5.6.** Selected ASTM standards for simulated weathering, classified as outdoor exposure, marine exposure or solid waste conditions: (a) timeline including the creation and revision of each standard, compared with the surge in scientific publications including microplastic\* or nanoplastic\* in title, abstract or keywords (Scopus, May 4, 2021); (b) publications including microplastic\* or nanoplastic\* and at least one code (e.g., D6400) of the selected ASTM standards in any field, including the body text (Google Scholar, May 4, 2021); (c) simulated degradation pathway and the outcome properties measured within each type of exposure. Standards of natural exposure were not included in this selection. .... 144

**Figure 6.1.** Physical characterization of the pristine and aged microplastics (a, b) colour changes of the microplastic, (c, d) surface morphology of microplastics (outer side) using SEM, (e, f) roughness profile of the microplastics (inner side) using a profilometer, (g, h) representative image of water droplet for contact angle measurement on pristine and aged microplastics (inner side), (i, j) roughness parameters,  $S_a$  and  $S_z$  at 50× magnification, (k) mass change of microplastic disks before and after weathering. Pristine-in and aged-in refer to the inner surface of the original cup, while pristine-out and aged-out refer to the outer surface of the cup..... 184

**Figure 6.2.** Surface composition characterization of microplastics. (a) representative FTIR spectra of pristine versus aged microplastics. Inset: zoom-in of FTIR spectra; (b) representative deconvoluted XPS spectra of C1s for pristine disk at depth 0; (c) representative deconvoluted XPS spectra of C1s for aged disk at depth 0; (d) XPS analysis of O1s at depth 0; (e) difference in

oxygen content at depths 0, 1 and 2 for inner and outer surfaces. XPS etching done at 400 eV at 0.21 nm/s; depth 0 = outermost surface = 0 s of etching, depth 1 = 3 s, depth 2 = 6 s..... 186

**Figure 6.3.** (a) experimental settling velocity of microplastic disks in 10 mM NaCl ( $d_e = 1952 \mu\text{m}$ ), and (b) simulated transport distance of microplastic disks in a freshwater system ( $d_e = 1952 \mu\text{m}$ ). (c, e) calculated settling velocity of polystyrene disk and spheres, (d, f) simulated transport depth of 100  $\mu\text{m}$  polystyrene disk and sphere. .... 189

**Figure 6.4.** Effect of weathering on the (a) contaminant adsorption kinetics at 20  $\mu\text{g/L}$  triclosan; (b) at 100  $\mu\text{g/L}$  triclosan; (c) adsorption isotherm at pH 6; (d) comparison of hydrophobic contaminant ( $\log K_{ow} 3.09 - 4.76$ ) equilibrium adsorption capacity between different polystyrene microplastics in literature. Error bars denote standard deviations between triplicate runs. .... 191

**Figure 6.5.** Desorption data for triclosan in 10 mM NaCl. (a) desorption kinetics at  $C_0 = 100 \mu\text{g/L}$ , (b) desorption isotherm of pristine microplastics, (c) desorption isotherm of aged microplastics. Dotted line drawn to connect each adsorption data with its desorption data. Error bars denote standard deviations of 3 experimental runs. HI = hysteresis index. .... 194

**Figure S6.1.** Surface topography of the microplastics showing the glossy outer surface versus the non-glossy inner side. .... 202

**Figure S6.2.** Different scenarios where changes to mass, diameter, thickness or different combinations of all parameters will impact the density of the microplastic disk. .... 204

**Figure S6.3.** Representative SEM images showing the morphology of the inner and outer surfaces of the pristine versus aged microplastic disks. .... 204

**Figure S6.4.** Representative 3D structures showing the surface topography of the microplastic disks. .... 205

**Figure S6.5.** Contact angle measurements of pristine versus aged microplastics. out and in refer to inner and outer parts of the single-use cup. N = 60 measurements from 3 independent samples (n = 20 each) for each condition. Asterisks represent significant difference at  $p < 0.05$ . .... 205

**Figure S6.6.** XPS spectra of pristine versus aged microplastics for C1s and O1s. a-d indicates that additional peaks are observed at depth 0 (surface) for both inner and outer sides. .... 206

**Figure S6.7.** Stress-strain curves. Samples A, B, C are three independent samples for each treatment. The parameters were calculated as described in <sup>9</sup>. The Young's modulus was calculated as the slope of the stress-strain curve while ignoring the first few flat data points. The ultimate elongation is the plastic strain value where the plastic broke.<sup>9</sup> .... 206

**Figure S6.8.** Effect of weathering on the amount of triclosan released from microplastics (approx. 30 mg) in 10 mM NaCl solution (40 mL). Values on x-axis are the approximate initial starting concentrations during the sorption phase. Error bars represent standard deviation of 3 independent measurements from three separate vials..... 207

**Figure S6.9.** Effect of weathering on the desorption of triclosan as function of depth for a smaller microplastic disk (diameter of 220  $\mu\text{m}$ ) and sphere both having equivalent diameters of 100  $\mu\text{m}$ . .... 208

## List of Tables

<b>Table 2.1.</b> Laboratory studies investigating NP and MP aggregation.....	20
<b>Table 2.2.</b> Laboratory studies investigating NP and MP deposition.....	26
<b>Table S2.1.</b> Data and references for Figure 2.1.....	54
<b>Table S2.2.</b> Summary of sorption studies of contaminants to plastic particles.....	56
<b>Table 3.1.</b> Measured hydrodynamic diameters, electrophoretic mobility (EPM), zeta potential (ZP), calculated elution (C/C0) and attachment efficiencies of the nanoplastics (NP) in quartz sand porous media.....	70
<b>S3.7.</b> Parameters used in calculating attachment efficiency.....	89
<b>Table S4.1.</b> The properties and conditions of plastic and electrolyte used in the study .....	114
<b>Table S4.2.</b> Properties of the natural surface water.....	114
<b>Table S4.3.</b> Experimental details for aggregation versus plastic-surface interaction experiments.....	115
<b>Table S4.4.</b> Relationship between CCC in divalent salts and polystyrene plastic size from literature .....	116
<b>Table S4.5.</b> Surface coverage calculation of natural organic matter present in working solution .....	119
<b>Table S4.6.</b> Debye length in CaCl <sub>2</sub> concentration.....	119
<b>Table S4.7.</b> Elemental composition of organic matter used as reported by the International Humic Substances Society.....	120
<b>Table S4.8.</b> Fitting parameters from plastic-surface interaction.....	120
<b>Table 5.1.</b> Comparison of characteristics and weathering conditions of effect studies using microplastics aged in the laboratory or collected in the environment. Detailed references in Tables S5.2 and S5.3.....	143
<b>Table 5.2.</b> Proposed reporting guidelines for studies on effects of weathered microplastics ....	152
<b>Table S5.1.</b> Literature search criteria .....	161
<b>Table S5.2.</b> Summary of laboratory studies investigating the effect of weathered microplastics, nanoplastics and leachates .....	161
<b>Table S5.3.</b> Summary of effect studies using microplastics collected from the environment ...	164
<b>Table S5.4.</b> Summary of international standard weathering protocols developed for plastics and other polymers .....	165
<b>Table 6.1.</b> Summary of parameters related to changes in physical, chemical and mechanical properties of the microplastics after aging.....	185
<b>Table 6.2.</b> Kinetic model fitting parameters for triclosan adsorption and desorption on microplastics .....	192

<b>Table S6.1.</b> LC-MS measurement parameters .....	200
<b>Table S6.2.</b> List of kinetic, isotherm models and other adsorption models used in this study. .	201
<b>Table S6.3.</b> Calculated changes to density after aging.. Below is a description of different scenarios that may lead to increased density. All values used are approximate average values measured: mass (from 4.4 – 3.8 mg), thickness (from 0.25 to 0.24 mm), and diameter (from 4.5 – 4.44 mm) for pristine and aged microplastics, respectively. ....	203
<b>Table S6.3.</b> Isotherm model fitting parameters for triclosan adsorption on microplastics .....	207

## List of Abbreviations

ABS	acrylonitrile butadiene styrene
AMP	amidine-modified plastics
CCC	critical coagulation concentration
ChMP	chloromethyl-modified plastic.
CMP	carboxyl-modified plastics
CTR	car tire rubber
DDE	dichlorodiphenyldichloroethylene
DDT	dichloro diphenyl trichloroethane
DLS	dynamic light scattering
EDL	electrical double layer
ENP	engineered nanoparticle
FOSA	Perfluorooctanesulfonamide
FTIR	Fourier-transform infrared spectroscopy
GFA	Georgetown fulvic acid
HCH	hexachlorocyclohexane
HDPE	high-density polyethylene
LDPE	low-density polyethylene
LPEI	linear polyethyleneimine
MP	microplastic
NOM	natural organic matter
NP	nanoplastic
PA	polyamide
PAA	polyacrylic acid
PAH	polycyclic aromatic hydrocarbon
PCB	polychlorinated biphenyl
PDAPMAC	polydiallyldimethylammonium chloride
PE	polyethylene
PET	polyethylene terephthalate
PEVA	polyethylene vinyl acetate
PFOS	perfluorooctanesulfonate
PHA	peat humic acid
PLA	polylactic acid
POM	polyoxymethylene
POP	persistent organic pollutant
PP	polypropylene
PPCP	pharmaceuticals and personal care product
PU	polyurethane
PVC	polyvinyl chloride
QCM-D	quartz crystal microbalance with dissipation

SEM	scanning electron microscope
SMP	sulfate-modified plastic
SRHA	Suwannee river humic acid
TEM	transmission electron microscope
TWP	tire wear particles

# Chapter 1: Introduction

## 1.1 Motivation

Plastic pollution has received a lot of attention in the last decade. Varying concentrations of tiny plastics have been documented in most environmental compartments<sup>1-4</sup> including remote areas.<sup>5,6</sup> Even with the current pollution prevention strategies, plastic emissions to the environment are expected to increase.<sup>7</sup> The major concern surrounding plastic pollution is the formation of microplastics and nanoplastics because of their potential to bioaccumulate, biomagnify, and act as transport vehicles for other contaminants.<sup>8</sup> These tiny plastics are either formed/manufactured intentionally (primary) or breakdown from discarded bulk plastics (secondary).<sup>9</sup> Amongst the prerequisite for assessing and predicting the risks associated with microplastics pollution, is understanding their transformations and persistence in the environment. These transformations may include aggregation, transport, deposition, sedimentation, adsorption of other contaminants, degradation etc.<sup>9</sup> These processes could determine whether microplastics will undergo long-range transport, accumulate within the vicinity of their release or be bioavailable. Nanoplastics from surface runoffs, and landfill leachates, etc. can potentially be transported to groundwater. The stability of nanoplastics in surface waters will also determine their bioavailability to pelagic or benthic organisms; hence, the aggregation behaviour of nanoplastics has been studied in synthetic water matrices.<sup>9</sup> The ability of microplastics to act as transport vehicles for other toxic and persistent chemicals has also been documented in laboratory and field studies.<sup>10,11</sup>

Despite the numerous studies attempting to quantify the effects and risks of microplastics and nanoplastics in these environmental compartments, there exist numerous knowledge gaps on the factors that influence their behaviour and interactions. Microplastics are expected to encounter and undergo various weathering processes (physical, chemical, or biological weathering) before and after release into the environment, yet the effect of weathering on the environmental risks of microplastics is largely overlooked.<sup>12</sup> Most studies investigating the transport and stability of microplastics have focused on other factors associated with the properties of the plastic and background media.<sup>9</sup> Considering that most microplastics will rarely be in their pristine state in the environment, it is important to investigate the effect of weathering on their behaviour. There are also numerous studies investigating the fate of primary microplastics, and less so from secondary

sources. In addition, the mass of natural organic and inorganic colloids and molecules are estimated to outweigh the mass of plastics in the environment;<sup>13</sup> yet, studies that assess the stability of nanoplastics are often limited by the use of high concentrations of plastics relative to natural colloids or natural organic matter (NOM). Moreover, there is lack of quantitative and comparative data on the colloidal stability of nanoplastics in natural waters.

## **1.2 Research objectives**

Clearly, there are several knowledge gaps regarding the fate and behaviour of microplastics and nanoplastics in the environment. With the increasing production of plastics and inadequate waste management strategies, a better understanding of their interactions and impact in natural environments is crucial. Therefore, the four main objectives of this thesis were as follows:

1. To examine how environmental weathering in cold climates (exposure to freeze-thaw) impacts the physicochemical properties and transport behaviour of nanoplastics in a model groundwater environment.
2. To systematically and comparatively examine the effect of environmental organic matter on the aggregation behaviour of different nanoplastics sizes in simple and complex synthetic water matrices. Thereafter, to quantitatively compare the findings between synthetic water and natural water matrices.
3. To examine the effect of UV weathering on the physicochemical properties of secondary microplastics. Then investigate how these changes in the particle properties influence microplastic settling and transport behaviour in freshwater.
4. To investigate the effect of UV weathering on the potential of secondary microplastics to act as transport vehicles for hydrophobic contaminants.

## **1.3 Thesis organisation**

- Chapter 2 provides an extensive literature review that estimates and describes the pathways and loads of plastics in different environmental compartments. Studies investigating the aggregation, deposition and contaminant transport of microplastics in the aquatic environment were critically assessed. Critical links between different plastic types and their adsorption capacities were provided.
- In Chapter 3, the effect of a physical weathering process (freeze-thaw) on nanoplastic transport is examined. The influence of repeated freeze-thaw cycles on the transformation

and transport of primary nanoplastics was investigated in a saturated porous media. The ability of natural organic matter to stabilize the nanoplastics suspension was investigated as well as the disaggregation behaviour of the freeze-thaw induced aggregates. Other studies reporting the transport of nanoplastics at different temperatures were compared with this work. Finally, the transport distance needed to remove 99.9% of nanoplastics from the fluid phase was estimated.

- In Chapter 4, the impact of environmental organic matter on the colloidal stability of two nanoplastic sizes was investigated in simple and complex synthetic water matrices. The nanoplastic to organic matter ratio was kept realistic (low) to gain better mechanistic interpretations of possible interactions. Thereafter, the aggregation behaviour of the two nanoplastics were quantitatively examined and compared in synthetic versus natural complex water matrices (with salinity gradients from fresh to seawater matrix).
- In Chapter 5, the expected and overlooked weathering pathways that plastics will undergo throughout their lifecycle before and after release into the environment was examined. The current weathering protocols used in microplastic research were critically analysed and compared to international standard weathering protocols developed for polymers, for their appropriateness, which highlighted important knowledge gaps. Finally, we developed and proposed a quality reporting system for weathering protocols and characterization, harmonization and reproducibility across different studies.
- In Chapter 6, the effect of UV weathering on the fate and behaviour of microplastic from a secondary source was investigated. The changes to the physicochemical properties were probed using a range of profilometry, spectroscopy and microscopy techniques. The effect of weathering on the settling velocities of the microplastic was measured experimentally and used to estimate their transport distance in a typical lake. Thereafter, the ability of the secondary microplastics to act as transport vehicles in freshwater was investigated.
- Chapter 7 provides a conclusion of the thesis and general implications of the findings to the global audience and suggestions for future research.

#### **1.4 Contributions to knowledge**

This doctoral thesis has addressed significant knowledge gaps in the literature and made novel and original contributions to advance our knowledge towards accurate risk assessment of microplastic

and nanoplastic pollution. The specific contributions on the fate and transformations of nanoplastics and microplastics are:

- 1. Demonstrated the impact of repeated environmental freeze-thaw on the stability and transport of nanoplastics in saturated porous media.** Although, there are several studies looking at the effect of various factors on the transport of nanoplastics or nanoplastic proxies in model groundwater environments, the effect of freeze-thaw (FT), a physical weathering process typical of cold climates is unknown. This is the first study that showed that by ignoring this component of environmental weathering, previous conclusions drawn on the effect of cold temperatures on nanoplastic transport may be inconclusive or overestimated. Repeated FT process was shown to induce nanoplastics aggregation which resulted in heightened retention in the porous media. This is also one of the first studies to show the coupled effect of cold temperature and the presence of natural organic matter on nanoplastics transport. The impact of FT outweighed the effect of NOM even though the presence of NOM significantly increased the transport of nanoplastics. We show that the FT-induced aggregation process was irreversible suggesting that the aggregates may be stable over long time periods.
- 2. Improved mechanistic understanding of the effect of environmental organic matter on the stability of nanoplastics.** Previous studies only focused on single particle sizes per study whereas plastic particles in the environment are made up of various size populations that may interact with organic matter differently. Moreover, the bulk of aggregation studies use unrealistic plastic/NOM ratios. It was shown that by using low plastic/NOM ratios, plastics will interact with different natural organic matters in a size specific manner. The presence of polysaccharides which are sometimes in excess during seasonal algal blooms destabilized the nanoplastics in simple divalent matrices and stabilized them in complex ion matrices. In addition, the effect of NOM was more pronounced for the larger nanoplastics. This provides an improved understanding of how different plastic sizes will behave in the marine environment.
- 3. Quantitative comparison of nanoplastics behaviour in synthetic waters and natural water matrices.** Numerous studies have examined the aggregation behaviour of nanoplastics in synthetic water using single particle sizes, while the natural marine water is more complex. This study shows that the attachment efficiency of two nanoplastic sizes

is similar in synthetic water (which is often used as proxy for marine water in laboratory studies), but different in natural seawater matrix. These observed differences have huge implications for risk assessment.

- 4. Demonstrated the effect of photodegradation on the interaction of a model contaminant with microplastics.** The effect of UV weathering on the sorption behaviour of microplastics is sparse. Moreover, even though polystyrene is widely studied in the literature, there are limited studies using those from secondary sources. This is the first study to examine the sorption behaviour of a secondary microplastic made of polystyrene while investigating the effect of plastic aging. The aged microplastics exhibit higher adsorption capacity compared to the pristine ones at high contaminant concentration. This provides improved understanding about the impact of weathering on microplastic behaviour.
- 5. Investigated the effect of UV weathering on the settling behaviour of secondary microplastics.** The few microplastics settling velocity studies only focused on biofouling as a form of plastic aging. In fact, biofouling is often attributed to why some microplastics are lost from the sea and found in the seafloor, whereas microplastics will also undergo other non-biological aging processes in the environment. This is the first study to show the effect of UV weathering on the settling velocity of microplastics. The physicochemical properties of the microplastics were altered after weathering which affected their buoyancy leading to increased settling velocities. This data was used to estimate the retention of microplastics in lakes.
- 6. Novel perspective and critical evaluation of the microplastics literature on plastic loads, weathering, aggregation, deposition and contaminant sorption.** A critical literature review revealed an important trend between microplastic types and their contaminant adsorption capacities. An up-to-date overview of plastic concentrations in different environmental compartments was also presented. Weathering protocols vary across microplastic research which can potentially confound findings. Hence, there is an urgent need for the development of standardized protocols. The appropriateness of international weathering standards for microplastics research was critically evaluated and a framework of quality reporting system for method harmonization developed. This will help with the design of experiments attempting to mimic environmentally relevant

microplastics. Critical knowledge gaps about the fate and behaviour of microplastics were highlighted for future research.

### **1.5 Contributions of the author**

This thesis consists of 5 articles and is presented in a manuscript-based format. Two of these articles have been published in peer-reviewed scientific journals, one is submitted while the remaining two articles are being prepared for submission. In all the publications, the first author of each manuscript is the primary author of this thesis. Below is a detailed description of the contributions of each author:

1. "Microplastics and nanoplastics in aquatic environments: Aggregation, deposition, and enhanced contaminant transport" *Environmental Science and Technology*. 52(4), 1704-1724. 2018

**Authors:** Alimi, O.S., Farner Budarz, J., Hernandez, L.M. and Tufenkji, N.

**Contributions:** This manuscript was an extension of Alimi, O.S's PhD Thesis proposal in 2017. Alimi, O.S conceptualized, conducted literature review, synthesized data and wrote the initial draft of the manuscript. Farner, J and Hernandez, L.M wrote subsections and edited the manuscript. Tufenkji, N. conceptualized, reviewed, and edited the manuscript.

2. "Exposure of nanoplastics to freeze-thaw leads to aggregation and reduced transport in model groundwater environments", *Water Research*, 116533. 2020

**Authors:** Alimi, O.S., Farner, J.M. and Tufenkji, N.

**Contributions:** Alimi, O.S and Tufenkji, N. designed the experiments. Alimi, O.S conducted all the experiments, analysed the data and wrote the manuscript. Farner, J assisted with data interpretation and reviewed the manuscript. Tufenkji, N. reviewed the manuscript and supervised the project.

3. "Mechanistic understanding of the aggregation kinetics of nanoplastics in marine environments", *To be submitted to Water Research*. 2021

**Authors:** Alimi, O.S., Farner, J., Roweczyk L., Petosa, A.R., Claveau-Mallet, D., Hernandez, L.M., Wilkinson, K.J. and Tufenkji, N.

**Contributions:** Alimi, O.S, Tufenkji, N. and Farner, J. designed the initial aggregation experiments. Alimi, O.S conducted most of the aggregation experiments, characterised the nanoplastic aggregate structures, analysed the data and wrote the manuscript. Roweczyk L. and Farner, J assisted with data interpretation. Roweczyk L., Claveau-Mallet, D. Petosa, A.R. and Farner, J. assisted with the aggregation experiments. Hernandez, L.M. carried out the optical tweezer experiments and analysis. Wilkinson, K.J. and Tufenkji N, supervised the project, reviewed and edited the manuscript.

4. "Weathering pathways and protocols for environmentally relevant microplastics and nanoplastics: What are we missing?", *Journal of Hazardous Materials*, **126955** 2021

**Authors:** Alimi, O.S., Claveau-Mallet, D., Kurusu, R., Lapointe, M., Stephane, B. and Tufenkji, N.

**Contributions:** The idea for this review paper arose during a progress meeting at the beginning of the COVID-19 pandemic when all laboratories were shut down for experimental work. Alimi, O.S. and Claveau-Mallet, D. conceptualized the review idea and designed the study. Alimi, O.S. conducted the literature review, synthesized, analysed the data, and wrote the initial draft of the manuscript. Claveau-Mallet, D, Kurusu, R., Lapointe, M., contributed to writing sections of the manuscript. Bayen, S. and Tufenkji, N. reviewed and supervised the work.

5. "Effects of weathering on the properties and fate of secondary microplastics from a disposable cup" *To be submitted.*

**Authors:** Alimi, O.S., Claveau-Mallet, D., Lapointe, M., Tinh, B., Liu, L., Hernandez, L.M., Stephane, B. and Tufenkji, N.

**Contributions:** Alimi, O.S. and Claveau-Mallet, D. conceptualized and designed the study. Alimi, O.S. conducted the adsorption and desorption experiments, settling experiments, led the characterization of the microplastics, analyzed the data and wrote the manuscript. Tinh, B., (a McGill University undergraduate student engaged at the time in a summer project in the Biocolloids and Surfaces Laboratory) assisted with conducting some preliminary experiments. Hernandez, L assisted with the SEM and XPS measurements. Lapointe, M assisted with the

transport simulations. Liu L. assisted with contaminant analysis using the LC-MS. Bayen, S. and Tufenkji, N. supervised the project and reviewed the manuscript.

## References

1. Panno, S. V.; Kelly, W. R.; Scott, J.; Zheng, W.; McNeish, R. E.; Holm, N.; Hoellein, T. J.; Baranski, E. L., Microplastic Contamination in Karst Groundwater Systems. *Ground Water* **2019**, *57* (2), 189-196.
2. Panko, J. M.; Chu, J.; Kreider, M. L.; Unice, K. M., Measurement of airborne concentrations of tire and road wear particles in urban and rural areas of France, Japan, and the United States. *Atmos. Environ.* **2013**, *72*, 192-199.
3. Browne, M. A.; Crump, P.; Niven, S. J.; Teuten, E.; Tonkin, A.; Galloway, T.; Thompson, R., Accumulation of microplastic on shorelines worldwide: sources and sinks. *Environ. Sci. Technol.* **2011**, *45* (21), 9175-9.
4. Thompson, R. C.; Olsen, Y.; Mitchell, R. P.; Davis, A.; Rowland, S. J.; John, A. W.; McGonigle, D.; Russell, A. E., Lost at sea: Where is all the plastic? *Sci* **2004**, *304* (5672), 838.
5. Allen, S.; Allen, D.; Phoenix, V. R.; Le Roux, G.; Durántez Jiménez, P.; Simonneau, A.; Binet, S.; Galop, D., Atmospheric transport and deposition of microplastics in a remote mountain catchment. *Nature Geoscience* **2019**, *12* (5), 339-344.
6. Napper, I. E.; Davies, B. F. R.; Clifford, H.; Elvin, S.; Koldewey, H. J.; Mayewski, P. A.; Miner, K. R.; Potocki, M.; Elmore, A. C.; Gajurel, A. P.; Thompson, R. C., Reaching New Heights in Plastic Pollution—Preliminary Findings of Microplastics on Mount Everest. *One Earth* **2020**, *3* (5), 621-630.
7. Borrelle, S. B.; Ringma, J.; Law, K. L.; Monnahan, C. C.; Lebreton, L.; McGivern, A.; Murphy, E.; Jambeck, J.; Leonard, G. H.; Hilleary, M. A., Predicted growth in plastic waste exceeds efforts to mitigate plastic pollution. *Sci* **2020**, *369* (6510), 1515-1518.
8. Rochman, C. M., The role of plastic debris as another source of hazardous chemicals in lower-trophic level organisms. Springer Berlin Heidelberg: Berlin, Heidelberg, 2016; pp 1-15.
9. Alimi, O. S.; Farner Budarz, J.; Hernandez, L. M.; Tufenkji, N., Microplastics and nanoplastics in aquatic environments: Aggregation, deposition, and enhanced contaminant transport. *Environ. Sci. Technol.* **2018**, *52* (4), 1704-1724.
10. Rochman, C. M.; Hentschel, B. T.; Teh, S. J., Long-term sorption of metals is similar among plastic types: implications for plastic debris in aquatic environments. *PLoS One* **2014**, *9* (1).
11. Rochman, C. M.; Hoh, E.; Hentschel, B. T.; Kaye, S., Long-term field measurement of sorption of organic contaminants to five types of plastic pellets: implications for plastic marine debris. *Environ. Sci. Technol.* **2013**, *47* (3), 1646-54.
12. Alimi, O. S.; Claveau-Mallet, D.; Kurusu, R. S.; Lapointe, M.; Bayen, S.; Tufenkji, N., Weathering pathways and protocols for environmentally relevant microplastics and nanoplastics: What are we missing? *J. Hazard. Mater.* **2022**, *423*, 126955.
13. Koelmans, A. A.; Bakir, A.; Burton, G. A.; Janssen, C. R., Microplastic as a vector for chemicals in the aquatic environment: Critical review and model-supported reinterpretation of empirical studies. *Environ. Sci. Technol.* **2016**, *50* (7), 3315-26.

## **Preamble to Chapter 2**

Little is known about the concentrations, mobility, and impacts of nanoplastics and microplastics in the environment. In this critical literature review, we presented a comprehensive overview and perspective of micro- and nanoplastic aggregation and deposition and highlight key factors such as water chemistry, surface coating, and plastic type and functionalization that influence particle behavior. We included an overview of studies examining micro- and nanoplastic concentrations and transport between major environmental compartments. We also discussed the potential for plastics to act as transport vectors for other contaminants such as persistent organic pollutants, metals, and pesticides in surface water and saturated porous media. Our data synthesis revealed that the rubbery polymer, polyethylene generally has a higher sorption capacity than other polymer types. Major knowledge gaps that need to be addressed to improve our understanding of the risks associated with microplastic pollution were highlighted. This critical review chapter laid the foundation for other chapters reported in this thesis.

The results and findings from this chapter have been published in *Environmental Science and Technology Journal* in December 2017.

## **Chapter 2: Microplastics and Nanoplastics in Aquatic Environments: Aggregation, Deposition, and Enhanced Contaminant Transport**

### **Abstract**

Plastic litter is widely acknowledged as a global environmental threat and poor management and disposal lead to increasing levels in the environment. Of recent concern is the degradation of plastics from macro- to micro- and even to nanosized particles smaller than 100 nm in size. At the nanoscale, plastics are difficult to detect and can be transported in air, soil and water compartments. While the impact of plastic debris on marine and fresh waters and organisms has been studied, the loads, transformations, transport, and fate of plastics in terrestrial and subsurface environments are largely overlooked. In this review, we first present estimated loads of plastics in different environmental compartments. We also provide a critical review of the current knowledge vis-à-vis nanoplastic (NP) and microplastic (MP) aggregation, deposition, and contaminant co-transport in the environment. Important factors that affect aggregation and deposition in natural subsurface environments are identified and critically analyzed. Factors affecting contaminant sorption onto plastic debris are discussed, and we show how polyethylene generally exhibits a greater sorption capacity than other plastic types. Finally, we highlight key knowledge gaps that need to be addressed to improve our ability to predict the risks associated with these ubiquitous contaminants in the environment by understanding their mobility, aggregation behavior and their potential to enhance the transport of other pollutants.

## 2.1 Introduction

Currently, the global production of plastics exceeds 320 million tons (Mt) per year,<sup>1</sup> with production expected to double in the next 20 years.<sup>2</sup> Of this, only 6-14% is recycled, meaning up to 86% ends up either in landfills (21–42%) or released into the environment due to mismanagement through a variety of pathways (Figure 2.1).<sup>2-6</sup> Indeed, with the widespread use of different plastics, the current era has been referred to as the *Plasticene*.<sup>7</sup> Plastic debris has been detected in air,<sup>8</sup> oceans,<sup>5, 9, 10</sup> soils,<sup>11-13</sup> sediments,<sup>14, 15</sup> and surface waters worldwide.<sup>16</sup> It is estimated that in Europe and North America, the amount of microplastics (MPs) transferred every year from wastewater treatment plants (WWTPs) to agricultural soils as biosolids is greater than the total burden of MPs currently present in ocean water.<sup>3</sup>

Plastics are produced through the polymerization of various monomers and additives resulting in a spectrum of characteristics such as polarity and “glassiness”.<sup>17, 18</sup> These differences in composition will impact their affinity for other pollutants and potential risks associated with them.<sup>19</sup> The most commonly detected plastics in the environment are polyethylene (PE), polyvinyl chloride (PVC), polypropylene (PP), polyethylene terephthalate (PET) and polystyrene (PS).<sup>20</sup>

The presence of MPs in the environment had been largely overlooked until recently; however, the number of studies is now growing rapidly due to the global ubiquity of plastic and its potential threat to human health and biota. Large plastic debris breaks down to form macroplastics (herein defined as >25 mm in size), mesoplastics (5-25 mm), MPs (<5 mm) and nanoplastics (NPs) (<100 nm).<sup>21, 22</sup> There is no clear consensus on the definition of MP and NP size in the literature;<sup>5, 23-27</sup> in this review, we define MPs and NPs as plastic debris with diameters of 100 nm-5 mm and <100 nm, respectively.

MPs/NPs are either primary or secondary in origin. One example of primary MPs is the plastic beads used as exfoliants in personal care products.<sup>28</sup> Primary NPs have also been detected in facial cleansers.<sup>29</sup> When these consumer goods are used, MPs and NPs are released into waste streams, with 95–99% partitioning into biosolids or removed in oil skimming in WWTPs.<sup>3, 11, 30, 31</sup> Nonetheless, an estimated 8 trillion pieces of MP (including microfibers) enter the aquatic environment via WWTP effluents.<sup>32</sup> Other sources of primary MPs in the environment include industrial abrasives and accidental spills.<sup>33, 34</sup>

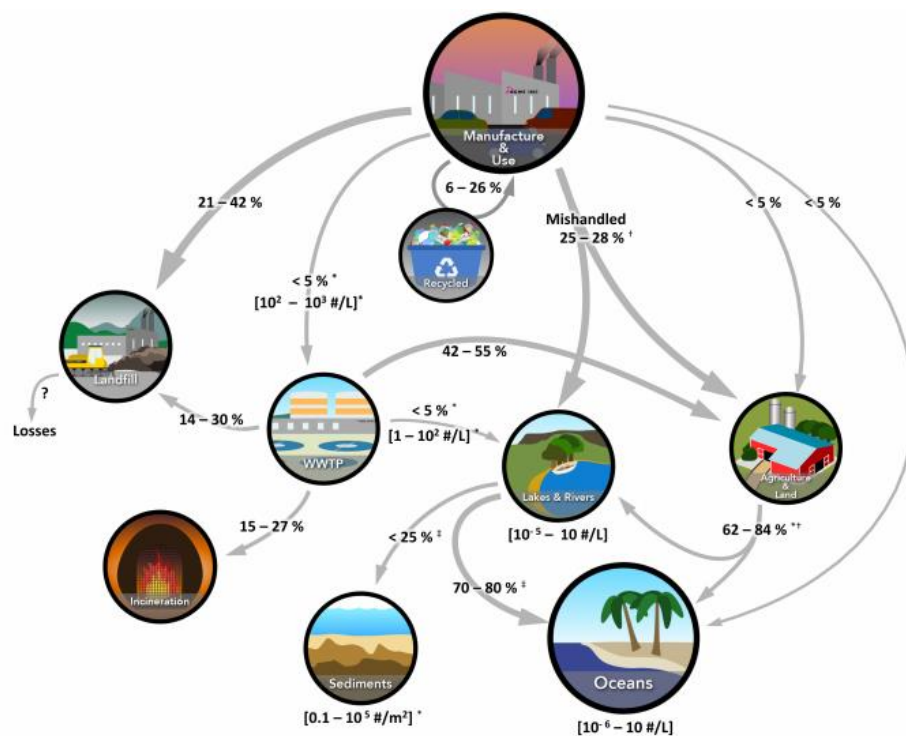


**Figure 2.1.** Estimates of plastic loading and transport pathways in the environment aggregated from reports in the literature. Percentages indicate the fraction of plastics in a given compartment moving to a subsequent compartment, with wider arrows representing greater plastic transfer. Ranges of concentrations measured, either in number of particles per liter or per area, are given where reliable values were observed. Values indicated are for macro and microplastics. \*corresponds to estimates for microplastics only. †corresponds to values divided between two compartments. ‡corresponds to best estimates in the absence of data in the literature. Data and references are summarized in Table S2.1.

Secondary MPs are the unintentional product of larger plastics degrading in the environment due to weathering processes (e.g., hydrolysis, UV photodegradation, mechanical abrasion, biodegradation). Sources include car tires, agricultural plastic mulch, microfibers from textiles, and larger plastics in the ocean (e.g., plastic bags, bottles, ropes, nets).<sup>33, 35-37</sup> Secondary MPs can often be identified by their irregular shapes and changes to the chemical structure.<sup>38</sup>

The increasing load of plastic in the ocean has received considerable attention.<sup>1, 10, 25, 33</sup> It is estimated that there will be over 250 Mt of plastic accumulated in the ocean by 2025.<sup>1, 39</sup> Though the processes may be slow, plastic will inevitably break down into MPs and NPs due to exposure to UV radiation, mechanical abrasion, and wave action. The combination of primary and secondary sources leads to estimates that 5.25 trillion plastic particles contaminate the global sea surface,<sup>40</sup> the majority of which are less than 10 mm in size.<sup>36</sup>

In contrast to marine plastics, there is limited information on the behavior, fate, and loading of MPs and NPs in the terrestrial environment. MPs and NPs may be introduced to soils as a result of landfill leachate, agricultural mulches, application of wastewater biosolids to agricultural land, or by direct releases of secondary MPs and NPs from abrasion or maintenance of outdoor plastic goods and coated surfaces.<sup>2, 13, 41-45</sup> Following release into the environment, MPs and NPs may undergo various transformations commonly associated with natural or anthropogenic colloids;<sup>46</sup> namely, homo- and heteroaggregation, interactions with microorganisms and macromolecules (e.g., adsorption of proteins, natural organic matter) and biodegradation. These processes, as well as the mobility of the particles in natural soils and ground waters, are strongly influenced by porewater chemistry (e.g., pH, ionic strength, natural organic matter content) as well as the properties of the plastics (e.g., size, shape, chemical composition) and soil/aquifer sediments (e.g., composition, size distribution). While a large number of laboratory studies have examined the transformations and transport of natural colloids and engineered nanomaterials such as metals and metal oxides in terrestrial environments,<sup>46-50</sup> there is little data on how these environmental processes and conditions affect different types of NPs and MPs that are present in soils.

Natural colloids such as iron oxides and clays have been shown to affect the transport of contaminants such as radionuclides, pesticides, and polycyclic aromatic hydrocarbons in the subsurface environment.<sup>51-56</sup> Likewise, MPs and NPs can act as vectors for the transport of contaminants such as heavy metals<sup>57-59</sup> and persistent organic pollutants (POPs).<sup>20, 60-65</sup> Yet, the extent to which sorption of contaminants onto different types of MPs and NPs enhances or mitigates the environmental and health impacts of these pollutants remains unclear.

This paper provides a critical review of the existing scientific literature examining the aggregation and transport of NPs and MPs in soil and groundwater systems. First, we estimate the loads of plastics in different environmental compartments. Next, we critically assess existing studies on the aggregation, transport and contaminant sorption behavior of NPs and MPs in terrestrial and subsurface environments. Finally, the current gaps in knowledge precluding a comprehensive understanding of MP and NP fate and impacts are discussed.

### **2.1.1 From macro to micro to...nano?**

Macroplastics can degrade to form MPs through stresses that impact the structure and reactivity of the plastic polymer.<sup>66, 67</sup> Degradation of plastics can occur by multiple processes including hydrolysis, photodegradation due to UV exposure, mechanical abrasion by sand or wave action,

and biodegradation.<sup>68, 69</sup> These processes may also act synergistically. For example, UV exposure leads to carbonyl group formation, rendering the materials more brittle and increasing the likelihood of mechanical degradation.<sup>36</sup> Degradation mechanisms are not uniform for all plastics; for instance, PS and PE are more prone to weathering by UV radiation than other plastics.<sup>70</sup> While the occurrence of MPs in the natural environment is increasingly well documented,<sup>16, 68, 71, 72</sup> to date, no study reports on the presence of NPs in aquatic or soil environments. This is mainly due to methodological challenges associated with detection and recovery of such small, carbon-based particles in complex natural matrices. Although there is no data available on environmental loads of NPs, weathering of macroplastics and MPs is expected to yield secondary NPs.<sup>67</sup> Indeed, a controlled laboratory study<sup>66</sup> shows that NPs and MPs (ranging in size from 30-2000 nm) are released during weathering of macroplastic (a polystyrene coffee cup lid) in a simulated marine environment. A recent study further reveals that consumer products such as facial scrubs can act as an unintentional yet important source of primary NPs to natural waters and soils.<sup>29</sup> Thus, although environmental levels of NPs are yet to be quantified, plastic nano-litter is expected to be as ubiquitous as its bulk counterparts.

## **2.2 Living in the Plasticene: Plastic in every corner of the earth**

Plastics can be found throughout the globe. Despite their ubiquity, the global cycling of MPs and NPs is not well understood. Figure 2.1 illustrates the existing knowledge of global plastic cycling. Significant transport pathways are identified and loads in selected environmental compartments are reported; however, the relative flux of plastics from one compartment to another is often unknown or associated with large uncertainty. Despite numerous studies to date, wide ranges in reported concentrations are observed, representing both spatial variation and measurement uncertainty. For example, estimates of plastic loads in the oceans range six orders of magnitude,<sup>14, 25, 73</sup> while no comprehensive data exist for MPs in soils despite considerable agricultural use.<sup>74, 75</sup> Finally, atmospheric deposition of MPs and NPs is expected, but largely unexamined<sup>76</sup> except for few studies.<sup>16, 77</sup>

### **2.2.1 Freshwaters are key vectors for microplastic transport**

Rivers are estimated to transport 70-80% of plastics that eventually arrive in the oceans, with primary inputs from mishandled debris either during manufacture and use, from agriculture and land, and WWTP effluent (Figure 2.1).<sup>30</sup> Concentrations of plastics in freshwater can rival marine levels, though there is great spatial variation, depending on proximity to urban or industrial sites,

or the presence of WWTPs.<sup>68, 78-80</sup> Freshwaters are generally closer to plastics sources than marine waters and have more shoreline to retain particles, facilitating accumulation and mechanical degradation.<sup>71</sup> Branches, logs, and dams have been identified as local hotspots of plastics.<sup>81, 82</sup>

Several studies have focused on large rivers, such as the Chicago River, Rhine-Main, Danube, and Thames.<sup>34, 79, 80, 83</sup> In general, significant differences are seen in concentrations of MPs upstream of a point source versus downstream.<sup>79</sup> However, the presence of multiple sources along the length of a river makes identifying the origin of specific particles difficult.<sup>80</sup> Additionally, changes in flow due to bends, particularly deep or shallow sections, etc. can cause particle buildup and influence transport. Pulsed, accidental releases have been identified as a primary source of peak loading events.<sup>34</sup> Furthermore, periods of high flow are capable of both re-suspending particles that may have settled to the sediments and depositing MPs onto adjacent shorelines.<sup>30</sup>

WWTPs, ubiquitous along populated waterways, act as significant point sources of MPs to freshwaters. McCormick et al. demonstrated a 10-fold increase in plastic fibers downstream of a WWTP in the Chicago River<sup>79</sup> despite the fact that 95-99% of plastics partition into the wastewater biosolids.<sup>16, 84, 85</sup> Likewise, in a WWTP with tertiary treatment, as little as 0.1% of the incoming MPs and microfibers were released in the effluent water.<sup>31</sup> Although a relatively large fraction of MPs/NPs are expected to be trapped in wastewater biosolids, it is estimated that 520,000 tons/year of plastic waste is still released in wastewater effluents in Europe alone.<sup>30</sup> It is noteworthy that application of sludge can represent a significant source of MPs (and very likely NPs) to agricultural lands.

Lakes can act as temporary or long-term sinks of MPs. Areas of the Laurentian Great Lakes are as polluted as ocean gyres, but there are large spatial variations, both within a single lake and between lakes.<sup>78</sup> Transport in lakes is driven by currents, similar to rivers and streams, but also by wind patterns that can produce areas of seasonally high local MP concentrations.<sup>86</sup> Hoffman and Hittinger estimate plastic introduction into the Great Lakes at 10,000 metric tons/year.<sup>87</sup>

Estimates of plastic loading in rivers and lakes range from  $10^{-5}$  to 10s of pieces/L (Figure 2.1).<sup>30, 73, 79</sup> Making precise estimates of plastic loading in lakes is difficult however, as sampling generally takes place at the water surface, while large concentrations of MPs can also exist below the surface, depending on the biological, physicochemical, and hydrodynamic conditions (e.g., plastic density, mixing of water column and aggregation/attachment of bacteria/algae).<sup>81</sup>

### **2.2.2 Aquatic species are at high risk**

With the high loads of MPs (and likely NPs) in natural waters, aquatic species are expected to experience chronic exposure and to potentially bioaccumulate the plastic particles.<sup>88-90</sup> Invertebrates such as crustaceans, barnacles, polychaete worms, mussels, and amphipods have ingested MP fragments in controlled studies.<sup>15, 91, 92</sup> These tests often employ high MP concentrations, limiting their environmental significance.<sup>1</sup> A few researchers investigated plastic accumulation in organisms in their natural habitat confirming MP ingestion and accumulation in the gut and stomach of various species of fish,<sup>90,93</sup> shellfish,<sup>94</sup> and fur seals.<sup>95</sup> Although there is a growing number of studies on MP accumulation in aquatic organisms, the (likely) biouptake of NPs has not been examined. The small size and organic composition of NPs present significant methodological challenges to their detection and quantification in complex biological samples. Techniques that may hold promise for future studies in this area include pyrolysis combined with chromatography, mass spectrometry, infrared spectroscopy, scanning electron microscopy with energy dispersive x-ray spectroscopy, field flow fractionation with pyrolysis and multi-angle light scattering.<sup>96</sup>

### **2.2.3 Plastic loads in soils and sediments are less understood**

In comparison to aquatic environments, relatively few studies have investigated plastics levels in soils and sediments.<sup>5, 68</sup> Significant sources of MPs and NPs to soils are likely land application of biosolids, plastic agricultural products, and litter. Moreover, a considerable fraction of the global production of plastic waste (21-42%) (Figure 2.1) is stored in landfills,<sup>11</sup> often under poorly managed conditions that can result in release to soils. Not surprisingly, MPs and synthetic polymer fibers found in sewage sludge were still detectable up to fifteen years after being applied to soils.<sup>12, 13</sup> Indeed, the US market for agricultural plastic was estimated at \$5.8 billion in 2012, including products such as plastic seed casings, ground covers, crop mulch, greenhouse coverings, labels, and wraps.<sup>97</sup> Despite this, little is known about the retention and fate of agricultural plastics after their use. Bioturbation by earthworms can increase soil plastic retention; particles were observed to move downward in the soil profile, with smaller particles being transported to a greater extent.<sup>75, 98</sup> Modeling the fate of plastics in biosolids applied to soils, Nizzetto et al. estimate that only 16-38% of deposited MPs are retained in soils.<sup>3</sup>

Analysis of river sediment cores suggest plastic accumulation over the past four decades.<sup>99</sup> In the Rein-Main river, plastics <5 mm were found in all sediments sampled, with loads up to 1 g/kg (4,000 particles/kg).<sup>80</sup> In general, less plastic mass but similar particle numbers – highlighting

the fact that small particles are generally more mobile – were found in areas of lower population density and nature preserves. Despite this, no clear correlation was established between sediment MP levels and population density, industrial proximity, or WWTPs, illustrating the complex influences of a river system. Lastly, Browne et al.<sup>68</sup> found polyester and acrylic fibers used in clothing were present at over 250% greater concentrations in coastal sediments at historical sewage discharge locations versus reference sites.

Although soils – particularly agricultural lands – are expected to be important sinks for MPs and NPs, significant research is needed to better understand their loads, fate and potential for biouptake in these complex heterogeneous environments. Plastic laden soils also pose a risk for contamination of natural subsurface environments, including groundwaters that may be used as drinking water sources. Thus, there is also an urgent need to characterize the behavior and mobility of MPs and NPs in natural soils and subsurface environments such as groundwater aquifers.

#### **2.2.4 Modeling with incomplete data**

Because the data on MP and especially NP loads are limited and the uncertainty is high, there are few reliable models for MP (or NP) transport.<sup>11</sup> Jambeck et al.<sup>39</sup> calculated broad estimates of future land-based (terrestrial and freshwater) plastics entering the ocean based on waste management data, suggesting that between 100 and 250 million tons of plastics will be released into the ocean by 2025. On a finer scale, Nizzetto et al. developed the first mathematical study of MP fate in terrestrial environments and rivers using an integrated catchment model.<sup>11</sup> This work focused on the mechanisms of MP particle storage, entrainment and deposition in soils and streams to calculate the retention efficiency of soils and river sediments during MP transport toward the sea.<sup>3, 11</sup> One of the primary shortcomings of many models is the lack of 3-dimensional resolution, with models assuming that all particles exist at the water surface which does not account for the variability of plastic concentrations with depth.<sup>83</sup> Furthermore, validating models becomes difficult as not all plastics are captured due to limitations in sampling methods that are unable to detect the smallest particles.<sup>87</sup> To overcome these shortcomings, it could be of interest to implement transport and fate models that have recently been developed for engineered nanoparticles (ENPs).<sup>100</sup> Several models that take aggregation and heteroaggregation into account have been developed for ENPs that could be applicable to NPs.<sup>101-103</sup> Currently, the lack of robust models prohibits a comprehensive understanding of the risks posed by MPs and NPs and reflects the shortcomings in existing data sets of MP and NP behavior and fate in environmental systems.

To address this, considerable fundamental research is needed to characterize the aggregation and deposition kinetics of MPs and NPs over a broad range of environmental conditions.

### **2.3 Current state of knowledge on micro- and nanoplastic aggregation and deposition**

NPs and MPs in natural soils and waters will undergo various transformations (e.g., degradation, coating with environmental macromolecules) that will influence their aggregation, deposition, and transport. These processes will depend largely on the aquatic chemistry of the water column, aquifer porewaters, and sediment properties and will directly influence the environmental fate of the plastic particles.

Aggregation involves the transport of two particles towards each other to collide, followed by attachment. This can occur with two particles of the same type (homoaggregation), or two different particles (heteroaggregation). Deposition is the process of a particle attaching to a larger, immobile collector surface, such as an aquifer/sediment grain.<sup>104</sup> The fundamental mechanisms governing particle aggregation and deposition have been extensively described.<sup>47, 105, 106</sup> Once particles collide with each other (aggregation) or with a collector grain surface (deposition), the likelihood of attachment is controlled by van der Waals and electrical double layer forces described by the Derjaguin-Landau-Verwey-Overbeek (DLVO) theory,<sup>107, 108</sup> as well as non-DLVO interactions (including steric forces).<sup>109, 110</sup> The likelihood of attachment or “attachment efficiency” ( $\alpha$ ) is the ratio of collisions that result in attachment to the number of total collisions. If attractive forces dominate, the process is considered diffusion-limited and  $\alpha$  approaches 1. Conversely, if  $\alpha < 1$ , repulsive forces influence the likelihood of attachment, and the process is considered reaction-limited. According to DLVO theory, increasing the ionic strength (IS) of a solution compresses the electrical double layer and decreases repulsive forces, resulting in a higher rate of aggregation or deposition. The minimum electrolyte concentration needed to completely destabilize a particle suspension is the critical coagulation concentration (CCC). The CCC represents the point at which  $\alpha$  reaches unity, beyond which the aggregation rate is insensitive to an increase in IS.<sup>111</sup> Additionally, according to the Schulze-Hardy rule, multivalent electrolytes will have lower CCC values.

Besides water chemistry, particle-specific properties (e.g., size, density, shape, chemical composition, surface charge, surface coating), hydrodynamic conditions, and soil/sediment properties (e.g., grain size distribution, organic matter content)<sup>104, 111, 112</sup> also influence the

potential mobility of particles in natural aquatic environments. Below, the existing literature on NP and MP aggregation and deposition has been summarized and critically analyzed.

### **2.3.1 Laboratory studies investigating the aggregation of nanoplastics and microplastics.**

Aggregation largely determines the fate, mobility, persistence, and bioavailability of particles in the environment. It is generally controlled by the IS and valence of the electrolytes in the surrounding medium; however, aggregation can also be impaired for NPs/MPs that are polymer-coated, either intentionally or incidentally.<sup>46</sup> Heteroaggregation, in which two or more different types of particles form aggregates, is more likely to take place than homoaggregation for MPs and NPs due to the overwhelmingly greater number of natural colloids.<sup>46</sup> While this has been shown for ENPs and natural colloids,<sup>113</sup> the impact of heteroaggregation on the state or fate of MPs and NPs is unknown. Table 2.1 summarizes the laboratory studies that have investigated the aggregation rates, CCCs and general aggregation behavior of MPs and NPs.

A large number of studies have examined the homoaggregation behavior of PS NPs and MPs. In general, the data in Figure 2.2 show that the particle-particle attachment efficiency ( $\alpha_{pp}$ ) increases with increasing IS due to compression of the electrical double layer, in agreement with the DLVO theory. For example, Wegner et al.<sup>88</sup> report that carboxylated 30 nm PS particles in seawater rapidly aggregated to over 1000 nm in less than 30 minutes. Data in Figure 2.2 show how the electrolyte valence impacts the aggregation rates of PS NPs and MPs. For instance, the CCC for sulfonated PS particles was an order of magnitude greater in monovalent electrolytes compared to divalent electrolytes.<sup>114</sup> The importance of valence is further highlighted in Figure 2.2a, where trivalent cations destabilized carboxylate- and sulfate-modified PS at lower concentrations than divalent cations.<sup>115-117</sup>

A study by Ruiz Cabello et al.<sup>118</sup> shows that sulfate-functionalized PS behaves similarly in two different monovalent electrolytes at pH 4 (in NaCl and KCl, Figure 2.2b). Interestingly, Oncsick et al. also examined sulfate-functionalized PS, at pH 4 in NaCl, but report different behavior. The 530 nm sulfate-functionalized PS used by Oncsick et al.<sup>117</sup> (Figure 2.2b) is less stable in NaCl when compared to a 960 nm PS employed by Ruiz Cabello et al. The observed difference in particle stability may arise from differing surface charge densities and/or disparities in diffusion kinetics due to particle size.

1 **Table 2.1.** Laboratory studies investigating NP and MP aggregation

Plastic type and surface functionality	Nominal size and concentration	Solution chemistry	Experimental approach	Main findings and conclusion	References
<b>PVC latex</b>	d= 480 nm C <sub>0</sub> =36 – 1800 mg/L	Na <sup>+</sup> and Mg <sup>2+</sup>	spectrophotometry	<ul style="list-style-type: none"> <li>• Aggregation kinetics in agreement with DLVO theory</li> <li>• Aggregation follows Schulze–Hardy rule</li> </ul>	Bibeau and Matijević, 1973 <sup>119</sup>
<b>PVC latex</b>	d= 338 , 510 nm C <sub>0</sub> = 3 × 10 <sup>8</sup> particles/mL	NaNO <sub>3</sub> , Ca(NO <sub>3</sub> ) and La(NO <sub>3</sub> ) <sub>3</sub>	DLS	<ul style="list-style-type: none"> <li>• Qualitative but not quantitative agreement with DLVO theory</li> </ul>	Bleier and Matijević, 1976 <sup>120</sup>
<b>PS latex (carboxylate)</b>	d = 90 - 244 nm C <sub>0</sub> = 0.001- 0.005 wt %	NaCl, BaCl <sub>2</sub> , LaCl <sub>3</sub>	photoelectric colorimetry	<ul style="list-style-type: none"> <li>• Aggregation follows Schulze–Hardy rule</li> <li>• Stability increases with addition of surface carboxyl groups</li> </ul>	Sakota et al., 1977 <sup>121</sup>
<b>PS latex (casein coating)</b>	d = 348 ± 4 nm C <sub>0</sub> = 2.1 × 10 <sup>9</sup> particles/mL	100 – 1000 mM NaCl pH 7.3	DLS	<ul style="list-style-type: none"> <li>• Casein coating imparts stability</li> <li>• Stability increases with casein coverage</li> </ul>	Dickinson et al., 1983 <sup>122</sup>
<b>PS latex (sulfate)</b>	d = 297 ± 3 nm C <sub>0</sub> = 3 × 10 <sup>-4</sup> (solid volume fraction)	KCl, CaCl <sub>2</sub> and La(NO <sub>3</sub> ) <sub>3</sub>	spectrophotometry	<ul style="list-style-type: none"> <li>• Good agreement between theory and experiment for all electrolytes studied</li> <li>• Aggregation follows Schulze–Hardy rule</li> </ul>	Carrique et al., 1991 <sup>123</sup>
<b>PS latex (sulfate)</b>	d = 179 ± 12 nm C = 10 <sup>10</sup> particles/mL	KBr , MgSO <sub>4</sub> pH 3 - 9	spectrophotometry	<ul style="list-style-type: none"> <li>• Aggregation follows Schulze–Hardy rule</li> </ul>	Bastos and de las Nieves, 1993 <sup>114</sup>
<b>PS latex (sulfate)</b>	d= 156 nm C <sub>0</sub> = 7×10 <sup>7</sup> particles/mL	15 – 100 mM NaCl 1 mg/L organic matter pH 7.4	DLS	<ul style="list-style-type: none"> <li>• Coated NPs stable over 24 hours</li> <li>• NPs more stable with larger size fraction of humic acid</li> <li>• Steric interactions dominate stability</li> </ul>	Amirbahman and Olson , 1993 <sup>124</sup>
<b>PS latex</b>	d = 789 ± 3 nm C <sub>0</sub> = 3.5% m/m solids	250 mM NaCl + polyelectrolytes (HEC, SCMC, SPSS)	DLS	<ul style="list-style-type: none"> <li>• Polymer depletion led to NP aggregation</li> <li>• Stabilization by polyelectrolytes dependent on molecular size and osmotic pressure</li> </ul>	Smith and Williams, 1995 <sup>125</sup>
<b>PS latex (sulfate and amidine)</b>	d = 110, 120 nm	500 mM NaCl 20 mg/L humic acid and polysaccharides pH 7	DLS	<ul style="list-style-type: none"> <li>• Smaller humic acid fractions impart greater stability on smaller aggregates than polysaccharides. Impact is less significant for larger aggregates</li> <li>• Stability increases with adsorbed organic matter; positively charged particles adsorb more humic acid than the negatively charged counterpart</li> <li>• Stability of aggregates inversely proportional to aggregate size</li> </ul>	Walker and Bob, 2001 <sup>126</sup>
<b>Synthetic amphiphilic polyurethane (APU)</b>	d = 17- 97 nm C <sub>0</sub> = 1.5×10 <sup>4</sup> mg/L	0.2, 5 mM CaSO <sub>4</sub> 0.02% NaN <sub>3</sub>	DLS	<ul style="list-style-type: none"> <li>• Stability decreased with increasing ionic strength for all except particles with poly(ethylene glycol)-modified urethane acrylate precursor chains</li> </ul>	Tungittiplakorn et al., 2004 <sup>127</sup>

<b>PS latex (carboxylate and amphoteric)</b>	$d_{\text{TEM}} = 364 \pm 13, 320 \pm 15$ nm $C_0 = 110, 180$ mg/L	NaCl pH 5, 7, 9	Low-angle light-scattering	<ul style="list-style-type: none"> <li>• Surfactant-complexed particles more stable than bare particles</li> <li>• Electrostatic repulsion imparts stability</li> <li>• At low electrolyte concentrations, colloids remain stable after addition of surfactants</li> </ul>	Jódar-Reyes et al., 2006 <sup>128</sup>
<b>PS latex (sulfate and amidine)</b>	$d = 200, 270$ nm $C_0 = n. s.$	KCl + polyelectrolytes pH 4, 5.8	DLS	<ul style="list-style-type: none"> <li>• Both particles behave similarly in the presence of oppositely charged polyelectrolytes</li> <li>• In the presence of polyelectrolyte coatings, EDL forces responsible for stabilization</li> </ul>	Hierrezuelo et al., 2010 <sup>129</sup>
<b>PS latex (sulfate)</b>	$d = 115 \pm 7$ nm $C_0 = 1.3 \times 10^8, 1 \times 10^{10}$ particles/mL	0.1 – 1000 mM KCl, MgCl <sub>2</sub> , LaCl <sub>3</sub> pH 6- 7.5	DLS	<ul style="list-style-type: none"> <li>• Aggregation follows Schulze–Hardy rule</li> <li>• Multivalent counterion concentration determines counterion adsorption</li> <li>• DLVO theory assumption of constant charge is in agreement for monovalent salt.</li> </ul>	Schneider et al., 2011 <sup>115</sup>
<b>PS latex (carboxylate)</b>	$d = 30$ nm $C_0 = 100, 200, 300$ mg/L	sea water	DLS	<ul style="list-style-type: none"> <li>• NP destabilized shortly after being introduced to seawater (~1000 nm aggregates)</li> </ul>	Wegner et al., 2012 <sup>88</sup>
<b>PS latex (carboxylate)</b>	$d = 1000$ nm $C_0 = 80$ mg/L	KCl, MgCl <sub>2</sub> , LaCl <sub>3</sub> , ZrCl <sub>4</sub> pH 4	DLS	<ul style="list-style-type: none"> <li>• Aggregation follows Schulze–Hardy rule</li> </ul>	Ruiz-Cabello et al., 2013 <sup>116</sup>
<b>PS latex (carboxylate and amidine)</b>	$d = 40, 50$ nm $C_0 = 1 \times 10^4$ mg/L	natural seawater	DLS	<ul style="list-style-type: none"> <li>• Carboxylate modified NP formed large aggregates of ~1700 nm while amine modified ones was dispersed at ~90 nm</li> </ul>	Della Torre et al., 2014 <sup>130</sup>
<b>PS latex (carboxylate and sulfate)</b>	$d = 530, 1000$ nm $C_0 = 4.5$ mg/L	5 – 1000 mM NaCl, KCl, CsCl, MgCl <sub>2</sub> , CaCl <sub>2</sub> , LaCl <sub>3</sub> pH 4	DLS	<ul style="list-style-type: none"> <li>• Aggregation follows Schulze–Hardy rule</li> <li>• Aggregation highly dependent on valence of counter ion</li> <li>• Aggregation insensitive to ion type for the same valence</li> </ul>	Oncsik et al., 2014 <sup>117</sup>
<b>PS latex (sulfate and amidine)</b>	$d_{\text{TEM}} = 960, 980$ nm $C_0 = 50\text{--}200$ mg/L	10 - 200 mM NaCl 8 - 100 mM NaSCN 9 - 180 mM NaBr 10 - 500 mM KCl 10 - 500 mM CsCl pH 4	DLS	<ul style="list-style-type: none"> <li>• Both MPs behave similarly in all electrolytes</li> </ul>	Ruiz-Cabello et al., 2015 <sup>118</sup>
<b>PS latex</b>	$d = 70, 1050$ nm $C_0 = 50$ mg/L	natural fresh water	DLS	<ul style="list-style-type: none"> <li>• Heteroaggregation observed with kaolin or bentonite clays in natural freshwater</li> </ul>	Besseling et al., 2016 <sup>131</sup>
<b>PS latex (carboxylate)</b>	$d = 24 - 495$ nm $C_0 = 1.5 \times 10^8 - 1 \times 10^{12}$ particles/mL	500 mM NaCl 2000 mM CaCl <sub>2</sub> pH 7	DLS	<ul style="list-style-type: none"> <li>• Aggregation rate directly proportional to particle concentration</li> </ul>	Henry et al., 2016 <sup>132</sup>
<b>PS latex (sulfate and amidine)</b>	$d_{\text{TEM}} = 110, 265$ nm $C_0 = 2\text{--}10$ and $50\text{--}200$ mg/L; $0.3 - 2 \times 10^9$ particles/mL	NaCl, NaBr, NaSCN, NaN(CN) <sub>2</sub> pH 4	DLS TEM	<ul style="list-style-type: none"> <li>• Surface charge and aggregation rate both sensitive to the type of ion</li> <li>• Aggregation follows Schulze–Hardy rule</li> </ul>	Oncsik et al., 2016 <sup>133</sup>

Changes to the particles resulting from engineered functionalization or incidental coatings will also impact NP aggregation. Hierrezuelo et al.<sup>129</sup> show that a 270 nm sulfate-modified PS is more stable than a 200 nm amidine-modified PS under the same experimental conditions (open red squares and circles). Della Torre et al. observed that 40 nm carboxylated PS NPs rapidly formed aggregates of ~1700 nm in natural seawater, while 50 nm amino-modified PS NPs remained temporarily stable at ~90 nm, but moderately aggregated at longer times.<sup>130</sup> Sakota and Okaya demonstrated that increasing the extent to which PS particles are carboxylated increased stability, due to an increase in surface charge.<sup>121</sup> Similarly, the stability of sulfonated PS latex was observed to depend on surface charge density.<sup>114</sup> Thus, particle aggregation will not only depend on water chemistry but also on the particle surface functionalization.

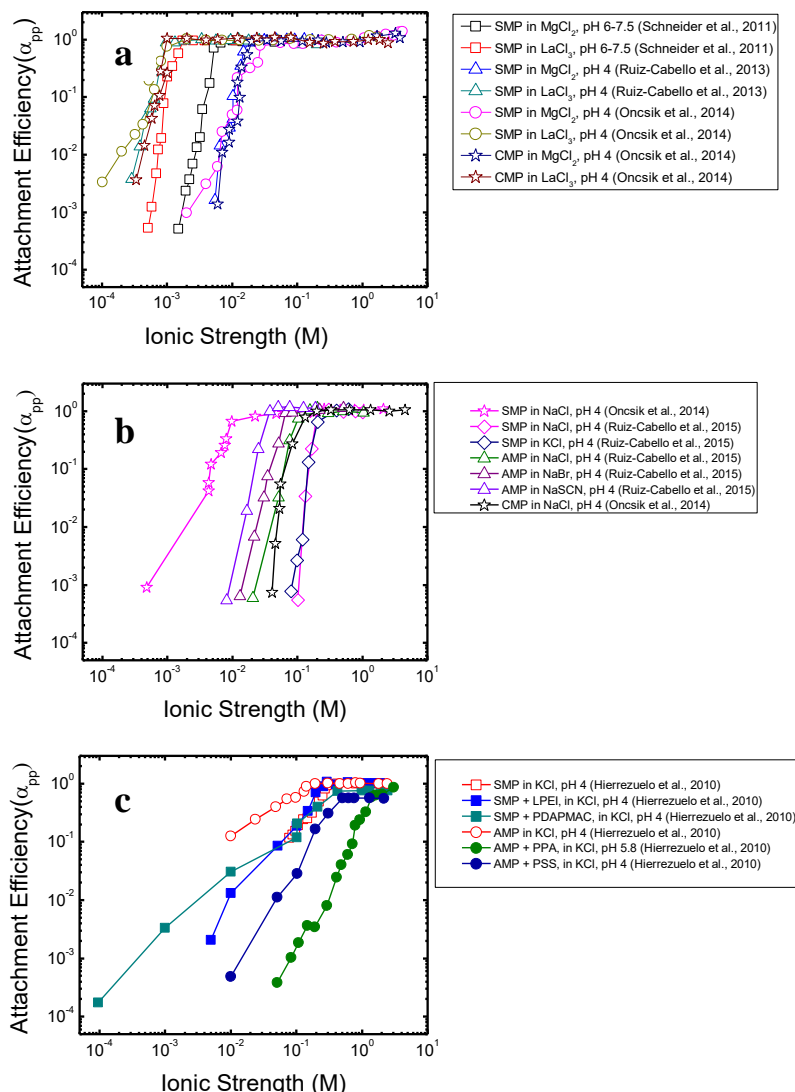


**Figure 2.2.** Aggregation stability curves of selected PS NPs and MPs in (a) multivalent salts (b) monovalent salts without coating and (c) monovalent salts with coatings from studies summarized in Table 2.1.<sup>116-118, 129</sup> Here,  $\alpha_{pp}$  = particle-particle attachment efficiency and SMP, CMP and AMP = sulfate-, carboxyl- and amidine-modified plastics, respectively. Solid symbols indicate addition of polyelectrolyte to the background solution.

Few studies have examined the effect of coatings on the stability of NPs and MPs. In Figure 2.2c, solid symbols represent coated NPs and MPs while open symbols represent uncoated particles. Although polymer coatings are generally observed to stabilize ENP suspensions due to steric or electrosteric stabilization,<sup>47</sup> their impact on NP and MP aggregation is not clear. For example, Hierrezuelo et al. report that 200 nm uncoated amidine-modified PS particles are less stable than those coated with either polyacrylic acid (PAA) or polystyrene sulfonate (PSS) polymers (Figure 2.2c, circles). However, they also show that a 270 nm linear polyethyleneimine

(LPEI)- and polydiallyldimethylammonium chloride (PDAPMAC)-coated sulfate-modified PS have a comparable stability to the bare particles (Figure 2.2c, squares).<sup>129</sup>

Natural organic matter (NOM), which is ubiquitous in natural waters, is expected to adsorb on the surface of plastic particles, as has been demonstrated for natural colloids and ENPs.<sup>134-139</sup> Studies on plastic aggregation in the presence of NOM are sparse,<sup>124, 126</sup> precluding generalizations of the impact of these diverse environmental molecules. Two studies<sup>124, 126</sup> show that PS NP aggregation is reduced in the presence of polysaccharides, humic and fulvic acids; however, additional research is needed to develop a more comprehensive understanding of the effects of these ubiquitous and heterogeneous environmental macromolecules on plastic stability.

The existing literature on the aggregation of spherical PS particles is generally in qualitative agreement with the DLVO theory of colloidal stability. Namely, the data in Figure 2.2 show that  $\alpha_{pp}$  increases with increasing solution IS until the mass transport-limited aggregation rate is reached (where  $\alpha_{pp}=1$ ). In all studies, spherical particles are used; however, since a large proportion of MPs and NPs in the environment is expected to have variable and non-spherical shapes, the aggregation behavior of different-shaped plastics warrants further investigation. Moreover, plastic debris in the environment is not restricted to PS. While the aggregation behavior of PVC latex and polyurethane (PU) particles have been observed to generally follow the DLVO theory and Schulze-Hardy rule,<sup>119, 120</sup> little attention has been paid to these materials. Thus, future research should take into account the diversity of plastics to better understand environmental fate and associated risks.

### **2.3.2 Laboratory studies investigating the deposition of nanoplastics and microplastics.**

Different experimental approaches have been used to investigate NP and MP deposition kinetics in systems representative of the unsaturated (vadose) and water saturated zones of the subsurface environment.<sup>111, 140</sup> Fully or partially water-saturated columns filled with well-characterized granular media (*e.g.*, glass beads, sand, or soil) are commonly used to study particle transport and deposition by monitoring changes in the column effluent particle concentration as a function of time.<sup>124, 140-171</sup> Alternatively, the quartz crystal microbalance with dissipation monitoring (QCM-D) has been used to characterize NPs deposition onto model aquifer grain surfaces.<sup>167</sup> Nearly all studies on the deposition of NPs or MPs have focused on spherical PS particles modified with sulfate, amine or carboxyl groups (Table 2.2). Figure 2.3 summarizes data from some of these

studies. As noted in the case of particle aggregation, the particle-collector attachment efficiency ( $\alpha_{pc}$ ) also increases with IS due to electrical double layer compression.

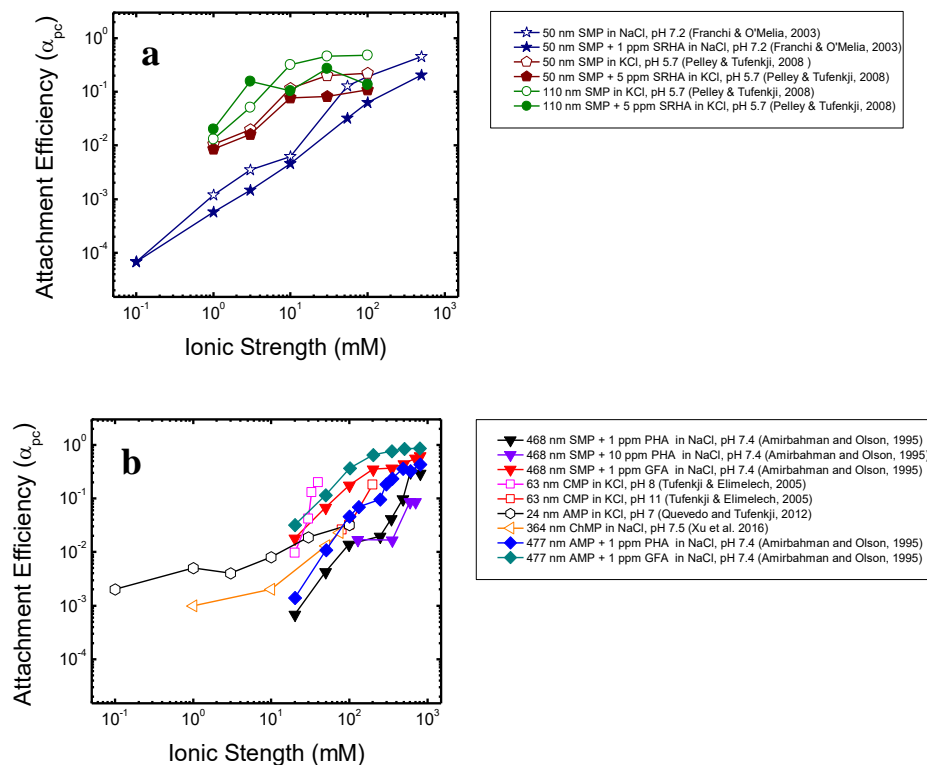


**Figure 2.1.** Deposition stability curves of PS NPs and MPs from studies in Table 2.2,<sup>141, 157, 160, 161, 164, 167</sup> (a) SMP with and without SRHA and (b) SMP, AMP, and CMP with and without various types of NOM. Here,  $\alpha_{pc}$  = particle-collector attachment efficiency and solid symbols indicate addition of NOM. PHA = peat humic acid, GFA = Georgetown fulvic acid, SRHA = Suwannee river humic acid and ChMP = chloromethyl-modified plastic.

**Table 2.2.** Laboratory studies investigating NP and MP deposition

Plastic type and surface functionality	Particle size and concentration	Deposition system	Collector surfaces	Solution chemistry	Main findings and conclusions	References
PS latex (sulfate)	d = 46,378,753 nm C <sub>0</sub> = 1 - 4 mg/L	packed column H:15, 20 cm, D:n.s.	glass beads d= 200,400 μm	3-300 mM KCl, CaCl <sub>2</sub> pH 6.7	<ul style="list-style-type: none"> <li>• Deposition rate increases with increasing IS until 0.1M KCl and 0.01M CaCl<sub>2</sub> (above which deposition rate decreases)</li> </ul>	Elimelech & O'Melia, 1990a <sup>155</sup>
PS latex (sulfate)	d= 46, 121,378,753 nm C <sub>0</sub> = 0.5 - 4 mg/L	packed column H: 20 cm, D:n.s.	glass beads d= 200,400 μm	3-300 mM KCl pH 6.7	<ul style="list-style-type: none"> <li>• Deposition rate increases with IS</li> <li>• Stability curve slope independent of particle size</li> </ul>	Elimelech & O'Melia, 1990b <sup>154</sup>
PS latex (sulfate)	d = 156 nm C <sub>0</sub> = 7×10 <sup>7</sup> particles/mL	packed column H:n.s, D:n.s	quartz sand d= 275 μm	15 – 100 mM NaCl 1 mg/L humic matter pH = 7.4	<ul style="list-style-type: none"> <li>•Steric repulsion responsible for stability at high ionic strengths</li> <li>•Peat humic acid imparts more stability than Georgetown fulvic acid</li> </ul>	Amirbahman and Olson, 1993 <sup>124</sup>
PS latex (sulfate and carboxylate)	d = 190, 220 nm C <sub>0</sub> = 5 × 10 <sup>7</sup> particles/mL	packed column H:30 cm, D:2.5 cm	unsaturated quartz sand d <sub>50</sub> =212 - 315 μm	1 mM NaNO <sub>3</sub> pH 7.0	<ul style="list-style-type: none"> <li>• Presence of air at collector surface increases retention</li> <li>• Retention greater for hydrophobic particles</li> </ul>	Wan and Wilson, 1994 <sup>156</sup>
PS latex (sulfate and amidine)	d = 468, 477 nm C <sub>0</sub> = 10 <sup>7</sup> particles/mL	packed column H:n/a	quartz sand d <sub>50</sub> =275 μm	20 - 800 mM NaCl pH 7.4 1, 10 mg/L Georgetown fulvic acid, peat humic acid	<ul style="list-style-type: none"> <li>• Negatively charged particles more stable than positively charged when coated due to greater magnitude of repulsive force</li> <li>• Larger molecular sized NOM shows less retention due to steric contribution</li> </ul>	Amirbahman and Olson, 1995 <sup>157</sup>
PS latex	d = 76, 301 nm C <sub>0</sub> = n/a	packed column H:15 cm, D:3.2 mm	glass beads 100, 200 μm quartz sand 74, 149 μm	0 - 1 mM KCl	<ul style="list-style-type: none"> <li>• At higher IS, particles deposited on porous media</li> </ul>	Sojitra, 1995 <sup>153</sup>
PS latex (sulfate and amidine)	d = 2500 nm C <sub>0</sub> = 2.3 × 10 <sup>9</sup> particles/mL	packed column H:10 cm, D:2.5 cm	Ottawa sand d <sub>50</sub> =580 μm	10 mM NaCl 0 - 20 mg/L Georgetown NOM, pH 5.4	<ul style="list-style-type: none"> <li>• Presence of NOM imparts stability due to contribution of steric and electrostatic repulsion</li> </ul>	Deshiikan et al., 1998 <sup>158</sup>
PS latex	d = 53 – 1960 nm C <sub>0</sub> = n.s.	packed column H:20 cm, D:10 cm	Munich gravel d= 250 μm Sengenthal sand d= 100 μm	Milli- Q water 1, 10 mM NaCl, CaCl <sub>2</sub> pH = n/a	<ul style="list-style-type: none"> <li>•Deposition in agreement with DVLO: particle transport increases with decreasing IS</li> <li>•Impact of counterion valence more apparent in sand gravel</li> </ul>	Huber et al., 2000 <sup>152</sup>
PS latex (fluorescent) (carboxylate)	d = 450, 1000, 2000, 3200 nm C <sub>0</sub> = n.s.	packed column H:15 cm, D: 4.8 cm H:10 cm, D: 5 cm	Ottawa sand d <sub>50</sub> = 150 – 710 μm glass beads d <sub>50</sub> = 260 μm	1 mM NaCl pH 7	<ul style="list-style-type: none"> <li>• Model included; particle and grain size influence retention due to straining</li> <li>• Retention increases with decreasing grain size and increasing colloid size</li> </ul>	Bradford et al., 2002 <sup>159</sup>

PS latex (sulfate)	d = 98 nm C <sub>0</sub> = 1 mg/L	packed column H: 250 cm, D: 2.5 cm	glass beads d= 200 μm	0-500 mM NaCl 0,1 mg/L SRHA 13-960 mM KCl, CaCl <sub>2</sub> pH 6.7, 7.2	<ul style="list-style-type: none"> <li>• Deposition increases with IS; particle depositing at lower IS more prone to reentrainment</li> <li>• Deposition decreases with SRHA (except at low IS)</li> </ul>	Franchi and O'Melia, 2003 <sup>160</sup>
PS latex (sulfate)	d = 308 nm C <sub>0</sub> = 1 mg/L	packed column H:20 cm, D:2.5 cm	glass beads d= 200, 400 μm	10 - 100 mM KCl 200 mM CaCl <sub>2</sub> pH 5, 6.7-6.8	<ul style="list-style-type: none"> <li>• Latex particle exhibit little affinity for glass beads</li> </ul>	Hahn et al., 2004 <sup>151</sup>
PS latex (carboxylate)	d = 63, 320, 3000 nm C <sub>0</sub> = 1 × 10 <sup>7</sup> - 3.6 × 10 <sup>9</sup> particles/mL	packed column H: 12.6 cm, D:1.6 cm	glass beads d <sub>50</sub> = 330 μm	3 - 300 mM KCl 0.06 mM SDS pH 8, 11	<ul style="list-style-type: none"> <li>• Retention increases with IS</li> <li>• Deviations from colloid filtration theory investigated</li> </ul>	Tufenkji and Elimelech, 2005 <sup>161</sup>
PS latex (sulfate)	d =20 - 420 nm C <sub>0</sub> = 100 mg/L	packed column H:10 cm, D:4.5 cm	quartz sand d= 300 - 355 μm	1 mM (NaCl + NaHCO <sub>3</sub> ) pH 7.5	<ul style="list-style-type: none"> <li>• Particle retention lower in saturated flow conditions</li> <li>• Deposition decreases reaching a minimum then increases as plastic size increases to MP</li> </ul>	Zhuang et al., 2005 <sup>162</sup>
PS latex (carboxylate)	d = 1000, 3200 nm C <sub>0</sub> = 0.25,0.5,1,2 × C <sub>T</sub> C <sub>T</sub> = 3.68 × 10 <sup>7</sup> , 1.18 × 10 <sup>6</sup> particles/mL	packed column H:15 cm, D: 4.8 cm H:10 cm, D: 5 cm	Ottawa quartz sand d= 150, 240, 360 μm	1 mM NaCl pH 7	<ul style="list-style-type: none"> <li>• Retention increase with increasing MPs size and decreasing sand size</li> <li>• Less deposition with increase in C<sub>0</sub></li> </ul>	Bradford and Bettahar, 2006 <sup>150</sup>
PS latex (carboxylate and amidine)	d = 100 - 2000 nm C <sub>0</sub> = 1 × 10 <sup>6</sup> , 1 × 10 <sup>7</sup> particles/mL	packed column H:20 cm, D:3.8 cm	glass beads and quartz sand 417 – 600 μm	1 – 50 mM NaCl pH 2, 6.7	<ul style="list-style-type: none"> <li>• Particle retention increases with increasing velocity</li> </ul>	Tong and Johnson, 2006 <sup>172</sup>
PS latex (sulfate)	d = 30, 66, 1156, 3000 nm C <sub>0</sub> = 10, 40 mg/L	packed column H:10 cm, D:3.8 cm	glass beads (3 fraction sizes) d= 88 - 125 μm d=180 - 250 μm d= 590 - 840 μm	DI water 200 mM NaCl pH 10	<ul style="list-style-type: none"> <li>• Using DI water, 0% particle deposition observed except for 3 μm PS</li> <li>• High IS imparts a lower critical straining ratio</li> </ul>	Shen et al., 2008 <sup>149</sup>
PS latex (carboxylate)	d = 1100 nm C <sub>0</sub> = 2.5 - 2.8 × 10 <sup>7</sup> particles/mL	packed column H:10 cm, D:5 cm	unsaturated Ottawa sand d <sub>50</sub> =240, 360 μm	6, 30 and 60 mM KCl pH 10	<ul style="list-style-type: none"> <li>• Retention decrease with level of saturation</li> </ul>	Torkzaban et al., 2008 <sup>140</sup>
PS latex (sulfate)	d = 2000 nm C <sub>0</sub> = 7.5 mg/L	packed column H:6.7 cm, D:1.8 cm	Zirconia beads d <sub>50</sub> = 326 μm	0.1 - 100 mM KCl pH 3 - 11	<ul style="list-style-type: none"> <li>• Retention increases with IS</li> <li>• pH effects on transport not significant</li> </ul>	Kobayashi et al., 2008 <sup>163</sup>

PS latex (sulfate)	d = 50, 110, 1500 nm C <sub>0</sub> = 1.2 × 10 <sup>11</sup> , 1.2 × 10 <sup>10</sup> , 8.6 × 10 <sup>6</sup> particles/mL	packed column H: 15 - 16.5 cm, D:1cm	quartz sand d <sub>50</sub> = 256 μm	1 – 100 mM KCl 0, 5 mg/L SRHA pH 5.7	<ul style="list-style-type: none"> <li>• Deposition increases with IS</li> <li>• Addition of SRHA generally decreases deposition due to steric contribution</li> </ul>	Pelley and Tufenkji, 2008 <sup>164</sup>
PS latex (carboxylate)	d = 20, 200, 1000 nm C <sub>0</sub> = n.s.	packed column H:20 cm, D:5.4 cm	Dune sand d <sub>50</sub> = 310 - 320 μm	3-4 mM artificial rainwater pH 7.8	<ul style="list-style-type: none"> <li>• Particle transport: acid washed sand &gt; distilled water washed &gt; natural sand</li> </ul>	Shani et al., 2008 <sup>165</sup>
PS latex	d = 980 nm C <sub>0</sub> = n/a	packed column H:30 cm, D:2.05 cm	unsaturated and saturated sand d <sub>50</sub> = 250 μm	2 - 50 mM NaNO <sub>3</sub> pH 7	<ul style="list-style-type: none"> <li>•Saturated flow: decreasing solution surface tension and IS, decreases deposition</li> <li>•Unsaturated flow: deposition decreases exponentially with travel distance.</li> </ul>	Zhuang et al., 2010 <sup>148</sup>
PS latex (carboxylate)	d = 40, 500 nm C <sub>0</sub> = 7.8 × 10 <sup>11</sup> / 1.2 × 10 <sup>8</sup> particles/mL	packed column H:30 cm, D:1cm	saturated quartz sand d = 270μm	0.05 – 100 mM NaCl pH 6.7, 9.6	<ul style="list-style-type: none"> <li>•Deposition is IS dependent, and increases with increasing IS</li> </ul>	Qing, 2011 <sup>173</sup>
PS latex (carboxylate)	d = 1000 nm C <sub>0</sub> = 3.64 × 10 <sup>7</sup> particles/mL	packed column H:7 cm, D:1.4 cm H:30 cm, D:5.5 cm	natural quartz sand d = 800 μm	Dead sea water 8.5 M	<ul style="list-style-type: none"> <li>•Particle deposition accelerates at high IS</li> </ul>	Magal et al., 2011 <sup>147</sup>
PS latex (sulfate and carboxylate)	d = 20, 1000 nm C <sub>0</sub> = 8 × 10 <sup>11</sup> , 10 <sup>7</sup> particles/mL	packed column H:8cm, D:1.6 cm	clean and biofilm coated quartz sand ( <i>Pseudomonas aeruginosa</i> biofilm) d <sub>50</sub> = 763 μm	10 mM KCl pH 7.2	<ul style="list-style-type: none"> <li>• Retention increased in biofilm coated sand vs. clean sand</li> <li>• Higher retention with sulfate functionalized particles than carboxylate</li> </ul>	Tripathi et al., 2011 <sup>166</sup>
PS latex (sulfonated)	d = 800 nm C <sub>0</sub> = n.s.	n.s.	hematite covered mica monolayer	IS = 0.1- 10 mM pH 3.5	<ul style="list-style-type: none"> <li>• Deposition deviates from the mean-field DLVO theory but agrees with DLVO theory at low IS</li> </ul>	Nattich-Rak et al., 2012 <sup>146</sup>
PS latex (carboxylate)	d= 24 nm C <sub>0</sub> = 10 <sup>12</sup> particles/mL	packed column H :10 cm, D:1cm	loamy and quartz sand d = 225 μm, loamy d = 256 μm, quartz	0.1 -100 mM KCl 0.1 -10 mM CaCl <sub>2</sub> pH 7	<ul style="list-style-type: none"> <li>• Retention increases with IS</li> <li>• Higher deposition with divalent electrolyte vs. monovalent in quartz sand</li> <li>• Retention greater in loamy than quartz sand</li> </ul>	Quevedo and Tufenkji, 2012 <sup>167</sup>
PS latex (carboxylate)	d = 100, 1050 nm C <sub>0</sub> = 10.5 mg/L	chamber bed L×W×H: 20×10×10 cm	glass rod d = 5000 μm	1- 100 mM KCl pH 7	<ul style="list-style-type: none"> <li>• Retention decreases with increasing flow velocity and increases with increasing IS</li> </ul>	Wu et al., 2012 <sup>168</sup>
PS latex	d = 60 nm C <sub>0</sub> = 50 mg/L	deep well plate columns H:3.4 cm	Iota quartz sand and Calls Creek sediment d = 200, 361 μm	0.001–0.1% sodium dodecyl sulfate (SDS)	<ul style="list-style-type: none"> <li>•Greater deposition in the sediment than in Iota quartz sand.</li> </ul>	Bouchard et al., 2013 <sup>145</sup>
PS latex (carboxylate)	d = 75, 300 and 2100 nm C <sub>0</sub> = 4.31 × 10 <sup>10</sup> and 1.35 × 10 <sup>8</sup> particles/mL	packed column H:15.2 cm, D:2.61 cm	fine and medium quartz sand d <sub>50</sub> = 181, 513 μm	0.1 - 1000 mM NaCl 83-95% saturation	<ul style="list-style-type: none"> <li>• Less attachment onto fine than medium quartz sand</li> <li>• Deposition slighter higher with large particles</li> </ul>	Mitropoulou et al., 2013 <sup>144</sup>

PS latex (carboxylate)	d = 100, 500, 2000 nm $C_0 = 1.1 \times 10^6, 7.3 \times 10^7, 2.3 \times 10^{10}$ particles/mL	packed column H:11 cm, D:2 cm	quartz sand $d_{50} = 250 \mu\text{m}$	0 - 800 mM NaCl, pH 5.6 - 5.8	<ul style="list-style-type: none"> <li>• Deposition behavior in column experiments not consistent with batch experiments</li> </ul>	Treumann et al., 2014 <sup>169</sup>
PS latex (carboxylate)	d= 300 nm $C_0 = 5.8 \times 10^7$ particles/mL	physical micromodel	polydimethylsiloxane (PDMS)	DI water IS = 0.0012 mM pH 7.0	<ul style="list-style-type: none"> <li>• Retention decreases with flow velocity</li> </ul>	Zhang et al., 2015 <sup>170</sup>
PS latex (sulfate and carboxylate)	d = 20 nm $C_0 = 20 \text{ mg/L}$ ( $\sim 2.62 \times 10^{12}$ particles/mL)	packed column H:8.1 cm, D:1.6 cm	clean and biofilm coated quartz sand ( <i>Pseudomonas aeruginosa</i> biofilm) $d_c = 760 \mu\text{m}$	1 - 100 mM NaCl 1 - 100 mM $\text{CaCl}_2$ pH 7.0	<ul style="list-style-type: none"> <li>• At lower IS, high retention observed in biofilm coated than clean sand</li> <li>• Both functionalized particles behaved comparably</li> </ul>	Mitzel et al., 2016 <sup>171</sup>
PS latex	d = 240 nm $C_0 = 25 \text{ mg/L}$	packed column H:25 cm, D:2.5 cm	fine and medium unsaturated and saturated sand $d_{50} = 140, 323 \mu\text{m}$	0.4 mM NaCl pH 6.7	<ul style="list-style-type: none"> <li>• Deposition in unsaturated media greater than saturated media</li> </ul>	Hoggan, 2016 <sup>143</sup>
PS latex (carboxylate)	d = 1156 nm $C_0 = 10 \text{ mg/L}$	packed column H:10 cm, D:3.8 cm	quartz sand 300 - 355 $\mu\text{m}$	0.0001 - 0.2 M NaCl pH 10	<ul style="list-style-type: none"> <li>• Detachment of particles from the primary energy well can be achieved by Brownian diffusion.</li> </ul>	Wang et al., 2016 <sup>142</sup>
PS latex (chloromethyl)	d = 364 nm $C_0 = 5, 100 \text{ mg/L}$	packed column H:200 cm, D:2.6 cm	unsaturated quartz sand 300–350 $\mu\text{m}$	1 - 75 mM NaCl pH 7.5	<ul style="list-style-type: none"> <li>• Increase in electrostatic repulsion leads to decreasing particle deposition</li> <li>• Effect of saturation on deposition more important at high IS</li> </ul>	Xu et al., 2016 <sup>141</sup>

The porewater flowrate in subsurface environments has been shown to affect the transport of NPs and MPs.<sup>168, 170</sup> Generally, decreased plastic deposition is observed at high porewater velocities, in agreement with studies involving other types of colloids (*e.g.* titanium dioxide, fullerenes).<sup>48, 170, 172, 174</sup> Tong and Johnson observed a decrease in retention of PS MPs in columns packed with quartz sand as flow velocity increased.<sup>172</sup> This behavior was observed by others when the plastic particle and collector have the same charge (unfavorable condition).<sup>175, 176</sup>

The type of granular media will play a large role in determining the fate of NPs and MPs in the environment. Despite this, most studies have used clean glass beads and high purity quartz sand that poorly represent natural environments. Researchers that investigated the behavior of plastic particles in realistic media other than quartz sand and glass beads suggest that retention is much higher under ‘dirty’ conditions. Bouchard et al. showed that PS MP retention was greater in sediments from a creek in Georgia, USA than in pure Iota quartz sand.<sup>145</sup> The observed retention was attributed to the high aluminum hydroxide content and rougher surface of the sediment that can provide positive charge and localized sites for deposition, respectively. Additionally, using comparable media grain sizes, Quevedo and Tufenkji showed that PS NP retention was greater in an agricultural loamy sand than high purity quartz sand.<sup>167</sup> These studies suggest that retention is higher in more heterogeneous granular media, although further investigations using environmentally relevant granular materials are needed to establish a comprehensive understanding of the effect of geochemistry and grain size distribution on the transport of NPs and MPs.

Microorganisms and biofilms are ubiquitous in natural aquatic environments; yet, their impact on the mobility of NPs and MPs has not been well studied. Tripathi et al observed that PS NPs and MPs with different surface functionalities (carboxylate and sulfate) exhibit increased retention in columns packed with quartz sand coated with *Pseudomonas aeruginosa* biofilm.<sup>166</sup> Mitzel et al also reported higher retention of sulfate and carboxylate functionalized PS NPs when sand is coated with *Pseudomonas aeruginosa* biofilm. This trend is observed in the presence of other types of biofilms (*e.g.*, *Pseudomonas fluorescens*, *Stenotrophomonas maltophilia*, *Lactococcus lactis* etc.).<sup>177, 178</sup> The hydrophobicity of biofilm-coated sand can also influence the transport behavior of PS. For example, Mitzel et al observed dynamic NP transport behavior in sand coated with a hydrophilic biofilm, whereas NP transport was constant with time in the sand coated with a more hydrophobic biofilm.<sup>171</sup>

Few studies have examined the impact of NOM such as fulvic and humic acids on the transport and deposition of NPs and MPs in model subsurface environments.<sup>158, 160, 164</sup> Particles coated with NOM (Figure 2.3a, solid symbols) were generally observed to have lower attachment efficiencies than uncoated particles (open symbols) with few exceptions. Franchi and O'Melia showed that negatively charged sulfate functionalized PS particles coated with Suwannee River humic acid exhibit reduced retention (except at IS below 10 mM NaCl) in columns packed with glass beads (Figure 2.3a, star symbol). This was one of the first studies to report on the role of the secondary energy minimum in the reversible attachment of NPs or MPs.<sup>160</sup> In examining the effect of varying NOM concentrations, Amirbahman and Olson observed little difference in stability of negatively charged PS MPs when the concentration of peat humic acid increased from 1 to 10 ppm (Figure 2.3b, black and purple solid downward triangle).<sup>157</sup> Deshiikan et al looked at the effect of increasing Georgetown NOM concentration on two PS MPs. The stability of the positively charged PS MPs increased significantly as NOM concentration increased from 5 to 20 ppm. This was associated with a reversal of MP surface charge from positive to negative. However, no substantial difference in stability was observed for the negatively charged particles in the presence versus absence of NOM, a result attributed to less NOM having sorbed to the negatively-charged particles.<sup>158</sup> As humic substances are commonly negatively charged at environmentally relevant pH, adsorption of NOM onto positively charged MPs will reduce the magnitude of the surface charge.<sup>48</sup> The type of NOM sorbed to the surface also influences particle stability. In comparing adsorption of two NOMs having differing average molecular sizes (Georgetown fulvic and peat humic acid, both at 1 ppm) onto positively and negatively charged PS MPs, particles coated with the lower molecular-sized Georgetown fulvic acid were more likely to deposit onto quartz sand (Figure 2.3b, solid diamonds), despite similar electrophoretic mobilities.<sup>157</sup> This was attributed to the reduced steric-stabilizing effect of the smaller organic molecule.

A significant fraction of NPs and MPs is expected to enter groundwater via the unsaturated (vadose) zone, where particle mobility is often reduced compared to water saturated environments due to the role of the air-water interface and film straining.<sup>140, 143, 156, 162</sup> For example, Wan and Wilson attributed increased retention of PS MPs in sand-packed columns with increasing gas content to the air-water interface;<sup>156</sup> however, Torkzaban et al. suggest that for similarly charged surfaces, straining is the predominant retention mechanism.<sup>140</sup> Colloid hydrophobicity also plays an increased role in particle retention in the vadose zone, resulting in greater partitioning to the

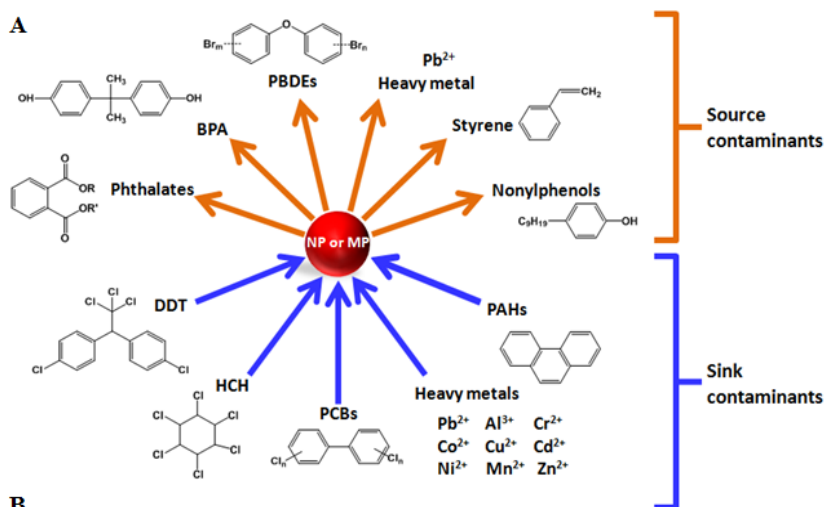
air-water interface.<sup>156</sup> Thus, the transport of hydrophobic plastics is expected to be significantly mitigated when moving through the vadose zone.

A review of the existing literature (Table 2.2) shows that few studies have examined the transport and deposition behavior of NPs and MPs in environmentally relevant systems. The subsurface environment is heterogeneous and complex, and laboratory studies using pristine granular media are likely to underestimate NP and MP deposition. As is also the case for plastic aggregation, most of the studies on plastic deposition were performed using spherical primary plastics that are less likely to be encountered in the environment. The transport behavior of more environmentally relevant secondary plastics comprised of fragments, films, rods, etc. requires investigation. Furthermore, studies have largely been limited to PS; thus, there is a need for additional research to understand the impacts of factors such as water chemistry, microbial biofilms, and soil type on the mobility of different plastics.

## **2.4 Plastics may act as vectors for other contaminants**

### **2.4.1 Plastics as contaminant source and sink**

NPs and MPs can serve as both sources and sinks for contaminants in the environment (Figure 2.4a). Chemical byproducts, monomers, and additives (*e.g.*, bisphenol A, triclosan, bisphenone, flame retardants, phthalates, organotins) are added during the manufacturing of plastics. Several of these additives, that may leach from the plastic into the environment,<sup>179</sup> are of significant concern (endocrine disrupting, carcinogenic and/or mutagenic).<sup>180</sup> On the other hand, plastics can also sorb inorganic and organic contaminants,<sup>20, 58, 59, 63, 181</sup> as MPs in the aquatic environment were found to be contaminated with POPs and heavy metals. For example, MPs were reported to exhibit concentrations of POPs up to six orders of magnitude greater than the background concentration in the surrounding seawater.<sup>62, 182-184</sup> These interactions with contaminants are increasingly being studied to better understand the risks associated with plastics in the environment.<sup>18, 57, 62, 64, 182, 185</sup> Furthermore, the bioavailability of these sorbed contaminants to aquatic organisms may be considerable, with significant rates of desorption for DDT and phenanthrene observed across a range of salinities.<sup>60</sup>



Plastic type	Average ranking										Glass transition temperature * T <sub>g</sub> (°C)				
	Wu et al., 2001	Muller et al., 2001	Mato et al., 2001	Pascall et al., 2002	Teuten et al., 2005	Fries and Klontza, 2007	Rochman et al., 2008	Huffer et al., 2012	Wang et al., 2013(a)	Wang et al., 2014	Wang and Hofman, 2015	Wang and Wang, 2016	Average ranking	T <sub>g</sub> (°C)	
PE				1	1	1	1			2	1	3	1	1.4	-125
HDPE	2	1						2	1					1.5	-90
LDPE		2						1	2					1.7	-110
PS					2					1	3	1	2	1.8	95-100
POM							2							2.0	-30
PP				2		2	3			3	3			2.6	0
PVC	1				3	3			5		2	2	3	2.7	87
PA												4		4.0	47
PET									4					4.0	69

**Figure 2.4.** (a) Contaminants that have been found to associate with plastic debris in the environment.<sup>17, 57, 59, 62, 186-189</sup> Schematic adapted from<sup>185</sup> (b) Relative ranking of sorption capacity as a function of plastic type. In a given study, a score of 1 indicates the highest sorption capacity and increasing values indicate plastics that exhibit lower sorption capacities. HDPE = high-density polyethylene; LDPE = low-density polyethylene; POM = polyoxymethylene; PA = polyamide; PET = polyethylene terephthalate. \*Glass transition temperature from<sup>190</sup>.

Table S2.2 summarizes existing studies on the sorption of contaminants on plastics, many of which have focused on micrometer and millimeter-sized particles. Sorption of contaminants onto plastic debris depends on several factors such as the physicochemical properties of the polymer, solution chemistry of the immediate environment, the degree of weathering, and temperature.<sup>18, 61, 62, 65, 183-185, 191</sup>

When plastics are released into the environment, several environmental factors will lead to fouling and weathering.<sup>61, 191</sup> Degradation and breakup of pristine plastics can increase the exposed

surface area, resulting in increased sorption capacity. For example, Napper et al. investigated PE microbeads extracted from personal care products and found that rough MPs adsorbed more DDT and phenanthrene than smooth ones.<sup>64</sup> Similar trends were observed with heavy metal contaminants; aged PE pellets adsorbed more cationic metals than pristine pellets.<sup>59</sup> Brennecke et al. observed that higher levels of  $Zn^{2+}$  and  $Cu^{2+}$  sorbed onto aged PVC compared with pristine PS particles, despite the fact that PS generally shows a greater sorption capacity than PVC (Figure 2.4b).<sup>57</sup> On the other hand, weathering via photodegradation oxidizes plastics (adding *e.g.* carbonyl groups) and increases their polarity which can decrease their sorption capacity. Fouling, sometimes indicated by discoloration, is also expected to affect the adsorption of contaminants onto plastics. Discolored plastic particles have been shown to adsorb more PCBs than non-discolored ones.<sup>61</sup>

Increasing temperatures will generally reduce the “glassiness” of a polymer, increasing its affinity for contaminants; however, increasing the temperature of the aqueous phase also leads to increased solubility of organic and inorganic contaminants.<sup>192</sup> Crawford and Quinn observed greater affinities for PE MP with 33 different PAHs at 21 °C versus 10 °C.<sup>18</sup> Hu et al. also reported an increase in sorption with temperature of lubricating oil on PE NP and PS MP.<sup>65</sup> In contrast, Zhan et al. showed that sorption of PCBs onto PP decreased as temperature increased from 19 to 27 °C.<sup>193</sup> These conflicting data highlight the difficulty in predicting changes in contaminant sorption, because temperature will impact both the properties of the plastic and the contaminant.

The salinity of the surrounding aqueous environment can also influence the sorption behavior of plastics by affecting the water solubility of organic compounds. Generally, an increase in salinity decreases the solubility of non-polar and weakly polar organic contaminants in water,<sup>192</sup> known as the *salting-out effect*. Hence, high salt levels can increase the availability of certain hydrophobic contaminants for adsorption onto plastics. Indeed, the adsorption of phenanthrene on PP MPs increased with salinity.<sup>194</sup> Hu et al reported that lubricating oil adsorbed more to PE NPs and PS MPs when salinity increased. This was attributed to the salts promoting outer-sphere surface complexation between the particles and the oil.<sup>65</sup> Increased salinity levels also resulted in greater sorption capacities of PCBs onto PE and PS.<sup>195</sup> However, this trend does not appear to be universal for plastics. As salinity increased from freshwater to seawater, sorption of heavy metals by PE was observed to decrease considerably, with the exceptions of  $Cu^{2+}$  and  $Cr^{2+}$ .<sup>196</sup> Decreased sorption of DDT onto either PVC or PE was noted when salinity increased from river to seawater

(no effect was noted on the sorption of phenanthrene).<sup>60</sup> Given the limited studies and contradictory reports, the effects of salinity on the sorption of inorganic and organic contaminants onto plastic merit further investigations.

Beyond environmental factors influencing sorption, the type of plastic also plays an important role. Figure 2.4b provides an integrated comparison of polymer sorption capacities to determine the expected relative contaminant association as a function of plastic type. For each study, the sorption capacity of different plastics was ranked by assigning a score of 1 to those that exhibited the highest sorption capacity and increasing values for plastics that exhibited lower sorption capacities. The average ranking for each type of plastic across the different studies was then calculated and reported alongside their glass transition temperatures ( $T_g$ ). In general, rubbery polymers such as PE and PP are expected to allow greater diffusion of contaminants into the polymer than glassy polymers such as PET and PVC.<sup>17</sup> At room temperature, rubbery polymers exist above their  $T_g$  which results in greater flexibility and facilitates contaminant sorption.<sup>17</sup> Indeed, the rubbery polymer PE commonly shows a greater affinity for contaminants than other types of plastics (i.e., in Figure 2.4b, PE most often receives a score of 1).<sup>4, 17, 20, 191, 197</sup> Conversely, PET and PVC generally exhibit lower sorption capacities (i.e., they receive higher scores of 4 or 5).<sup>20, 63</sup> However, this generalization does not hold for all types of contaminants (Figure 2.4b). For instance, PS appears to be an exception to the rule, whereby its average sorption capacity ranking is greater than would be predicted by its  $T_g$ . Five studies have compared the sorption of contaminants by PS and other plastics, and twice it ranked highest despite PS being a glassy polymer at room temperature.<sup>190</sup> A possible explanation for this is the presence of benzene in the PS monomer rather than, for example, hydrogen in PE (Figure S2.1). This benzene ring increases the distance between the polymer chains and can facilitate contaminant attachment and integration into the polymer.<sup>17</sup> Other exceptions to the general trend include the accumulation of less metal by high density PE than low density PE, PET, PVC and PP,<sup>58</sup> and sorption of more alkylbenzenes by PVC than PE.<sup>198</sup> Thus, whereas general sorption trends appear to be well correlated to  $T_g$ , these latter observations are likely related to the chemistries of a specific contaminant and plastic.

Contaminants are unlikely to exist in isolation in the environment; however, studies investigating the potential for competitive sorption onto plastics are nearly nonexistent. Competitive sorption between phenanthrene and DDT was demonstrated for PE and PVC, which sorbed more DDT than phenanthrene.<sup>64, 199</sup> The observed trend for DDT could be due to several

factors, including its greater hydrophobicity. There is a need to investigate the sorption capacity of plastics in environmentally relevant heterogeneous systems to further understand the mechanisms by which plastics preferentially interact with different organic and inorganic contaminants.

Figure 2.4a and Table S2.2 show that several investigations have focused on the association of plastic particles with persistent, bio-accumulative, and toxic compounds (*e.g.*, metals, PAHs, PCBs and DDT).<sup>60, 61, 64, 182, 195</sup> Pharmaceuticals and other endocrine-disrupting compounds which are contaminants of emerging concern are less studied in this context. Wu et al investigated the effect of salinity and presence of NOM on the sorption capacity of four pharmaceutical contaminants onto PE MPs.<sup>200</sup> They reported that sorption to PE MPs depends on contaminant hydrophobicity and that the presence of NOM decreased the affinity of all but one contaminant (carbamazepine).<sup>200</sup> Since the interaction of plastics with POPs can differ from pharmaceutical contaminants (some of which can be ionic), there is need for more research to understand the mechanisms by which pharmaceutical contaminants and NOM interact with plastic particles in aquatic environments.

#### **2.4.2 Nanoplastics and microplastics can facilitate the transport of contaminants**

The mobility of organic and inorganic contaminants can be enhanced by association with colloids in soils, surface waters, and groundwaters.<sup>52, 201, 202</sup> Natural colloids (*e.g.* iron oxides and clays) have been reported to increase the transport of metals such as copper, zinc, lead, cadmium, arsenic and nickel up to 50 times the rates observed in non-colloid associated tests.<sup>51, 53, 54, 203-207</sup> Colloids have also demonstrated the potential for promoting the transport of organic pollutants, such as prochloraz, glyphosate, and atrazine.<sup>208-210</sup> The movement of colloids can be faster than that of the porewater due to the size exclusion effect, in which colloids are excluded from small pores.<sup>211</sup>

Studies on the facilitated transport of contaminants by plastics (PS and polyurethane, PU) in model or natural subsurface systems are sparse,<sup>127, 212</sup> though they are in general agreement with the literature on natural colloids. PU used within a remediation paradigm improved the removal of phenanthrene from soil by facilitating the contaminant's mobility in porous media and increasing the bioavailability to microbial populations that can degrade the contaminant.<sup>127, 212</sup> Jaradat et al. showed that phenanthrene in leaf compost had a greater affinity for sulfate- and carboxylate-modified PS MPs than the compost materials.<sup>213</sup> Laboratory-scale columns packed with leaf compost media revealed that phenanthrene levels in the column effluent were significantly higher

in the presence of more hydrophobic sulfidated PS MPs than carboxylated PS. The potential for 76 and 301 nm sulfate-modified PS plastics to facilitate the transport of pyrene and phenanthrene has also been investigated in columns packed with glass beads or quartz sand.<sup>153</sup> At low IS, both pyrene and phenanthrene showed an earlier breakthrough in the presence of PS particles compared to that without particles. In contrast, at high IS, increased retention of PS particles in the granular medium resulted in increased retardation of contaminant compared to experiments with no particles. This suggests that the ability of plastics to facilitate the transport of contaminants is linked with the stability of the plastic itself. In their study with PS MPs, Roy and Dzombak identified slow desorption of contaminants from particles as an important prerequisite for significant colloid-facilitated transport.<sup>53</sup> Taken together, these studies show that MPs and NPs have the potential to facilitate the transport of contaminants but a great deal more research is needed to understand the scope of this problem.

## **2.5 Regulatory policy**

The increasing evidence of MP's potential for harm - either directly or indirectly, has led to numerous calls for regulations and bans on MP use in consumer products and release into the environment.<sup>28, 34, 89, 214-217</sup> In the U.S., most plastics are grandfathered into the Toxic Substances Control Act of 1977 and therefore are considered safe until proven otherwise.<sup>218</sup> MPs are considered non-hazardous solid waste from a regulatory standpoint, and governmental agencies have been hesitant to include MPs in water quality regulations such as turbidity or particulate matter, which would largely impact WWTPs.<sup>89, 214, 218</sup> In Austria, limits on plastic discharge into freshwater rivers and streams do exist, although the limit, at 30 mg L<sup>-1</sup> day<sup>-1</sup>, is so high as to be ineffective.<sup>34</sup> The European Marine Strategy Framework Directive, which requires member states to establish strategies for maintaining marine waters, includes MPs as marine litter but does not specify how countries should keep MPs from reaching their coastal waters (*e.g.*, improvements to WWTPs or MP bans).<sup>216</sup>

Amidst this backdrop, several governmental organizations have enacted legislation, primarily focused on MPs in single use cosmetics, to specifically ban microbeads or MPs. In 1999, the Canadian government classified microbeads as a toxin, which was coupled with the intent to prohibit importation, manufacture, or sale of some microbeads. Similar to other legislation however, this ban primarily covers personal care products and does not include abrasives, cleaning products, and other household uses. Nine US states have enacted legislation banning the use of

microbeads, with Illinois the first to do so in 2014.<sup>217</sup> These acts primarily ban either the manufacture or sale of personal care products containing microbeads, though significant loopholes exist. For example, California law does not apply to products containing less than 1 ppm plastic by weight.<sup>217</sup> Furthermore, the US government passed the Microbead Free Waters Act (MFWA) in 2015, which amends the Food Drug and Cosmetic Act to ban the sale or distribution of MBs under a tiered timeline. The primary shortcoming of regulations that exist is that the scope is narrow and sufficient loopholes exist such that microbeads/MPs continue to be introduced into the environment. The characterization of microbeads and MPs as non-biodegradable entities is commonly included in regulatory definitions. This suggests that any change in particle size – either incidental or engineered – would permit the incorporation of MPs in products despite the existing bans. Furthermore, penalties for circumventing plastic waste regulations either do not exist (Maryland and Maine)<sup>217</sup> or are not enforced.<sup>215</sup>

## **2.6 Environmental implications and outlook**

We have presented estimated loads of plastics in different environmental compartments and an overview of the key factors that govern the degradation, aggregation, and transport of NPs and MPs in aquatic and terrestrial environments. The fate and transport of NPs and MPs strongly depend on the physicochemical properties of the plastics and water and soil chemistries. A significant concern regarding MPs and NPs is their demonstrated ability to act as transport vectors for environmental contaminants. The rubbery polymer PE has shown a higher sorption capacity compared to other plastics for most contaminants reviewed. PE is also the most produced and frequently detected plastic in the environment widely used in packaging. As such, regulatory bodies would do well to consider PE in policy making. Additionally, regulations should not only consider the ability of plastics to act as sinks for environmental contaminants, but also the contaminants that originate from the plastics. For example, while PVC generally accumulates lower amounts of contaminants from its surroundings than other plastics (Figure 2.4b), it is composed of a high content of carcinogenic phthalates (~50%).<sup>219</sup>

Despite the considerable body of plastics research, important questions remain unanswered:

- How do we define NPs and MPs? And how can we make this definition uniform within literature? There is a need to improve detection and characterization techniques, as there is currently no rigorous methodology to detect NPs in the environment. How can we develop

new techniques or improve existing ones to push the resolution towards detection at the nanoscale?

- Does the transport of other commonly detected plastics (PE, PP, PVC, PET, etc.,) differ from that of PS in the subsurface environment? Do model primary plastics behave differently from environmentally relevant secondary plastics? Changes in the physicochemical properties of a particle will impact both aggregation and deposition behavior. Will plastic types of similar size/surface areas behave differently?
- Could plastic debris contamination in groundwaters be an important concern? What tools exist for the accurate detection of NPs/MPs in groundwaters?
- How do NPs and MPs interact with pharmaceuticals and other emerging contaminants? The effect of salinity on contaminant sorption remains unclear. How do complex aquatic environments containing natural organic matter, microorganisms, mixtures of contaminants, etc. affect sorption capacity? Does the formation of biofilms affect sorption/desorption capacities?

Answering these and other questions will significantly improve our understanding of the fate, transport, and risks associated with MPs and NPs that are already ubiquitous in the environment. Although policy makers are starting to acknowledge the potential risks and implications of MPs and NPs, which is leading to the ban of some products, these are important concerns, as MPs and NPs have been accumulating in the environment for decades. Understanding the behavior and prevalence of MPs and NPs in the environment is the first step towards mitigating the impacts of these contaminants.

## **Acknowledgements**

The authors acknowledge the financial support of the Canada Research Chairs program, the Natural Sciences and Engineering Research Council of Canada, the National Contaminants Advisory Group of Fisheries and Oceans Canada, the Petroleum Technology Development Fund (PTDF) of Nigeria for an award to OSA, and McGill University for a MEDA award to LMH and OSA.

## References

1. Wright, S. L.; Kelly, F. J., Plastic and human health: A micro issue? *Environ. Sci. Technol.* **2017**, *51*, (12), 6634-6647.
2. MacArthur, D. E.; Waughray, D.; Stuchtey, R. M., The new plastics economy rethinking the future of plastics. *World Economic Forum* **2016**.
3. Nizzetto, L.; Futter, M.; Langaas, S., Are agricultural soils dumps for microplastics of urban origin? *Environ. Sci. Technol.* **2016**, *50*, (20), 10777-10779.
4. O'Connor, I. A.; Golsteijn, L.; Hendriks, A. J., Review of the partitioning of chemicals into different plastics: Consequences for the risk assessment of marine plastic debris. *Mar. Pollut. Bull.* **2016**, *113*, (1-2), 1-2.
5. Barnes, D. K.; Galgani, F.; Thompson, R. C.; Barlaz, M., Accumulation and fragmentation of plastic debris in global environments. *Philos. Trans. R. Soc. London, Ser. B* **2009**, *364*, (1526), 1985-98.
6. O'Connor, M. C., Only 14% of plastics are recycled – can tech innovation tackle the rest? *The Guardian* 2017.
7. Reed, C., Dawn of the Plasticene age. *New Scientist* 225.3006 **2015**, *43*, (2), 28-32.
8. Panko, J. M.; Chu, J.; Kreider, M. L.; Unice, K. M., Measurement of airborne concentrations of tire and road wear particles in urban and rural areas of France, Japan, and the United States. *Atmospheric Environ.* **2013**, *72*, 192-199.
9. Thompson, R. C.; Moore, C. J.; vom Saal, F. S.; Swan, S. H., Plastics, the environment and human health: Current consensus and future trends. *Philos. Trans. R. Soc. London, Ser. B* **2009**, *364*, (1526), 2153-66.
10. da Costa, J. P.; Santos, P. S. M.; Duarte, A. C.; Rocha-Santos, T., (Nano)plastics in the environment - Sources, fates and effects. *Sci. Total Environ.* **2016**, *566-567*, 15-26.
11. Nizzetto, L.; Bussi, G.; Futter, M. N.; Butterfield, D.; Whitehead, P. G., A theoretical assessment of microplastic transport in river catchments and their retention by soils and river sediments. *Environ. Sci. Process Impacts* **2016**, *18*, (8), 1050-9.
12. Dubaish, F.; Liebezeit, G., Suspended microplastics and black carbon particles in the Jade system, Southern north sea. *Water, Air, & Soil Pollut. : An International Journal of Environmental Pollution* **2013**, *224*, (2), 1-8.
13. Zubris, K. A. V.; Richards, B. K., Synthetic fibers as an indicator of land application of sludge. *Environ. Pollut.* **2005**, *138*, (2), 201-211.
14. Hidalgo-Ruz, V.; Gutow, L.; Thompson, R. C.; Thiel, M., Microplastics in the marine environment: a review of the methods used for identification and quantification. *Environ. Sci. Technol.* **2012**, *46*, (6), 3060-75.
15. Thompson, R. C.; Olsen, Y.; Mitchell, R. P.; Davis, A.; Rowland, S. J.; John, A. W.; McGonigle, D.; Russell, A. E., Lost at sea: Where is all the plastic? *Science* **2004**, *304*, (5672), 838.
16. Dris, R.; Gasperi, J.; Rocher, V.; Saad, M.; Renault, N.; Tassin, B., Microplastic contamination in an urban area: A case study in Greater Paris. *Environ. Chem.* **2015**, *12*, (5), 592.
17. Pascall, M. A.; Zabik, M. E.; Zabik, M. J.; Hernandez, R. J., Uptake of polychlorinated biphenyls (PCBs) from an aqueous medium by polyethylene, polyvinyl chloride, and polystyrene films. *J. Agric. Food Chem.* **2005**, *53*, (1), 164-9.
18. Crawford, C. B.; Quinn, B., *Microplastic pollutants*. 2017.
19. Bergmann, M.; Gutow, L.; Klages, M., *Marine Anthropogenic Litter*. 2015.

20. Rochman, C. M.; Hoh, E.; Hentschel, B. T.; Kaye, S., Long-term field measurement of sorption of organic contaminants to five types of plastic pellets: implications for plastic marine debris. *Environ. Sci. Technol.* **2013**, *47*, (3), 1646-54.
21. Arthur, C.; Baker, J.; Bamford, H., *Proceedings of the International Research Workshop on the Occurrence, Effects and Fate of Microplastic Marine Debris*. NOAA Technical Memorandum: 2009.
22. Jahnke, A.; Arp, H. P. H.; Escher, B. I.; Gewert, B.; Gorokhova, E.; Kühnel, D.; Ogonowski, M.; Potthoff, A.; Rummel, C.; Schmitt-Jansen, M.; Toorman, E.; MacLeod, M., Reducing uncertainty and confronting ignorance about the possible impacts of weathering plastic in the marine environment. *Environ. Sci. Technol. Letters* **2017**, *4*, (3), 85-90.
23. Derraik, J. G. B., The pollution of the marine environment by plastic debris: a review. *Mar. Pollut. Bull.* **2002**, *44*, (9), 842-852.
24. Betts, K., Why small plastic particles may pose a big problem in the oceans. *Environ. Sci. Technol.* **2008**, *42*, (24).
25. Cole, M.; Lindeque, P.; Halsband, C.; Galloway, T. S., Microplastics as contaminants in the marine environment: a review. *Mar. Pollut. Bull.* **2011**, *62*, (12), 2588-97.
26. Ryan, P. G.; Moore, C. J. C. J.; Franeker, v. J. A.; Moloney, C. L., Monitoring the abundance of plastic debris in the marine environment. *Philos. Trans. R. Soc. London, Ser. B, Biological Sciences* **2009**, *364*, (1526), 1999-2012.
27. Browne, M.; Galloway, T.; Thompson, R., Microplastic - an emerging contaminant of potential concern? *Integr. Environ. Assess. Manag.* **2007**, *preprint*, (2007), 1.
28. Rochman, C. M.; Kross, S. M.; Armstrong, J. B.; Bogan, M. T.; Darling, E. S.; Green, S. J.; Smyth, A. R.; Verissimo, D., Scientific evidence supports a ban on microbeads. *Environ. Sci. Technol.* **2015**, *49*, (18), 10759-61.
29. Hernandez, L. M.; Yousefi, N.; Tufenkji, N., Are there nanoplastics in your personal care products? *Environ. Sci. Technol. Letters* **2017**, *4*, (7), 280-285.
30. Horton, A. A.; Walton, A.; Spurgeon, D. J.; Lahive, E.; Svendsen, C., Microplastics in freshwater and terrestrial environments: Evaluating the current understanding to identify the knowledge gaps and future research priorities. *Sci. Total Environ.* **2017**, *586*, 127-141.
31. Carr, S. A.; Liu, J.; Tesoro, A. G., Transport and fate of microplastic particles in wastewater treatment plants. *Water Res.* **2016**, *91*, 174-82.
32. Rochman, C. M.; Kross, S. M.; Armstrong, J. B.; Bogan, M. T.; Darling, E. S.; Green, S. J.; Smyth, A. R.; Verissimo, D., Scientific evidence supports a ban on microbeads. *Environ. Sci. Technol.* **2015**, *49*, (18), 10759-61.
33. McDevitt, J. P.; Criddle, C. S.; Morse, M.; Hale, R. C.; Bott, C. B.; Rochman, C. M., Addressing the issue of microplastics in the wake of the microbead-free waters act-a new standard can facilitate improved policy. *Environ. Sci. Technol.* **2017**, *51*, (12), 6611-6617.
34. Lechner, A.; Keckeis, H.; Lumesberger-Loisl, F.; Zens, B.; Krusch, R.; Tritthart, M.; Glas, M.; Schludermann, E., The Danube so colourful: a potpourri of plastic litter outnumbers fish larvae in Europe's second largest river. *Environ. Pollut.* **2014**, *188*, 177-81.
35. Hernandez, E.; Nowack, B.; Mitrano, D. M., Polyester textiles as a source of microplastics from households: A mechanistic study to understand microfiber release during washing. *Environ. Sci. Technol.* **2017**, *51*, (12), 7036-7046.
36. Mattsson, K.; Hansson, L. A.; Cedervall, T., Nano-plastics in the aquatic environment. *Environ. Sci. Process Impacts* **2015**, *17*, (10), 1712-21.

37. Reisser, J.; Shaw, J.; Wilcox, C.; Hardesty, B. D.; Proietti, M.; Thums, M.; Pattiaratchi, C., Marine plastic pollution in waters around Australia: characteristics, concentrations, and pathways. *PLoS One* **2013**, *8*, (11), e80466.
38. Zbyszewski, M.; Corcoran, P. L., Distribution and degradation of fresh water plastic particles along the beaches of Lake Huron, Canada. *Water, Air, & Soil Pollut.* **2011**, *220*, (1-4), 365-372.
39. Jambeck, J. R.; Geyer, R.; Wilcox, C.; Siegler, T. R.; Perryman, M.; Andrady, A.; Narayan, R.; Law, K. L., Marine pollution. Plastic waste inputs from land into the ocean. *Science (New York, N.Y.)* **2015**, *347*, (6223), 768-71.
40. Eriksen, M.; Lebreton, L. C.; Carson, H. S.; Thiel, M.; Moore, C. J.; Borerro, J. C.; Galgani, F.; Ryan, P. G.; Reisser, J., Plastic pollution in the world's oceans: More than 5 trillion plastic pieces weighing over 250,000 tons afloat at sea. *PLoS One* **2014**, *9*, (12), e111913.
41. Samolada, M. C.; Zabaniotou, A. A., Comparative assessment of municipal sewage sludge incineration, gasification and pyrolysis for a sustainable sludge-to-energy management in Greece. *Waste Manag.* **2014**, *34*, (2), 411-20.
42. Kyrikou, I.; Briassoulis, D., Biodegradation of agricultural plastic films: A critical review. *J. Polym. Environ.* **2007**, *15*, (2), 125-150.
43. Malinconico, M., Soil degradable bioplastics for a sustainable modern agriculture. **2017**.
44. Peccia, J.; Westerhoff, P., We should expect more out of our sewage sludge. *Environ. Sci. Technol.* **2015**, *49*, (14), 8271-6.
45. Scarascia, G.; Sica, C.; Russo, G., Plastic materials in European agriculture: Actual use and perspectives. *J. of Ag. Eng. - Riv. di Ing. Agr* **2011**, *42*.
46. Lowry, G. V.; Gregory, K. B.; Apte, S. C.; Lead, J. R., Transformations of nanomaterials in the environment. *Environ. Sci. Technol.* **2012**, *46*, (13), 6893-9.
47. Petosa, A. R.; Jaisi, D. P.; Quevedo, I. R.; Elimelech, M.; Tufenkji, N., Aggregation and deposition of engineered nanomaterials in aquatic environments: role of physicochemical interactions. *Environ. Sci. Technol.* **2010**, *44*, (17), 6532-49.
48. Garner, K. L.; Keller, A. A., Emerging patterns for engineered nanomaterials in the environment: a review of fate and toxicity studies. *J. Nanopart. Res.* **2014**, *16*, (8), 2503.
49. Hotze, E. M.; Phenrat, T.; Lowry, G. V., Nanoparticle aggregation: Challenges to understanding transport and reactivity in the environment. *J. Environ. Qual.* **2010**, *39*, (6), 1909.
50. Batley, G. E.; Kirby, J. K.; McLaughlin, M. J., Fate and risks of nanomaterials in aquatic and terrestrial environments. *Acc. Chem. Res.* **2013**, *46*, (3), 854-62.
51. Sun, H.; Gao, B.; Tian, Y.; Yin, X.; Yu, C.; Wang, Y.; Ma, L. Q., Kaolinite and lead in saturated porous media: Facilitated and impeded transport. *J. Environ. Eng.* **2010**, *136*, (11), 1305-1308.
52. Ryan, J.; Elimelech, M., *Colloid mobilization and transport in groundwater*. 1996; Vol. 107, p 1-56.
53. Roy, S. B.; Dzombak, D. A., Chemical factors influencing colloid-facilitated transport of contaminants in porous media. *Environ. Sci. Technol.* **1997**, *31*, (3), 656-664.
54. Puls, R. W.; Powell, R. M., Transport of inorganic colloids through natural aquifer material: implications for contaminant transport. *Environ. Sci. Technol.* **1992**, *26*, (3), 614-621.
55. Amrhein, C.; Mosher, P. A.; Strong, J. E., Colloid-assisted transport of trace metals in roadside soils receiving deicing salts. *Soil Sci. Soc. Am. J.* **1993**, *57*, (5), 1212-1217.

56. Grolimund, D.; Borkovec, M.; Barmettler, K.; Sticher, H., Colloid-facilitated transport of strongly sorbing contaminants in natural porous media: A laboratory column study. *Environ. Sci. Technol.* **1996**, *30*, (10), 3118-3123.
57. Brennecke, D.; Duarte, B.; Paiva, F.; Caçador, I.; Canning-Clode, J., Microplastics as vector for heavy metal contamination from the marine environment. *Estuar. Coast Shelf Sci.* **2016**, *178*, 189-195.
58. Rochman, C. M.; Hentschel, B. T.; Teh, S. J., Long-term sorption of metals is similar among plastic types: implications for plastic debris in aquatic environments. *PLoS One* **2014**, *9*, (1).
59. Holmes, L. A.; Turner, A.; Thompson, R. C., Adsorption of trace metals to plastic resin pellets in the marine environment. *Environ. Pollut. (Barking, Essex : 1987)* **2012**, *160*, (1), 42-8.
60. Bakir, A.; Rowland, S. J.; Thompson, R. C., Transport of persistent organic pollutants by microplastics in estuarine conditions. *Estuar. Coast Shelf Sci.* **2014**, *140*, 14-21.
61. Endo, S.; Takizawa, R.; Okuda, K.; Takada, H.; Chiba, K.; Kanehiro, H.; Ogi, H.; Yamashita, R.; Date, T., Concentration of polychlorinated biphenyls (PCBs) in beached resin pellets: Variability among individual particles and regional differences. *Mar. Pollut. Bull.* **2005**, *50*, (10), 1103-1114.
62. Lee, H.; Shim, W. J.; Kwon, J. H., Sorption capacity of plastic debris for hydrophobic organic chemicals. *Sci. Total Environ.* **2014**, *470-471*, 470-471.
63. Rochman, C. M.; Manzano, C.; Hentschel, B. T.; Simonich, S. L.; Hoh, E., Polystyrene plastic: a source and sink for polycyclic aromatic hydrocarbons in the marine environment. *Environ. Sci. Technol.* **2013**, *47*, (24), 13976-84.
64. Napper, I. E.; Bakir, A.; Rowland, S. J.; Thompson, R. C., Characterisation, quantity and sorptive properties of microplastics extracted from cosmetics. *Mar. Pollut. Bull.* **2015**, *99*, (1-2), 178-185.
65. Hu, J.-Q.; Yang, S.-Z.; Guo, L.; Xu, X.; Yao, T.; Xie, F., Microscopic investigation on the adsorption of lubrication oil on microplastics. *J. Mol. Liq.* **2017**, *227*, 351-355.
66. Lambert, S.; Wagner, M., Characterisation of nanoplastics during the degradation of polystyrene. *Chemosphere* **2016**, *145*, 265-268.
67. Andrady, A. L., Microplastics in the marine environment. *Mar. Pollut. Bull.* **2011**, *62*, (8), 1596-605.
68. Browne, M. A.; Crump, P.; Niven, S. J.; Teuten, E.; Tonkin, A.; Galloway, T.; Thompson, R., Accumulation of microplastic on shorelines worldwide: sources and sinks. *Environ. Sci. Technol.* **2011**, *45*, (21), 9175-9.
69. Imhof, H. K.; Schmid, J.; Niessner, R.; Ivleva, N. P.; Laforsch, C., A novel, highly efficient method for the separation and quantification of plastic particles in sediments of aquatic environments. *Limnol. Oceanogr. Methods* **2012**, *10*, (7), 524-537.
70. Feldman, D., Weathering of polymers, A. Davis and D. Sims, Applied Science Publishers, London, 1983, 294 pp. Price: \$64.75. *J. Polym. Sci., Part A: Polym. Chem.* **1984**, *22*, (7), 423.
71. Eerkes-Medrano, D.; Thompson, R. C.; Aldridge, D. C., Microplastics in freshwater systems: A review of the emerging threats, identification of knowledge gaps and prioritisation of research needs. *Water Res.* **2015**, *75*, 63-82.
72. Law, K. L.; Moret-Ferguson, S.; Maximenko, N. A.; Proskurowski, G.; Peacock, E. E.; Hafner, J.; Reddy, C. M., Plastic accumulation in the North Atlantic subtropical gyre. *Science* **2010**, *329*, (5996), 1185-8.

73. Zhao, S.; Zhu, L.; Wang, T.; Li, D., Suspended microplastics in the surface water of the Yangtze Estuary System, China: first observations on occurrence, distribution. *Mar. Pollut. Bull.* **2014**, *86*, (1-2), 562-568.
74. Steinmetz, Z.; Wollmann, C.; Schaefer, M.; Buchmann, C.; David, J.; Troger, J.; Munoz, K.; Fror, O.; Schaumann, G. E., Plastic mulching in agriculture. Trading short-term agronomic benefits for long-term soil degradation? *Sci. Total Environ.* **2016**, *550*, 690-705.
75. Rillig, M. C.; Ziersch, L.; Hempel, S., Microplastic transport in soil by earthworms. *Sci. Rep.* **2017**, *7*, (1), 1362.
76. Free, C. M.; Jensen, O. P.; Mason, S. A.; Eriksen, M.; Williamson, N. J.; Boldgiv, B., High-levels of microplastic pollution in a large, remote, mountain lake. *Mar. Pollut. Bull.* **2014**, *85*, (1), 156-63.
77. Dris, R.; Gasperi, J.; Mirande, C.; Mandin, C.; Guerrouache, M.; Langlois, V.; Tassin, B., A first overview of textile fibers, including microplastics, in indoor and outdoor environments. *Environ. Pollut.* **2017**, *221*, 453-458.
78. Driedger, A. G. J.; Dürr, H. H.; Mitchell, K.; Van Cappellen, P., Plastic debris in the Laurentian Great Lakes: A review. *J. Great Lakes Res.* **2015**, *41*, (1), 9-19.
79. McCormick, A.; Hoellein, T. J.; Mason, S. A.; Schlupe, J.; Kelly, J. J., Microplastic is an abundant and distinct microbial habitat in an urban river. *Environ. Sci. Technol.* **2014**, *48*, (20), 11863-71.
80. Klein, S.; Worch, E.; Knepper, T. P., Occurrence and spatial distribution of microplastics in river shore sediments of the Rhine-main area in Germany. *Environ. Sci. Technol.* **2015**, *49*, (10), 6070-6.
81. Hoellein, T.; Rojas, M.; Pink, A.; Gasior, J.; Kelly, J., Anthropogenic litter in urban freshwater ecosystems: distribution and microbial interactions. *PLoS One* **2014**, *9*, (6), e98485.
82. Zhang, K.; Gong, W.; Lv, J.; Xiong, X.; Wu, C., Accumulation of floating microplastics behind the Three Gorges Dam. *Environ. Pollut.* **2015**, *204*, 117-23.
83. Morritt, D.; Stefanoudis, P. V.; Pearce, D.; Crimmen, O. A.; Clark, P. F., Plastic in the Thames: a river runs through it. *Mar. Pollut. Bull.* **2014**, *78*, (1-2), 196-200.
84. Murphy, F.; Ewins, C.; Carbonnier, F.; Quinn, B., Wastewater treatment works (WWTW) as a source of microplastics in the aquatic environment. *Environ. Sci. Technol.* **2016**, *50*, (11), 5800-8.
85. Talvitie, J.; Mikola, A.; Setälä, O.; Heinonen, M.; Koistinen, A., How well is microlitter purified from wastewater? - A detailed study on the stepwise removal of microlitter in a tertiary level wastewater treatment plant. *Water Res.* **2017**, *109*, 164-172.
86. Dris, R.; Imhof, H.; Sanchez, W.; Gasperi, J.; Galgani, F.; Tassin, B.; Laforsch, C., Beyond the ocean: Contamination of freshwater ecosystems with (micro-) plastic particles. *Environ. Chem.* **2015**, *12*, 32.
87. Hoffman, M. J.; Hittinger, E., Inventory and transport of plastic debris in the Laurentian Great Lakes. *Mar. Pollut. Bull.* **2017**, *115*, (1-2), 273-281.
88. Wegner, A.; Besseling, E.; Foekema, E. M.; Kamermans, P.; Koelmans, A. A., Effects of nanopolystyrene on the feeding behavior of the blue mussel (*Mytilus edulis* L.). *Environ. Toxicol. Chem.* **2012**, *31*, (11), 2490-2497.
89. Rochman, C. M.; Browne, M. A.; Halpern, B. S.; Hentschel, B. T.; Hoh, E.; Karapanagioti, H. K.; Rios-Mendoza, L. M.; Takada, H.; Teh, S.; Thompson, R. C., Policy: Classify plastic waste as hazardous. *Nature* **2013**, *494*, (7436), 169-71.

90. Boerger, C. M.; Lattin, G. L.; Moore, S. L.; Moore, C. J., Plastic ingestion by planktivorous fishes in the North Pacific Central Gyre. *Mar. Pollut. Bull.* **2010**, *60*, (12), 2275-8.
91. Browne, M. A.; Dissanayake, A.; Galloway, T. S.; Lowe, D. M.; Thompson, R. C., Ingested microscopic plastic translocates to the circulatory system of the mussel, *Mytilus edulis* (L). *Environ. Sci. Technol.* **2008**, *42*, (13), 5026-31.
92. Graham, E. R.; Thompson, J. T., Deposit- and suspension-feeding sea cucumbers (Echinodermata) ingest plastic fragments. *J. Exp. Mar. Biol. Ecol.* **2009**, *368*, (1), 22-29.
93. Possatto, F. E.; Barletta, M.; Costa, M. F.; do Sul, J. A.; Dantas, D. V., Plastic debris ingestion by marine catfish: an unexpected fisheries impact. *Mar. Pollut. Bull.* **2011**, *62*, (5), 1098-102.
94. Murray, F.; Cowie, P. R., Plastic contamination in the decapod crustacean *Nephrops norvegicus* (Linnaeus, 1758). *Mar. Pollut. Bull.* **2011**, *62*, (6), 1207-17.
95. Eriksson, C.; Burton, H., Origins and biological accumulation of small plastic particles in fur seals from macquarie island. *AMBIO* **2003**, *32*, (6), 380-384.
96. Bouwmeester, H.; Hollman, P. C.; Peters, R. J., Potential health impact of environmentally released micro- and nanoplastics in the human food production chain: Experiences from nanotoxicology. *Environ. Sci. Technol.* **2015**, *49*, (15), 8932-47.
97. Brodhagen, M.; Goldberger, J. R.; Hayes, D. G.; Inglis, D. A.; Marsh, T. L.; Miles, C., Policy considerations for limiting unintended residual plastic in agricultural soils. *Environ. Sci. Policy* **2017**, *69*, 81-84.
98. Huerta Lwanga, E.; Gertsen, H.; Gooren, H.; Peters, P.; Salanki, T.; van der Ploeg, M.; Besseling, E.; Koelmans, A. A.; Geissen, V., Incorporation of microplastics from litter into burrows of *Lumbricus terrestris*. *Environ. Pollut.* **2017**, *220*, (Pt A), 523-531.
99. Corcoran, P. L.; Norris, T.; Ceccanese, T.; Walzak, M. J.; Helm, P. A.; Marvin, C. H., Hidden plastics of Lake Ontario, Canada and their potential preservation in the sediment record. *Environ. Pollut.* **2015**, *204*, 17-25.
100. Huffer, T.; Praetorius, A.; Wagner, S.; von der Kammer, F.; Hofmann, T., Microplastic exposure assessment in aquatic environments: Learning from similarities and differences to engineered nanoparticles. *Environ. Sci. Technol.* **2017**, *51*, (5), 2499-2507.
101. Therezien, M.; Thill, A.; Wiesner, M. R., Importance of heterogeneous aggregation for NP fate in natural and engineered systems. *Sci. Total Environ.* **2014**, *485-486*, 309-318.
102. Dale, A. L.; Casman, E. A.; Lowry, G. V.; Lead, J. R.; Viparelli, E.; Baalousha, M., Modeling nanomaterial environmental fate in aquatic systems. *Environ. Sci. Technol.* **2015**, *49*, (5), 2587-93.
103. Dale, A. L.; Lowry, G. V.; Casman, E. A., Stream dynamics and chemical transformations control the environmental fate of silver and zinc oxide nanoparticles in a watershed-scale model. *Environ. Sci. Technol.* **2015**, *49*, (12), 7285-93.
104. Wiesner, M. R.; Bottero, J.-Y., *Environmental nanotechnology : Applications and impacts of nanomaterials*. McGraw-Hill: New York, 2007.
105. Yao, K.-M.; Habibi, M. T.; O'Melia, C. R., Water and waste water filtration. Concepts and applications. *Environ. Sci. Technol.* **1971**, *5*, (11), 1105-1112.
106. Tufenkji, N.; Elimelech, M., Correlation equation for predicting single-collector efficiency in physicochemical filtration in saturated porous media. *Environ. Sci. Technol.* **2004**, *38*, (2), 529-36.

107. Derjaguin, B.; Landau, L., Theory of the stability of strongly charged lyophobic sols and of the adhesion of strongly charged particles in solutions of electrolytes. *Prog. Surf. Sci.* **1993**, *43*, (1-4), 30-59.
108. Verwey, E. J. W.; Overbeek, J. T. G.; Nes, K. v., Theory of the stability of lyophobic colloids : the interaction of sol particles having an electric double layer. **1948**.
109. Alexander, S., Adsorption of chain molecules with a polar head a scaling description. *J. Phys. France* **1977**, *38*, (8), 983-987.
110. de Gennes, P. G., Dry spreading of a liquid on a random surface. *C. R. Seances Acad. Sci., Ser. 2* **1985**, *300* (4), 129-132.
111. Elimelech, M., Particle deposition and aggregation : Measurement, modelling, and simulation. **1998**.
112. Klaine, S. J.; Alvarez, P. J. J.; Batley, G. E.; Fernandes, T. F.; Handy, R. D.; Lyon, D. Y.; Mahendra, S.; McLaughlin, M. J.; Lead, J. R., Nanomaterials in the environment: Behavior, fate, bioavailability, and effects. *Environ. Toxicol. Chem.* **2008**, *27*, (9), 1825-1851.
113. Praetorius, A.; Labille, J.; Scheringer, M.; Thill, A.; Hungerbühler, K.; Bottero, J. Y., Heteroaggregation of titanium dioxide nanoparticles with model natural colloids under environmentally relevant conditions. *Environ. Sci. Technol.* **2014**, *48*, (18), 10690-8.
114. Bastos, D.; de las Nieves, F. J., Colloidal stability of sulfonated polystyrene model colloids. Correlation with electrokinetic data. *Colloid Polym. Sci.* **1994**, *272*, (5), 592-597.
115. Schneider, C.; Hanisch, M.; Wedel, B.; Jusufi, A.; Ballauff, M., Experimental study of electrostatically stabilized colloidal particles: Colloidal stability and charge reversal. *J. Colloid Interface Sci.* **2011**, *358*, (1), 62-67.
116. Ruiz-Cabello, F. J.; Trefalt, G.; Csendes, Z.; Sinha, P.; Oncsik, T.; Szilagyi, I.; Maroni, P.; Borkovec, M., Predicting aggregation rates of colloidal particles from direct force measurements. *J. Phys. Chem. B* **2013**, *117*, (39), 11853-62.
117. Oncsik, T.; Trefalt, G.; Csendes, Z.; Szilagyi, I.; Borkovec, M., Aggregation of negatively charged colloidal particles in the presence of multivalent cations. *Langmuir* **2014**, *30*, (3), 733-41.
118. Montes Ruiz-Cabello, F. J.; Trefalt, G.; Oncsik, T.; Szilagyi, I.; Maroni, P.; Borkovec, M., Interaction forces and aggregation rates of colloidal latex particles in the presence of monovalent counterions. *J. Phys. Chem. B* **2015**, *119*, (25), 8184-93.
119. Bibeau, A. A.; Matijevic, E., Stability of polyvinyl chloride latex:III. Effects of simple electrolytes. *J. Colloid Interface Sci.* **1973**, *43*, (2), 330-338.
120. Bleier, A.; Matijevic, E., Heterocoagulation. I. Interactions of monodispersed chromium hydroxide with polyvinyl chloride latex. *J. Colloid Interface Sci.* **1976**, *55*, (3), 510-524.
121. Sakota, K.; Okaya, T., Electrolyte stability of carboxylated latexes prepared by several polymerization processes. *J. Appl. Polym. Sci.* **1977**, *21*, (4), 1025-1034.
122. Dickinson, E.; Robson, E. W.; Stainsby, G., Colloid stability of casein-coated polystyrene particles. *J. Chem. Soc. Faraday Trans.* **1983**, *79*, (12), 2937.
123. Carrique, F.; Salcedo, J.; Cabrerizo, M. A.; González-Caballero, F.; Delgado, A. V., Further studies on the stability of polystyrene suspensions. *Acta Polym.* **1991**, *42*, (6), 261-266.
124. Amirbahman, A.; Olson, T. M., Transport of humic matter-coated hematite in packed beds. *Environ. Sci. Technol.* **1993**, *27*, (13), 2807-2813.
125. Smith, N. J.; Williams, P. A., Depletion flocculation of polystyrene latices by water-soluble polymers. *J. Chem. Soc. Faraday Trans.* **1995**, *91*, (10), 1483.
126. Walker, H. W.; Bob, M. M., Stability of particle flocs upon addition of natural organic matter under quiescent conditions. *Water Res.* **2001**, *35*, (4), 875-882.

127. Tungittiplakorn, W.; Lion, L. W.; Cohen, C.; Kim, J. Y., Engineered polymeric nanoparticles for soil remediation. *Environ. Sci. Technol.* **2004**, *38*, (5), 1605-10.
128. Jódar-Reyes, A. B.; Ortega-Vinuesa, J. L.; Martín-Rodríguez, A., Electrokinetic behavior and colloidal stability of polystyrene latex coated with ionic surfactants. *J. Colloid Interface Sci.* **2006**, *297*, (1), 170-181.
129. Hierrezuelo, J.; Sadeghpour, A.; Szilagyi, I.; Vaccaro, A.; Borkovec, M., Electrostatic stabilization of charged colloidal particles with adsorbed polyelectrolytes of opposite charge. *Langmuir* **2010**, *26*, (19), 15109-11.
130. Della Torre, C.; Bergami, E.; Salvati, A.; Faleri, C.; Cirino, P.; Dawson, K. A.; Corsi, I., Accumulation and embryotoxicity of polystyrene nanoparticles at early stage of development of sea urchin embryos *Paracentrotus lividus*. *Environ. Sci. Technol.* **2014**, *48*, (20), 12302-11.
131. Besseling, E.; Quik, J. T. K.; Sun, M.; Koelmans, B., Fate of nano- and microplastic in freshwater systems: A modeling study. *Environ. Pollut.* **2016**, *220*, (Part A), 540-548.
132. Henry, C.; Norrfors, K. K.; Olejnik, M.; Bouby, M.; Luetzenkirchen, J.; Wold, S.; Minier, J.-P., A refined algorithm to simulate latex colloid agglomeration at high ionic strength. *Adsor* **2016**, *22*, (4-6), 503-515.
133. Oncsik, T.; Desert, A.; Trefalt, G.; Borkovec, M.; Szilagyi, I., Charging and aggregation of latex particles in aqueous solutions of ionic liquids: towards an extended Hofmeister series. *PCCP* **2016**, *18*, (10), 7511-20.
134. Saleh, N. B.; Pfefferle, L. D.; Elimelech, M., Aggregation kinetics of multiwalled carbon nanotubes in aquatic systems: measurements and environmental implications. *Environ. Sci. Technol.* **2008**, *42*, (21), 7963-9.
135. Saleh, N. B.; Pfefferle, L. D.; Elimelech, M., Influence of biomacromolecules and humic acid on the aggregation kinetics of single-walled carbon nanotubes. *Environ. Sci. Technol.* **2010**, *44*, (7), 2412-2418.
136. Chen, K. L.; Elimelech, M., Influence of humic acid on the aggregation kinetics of fullerene (C60) nanoparticles in monovalent and divalent electrolyte solutions. *J. Colloid Interface Sci.* **2007**, *309*, (1), 126-134.
137. Johnson, R. L.; Johnson, G. O.; Nurmi, J. T.; Tratnyek, P. G., Natural organic matter enhanced mobility of nano zerovalent iron. *Environ. Sci. Technol.* **2009**, *43*, (14), 5455-60.
138. Domingos, R. F.; Baalousha, M. A.; Ju-Nam, Y.; Reid, M. M.; Tufenkji, N.; Lead, J. R.; Leppard, G. G.; Wilkinson, K. J., Characterizing manufactured nanoparticles in the environment: multimethod determination of particle sizes. *Environ. Sci. Technol.* **2009**, *43*, (19), 7277-84.
139. Arvidsson, R.; Molander, S.; Sandén, B. A.; Hassellöv, M., Challenges in exposure modeling of nanoparticles in aquatic environments. *Hum. Ecol. Risk Assess.* **2011**, *17*, (1), 245-262.
140. Torkzaban, S.; Bradford, S. A.; van Genuchten, M. T.; Walker, S. L., Colloid transport in unsaturated porous media: The role of water content and ionic strength on particle straining. *J. Contam. Hydrol.* **2008**, *96*, (1), 113-127.
141. Xu, S.; Qi, J.; Chen, X.; Lazouskaya, V.; Zhuang, J.; Jin, Y., Coupled effect of extended DLVO and capillary interactions on the retention and transport of colloids through unsaturated porous media. *Sci. Total Environ.* **2016**, *573*, (11), 564-572.
142. Wang, Z.; Jin, Y.; Shen, C.; Li, T.; Huang, Y.; Li, B.; Zheng, J., Spontaneous detachment of colloids from primary energy minima by Brownian diffusion. *PLoS One* **2016**, *11*, (1), e0147368.

143. Hoggan, J. L.; Sabatini, D. A.; Kibbey, T. C. G., Transport and retention of TiO<sub>2</sub> and polystyrene nanoparticles during drainage from tall heterogeneous layered columns. *J. Contam. Hydrol.* **2016**, *194*, (12), 30-35.
144. Mitropoulou, P. N.; Syngouna, V. I.; Chrysikopoulos, C. V., Transport of colloids in unsaturated packed columns: Role of ionic strength and sand grain size. *Chem. Eng. J.* **2013**, *232*, (5), 237-248.
145. Bouchard, D.; Zhang, W.; Chang, X., A rapid screening technique for estimating nanoparticle transport in porous media. *Water Res.* **2013**, *47*, (12), 4086-4094.
146. Nattich-Rak, M.; Adamczyk, Z.; Sadowska, M.; Morga, M.; Ocwieja, M., Hematite nanoparticle monolayers on mica: Characterization by colloid deposition. *Colloids Surf. A. Physicochem Eng. Asp.* **2012**, *412*, 72-81.
147. Magal, E.; Weisbrod, N.; Yechieli, Y.; Walker, S. L.; Yakirevich, A., Colloid transport in porous media: Impact of hyper-saline solutions. *Water Res.* **2011**, *45*, (11), 3521-3532.
148. Zhuang, J.; Goepfert, N.; Tu, C.; McCarthy, J.; Perfect, E.; McKay, L., Colloid transport with wetting fronts: interactive effects of solution surface tension and ionic strength. *Water Res.* **2010**, *44*, (4), 1270-8.
149. Shen, C.; Huang, Y.; Li, B.; Jin, Y., Effects of solution chemistry on straining of colloids in porous media under unfavorable conditions. *Water Resour. Res.* **2008**, *44*, (5).
150. Bradford, S. A.; Bettahar, M., Concentration dependent transport of colloids in saturated porous media. *J. Contam. Hydrol.* **2006**, *82*, (1), 99-117.
151. Hahn, M. W.; Abadzic, D.; O'Melia, C. R., Aquasols: On the role of secondary minima. *Environ. Sci. Technol.* **2004**, *38*, (22), 5915-24.
152. Huber, N.; Baumann, T.; Niessner, R., Assessment of colloid filtration in natural porous media by filtration theory. *Environ. Sci. Technol.* **2000**, *34*, (17), 3774-3779.
153. Sojitra, I.; Valsaraj, K. T.; Reible, D. D.; Thibodeaux, L. J., Transport of hydrophobic organics by colloids through porous media 1. Experimental results. *Colloids Surf. A. Physicochem Eng. Asp.* **1995**, *94*, (2), 197-211.
154. Elimelech, M.; O'Melia, C. R., Effect of particle size on collision efficiency in the deposition of Brownian particles with electrostatic energy barriers. *Langmuir* **1990**, *6*, (6), 1153-1163.
155. Elimelech, M.; O'Melia, C. R., Kinetics of deposition of colloidal particles in porous media. *Environ. Sci. Technol.* **1990**, *24*, (10), 1528-1536.
156. Wan, J.; Wilson, J. L., Colloid transport in unsaturated porous media. *Water Resour. Res.* **1994**, *30*, (4), 857-864.
157. Amirbahman, A.; Olson, T. M., The role of surface conformations in the deposition kinetics of humic matter-coated colloids in porous media. *Colloids Surf. A. Physicochem Eng. Asp.* **1995**, *95*, (2), 249-259.
158. Deshiikan, S. R.; Eschenazi, E.; Papadopoulos, K. D., Transport of colloids through porous beds in the presence of natural organic matter. *Colloids Surf. A. Physicochem Eng. Asp.* **1998**, *145*, (1), 93-100.
159. Bradford, S. A.; Yates, S. R.; Bettahar, M.; Simunek, J., Physical factors affecting the transport and fate of colloids in saturated porous media. *Water Resour. Res.* **2002**, *38*, (12), 63-1-63-12.
160. Franchi, A.; O'Melia, C. R., Effects of natural organic matter and solution chemistry on the deposition and reentrainment of colloids in porous media. *Environ. Sci. Technol.* **2003**, *37*, (6), 1122-9.

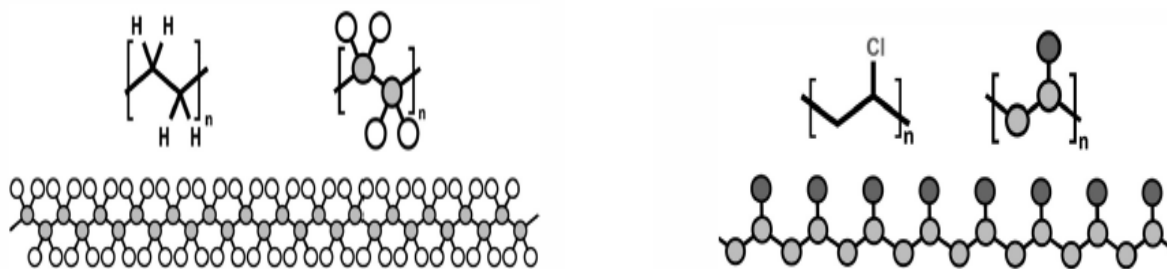
161. Tufenkji, N.; Elimelech, M., Breakdown of colloid filtration theory: Role of the secondary energy minimum and surface charge heterogeneities. *Langmuir* **2005**, *21*, (3), 841-52.
162. Zhuang, J.; Qi, J.; Jin, Y., Retention and transport of amphiphilic colloids under unsaturated flow conditions: effect of particle size and surface property. *Environ. Sci. Technol.* **2005**, *39*, (20), 7853-9.
163. Kobayashi, M.; Nanaumi, H.; Muto, Y., Initial deposition rate of latex particles in the packed bed of zirconia beads. *Colloids Surf. A. Physicochem Eng. Asp.* **2009**, *347*, (1-3), 2-7.
164. Pelley, A. J.; Tufenkji, N., Effect of particle size and natural organic matter on the migration of nano- and microscale latex particles in saturated porous media. *J. Colloid Interface Sci.* **2008**, *321*, (1), 74-83.
165. Shani, C.; Weisbrod, N.; Yakirevich, A., Colloid transport through saturated sand columns: Influence of physical and chemical surface properties on deposition. *Colloids Surf. A. Physicochem Eng. Asp.* **2008**, *316*, (1-3), 142-150.
166. Tripathi, S.; Champagne, D.; Tufenkji, N., Transport behavior of selected nanoparticles with different surface coatings in granular porous media coated with *Pseudomonas aeruginosa* biofilm. *Environ. Sci. Technol.* **2012**, *46*, (13), 6942-9.
167. Quevedo, I. R.; Tufenkji, N., Mobility of functionalized quantum dots and a model polystyrene nanoparticle in saturated quartz sand and loamy sand. *Environ. Sci. Technol.* **2012**, *46*, (8), 4449-57.
168. Wu, L.; Gao, B.; Muñoz-Carpena, R.; Pachepsky, Y. A., Single collector attachment efficiency of colloid capture by a cylindrical collector in laminar overland flow. *Environ. Sci. Technol.* **2012**, *46*, (16), 8878-86.
169. Treumann, S.; Torkzaban, S.; Bradford, S. A.; Visalakshan, R. M.; Page, D., An explanation for differences in the process of colloid adsorption in batch and column studies. *J. Contam. Hydrol.* **2014**, *164*, (12), 219-229.
170. Zhang, Q.; Raoof, A.; Hassanizadeh, S. M., Pore-scale study of flow rate on colloid attachment and remobilization in a saturated micromodel. *J. Environ. Qual.* **2015**, *44*, (5).
171. Mitzel, M. R.; Sand, S.; Whalen, J. K.; Tufenkji, N., Hydrophobicity of biofilm coatings influences the transport dynamics of polystyrene nanoparticles in biofilm-coated sand. *Water Res.* **2016**, *92*, (7), 113-120.
172. Tong, M.; Johnson, W. P., Excess colloid retention in porous media as a function of colloid size, fluid velocity, and grain angularity. *Environ. Sci. Technol.* **2006**, *40*, (24), 7725-7731.
173. Qing, Y. Evaluating the role of the secondary energy minimum in colloid deposition and release in saturated porous media. The Ohio State University, 2011.
174. Wu, L.; Gao, B.; Munoz-Carpena, R.; Pachepsky, Y. A., Single collector attachment efficiency of colloid capture by a cylindrical collector in laminar overland flow. *Environ. Sci. Technol.* **2012**, *46*, (16), 8878-86.
175. Brow, C. N.; Li, X.; Rička, J.; Johnson, W. P., Comparison of microsphere deposition in porous media versus simple shear systems. *Colloids Surf. A. Physicochem Eng. Asp.* **2005**, *253*, (1), 125-136.
176. Li, X.; Zhang, P.; Lin, C. L.; Johnson, W. P., Role of hydrodynamic drag on microsphere deposition and re-entrainment in porous media under unfavorable conditions. *Environ. Sci. Technol.* **2005**, *39*, (11), 4012-4020.
177. Peulen, T. O.; Wilkinson, K. J., Diffusion of nanoparticles in a biofilm. *Environ. Sci. Technol.* **2011**, *45*, (8), 3367-73.

178. Guiot, E.; Georges, P.; Brun, A.; Fontaine-Aupart, M. P.; Bellon-Fontaine, M. N.; Briandet, R., Heterogeneity of diffusion inside microbial biofilms determined by Fluorescence Correlation Spectroscopy under two-photon excitation & para. *Photochem. Photobiol.* **2002**, *75*, (6), 570-578.
179. Suhrhoff, T. J.; Scholz-Bottcher, B. M., Qualitative impact of salinity, UV radiation and turbulence on leaching of organic plastic additives from four common plastics - A lab experiment. *Mar. Pollut. Bull.* **2016**, *102*, (1), 84-94.
180. Lithner, D.; Larsson, Å.; Dave, G., Environmental and health hazard ranking and assessment of plastic polymers based on chemical composition. *Sci. Total Environ.* **2011**, *409*, (18), 3309-3324.
181. Hüffer, T.; Hofmann, T., Sorption of non-polar organic compounds by micro-sized plastic particles in aqueous solution. *Environ. Pollut.* **2016**, *214*, (17), 194-201.
182. Mato, Y.; Isobe, T.; Takada, H.; Kanehiro, H.; Ohtake, C.; Kaminuma, T., Plastic resin pellets as a transport medium for toxic chemicals in the marine environment. *Environ. Sci. Technol.* **2001**, *35*, (2), 318-24.
183. Hirai, H.; Takada, H.; Ogata, Y.; Yamashita, R.; Mizukawa, K.; Saha, M.; Kwan, C.; Moore, C.; Gray, H.; Laursen, D.; Zettler, E. R.; Farrington, J. W.; Reddy, C. M.; Peacock, E. E.; Ward, M. W., Organic micropollutants in marine plastics debris from the open ocean and remote and urban beaches. *Mar. Pollut. Bull.* **2011**, *62*, (8), 1683-1692.
184. Rios, L. M.; Moore, C.; Jones, P. R., Persistent organic pollutants carried by synthetic polymers in the ocean environment. *Mar. Pollut. Bull.* **2007**, *54*, (8), 1230-1237.
185. Rochman, C. M., The complex mixture, fate and toxicity of chemicals associated with plastic debris in the marine environment. In *Marine Anthropogenic Litter*, Bergmann, M.; Gutow, L.; Klages, M., Eds. Springer International Publishing: Cham, 2015; pp 117-140.
186. Wang, W.; Wang, J., Different partition of polycyclic aromatic hydrocarbon on environmental particulates in freshwater: Microplastics in comparison to natural sediment. *Ecotoxicol. Environ. Saf.* **2017**, *147*, (Supplement C), 648-655.
187. Wang, F.; Shih, K. M.; Li, X. Y., The partition behavior of perfluorooctanesulfonate (PFOS) and perfluorooctanesulfonamide (FOSA) on microplastics. *Chemosphere.* **2015**, *119*, 841-847.
188. Fries, E.; Zarfl, C., Sorption of polycyclic aromatic hydrocarbons (PAHs) to low and high density polyethylene (PE). *Environ. Sci. Pollut. Res.* **2012**, *19*, (4), 1296-1304.
189. Müller, J. F.; Manomanii, K.; Mortimer, M. R.; McLachlan, M. S., Partitioning of polycyclic aromatic hydrocarbons in the polyethylene/water system. *Fresenius J. Anal. Chem.* **2001**, *371*, (6), 816-822.
190. Misumi, Glass transition temperature Tg of plastics. **2011**.
191. Teuten, E. L.; Rowland, S. J.; Galloway, T. S.; Thompson, R. C., Potential for plastics to transport hydrophobic contaminants. *Environ. Sci. Technol.* **2007**, *41*, (22), 7759-64.
192. Berkowitz, B.; Dror, I.; Yaron, B., *Contaminant geochemistry : interactions and transport in the subsurface environment.* 2014.
193. Zhan, Z.; Wang, J.; Peng, J.; Xie, Q.; Huang, Y.; Gao, Y., Sorption of 3,3,4,4-tetrachlorobiphenyl by microplastics: A case study of polypropylene. *Mar. Pollut. Bull.* **2016**, *110*, (1), 559-563.
194. Karapanagioti, H. K.; Klontza, I., Testing phenanthrene distribution properties of virgin plastic pellets and plastic eroded pellets found on Lesvos island beaches (Greece). *Mar. Environ. Res.* **2008**, *65*, (4), 283-290.

195. Velzeboer, I.; Kwadijk, C. J. A. F.; Koelmans, A. A., Strong sorption of PCBs to nanoplastics, microplastics, carbon nanotubes, and fullerenes. *Environ. Sci. Technol.* **2014**, *48*, (9), 4869-4876.
196. Holmes, L. A.; Turner, A.; Thompson, R. C., Interactions between trace metals and plastic production pellets under estuarine conditions. *Mar. Chem.* **2014**, *167*, 25-32.
197. Mato, Y.; Takada, H.; P., Z. M.; Kanehiro, H.; Y., K., Toxic chemicals contained in plastic resin pellets in the marine environment: Spatial difference in pollutant concentrations and the effects of resin type. *Kankyo Kagakukaishi* **2002**, (15), 415-423.
198. Wu, B.; Taylor, C. M.; Knappe, D. R.; Nanny, M. A.; Barlaz, M. A., Factors controlling alkylbenzene sorption to municipal solid waste. *Environ. Sci. Technol.* **2001**, *35*, (22), 4569-76.
199. Bakir, A.; Rowland, S. J.; Thompson, R. C., Competitive sorption of persistent organic pollutants onto microplastics in the marine environment. *Mar. Pollut. Bull.* **2012**, *64*, (12), 2782-9.
200. Wu, C.; Zhang, K.; Huang, X.; Liu, J., Sorption of pharmaceuticals and personal care products to polyethylene debris. *Environ. Sci. Pollut. Res.* **2016**, *23*, (9), 8819-26.
201. Bin, G.; Cao, X.; Dong, Y.; Luo, Y.; Ma, L., Colloid deposition and release in soils and their association with heavy metals. *Environ. Sci. Technol.* **2011**, *41*, (4), 336-372.
202. Stumm, W., Chemical interaction in particle separation. *Environ. Sci. Technol.* **1977**, *11*, (12), 1066-1070.
203. Karathanasis, A., *Subsurface migration of copper and zinc mediated by soil colloids*. 1998; Vol. 63, p 830-838.
204. Grolimund, D.; Borkovec, M., Colloid facilitated transport of strongly sorbing contaminants in natural porous media: mathematical modeling and laboratory column experiments. *Environ. Sci. Technol.* **2005**, *39*, (17), 6378-86.
205. Chen, G.; Flury, M.; Harsh, J. B.; Lichtner, P. C., Colloid-facilitated transport of cesium in variably saturated Hanford sediments. *Environ. Sci. Technol.* **2005**, *39*, (10), 3435-42.
206. Roy, S. B.; Dzombak, D. A., Colloid release and transport processes in natural and model porous media. *Colloids Surf. A. Physicochem Eng. Asp.* **1996**, *107*, (1), 245-262.
207. Solovitch-Vella, N.; Garnier, J.-M.; Ciffroy, P., Influence of the colloid type on the transfer of <sup>60</sup>Co and <sup>85</sup>Sr in silica sand column under varying physicochemical conditions. *Chemosphere* **2006**, *65*, (2), 324-331.
208. de Jonge, L. W.; Kjaergaard, C.; Moldrup, P., Colloids and colloid-facilitated transport of contaminants in soils. *Vadose Zone J.* **2004**, *3*, (2), 321.
209. de Jonge, H.; Jacobsen, O. H.; de Jonge, L. W.; Moldrup, P., Particle-facilitated transport of prochloraz in undisturbed sandy loam soil columns. *J. Environ. Qual.* **1998**, *27*, (6), 1495.
210. Sprague, L. A.; Herman, J. S.; Hornberger, G. M.; Mills, A. L., Atrazine adsorption and colloid-facilitated transport through the unsaturated zone. *J. Environ. Qual.* **2000**, *29*, (5), 1632.
211. Kretzschmar, R.; Borkovec, M.; Grolimund, D.; Elimelech, M., Mobile subsurface colloids and their role in contaminant transport. In *Adv. Agron.*, Sparks, D. L., Ed. Academic Press: 1999; Vol. 66, pp 121-193.
212. Johari, W. L. W.; Diamessis, P. J.; Lion, L. W., Mass transfer model of nanoparticle-facilitated contaminant transport in saturated porous media. *Water Res.* **2010**, *44*, (4), 1028-1037.
213. Jaradat, A. Q.; Fowler, K.; Grimberg, S. J.; Holsen, T. M., Transport of colloids and associated hydrophobic organic chemicals through a natural media filter. *J. Environ. Eng.* **2009**, *135*, (1), 36.

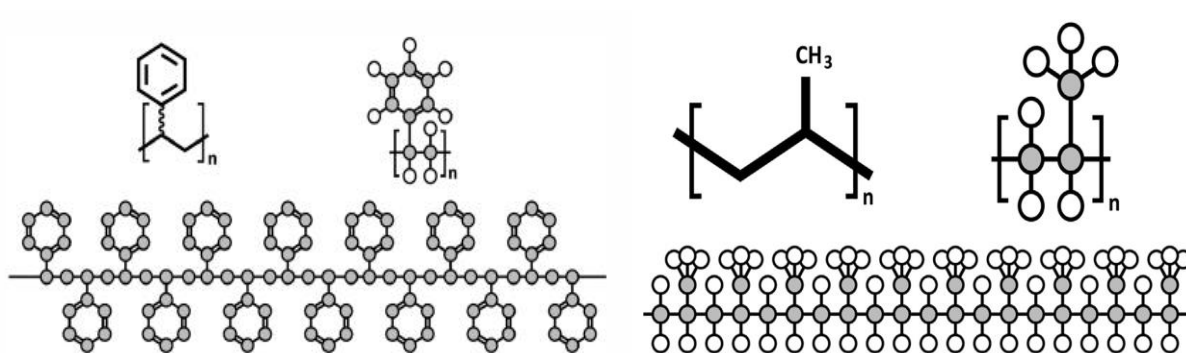
214. Doughty, R.; Eriksen, M., The case for a ban on microplastics in personal care products. *Tulane Environ. Law J* **2014**, *27*, 277–393.
215. Pettipas, S.; Bernier, M.; Walker, T. R., A Canadian policy framework to mitigate plastic marine pollution. *Mar. Policy* **2016**, *68*, 117-122.
216. Graney, G., Slipping through the cracks: How tiny plastic microbeads are currently escaping water treatment plants and international pollution regulation. *Fordham Int'l L. J.* **2016**, *39*, (4), 1023-1044.
217. Schroeck, N. J., Microplastic pollution in the Great lakes: State, federal, and common law solutions. *University of Detroit Mercy Law Review* **2016**, 273-291.
218. Truslow, D., Microbeads and the toxic use reduction act: Preventing pollution at its source. *Envtl. Aff. L. Rev.* **2017**, *44*, (1), 149.
219. Bauer, M. J.; Herrmann, R., Estimation of the environmental contamination by phthalic acid esters leaching from household wastes. *Sci. Total Environ.* **1997**, *208*, (1), 49-57.

## Supporting information



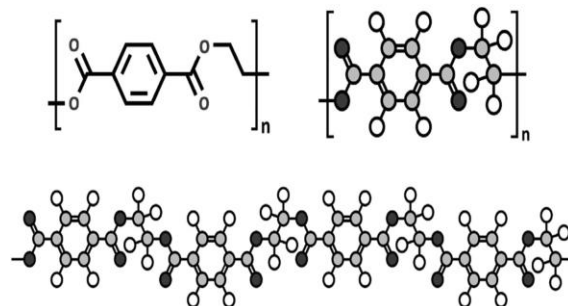
Polyethylene (PE)

Polyvinyl chloride (PVC)



Polystyrene (PS)

Polypropylene (PP)



Polyethylene terephthalate (PET)

**Figure S2.1.** Molecular structures of some commonly detected plastics in the environment. (Adapted from Quinn and Crawford, 2016)

**Table S2.1.** Data and references for Figure 2.1

<b>Compartment leaving</b>	<b>Compartment entering</b>	<b>% of Plastic leaving compartment</b>	<b>Reference</b>
Manufacture & Use	Mishandled (Ag & Land + Lakes & Rivers)	25.6 - 28.0 %	Calculated from Jambeck et al., 2015 <sup>1</sup>
Manufacture & Use	Agriculture & Land	0.5 - 5 %	Kyrikou and Briassoulis, 2007 <sup>2</sup> ; Scarascia-Mugnozza et al 2011 <sup>3</sup> ; Sintim and Flury, 2017 <sup>4</sup> ; Maliconico, 2017 <sup>5</sup>
Manufacture & Use	Landfill	21 - 42 %	Nizzetto et al., 2016 <sup>6</sup>
Manufacture & Use	WWTP	0.8 - 4.6 %	Calculated from Nizzetto et al., 2017 <sup>7</sup>
Manufacture & Use	Oceans	1.5 - 4.5 %	Nizzetto et al., 2016 <sup>6</sup>
Manufacture & Use	Recycled	6 - 26 %	Barnes et al., 2009 <sup>8</sup> ; Dris et al., 2015 <sup>9</sup>
WWTP	Effluent - Rivers & Lakes	* 0.1 - 5% (MP only)	Nizzetto et al., 2017; Horton et al., 2017 <sup>10</sup> ; Carr et al., 2016 <sup>11</sup>
WWTP	Solids - Land & Agriculture	42 - 55% (of sludge)	Peccia and Westerhoff, 2015 <sup>12</sup> ; Samolada and Zabaniotou, 2013 <sup>13</sup>
WWTP	Solids - Landfill	14 - 30 % (of sludge)	Peccia and Westerhoff, 2015 <sup>12</sup> ; Samolada and Zabaniotou, 2013 <sup>13</sup>
WWTP	Solids - Incineration	15 - 27 % (of sludge)	Peccia and Westerhoff, 2015; Samolada and Zabaniotou, 2013
Mishandled	Lakes & Rivers	† (25.6 - 28 %) w/ Land & Agriculture	Calculated from Jambeck et al., 2015
Agriculture & Land	Lakes & Rivers	† (62 - 84 % ) w/ Oceans	Nizzetto et al., 2016
Mishandled	Land & Agriculture	† (25.6 - 28 %) w/ Rivers & Lakes	Calculated from Jambeck et al., 2015
Agriculture & Land	Oceans + Lakes & Rivers	62 - 84 %	Nizzetto et al., 2016
Fishing Industry	Oceans	18 - 22.3 %	Andrady, 2011 <sup>14</sup> ; Ivar do Sul and Costa, 2013 <sup>15</sup>
All terrestrial sources	Oceans	80 %	Andrady, 2011 <sup>14</sup>
Lakes & Rivers	Oceans	70-80 % (ocean plastics coming from rivers)	Horton et al., 2017 <sup>10</sup>
Agriculture & Land	Oceans	0-10 %	Calculated from Andrady, 2011 <sup>14</sup> ; Horton et al., 2017 <sup>10</sup>

<b>Compartment</b>	<b>Concentration (#/m<sup>2</sup>)</b>	<b>Concentration (#/L)</b>	<b>Reference</b>
Lakes & Rivers	0.020 - 0.892	0.0024 - 0.3168	Horton et al., 2017 <sup>10</sup>
Lakes & Rivers		0.00005 - 0.032	Horton et al., 2017 <sup>10</sup>
Lakes & Rivers		4.1373 (+/-2.4615)	Zhao et al., 2014 <sup>16</sup>
Lakes & Rivers	0.020		EerkesMedrano et al., 2015 <sup>17</sup>
Lakes & Rivers		0.000028	EerkesMedrano et al., 2015 <sup>17</sup>
Lakes & Rivers	0.01 - 20		Dris et al., 2016 <sup>9</sup>
Lakes & Rivers	0.043		EerkesMedrano et al., 2015 <sup>17</sup>
Lakes & Rivers		0.0003168 (+/-0.00046646)	Lechner et al., 2014 <sup>18</sup>
Lakes & Rivers		0.00194 (+/-0.00081)	McCormick et al., 2014 <sup>19</sup>
Lakes & Rivers		0.01793 (+/-0.01105)	McCormick et al., 2014 <sup>19</sup>
Lakes & Rivers	8.465		Zhang et al., 2015 <sup>20</sup>
Lakes & Rivers	3.807		Zhang et al., 2015 <sup>20</sup>
WWTP Influent		260 - 320	Dris et al., 2015 <sup>9</sup>
WWTP Effluent		14 - 50	Dris et al., 2015 <sup>9</sup>
WWTP Influent		636.7 (+/-38.8)	Talvitie et al., 2017 <sup>21</sup>
WWTP Effluent		3.2 (+/-0.7)	Talvitie et al., 2017 <sup>21</sup>
Sediments	~0.21 - ~77,000	0.185 - 80	HidalgoRuz et al., 2012 <sup>22</sup>
Sediments	13,759 (+/-16,685)		EerkesMedrano et al., 2015 <sup>17</sup>
Sediments	1108 (+/-983)		Imhof et al., 2013 <sup>23</sup>
Sediments	108 (+/-55)		Imhof et al., 2013 <sup>23</sup>
Sediments	~0.05 - ~200		Dris et al., 2016 <sup>24</sup>
Sediments	75 - 1,300 (13,759)		Horton et al., 2017 <sup>10</sup>
Agriculture & Land		16 - 20 (+/-6)	Browne et al., 2011 <sup>25</sup>
Agriculture & Land		4 - 8 (+/-4)	Browne et al., 2011 <sup>25</sup>
Oceans		0.150 - 2.400	Cole et al., 2011 <sup>26</sup>
Oceans	~0.00005 - ~5	0.000022 - 8.654	HidalgoRuz et al., 2012 <sup>22</sup>
Oceans	0.0269		Zhang et al., 2015 <sup>20</sup>
Oceans	10 <sup>-6</sup> - 0.000250		Hinojosa and Thiel, 2009 <sup>27</sup>
Oceans		0.000167 (+/-0.000138)	Zhao et al., 2014 <sup>16</sup>

**Table S2.2.** Summary of sorption studies of contaminants to plastic particles

Plastic type and size	Contaminant	Key findings	References
PP virgin pellets	PCBs, DDE, and nonylphenols (NP) seawater	• Contaminants sorb about 1 million times more contaminants than immediate seawater	Mato et al., 2001 <sup>28</sup>
HDPE, PVC (d = 140 µm, PVC)	alkylbenzene; toluene and o-xylene	• PVC > HDPE > biopolymers	Wu et al., 2001 <sup>29</sup>
LDPE and HDPE	PAH	• HDPE > LDPE (four times more; as a result of the higher surface area of the former)	Muller et al., 2001 <sup>30</sup>
PP, PE	PCBs (sea water)	• PE > PP	Mato et al., 2002 <sup>31</sup>
Plastic pellets	PCBs	• Weathered pellets sorbed more PCBs • PE > PS • Sorbed chemicals unevenly distributed among pellets	Endo et al., 2005 <sup>32</sup>
PE (t = 2.286 × 10 <sup>-3</sup> cm) PVC (t = 1.78 × 10 <sup>-3</sup> cm) PS (t = 3.05 × 10 <sup>-3</sup> cm)	PCBs	• Average sorption: PE > PS > PVC • PE showed the highest uptake of PCBs and partition coefficients	Pascall et al., 2005 <sup>33</sup>
Plastic particles (d = 200 – 250 µm)	phenanthrene	• Desorption rate: sediments > plastics • PE >> PP > PVC > natural sediments	Teuten et al., 2007 <sup>34</sup>
PE (d = 2-3 mm) PP (d = 2-3 mm) POM (d < 2 mm) Plastic eroded pellets (PEP)	phenanthrene synthetic fresh water	• Equilibrium distribution coefficient: PEP > PE > POM > PP • Phenanthrene partitions to plastic debris several magnitudes over seawater	Karapanagioti and Klontza, 2008 <sup>35</sup>
HDPE, MDPE, LDPE and PVC (0.25 mm screen)	toluene (landfill)	• Affinity for contaminants in landfills: Plastic > lignocellulosic materials • Fast desorption from rubbery plastics compared to glassy plastics	Saquin et al., 2010 <sup>36</sup>
PET, HDPE, LDPE, PVC, and PP	PAHs and PCBs	• Long term field investigation as opposed to laboratory studies where temperature is controlled • Sorption of both contaminants consistent: HDPE > LDPE > PP >> PET > PVC	Rochman et al., 2013(a) <sup>37</sup>
PE beached and virgin	Cr, Co, Ni, Cu, Zn, Cd and Pb (filtered seawater)	• Beached PE > virgin PE	Holmes et al., 2012 <sup>38</sup>
HDPE (w×l×h= 4.2×4.7×2.8) LDPE (w×l×h=4×4.4× 2) mm	PAHs	LDPE > HDPE	Fries and Zarfl, 2012 <sup>39</sup>
PP, PS, PET, PVC, HDPE, LDPE (l= 3 mm, d= 2 mm)	PAHs (marine water)	• PS ≈ HDPE ≈ LDPE > PP > PET and PVC • PS appears to be a source and sink for PAHs	Rochman et al., 2013(b) <sup>40</sup>
PVC and PE (200–250 µm)	phenanthrene (Phe) and 4,4'-DDT	• Contaminant transport rely more on concentration than on salinity • Phe-PE >> DDT-PVC = DDT-PE >> Phe-PVC • Phe: PE > PVC, DDT: PVC > PE	Bakir et al., 2014 <sup>41</sup>
HDPE, PVC, LDPE and PP (d = 3 mm) PET (l × d = 2 × 3 mm)	Al, Cr, Mn, Fe, Co, Ni, Zn, Cd and Pb (sea water)	HDPE < LDPE, PVC, PET, PP and PS.	Rochman et al., 2014 <sup>42</sup>

PS, PE and PP ( $d < 250 \mu\text{m}$ )	PAHs; HCHs CBs (Sea water)	<ul style="list-style-type: none"> <li>•PS show greater affinity for the three contaminants studied except the few most hydrophobic PAHs;</li> <li>•HCHs: PP &gt; PE</li> <li>•CBs: PE &gt; PP</li> <li>•PAHs: PS &gt; PE &gt; PP</li> </ul>	Lee et al., 2014 <sup>43</sup>
PE (d = 10–180 $\mu\text{m}$ ) PS (d = 70 nm)	PCBs	<ul style="list-style-type: none"> <li>•Salinity increased sorption for both plastic types</li> <li>•PS &gt; PE</li> </ul>	Velzeboer et al., 2014 <sup>44</sup>
PE microbeads (d = 164 - 327 $\mu\text{m}$ )	3 H-phenanthrene 14 C- DDT (sea water)	<ul style="list-style-type: none"> <li>•DDT preferentially sorbed than phenanthrene in binary mixture</li> <li>•Rough particles adsorb higher contaminants than smooth ones.</li> </ul>	Napper et al, 2015 <sup>45</sup>
PE, PS and PVC (d = 150, 230, 250 $\mu\text{m}$ )	Perfluorochemicals: PFOS and FOSA	<ul style="list-style-type: none"> <li>•<math>K_{d \text{ FOSA}} &gt; K_{d \text{ PFOS}}</math></li> <li>•pH and salinity: FOSA unaffected while low values favour PFOS sorption</li> <li>•FOSA: PE &gt; PVC &gt; PS</li> </ul>	Wang et al., 2015 <sup>46</sup>
PE (d = 3.8 mm)	PAHs	<ul style="list-style-type: none"> <li>• Sorption capacity: 21°C &gt; 10°C</li> </ul>	Crawford and Quinn, 2017 <sup>47</sup>
PS (d = 70 nm)	PAHs (fresh water)	<ul style="list-style-type: none"> <li>• Sorption unaffected by aggregate size</li> </ul>	Liu et al., 2016 <sup>48</sup>
PE (d = 152.53 ± 57.92 $\mu\text{m}$ ) PA (d = 109.44 ± 44.53 $\mu\text{m}$ ) PS (d = 168.55 ± 57.50 $\mu\text{m}$ ) PVC (d = 57.64 ± 26.50 $\mu\text{m}$ )	n-Hexane, cyclohexane, benzene, toluene, chlorobenzene, ethylbenzoate, and naphthalene	<ul style="list-style-type: none"> <li>•Sorption capacity: PS &gt; PVC &gt; PE &gt; PA</li> </ul>	Huffer and Hofman, 2016 <sup>49</sup>
PE debris (d = 250 - 280 $\mu\text{m}$ )	PPCPs Dissolved organic matter (humic acid): 0-20 mg/L	<ul style="list-style-type: none"> <li>• PPCPs sorbed to plastics according to their hydrophobicity</li> <li>•Increase in humic acid decreased affinity for only three contaminant.</li> <li>•Increase in salinity affected sorption of one contaminant and not significant for the rest</li> </ul>	Wu et al., 2016 <sup>50</sup>
PP (d = 0.425–0.85 mm)	PCB: 3,3',4,4'-tetrachlorobiphenyl (simulated seawater, 3.5% NaCl solution) $C_{\text{PCB}} = 1 \text{ mg/L}$	<ul style="list-style-type: none"> <li>•Sorption capacity increases as particle size and temperature decreases</li> <li>•Sorption capacity: simulated seawater &gt; ultrapure water &gt; n hexane</li> </ul>	Zhan et al., 2016 <sup>51</sup>
PVC (d = 1.6 × 0.8 mm) PS (d = 0.7–0.9 mm)	Cu and Zn (seawater)	<ul style="list-style-type: none"> <li>•Maximum concentration of Cu and Zn greater in PVC than PS</li> <li>•Cu sorbed faster than Zn on PVC</li> </ul>	Brennecke et al., 2016 <sup>52</sup>
PE (d = 50 nm) PS (d = 20 - 40 $\mu\text{m}$ )	lubricating oil	<ul style="list-style-type: none"> <li>•Sorption: PE &gt; PS</li> <li>•Sorption capacity: independent of pH but increases with salinity and temperature</li> </ul>	Hu et al., 2017 <sup>53</sup>
PE (d = 100 - 150 $\mu\text{m}$ ) PS PVC	phenanthrene	<ul style="list-style-type: none"> <li>•Sorption: PE &gt; PS &gt; PVC &gt; natural sediment</li> </ul>	Wang and Wang 2017 <sup>54</sup>

d = diameter, l = length, t = thickness, w = width

PE = polyethylene; HDPE=high-density polyethylene; LDPE = low-density polyethylene; POM = polyoxymethylene; PP = polypropylene; PS = polystyrene; PVC= polyvinyl chloride; PA = polyamide; PET = polyethylene terephthalate. FOSA = Perfluorooctanesulfonamide, PFOS perfluorooctanesulfonate, PAH = polycyclic aromatic hydrocarbon, PPCPs = pharmaceuticals and personal care products, PCB = polychlorinated biphenyls, HCH = hexachlorocyclohexane, DDE = dichlorodiphenyldichloroethylene, DDT = dichloro diphenyl trichloroethane

## References

1. Jambeck, J. R.; Geyer, R.; Wilcox, C.; Siegler, T. R.; Perryman, M.; Andrady, A.; Narayan, R.; Law, K. L., Marine pollution. Plastic waste inputs from land into the ocean. *Science (New York, N.Y.)* **2015**, *347*, (6223), 768-71.
2. Kyrikou, I.; Briassoulis, D., Biodegradation of agricultural plastic films: A critical review. *J. Polym. Environ.* **2007**, *15*, (2), 125-150.
3. Scarascia, G.; Sica, C.; Russo, G., Plastic materials in European agriculture: Actual use and perspectives. *J. of Ag. Eng. - Riv. di Ing. Agr* **2011**, *42*.
4. Sintim, H. Y.; Flury, M., Is biodegradable plastic mulch the solution to agriculture's plastic problem? *Environ. Sci. Technol.* **2017**, *51*, (3), 1068-1069.
5. Malinconico, M., Soil degradable bioplastics for a sustainable modern agriculture. **2017**.
6. Nizzetto, L.; Bussi, G.; Futter, M. N.; Butterfield, D.; Whitehead, P. G., A theoretical assessment of microplastic transport in river catchments and their retention by soils and river sediments. *Environ. Sci. Process Impacts* **2016**, *18*, (8), 1050-9.
7. Nizzetto, L.; Futter, M.; Langaas, S., Are Agricultural Soils Dumps for Microplastics of Urban Origin? *Environ. Sci. Technol.* **2016**, *50*, (20), 10777-10779.
8. Barnes, D. K.; Galgani, F.; Thompson, R. C.; Barlaz, M., Accumulation and fragmentation of plastic debris in global environments. *Philos. Trans. R. Soc. London, Ser. B* **2009**, *364*, (1526), 1985-98.
9. Dris, R.; Imhof, H.; Sanchez, W.; Gasperi, J.; Galgani, F.; Tassin, B.; Laforsch, C., Beyond the ocean: Contamination of freshwater ecosystems with (micro-) plastic particles. *Environ. Chem.* **2015**, *12*, 32.
10. Horton, A. A.; Walton, A.; Spurgeon, D. J.; Lahive, E.; Svendsen, C., Microplastics in freshwater and terrestrial environments: Evaluating the current understanding to identify the knowledge gaps and future research priorities. *Sci. Total Environ.* **2017**, *586*, 127-141.
11. Carr, S. A.; Liu, J.; Tesoro, A. G., Transport and fate of microplastic particles in wastewater treatment plants. *Water Res.* **2016**, *91*, 174-82.
12. Peccia, J.; Westerhoff, P., We should expect more out of our sewage sludge. *Environ. Sci. Technol.* **2015**, *49*, (14), 8271-6.
13. Samolada, M. C.; Zabaniotou, A. A., Comparative assessment of municipal sewage sludge incineration, gasification and pyrolysis for a sustainable sludge-to-energy management in Greece. *Waste Manag.* **2014**, *34*, (2), 411-20.
14. Andrady, A. L., Microplastics in the marine environment. *Mar. Pollut. Bull.* **2011**, *62*, (8), 1596-605.
15. Ivar do Sul, J. A.; Costa, M. F., Plastic pollution risks in an estuarine conservation unit. *J. Coast. Res.* **2013**, *65*, 48-53.
16. Zhao, S.; Zhu, L.; Wang, T.; Li, D., Suspended microplastics in the surface water of the Yangtze Estuary System, China: first observations on occurrence, distribution. *Mar. Pollut. Bull.* **2014**, *86*, (1-2), 562-568.
17. Eerkes-Medrano, D.; Thompson, R. C.; Aldridge, D. C., Microplastics in freshwater systems: A review of the emerging threats, identification of knowledge gaps and prioritisation of research needs. *Water Res.* **2015**, *75*, 63-82.
18. Lechner, A.; Keckeis, H.; Lumesberger-Loisl, F.; Zens, B.; Krusch, R.; Tritthart, M.; Glas, M.; Schludermann, E., The Danube so colourful: a potpourri of plastic litter outnumbers fish larvae in Europe's second largest river. *Environ. Pollut.* **2014**, *188*, 177-81.

19. McCormick, A.; Hoellein, T. J.; Mason, S. A.; Schluep, J.; Kelly, J. J., Microplastic is an abundant and distinct microbial habitat in an urban river. *Environ. Sci. Technol.* **2014**, *48*, (20), 11863-71.
20. Zhang, K.; Gong, W.; Lv, J.; Xiong, X.; Wu, C., Accumulation of floating microplastics behind the Three Gorges Dam. *Environ. Pollut.* **2015**, *204*, 117-23.
21. Talvitie, J.; Mikola, A.; Koistinen, A.; Setälä, O., Solutions to microplastic pollution - Removal of microplastics from wastewater effluent with advanced wastewater treatment technologies. *Water Res.* **2017**, *123*, 401-407.
22. Hidalgo-Ruz, V.; Gutow, L.; Thompson, R. C.; Thiel, M., Microplastics in the marine environment: a review of the methods used for identification and quantification. *Environ. Sci. Technol.* **2012**, *46*, (6), 3060-75.
23. Imhof, H. K.; Ivleva, N. P.; Schmid, J.; Niessner, R.; Laforsch, C., Contamination of beach sediments of a subalpine lake with microplastic particles. *Curr. Biol.* **2013**, *23*, (19), R867-8.
24. Dris, R.; Gasperi, J.; Rocher, V.; Saad, M.; Renault, N.; Tassin, B., Microplastic contamination in an urban area: A case study in Greater Paris. *Environ. Chem.* **2015**, *12*, (5), 592.
25. Browne, M. A.; Crump, P.; Niven, S. J.; Teuten, E.; Tonkin, A.; Galloway, T.; Thompson, R., Accumulation of microplastic on shorelines worldwide: sources and sinks. *Environ. Sci. Technol.* **2011**, *45*, (21), 9175-9.
26. Cole, M.; Lindeque, P.; Halsband, C.; Galloway, T. S., Microplastics as contaminants in the marine environment: a review. *Mar. Pollut. Bull.* **2011**, *62*, (12), 2588-97.
27. Hinojosa, I. A.; Thiel, M., Floating marine debris in fjords, gulfs and channels of southern Chile. *Mar. Pollut. Bull.* **2009**, *58*, (3), 341-50.
28. Mato, Y.; Isobe, T.; Takada, H.; Kanehiro, H.; Ohtake, C.; Kaminuma, T., Plastic resin pellets as a transport medium for toxic chemicals in the marine environment. *Environ. Sci. Technol.* **2001**, *35*, (2), 318-24.
29. Wu, B.; Taylor, C. M.; Knappe, D. R.; Nanny, M. A.; Barlaz, M. A., Factors controlling alkylbenzene sorption to municipal solid waste. *Environ. Sci. Technol.* **2001**, *35*, (22), 4569-76.
30. Müller, J. F.; Manomanii, K.; Mortimer, M. R.; McLachlan, M. S., Partitioning of polycyclic aromatic hydrocarbons in the polyethylene/water system. *Fresenius J. Anal. Chem.* **2001**, *371*, (6), 816-822.
31. Mato, Y.; Takada, H.; P., Z. M.; Kanehiro, H.; Y., K., Toxic chemicals contained in plastic resin pellets in the marine environment: Spatial difference in pollutant concentrations and the effects of resin type. *Kankyo Kagakukaishi* **2002**, (15), 415-423.
32. Endo, S.; Takizawa, R.; Okuda, K.; Takada, H.; Chiba, K.; Kanehiro, H.; Ogi, H.; Yamashita, R.; Date, T., Concentration of polychlorinated biphenyls (PCBs) in beached resin pellets: Variability among individual particles and regional differences. *Mar. Pollut. Bull.* **2005**, *50*, (10), 1103-1114.
33. Pascall, M. A.; Zabik, M. E.; Zabik, M. J.; Hernandez, R. J., Uptake of polychlorinated biphenyls (PCBs) from an aqueous medium by polyethylene, polyvinyl chloride, and polystyrene films. *J. Agric. Food Chem.* **2005**, *53*, (1), 164-9.
34. Teuten, E. L.; Rowland, S. J.; Galloway, T. S.; Thompson, R. C., Potential for plastics to transport hydrophobic contaminants. *Environ. Sci. Technol.* **2007**, *41*, (22), 7759-64.
35. Karapanagioti, H. K.; Klontza, I., Testing phenanthrene distribution properties of virgin plastic pellets and plastic eroded pellets found on Lesbos island beaches (Greece). *Mar. Environ. Res.* **2008**, *65*, (4), 283-290.

36. Saquing, J. M.; Saquing, C. D.; Knappe, D. R.; Barlaz, M. A., Impact of plastics on fate and transport of organic contaminants in landfills. *Environ. Sci. Technol.* **2010**, *44*, (16), 6396-402.
37. Rochman, C. M.; Hoh, E.; Hentschel, B. T.; Kaye, S., Long-term field measurement of sorption of organic contaminants to five types of plastic pellets: implications for plastic marine debris. *Environ. Sci. Technol.* **2013**, *47*, (3), 1646-54.
38. Holmes, L. A.; Turner, A.; Thompson, R. C., Adsorption of trace metals to plastic resin pellets in the marine environment. *Environ. Pollut. (Barking, Essex : 1987)* **2012**, *160*, (1), 42-8.
39. Fries, E.; Zarfl, C., Sorption of polycyclic aromatic hydrocarbons (PAHs) to low and high density polyethylene (PE). *Environ. Sci. Pollut. Res.* **2012**, *19*, (4), 1296-1304.
40. Rochman, C. M.; Manzano, C.; Hentschel, B. T.; Simonich, S. L.; Hoh, E., Polystyrene plastic: a source and sink for polycyclic aromatic hydrocarbons in the marine environment. *Environ. Sci. Technol.* **2013**, *47*, (24), 13976-84.
41. Bakir, A.; Rowland, S. J.; Thompson, R. C., Transport of persistent organic pollutants by microplastics in estuarine conditions. *Estuar. Coast Shelf Sci.* **2014**, *140*, 14-21.
42. Rochman, C. M.; Hentschel, B. T.; Teh, S. J., Long-term sorption of metals is similar among plastic types: implications for plastic debris in aquatic environments. *PLoS One* **2014**, *9*, (1).
43. Lee, H.; Shim, W. J.; Kwon, J. H., Sorption capacity of plastic debris for hydrophobic organic chemicals. *Sci. Total Environ.* **2014**, *470-471*, 470-471.
44. Velzeboer, I.; Kwadijk, C. J. A. F.; Koelmans, A. A., Strong sorption of PCBs to nanoplastics, microplastics, carbon nanotubes, and fullerenes. *Environ. Sci. Technol.* **2014**, *48*, (9), 4869-4876.
45. Napper, I. E.; Bakir, A.; Rowland, S. J.; Thompson, R. C., Characterisation, quantity and sorptive properties of microplastics extracted from cosmetics. *Mar. Pollut. Bull.* **2015**, *99*, (1-2), 178-185.
46. Wang, F.; Shih, K. M.; Li, X. Y., The partition behavior of perfluorooctanesulfonate (PFOS) and perfluorooctanesulfonamide (FOSA) on microplastics. *Chemosphere.* **2015**, *119*, 841-847.
47. Crawford, C. B.; Quinn, B., *Microplastic pollutants*. 2017.
48. Liu, L.; Fokink, R.; Koelmans, A. A., Sorption of polycyclic aromatic hydrocarbons to polystyrene nanoplastic. *Environ. Toxicol. Chem.* **2016**, *35*, (7), 1650-1655.
49. Hüffer, T.; Hofmann, T., Sorption of non-polar organic compounds by micro-sized plastic particles in aqueous solution. *Environ. Pollut.* **2016**, *214*, (17), 194-201.
50. Wu, C.; Zhang, K.; Huang, X.; Liu, J., Sorption of pharmaceuticals and personal care products to polyethylene debris. *Environ. Sci. Pollut. Res.* **2016**, *23*, (9), 8819-26.
51. Zhan, Z.; Wang, J.; Peng, J.; Xie, Q.; Huang, Y.; Gao, Y., Sorption of 3,3,4,4-tetrachlorobiphenyl by microplastics: A case study of polypropylene. *Mar. Pollut. Bull.* **2016**, *110*, (1), 559-563.
52. Brennecke, D.; Duarte, B.; Paiva, F.; Caçador, I.; Canning-Clode, J., Microplastics as vector for heavy metal contamination from the marine environment. *Estuar. Coast Shelf Sci.* **2016**, *178*, 189-195.
53. Hu, J.-Q.; Yang, S.-Z.; Guo, L.; Xu, X.; Yao, T.; Xie, F., Microscopic investigation on the adsorption of lubrication oil on microplastics. *J. Mol. Liq.* **2017**, *227*, 351-355.

54. Wang, W.; Wang, J., Different partition of polycyclic aromatic hydrocarbon on environmental particulates in freshwater: Microplastics in comparison to natural sediment. *Ecotoxicol. Environ. Saf.* **2017**, *147*, (Supplement C), 648-655.

### **Preamble to Chapter 3**

The critical literature review on nanoplastics and microplastics aggregation and deposition in chapter 2 revealed that the impact of environmental weathering on the transport of nanoplastics in the aquatic environment is largely overlooked. Nanoplastics found in the environment are not expected to be in their pristine state; hence, the goal of this chapter was to examine the impact of a physical weathering process (freeze-thaw) on nanoplastics transport in a model subsurface environment. The coupled effect of the presence of natural organic matter and the disaggregation behaviour of the nanoplastic suspension after weathering were also investigated.

The results from this research have been published in *Water Research* in October 2020.

## **Chapter 3: Exposure of Nanoplastics to Freeze-Thaw Leads to Aggregation and Reduced Transport in Model Groundwater Environments**

### **Abstract**

Despite plastic pollution being a significant environmental concern, the impact of environmental conditions such as temperature cycling on the fate of nanoplastics in cold climates remains unknown. To better understand nanoplastic mobility in subsurface environments following freezing and thawing cycles, the transport of 28 nm polystyrene nanoplastics exposed to either constant (10 °C) temperature or freeze-thaw (FT) cycles (-10 °C to 10 °C) was investigated in saturated quartz sand. The stability and transport of nanoplastic suspensions were examined both in the presence and absence of natural organic matter (NOM) over a range of ionic strengths (3-100 mM NaCl). Exposure to 10 FT cycles consistently led to significant aggregation and reduced mobility compared to nanoplastics held at 10 °C, especially at low ionic strengths in the absence of NOM. While NOM increased nanoplastic mobility, it did not prevent the aggregation of nanoplastics exposed to FT. We compare our findings with existing literature and show that nanoplastics will largely aggregate and associate with soils rather than undergo long range transport in groundwater in colder climates following freezing temperatures. As one of the first studies to examine the coupled effect of cold temperature and NOM, this work highlights the need to account for climate and temperature changes when assessing the risks associated with nanoplastic release in aquatic systems.

### **3.1 Introduction**

Plastic pollution is one of the major environmental challenges of the 21st century with recent evidence highlighting the potential risk in terrestrial and freshwater ecosystems<sup>1,2</sup>. Plastics have been detected in almost every environmental compartment<sup>3-6</sup> and will degrade over time due to various environmental stresses to produce smaller, secondary, plastic particles such as microplastics (100 nm–5 mm in size) and nanoplastics (<100 nm).<sup>7-9</sup> Additionally, some products containing intentionally produced (primary) microplastics have been shown to also include nanoplastics.<sup>10</sup> Although the fate of plastics in soils has received less attention, recent studies suggest that soils may be a larger reservoir for and source of plastics than other environmental compartments.<sup>11, 12</sup> Nanoplastics released from surface water run-off, landfill storage and agricultural activities such as biosolids application and plastic mulch may end up in soils which

could contaminate drinking water supplies via infiltration into groundwater. Thus, understanding the transport potential of nanoplastics in soils and aquifers is crucial to protecting human and environmental health.

The transport potential of nanoplastics and other nanoparticles in groundwater is typically assessed by measuring the amount of particles retained in laboratory based saturated porous media that mimic groundwater environments.<sup>13-15</sup> Several physicochemical factors that are associated with properties of the nanoplastic (e.g., size, surface functionalization), porous medium (grain size, geochemistry), pore water chemistry (pH, presence of organic matter, ionic strength), and hydrological conditions (flow velocity) have been shown to affect the transport of nanoplastics in saturated porous media.<sup>7, 14, 16-18</sup> The effect of temperature or freezing which could age or transform nanoplastic suspensions, however, has largely been overlooked. Most nanoplastic transport experiments have been conducted under ambient temperature conditions (20–25 °C).<sup>7</sup> Some studies have employed the typical range of groundwater temperatures (4–20 °C), however they do not cover cycles of freezing and thawing temperatures experienced in colder climates.<sup>13, 19-21</sup> From theory, the mass transfer rate of particles from bulk solution to the grain surface (described by the single-collector contact efficiency,  $\eta_0$ ) should decrease at lower temperatures due to a decrease in the diffusion coefficient, and thus cold climate regions might face higher risks of nanoplastic exposure to drinking water wells due to the higher particle mobility observed at lower temperatures.<sup>19, 20, 22</sup> This temperature-dependent behavior has also been observed with other colloids, such as graphene oxide,<sup>23</sup> bacteriophage<sup>24</sup> and *E. coli*<sup>25</sup>.

Beyond simple cold temperatures, many parts of the world experience cycles of freezing and thawing in early and late winter. Exposure to freeze-thaw (FT) cycling has been associated with changes in bacterial virulence and transport in porous media,<sup>26-29</sup> whereby contradictory results regarding enhanced or reduced mobility have been reported, depending on the bacterial species studied. In addition to the lack of clear trend, the transport behavior of biocolloids may be of limited use in predicting the mobility of non-biological colloids in saturated porous media, due to their unique features (e.g., cell hydrophobicity, motility, cell surface appendages)<sup>26, 27</sup> which may introduce additional transport and attachment mechanisms not considered in traditional filtration theory. A recent study investigating titanium dioxide (TiO<sub>2</sub>) nanoparticles demonstrated that FT induced aggregation, increased deposition, and limited particle transport.<sup>30</sup> While the

presence of NOM has generally been reported to stabilize particle suspensions at room temperature, thereby increasing particle mobility in porous media, TiO<sub>2</sub> subjected to FT in the presence of NOM was associated with larger, more irreversibly agglomerated particles.<sup>30</sup> Currently, there is no information on the impact of FT on nanoplastic transport in the environment or on the interaction between NOM and nanoplastic during and after FT. Within other contexts such as quality control, biological applications, etc., freeze-thaw has been employed to test suspension stability of colloids.<sup>31, 32</sup> For example, Barb and Mikucki reported that frozen suspensions of 50–100 nm polystyrene latex particles remained agglomerated even after thawing at room temperature.<sup>31</sup> Understanding the effect of FT on nanoplastic transport in model groundwater environments will be beneficial in risk assessments, especially for climates that experience repeated FT cycling.<sup>4</sup>

In this study, we systematically examined the influence of FT cycles on the transformations and transport of model primary nanoplastics in saturated porous media at a groundwater temperature relevant to southern Canada. Nanoplastic stability and transport were investigated over a range of ionic strengths (IS) in monovalent salt, in both the presence and absence of NOM, at 10 °C and after exposure to 10 FT cycles. Under all conditions, 10 FT cycles led to significant aggregation and reduced mobility compared to nanoplastics held at 10 °C. Although the presence of NOM increased nanoplastic mobility in column tests, it did not prevent the aggregation of nanoplastics exposed to FT.

## **3.2 Materials and methods**

### **3.2.1 Nanoplastic and natural organic matter suspension preparation**

Carboxylate-modified polystyrene latex Fluospheres® of 28 nm nominal diameter (Molecular Probes, Invitrogen) were used to represent model primary nanoplastics. The stock suspension (approximate number concentration of  $4.5 \times 10^{15}$  particles/mL) was bath sonicated for 3 min before the preparation of each working suspension. For transport and characterisation experiments, the stock suspension was diluted to an initial working concentration of 2 mg nanoplastics/L ( $\sim 2.3 \times 10^{11}$  particles/mL) at pH  $6.0 \pm 0.2$  in various electrolyte solutions ranging from 3-100 mM IS in either the presence or absence of NOM. All electrolyte solutions were prepared using analytical grade NaCl (Fisher Scientific) in filtered reverse osmosis water (Biolab Scientific), and the pH was adjusted with 0.01M NaOH and HCl. Suwannee river NOM (International Humic Substances

Society, RO Isolate, 2R101N) was used as a representative NOM. A stock solution of 100 mg/L NOM was prepared in reverse osmosis water, adjusted to pH 8, stirred overnight, and stored in the dark at 4 °C. This stock was spiked into suspensions at 5 mg/L for experiments conducted in the presence of NOM. Each working suspension was then vortexed for approximately 20 s to obtain a well-dispersed suspension and subjected to one of two temperature pre-treatments: either kept at 10 °C (control) for 10 days or exposed to 10 FT cycles. Prior to each experiment, the suspension was gently inverted to resuspend any settled nanoplastics.

### **3.2.2 Temperature pre-treatments**

Natural FT cycles were simulated in a recirculating chiller (Julabo CORIO CD-200F) filled with a 70/30 ratio of water/propylene glycol. The temperature profile (Figure S3.1) was selected to represent southern Quebec, Canada during the winter shoulder periods.<sup>26, 28</sup> Nanoplastic working suspensions were exposed to 10 FT cycles of 24 h each. During each FT cycle, the temperature was brought from +10 to -10 °C over 8 h, held at -10 °C for 4 h, brought back to +10 °C over 8 h, and then held at 10 °C for 4 h. In the second pre-treatment, samples were kept at a constant temperature of 10 °C for the same duration (240 h).

In separate experiments, nanoplastic suspensions in 10 mM NaCl were exposed to 1, 5, and 10 FT cycles to examine the effect of the number of FT cycles. The stability of the suspension after each treatment was then monitored over 5 days. For each stability test, the nanoplastic suspension was gently shaken (moderate shearing force applied to not exceed the low flowrate expected in groundwater) before each measurement. A separate stability test where the suspension was vigorously mixed for 30 s using a vortexer at 100 rpm each day post FT was also performed.

### **3.2.3 Nanoplastic characterization**

Nanoplastic suspensions were characterized following temperature pre-treatments. Nanoplastics and aggregate sizes were determined using dynamic light scattering (DLS) and transmission electron microscopy (TEM), while the zeta potential (ZP), which is an estimation of surface charge, was determined from the electrophoretic mobility measured by laser Doppler velocimetry. The electrophoretic mobility measurements were converted to ZP using the Smoluchowski approximation with the Henry equation.<sup>33</sup> Both DLS and laser Doppler velocimetry measurements were conducted using a Malvern Zetasizer Nano (Malvern Panalytical). For DLS measurements, the Z-average diameter ( $d_{h, Z-avg}$ ) (cumulants mean diameter), intensity mean diameter ( $d_{h, intensity}$ )

and volume mean diameter ( $d_{h, volume}$ ) are reported. The polydispersity index (PDI) provides an indication of the heterogeneity of aggregate sizes within a suspension and ranges from 0 (monodisperse) to 1 (highly polydisperse). Aggregate morphology and primary particles were visualized using TEM (FEI Technai 120 kV TEM) coupled with a Gatan Ultrascan 4000 4k×4k CCD camera. TEM was performed on suspensions deposited onto thin carbon film grids (Pacific Grid-Tech, 300 mesh, 3.05 mm O.D., hole size) and allowed to dry at room temperature after wicking away the excess liquid with a Whatman filter paper.

### 3.2.4 Nanoplastic transport studies

Column experiments were performed at 10 °C inside a cold chamber (Danby, DWC032A2BDB), analogous to previous studies.<sup>13, 18, 27, 30, 34</sup> Glass chromatography columns (16 mm inner diameter, GE Life Sciences) were packed with high purity fine quartz sand (-50 +70 mesh size,  $d_{50} = 256 \mu\text{m}$ , Sigma-Aldrich). The sand was acid-washed before use following the protocol of Pelley and Tufenkji.<sup>18</sup> Prior to each column experiment, 26 g of sand was soaked in the desired electrolyte for a minimum of 10 days at 10 °C and then wet packed into the glass columns. Uniform packing of the sand bed was ensured by gentle vibration which resulted in a final packed bed length of 85 mm. The porous media was supported by a Nylon Spectra mesh filter (pore size: 70  $\mu\text{m}$ , thickness 70  $\mu\text{m}$ ). One pore volume (PV) was calculated by subtracting the volume of the sand used (density = 2.6 g/cm<sup>3</sup>) from the total volume of the packed column and confirmed using 0.01 M KNO<sub>3</sub> as a tracer. The column porosity, calculated as one PV divided by the total volume of the packed column, was 0.43. After packing, a minimum of 10 PVs of electrolyte solution were pumped through the porous medium to equilibrate the column. For experiments including NOM, the column was equilibrated with electrolyte containing 5 ppm NOM. Electrolyte and nanoplastic suspensions were introduced at a constant approach velocity of  $7.5 \times 10^{-5}$  m/s using syringe pumps (Kd Scientific). For deposition experiments, 5 PVs of nanoplastics suspension were injected into the column followed by the particle-free electrolyte until almost no nanoplastics were detected in the effluent. Influent ( $C_0$ ) and effluent ( $C$ ) nanoplastic concentrations were collected in real-time by spectrofluorometry (FluoroMax-4 Jobin Yvon Horiba, Edison, NY), where  $C_0$  was measured before each column experiment and by bypassing the sand column. The nanoplastic excitation (505 nm) and emission (515 nm) wavelengths were provided by the nanoplastic manufacturer and verified in the laboratory.

### 3.2.5 Interpreting transport experiments

To compare nanoplastic transport across treatments, the particle attachment efficiency,  $\alpha$ , was calculated using the influent sizes measured by DLS and the average  $C/C_0$  determined from the numerical integration of the area under the breakthrough curve (BTC, plotted as  $C/C_0$  versus PV) using Equation 3.1:<sup>15, 35</sup>

$$\alpha = -\frac{2}{3} \frac{d_c}{(1-\theta)L\eta_0} \ln \left[ \frac{C}{C_0} \right] \quad (3.1)$$

where  $L$  is the length of the packed filter medium,  $\theta$  is the porosity of the sand bed,  $d_c$  is the average diameter of the sand grains, and  $C/C_0$  is calculated by integrating the experimental particle BTCs. A detailed explanation can be found in Tufenkji and Elimelech, 2004.

## 3.3 Results and discussion

### 3.3.1 Physicochemical properties of nanoplastics exposed to freeze-thaw

One of the key factors determining the fate of nanoplastics in porous media is the particle size.<sup>7</sup> The hydrodynamic diameters ( $d_h$ ) of nanoplastics at 10 °C and after exposure to FT are reported as the  $Z$ -average ( $d_{h, z-avg}$ ), intensity mean ( $d_{h, intensity}$ ), and volume mean ( $d_{h, volume}$ ) diameters in Table 3.1.

1 **Table 3.1.** Measured hydrodynamic diameters, electrophoretic mobility (EPM), zeta potential (ZP), calculated elution (C/C<sub>0</sub>) and attachment efficiencies of the nanoplastics  
 2 (NP) in quartz sand porous media

3

Particle	Treatment	Ionic strength (mM NaCl)	C/C <sub>0</sub>	d <sub>h, Z-avg</sub> (nm)	PDI	d <sub>h, intensity</sub> (nm)	d <sub>h, volume</sub> (nm)	α <sub>Z-avg</sub>	α <sub>int mean</sub>	EPM (μmcm/Vs)	ZP (mV)
NP	10°C	3	0.95	55 ± 2	0.29	80 ± 3	50 ± 4	0.0040 ± 9.1×10 <sup>-4</sup>	0.0039 ± 9.0×10 <sup>-4</sup>	-1.5 ± 0.3	-22.1 ± 2.5
		10	0.72	46 ± 4	0.27	55 ± 4	43 ± 2	0.018 ± 6.4×10 <sup>-4</sup>	0.021 ± 5.7×10 <sup>-4</sup>	-1.8 ± 0.4	-25.5 ± 5.4
		30	0.024	46 ± 10	0.24	55 ± 16	43 ± 9	0.21 ± 4.4×10 <sup>-2</sup>	0.24 ± 6.4×10 <sup>-2</sup>	-1.6 ± 0.3	-22.5 ± 5.9
		100	0.026	58 ± 4	0.30	61 ± 8	66 ± 2	0.25 ± 0.0×10 <sup>0</sup>	0.27 ± 3.0×10 <sup>-2</sup>	-1.0 ± 0.1	-15.2 ± 1.1
	FT	3	0.49	1044 ± 156	0.81	462 ± 163	486 ± 94	0.40 ± 2.5×10 <sup>-2</sup>	0.24 ± 3.3×10 <sup>-2</sup>	-1.9 ± 0.3	-27.9 ± 7.0
		10	0.47	582 ± 331	0.73	407 ± 136	402 ± 221	0.30 ± 1.3×10 <sup>-1</sup>	0.24 ± 3.1×10 <sup>-2</sup>	-2.0 ± 0.4	-35.6 ± 6.5
		30	0.070	668 ± 85	0.76	687 ± 124	281 ± 28	1.1 ± 9.3×10 <sup>-2</sup>	1.2 ± 5.6×10 <sup>-2</sup>	-1.4 ± 0.2	-23.4 ± 1.5
		100	0.063	612 ± 353	0.78	484 ± 118	194 ± 15	1.1 ± 2.4×10 <sup>-1</sup>	1.0 ± 3.6×10 <sup>-1</sup>	-1.1 ± 0.1	-20.2 ± 1.8
NP + NOM	10°C	30	0.92	65 ± 10	0.36	66 ± 17	71 ± 20	0.0066 ± 6.9×10 <sup>-3</sup>	0.0070 ± 7.6×10 <sup>-3</sup>	-4.1 ± 0.5	-55.5 ± 7.2
		100	0.54	57 ± 13	0.33	70 ± 28	72 ± 27	0.040 ± 1.8×10 <sup>-3</sup>	0.047 ± 4.8×10 <sup>-3</sup>	-1.1 ± 0.2	-15.0 ± 4.1
	FT	30	0.47	2834 ± 1585	0.82	483 ± 121	475 ± 139	0.49 ± 4.2×10 <sup>-2</sup>	0.41 ± 2.0×10 <sup>-1</sup>	-2.5 ± 0.7	-34.9 ± 9.3
		100	0.38	519 ± 134	0.60	384 ± 32	405 ± 9	0.34 ± 7.5×10 <sup>-2</sup>	0.29 ± 2.8×10 <sup>-2</sup>	-1.6 ± 0.2	-20.4 ± 2.7

4 The ratio of particle radius (14 nm) to double layer thickness, κa = ~5.5, 3.0, 1.7 and 0.95 in 3, 10, 30 and 100 mM NaCl respectively, hence Smoluchowski  
 5 approximation was used to convert EPM to ZP using the Henry equation.

6

7

For monodisperse particle suspensions,  $d_{h,z-avg}$  and  $d_{h,intensity}$  will be the same, and either measurement would accurately describe the particle size in suspension. However, DLS becomes less accurate when the polydispersity index (PDI) is high ( $> 0.5$ ). Under these conditions, the Z-average diameter, calculated from the method of cumulants, may overestimate  $d_h$  since the scattering intensity is proportional to the sixth power of the particle diameter.<sup>36</sup> In such cases, the intensity peak may be more accurate in describing the system as it is the closest distribution to what is measured.<sup>37, 38</sup>

From Table 3.1, measured values of the influent  $d_{h,intensity}$  at 10 °C ranged from 55±4 – 80±3 nm in 3–100 mM IS. These values, together with the PDI ( $\leq 0.36$ ), suggest that the particles are generally stable under all conditions (at 10 °C) examined, even at high IS (100 mM NaCl). It is worth noting that the nanoplastic manufacturer suggests that the carboxylate-modified nanoplastics are stable in up to 1 M monovalent salt.<sup>39</sup> Inspection of the intensity-based particle size distribution (PSD) of the nanoplastics at 10 °C, (Figure 3.1a and b, Figure S3.2 open red squares) reveals that the PSD is reproducible across triplicate runs. In the presence of NOM (solid symbols), the nanoplastics are also stable at 10 °C. The PSD of the pristine nanoplastics at 10 °C occasionally indicated the presence of some aggregates greater than 2000 nm comprising ~1–10 % of the total particle population. Because even a small trace of large aggregates or artifacts will skew the intensity mean, the intensity weighted diameter peak with at least 90% of the particle population was reported as the  $d_{h,intensity}$  (Table 3.1) in such cases (refer to section S3.2 for further discussion).<sup>40</sup> The calculated volume mean diameter is in good agreement with this 90% intensity peak (see Figure S3.3 for comparison). The  $d_{h,intensity}$  and  $d_{h,z-avg}$  values observed in this study were 2-3 times larger than the nominal size (~28 nm) reported by the manufacturer and obtained via TEM. This is not surprising, as DLS hydrodynamic sizes are usually greater than those observed with TEM.<sup>36, 37</sup> Indeed, size analysis of TEM images for the stable nanoplastics at 10 °C (Figure 3.1 c and d) reveal sizes similar to the manufacturer's report ( $25 \pm 4$  nm,  $n = 48$  as determined via Image J analysis).

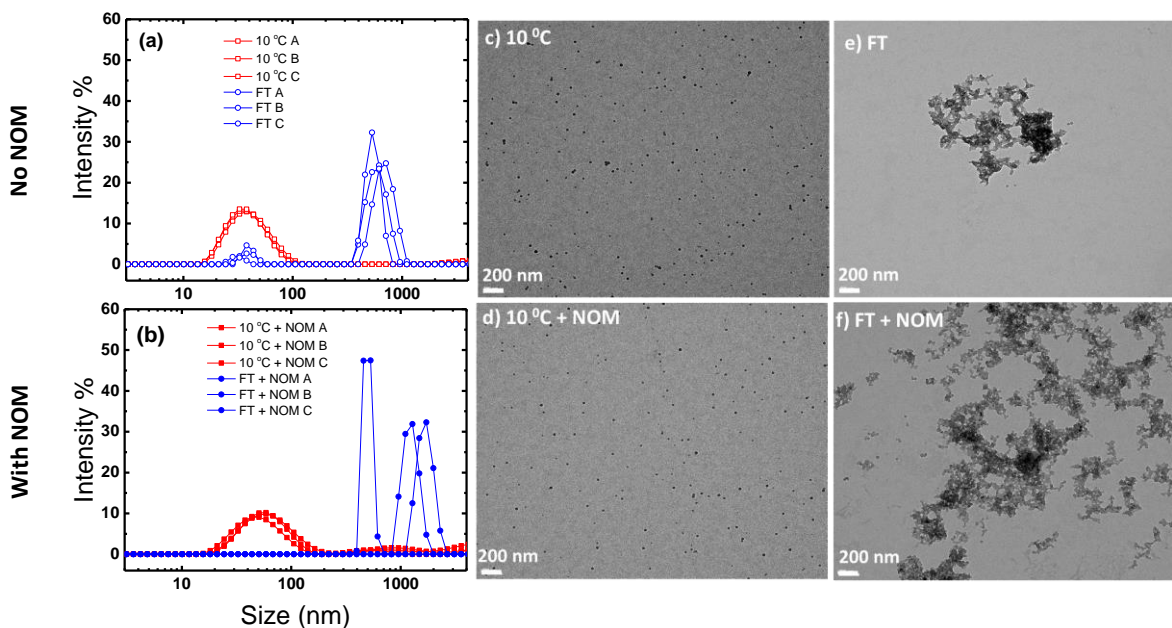


**Figure 3.1.** Representative intensity particle size distribution of nanoplastics in 30 mM NaCl (a) without NOM and (b) in the presence of NOM for three replicate samples (A, B, C). Representative TEM images of nanoplastics kept at 10°C for 240 hours (c and d) and after 10 FT cycles (e and f) all in 30 mM NaCl (a), (c), and (e) are suspensions without NOM. (b), (d), and (f) are suspensions with NOM.

Suspensions exposed to 10 FT cycles underwent aggregation that caused significant shifts in the PSD from 10–100 nm towards larger sizes of 100–1000 nm (Figure 3.1a and b, blue circles). The presence of NOM did not prevent the aggregation of nanoplastics following FT, and size ranges are on same order of magnitude for nanoplastics in the absence of NOM. For example, in 30 mM, the bare nanoplastics have  $d_{h,intensity} = 687 \pm 124$  while in the presence of NOM,  $d_{h,intensity} = 483 \pm 121$  (Table 3.1). TEM images confirm the formation of large aggregates upon exposure to repeated FT cycles (Figure 3.1c-f).

The effects of 3 different pre-treatment durations (1, 5, or 10 FT cycles) on the  $d_{h,z-avg}$  of the aggregates as well as on the disaggregation behavior of the aggregates were investigated. Figure 3.2 shows the  $d_{h,z-avg}$  of the aggregates before and after the 3 pre-treatments. After exposure to all 3 pre-treatments, the hydrodynamic size increased to  $\sim 2000$  nm and remain aggregated after 5 days. The aggregate size for the 1 FT cycle suspension post FT slightly decreased over the 5 days but did not fall below  $\sim 1000$  nm (Figure 3.2a). For all cycles, vigorously mixing the suspension did not result in an appreciable decrease in  $d_{h,z-avg}$  compared to day 5 post FT. This suggests that the aggregates formed after exposure to FT may be stable over longer time periods.

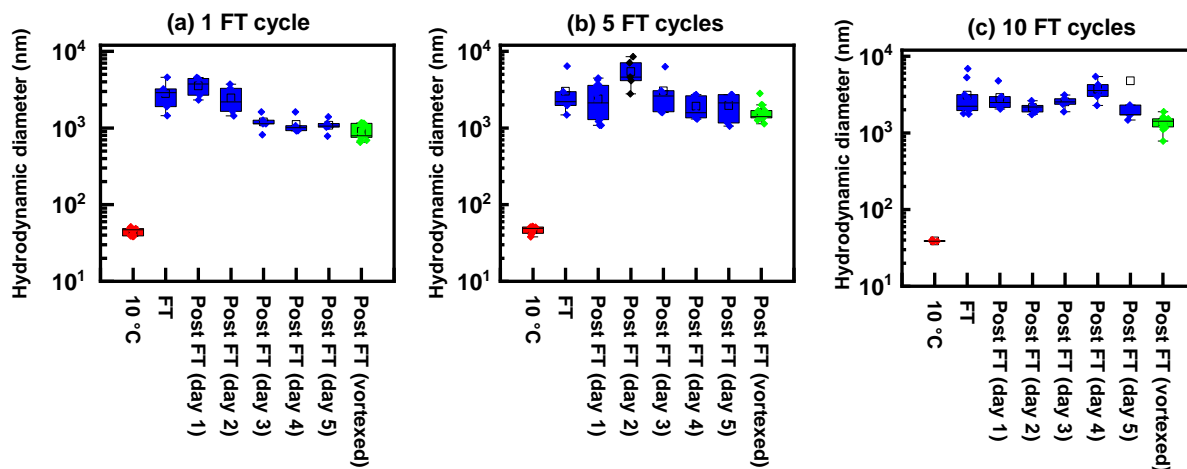


**Figure 3.2.** The stability of the nanoplastic suspension in 10 mM NaCl after exposure to (a) 1 FT cycle (b) 5 FT cycles and (c) 10 FT cycles. Sample stability was measured after FT exposure and named Post FT day 1 – 5. Samples that were vortexed Post FT from day 1 – 5 are collectively plotted as Post FT (vortexed).

Table 3.1 lists the ZP of nanoplastics in NaCl before and after FT treatment as well as in the presence and absence of NOM. All particles were negatively charged at pH 6 as anticipated given the carboxylic functional groups. The ZP was generally unchanged by increasing IS at 10 °C, except for nanoplastic suspensions in 100 mM IS ( $-15.2 \pm 1.1$  mV). This is seen both in the presence and absence of NOM which can be attributed to the screening of the electrical double layer as salt concentration increases. For bare nanoplastics, exposure to 10 FT cycles did not significantly alter the ZP when compared with those kept at 10 °C.

The ZP of nanoplastics in 30 mM NaCl and the presence of NOM ( $-55.5 \pm 7.2$  mV) was more negative compared to nanoplastics in the absence of NOM ( $-22.5 \pm 5.9$  mV). This was also generally observed for nanoplastics subjected to FT in the presence of NOM, although no differences in ZP are observed in 100 mM NaCl. The carboxyl and hydroxyl functional groups present in NOM will impart negative charges on microplastics and nanoplastics, leading to more negative ZPs<sup>18, 41, 42</sup>. We also observed some differences in ZP for the NOM coated nanoplastics when exposed to FT versus 10 °C. For example, after 10 FT cycles, nanoplastics in 30 mM IS + NOM, had a less negative ZP ( $-34.9 \pm 9.3$  mV) compared to those not exposed to FT ( $-55.5 \pm 7.2$  mV). It is important to note that the ZP values for the NP aggregates should be considered with caution as the aggregates are not solid spheres (see Figure 3.1).

### 3.3.2. Proposed mechanism of aggregation upon exposure to freeze-thaw

The formation of large aggregates after exposure to 10 FT cycles occurred irrespective of IS. This is also observed in the presence of NOM, which has been shown to stabilize nanoplastics and other colloids even at high monovalent IS.<sup>18, 43</sup> Previously, FT has been used to intentionally induce the aggregation of nanoparticles.<sup>32</sup> Similarly, Xiang *et al.* found only cryoprotectants (e.g. polyethylene glycols, Tween 20) to be effective in preventing FT induced aggregation of proteins.<sup>44</sup> We therefore hypothesize that aggregation is due to the solute rejection phenomenon in which the ordered crystalline structure of ice rejects impurities (e.g., insoluble particles) during freezing.<sup>45</sup> This increases the local concentration of nanoplastics in the still-unfrozen water,<sup>31, 45</sup> inducing aggregation. When the ice thaws, particles remain aggregated.

### 3.3.3 Nanoplastic transport in the absence of freeze-thaw

Figure 3.3 shows the BTCs for transport experiments conducted in the presence and absence of NOM. In agreement with DLVO theory,<sup>46, 47</sup> nanoplastic deposition increased with IS. Considerable transport ( $C/C_0 = 0.95$  and  $0.72$ ) is observed at low IS (3 and 10 mM NaCl, respectively) (Figure 3.3a). However, as IS increases to 30 and 100 mM, nearly all particles are retained in the column ( $C/C_0 = 0.024$  and  $0.026$ , respectively). Although the size and ZP of the bare nanoplastics in this study are not greatly impacted by increasing IS up to 30 mM (Table 3.1), the ZP of the quartz sand collector in the column has been shown to vary with IS:  $-18.9 \pm 0.3$  mV in 1 mM NaCl vs  $-12.7 \pm 0.5$  mV in 10 mM NaCl.<sup>34</sup> The ZP of the sand grain continuing to approach zero with increasing IS would explain the favorable deposition despite the similar ZP values of the nanoplastics themselves.

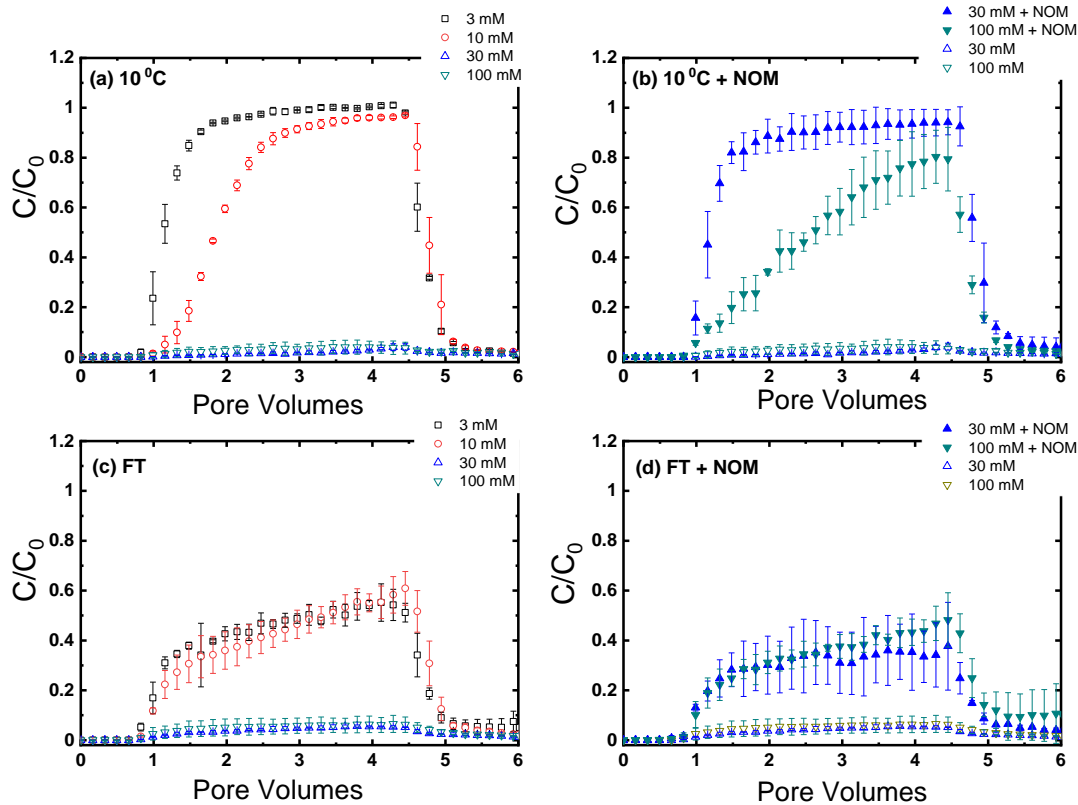


**Figure 3.3.** Breakthrough curves of nanoplastics conducted at (a) 10°C without NOM, (b) 10°C in the presence of NOM, (c) after 10 FT cycles without NOM, (d) after 10 FT cycles in the presence of NOM. Error bars represent standard deviation between duplicate runs.

It is worth noting the different shapes of the BTCs (Figure 3.3a and b) - which can give insight into the governing type of deposition mechanism in the porous medium. Typical BTCs observed in colloid transport studies are either constant, increasing (due to blocking) or decreasing (indicative of straining and/or ripening) with time.<sup>48</sup> Blocking occurs when deposited particles prevent subsequent deposition of incoming particles. Colloids may become physically strained when entrapped in smaller pores between grains, thereby clogging the pores and reducing elution over time. Ripening is a result of multi-layer deposition in which incoming particles are retained on already deposited particles.<sup>48</sup> In some cases, (e.g., 100 mM NaCl + NOM, Figure 3.3b), the BTCs exhibit a pronounced shape that is characteristic of blocking. Similarly, Quevedo and Tufenkji observed increasing BTCs indicative of blocking with 24 nm nanoplastics in 10 mM KCl using the same sand grains.<sup>13</sup> Similar behavior was observed by researchers working with cerium dioxide nanoparticles.<sup>49</sup>

To investigate how the presence of NOM, which is ubiquitous in the environment, would influence transport, 5 mg/L of NOM was added to nanoplastics suspensions of 30 and 100 mM IS. Figure 3.3b compares the BTCs in the presence (closed symbols) versus absence (open symbols) of NOM at 10°C. As previously discussed, bare nanoplastics show almost no elution through the column at 30 mM and 100 mM IS; however, nanoplastic mobility increased significantly in the presence of NOM. Increased retention is observed at 100 mM ( $C/C_0=0.54$ ) compared to 30 mM ( $C/C_0=0.92$ ) which is in agreement with the DLVO theory and consistent with the ZP measured ( $-55.5\pm 7.2$  mV at 30 mM compared to  $-15.0\pm 4.1$  mV at 100 mM). At 100 mM, BTCs characteristic of blocking are observed, though not at 30 mM IS. Interestingly, values of  $C/C_0$  in 30 mM IS + NOM are similar to bare nanoplastics in 3 mM IS (0.95 and 0.92, respectively). This highlights the ability of NOM to increase nanoplastic mobility, even at high IS (typical groundwater IS may reach up to 10 mM monovalent ions and 2 mM divalent ions),<sup>50</sup> and agrees with previous studies.<sup>14, 41, 51</sup> This has been observed in a natural groundwater where suspended organic matter increased the mobility of 50 nm carboxylated nanoplastics compared to the same groundwater where the organic matter had been previously removed.<sup>41</sup> The interaction between NOM and carboxylated PS has been well studied in the literature.<sup>52, 53</sup> NOM interacts with surfaces via electrostatic interaction, hydrophobic interaction or ligand exchange which imparts electrosteric, electrostatic or steric stability on negatively charged nanoparticles.<sup>42, 54, 55</sup> In one particularly relevant recent work, the authors demonstrated significant adsorption of Suwannee River NOM onto PS-COOH using initial NOM concentrations between 1 – 10 mg C/L.<sup>52</sup> This range covers the concentration used in this study (2.6 mg C/L). Additionally, the presence of NOM on sand surfaces has been reported to impart steric stabilization, significantly reducing particle retention.<sup>56</sup> Thus, the stabilizing effect observed at 30 and 100 mM (Figure 3.3b) is not surprising.

#### **3.3.4. Nanoplastic transport after exposure to 10 FT cycles**

Exposure to FT (Figure 3.3c) greatly decreases the transport of bare nanoplastics compared to controls held at 10 °C in 3 and 10 mM IS (Figure 3.3a). This is likely due to the FT-induced aggregation of nanoplastics, resulting in greater deposition. At low IS of 3 and 10 mM, differences in nanoplastic transport can be linked to aggregate size. Nanoplastic aggregates in suspensions held at 10 °C are smaller ( $d_{h,z-avg}$  of  $55\pm 2$  nm and  $46\pm 4$  nm, respectively) and more monodisperse than the suspensions exposed to FT ( $1044\pm 156$  nm and  $582\pm 331$  nm, respectively). At 3 mM,  $C/C_0$  reduces from 0.95 to 0.49 after FT exposure while at 10 mM,  $C/C_0$  reduces from 0.72 to 0.47. At

30 and 100 mM IS, FT does not significantly impact nanoplastic transport as almost complete retention of nanoplastics is observed in the sand column for particles exposed to both temperature pretreatments, even though the particles exposed to FT treatment form much larger aggregates ( $668\pm 85$  and  $612\pm 353$  nm, respectively) than those at  $10\text{ }^{\circ}\text{C}$  ( $46\pm 10$  and  $58\pm 4$  nm, respectively) (Table 3.1). Physical straining is thought to become important when aggregate diameter ( $d_a$ ) to collector diameter ( $d_c$ ) ratios ( $d_a/d_c$ ) are in the range of 0.002 to 0.008 or greater,<sup>17, 57</sup> or when the collector shape is irregular and angular,<sup>58</sup> likely leading to an increase in particle retention. For the  $256\text{ }\mu\text{m}$  collector (grain size) used here, these ratios translate to an aggregate diameter range of 512-2048 nm or greater. Since all  $d_a$  in this work range from  $384\pm 32$  –  $2834\pm 1585$  nm (for FT exposed particles), straining is likely in some cases. However, a decrease in  $C/C_0$  over time is not observed in all cases as would have been expected if physical straining was the dominant mechanism. Perhaps, some of the larger aggregates were entrapped in the pore spaces due to straining, but this does not appear to be the primary reason for the difference between  $10\text{ }^{\circ}\text{C}$  and FT BTCs.

As was observed at  $10\text{ }^{\circ}\text{C}$ , nanoplastic mobility in 30 and 100 mM after FT was greater in the presence of NOM (Figure 3.3d, solid symbols) compared to the absence (Figure 3.3d, open symbols). This can be due to steric stabilization by the NOM as the nanoplastic aggregates form. However, even in the presence of NOM, FT reduces transport which is readily observed when each IS is compared with the equivalent  $10\text{ }^{\circ}\text{C}$  control (Figure S3.4). Therefore, the increase in gravitational sedimentation and interception associated with larger aggregate size following FT outweighs the impact of steric stabilization.

### 3.3.5 Interpreting transport experiments

Attachment efficiencies,  $\alpha$ , calculated from Equation 3.1, are reported in blue and red symbols using both  $d_{h,z\text{-avg}}$  (Figure 3.4a) and  $d_{h,intensity}$  (Figure S3.5b) (Table 3.1). The influence of aggregate size is observed in the slight differences in reported  $\alpha$  values; however, both calculated  $\alpha_{z\text{-avg}}$  and  $\alpha_{int\text{-mean}}$  exhibit the same trend (See Figure S3.5). Thus, we focus on  $\alpha_{z\text{-avg}}$  in this discussion. The stability curves show qualitative agreement with the DLVO theory whereby  $\alpha$  generally increases with IS. For bare nanoplastics at  $10\text{ }^{\circ}\text{C}$ ,  $\alpha_{z\text{-avg}}$  varied over two orders of magnitude ( $\sim 0.004 < \alpha <$

0.25) in the range of 3–100 mM NaCl IS. Even at 100 mM IS,  $\alpha_{z\text{-avg}}$  does not approach unity, the point at which particles would be completely destabilized.

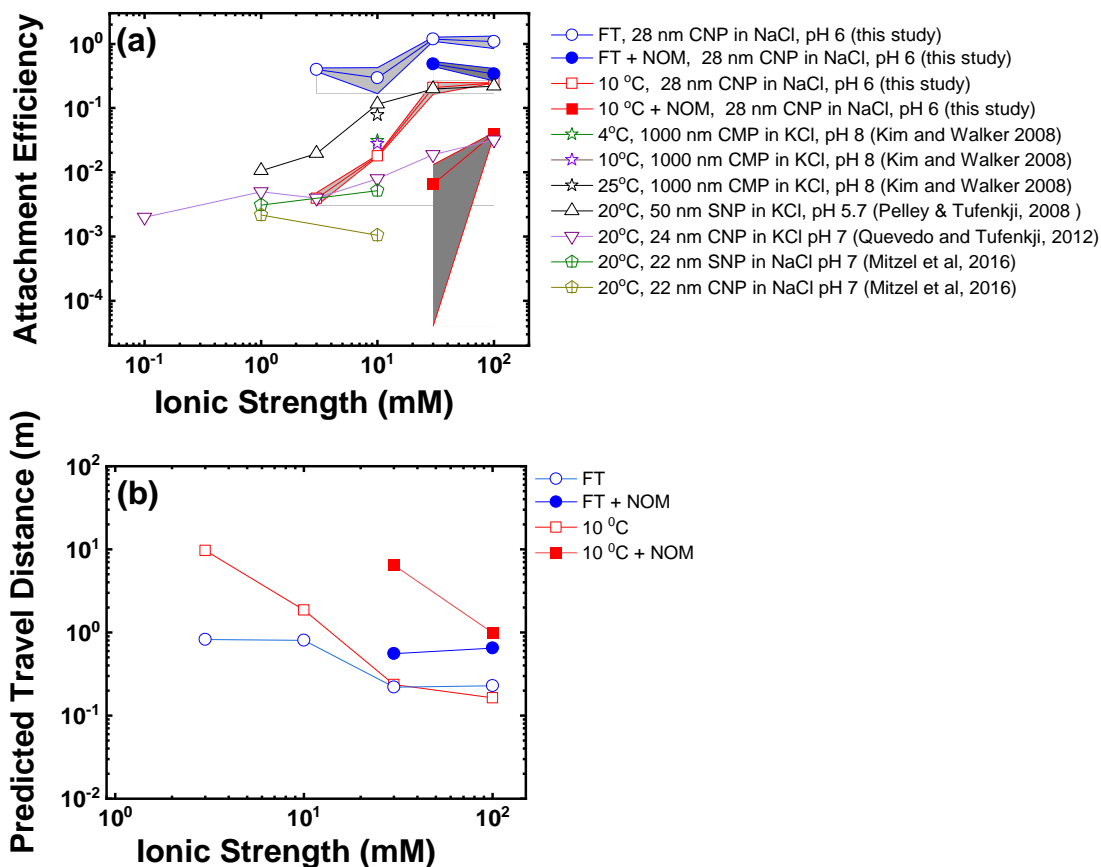


**Figure 3.4.** (a) Attachment efficiency as a function of IS calculated from  $d_{h,z\text{-avg}}$  for different nanoplastics and microplastics across different studies. CNP = carboxyl-modified nanoplastic, CMP = carboxyl-modified microplastic, SNP = sulfate-modified nanoplastics. The shaded regions indicate standard deviation (from duplicate measurement) around the mean for this study. Note that values for 4°C and 10°C from Kim and Walker 2008 overlap. (b) Predicted travel distances as a function of ionic strength at both 10°C and FT conditions.

For nanoplastics exposed to FT (blue symbols),  $\alpha_{z\text{-avg}}$  is significantly higher with more remarkable differences at low IS of 3 and 10 mM when compared to the 10 °C controls. The difference in  $\alpha_{z\text{-avg}}$  for nanoplastics exposed to FT versus 10 °C in 30 and 100 mM is nearly an order of magnitude (Figure 3.4a). Overall, the differences in  $\alpha_{z\text{-avg}}$  highlight the importance of considering FT-induced nanoplastic aggregation when making predictions of nanoplastic transport in cold climates. Under all conditions examined, the presence of NOM significantly reduced the

$\alpha_{z-avg}$  of the nanoplastics. This is consistent with previous studies that have examined the effect of NOM on  $\alpha$ .<sup>18, 42, 51</sup>

The current results are compared with previous studies using quartz sand grains with similar sizes and conducted with negatively charged nanoplastics and microplastics (Figure 3.4a). The  $\alpha$  values reported by Quevedo and Tufenkji are generally lower than this study even though the nanoplastics are relatively the same size and functionalization from the same manufacturer.<sup>13</sup> This can be attributed to the higher pH (pH 7 in their study compared to pH 6 in this study) resulting in significantly larger particle ZPs (-64 mV to -34 mV for 0.1 to 100 mM KCl IS). At 30 and 100 mM IS, the stability curve for 50 nm sulfonated nanoplastics reported by Pelley and Tufenkji at 20 °C is comparable with that at 10 °C in this study.<sup>13, 18</sup> Both studies were carried out at comparable pH but with different particle surface functionalization and size. This explains differences in the ZP (approximately -50 mV to -30 mV for 1-100 mM KCl IS) which is greater than the ZP measured in this work (-25.5±5.4 mV to -15±2 mV for 1-100 mM NaCl IS). The work of Mitzel *et al.* shows lower  $\alpha$  values compared to this study especially at 10 mM and for the carboxyl functionalized nanoplastics. Although Mitzel *et al.* used similarly sized nanoplastics, they worked at pH 7 with larger quartz sand grains. In their work, the ZP of the nanoplastics ranged between -57 mV to -43 mV. Kim and Walker investigated the effect of changing temperatures on the transport of 1000 nm carboxylate PS microplastics in 10 mM KCl and found that  $\alpha$  decreased in the order 25 °C > 10 °C  $\approx$  4 °C.<sup>19</sup> These  $\alpha$  values especially at 25 °C are all higher than this work at 10 °C, however the  $\alpha$  of nanoplastics exposed to FT are higher than those reported by Kim and Walker. Indeed, when comparing  $\alpha$  values at 10 mM, nanoplastics exposed to FT in this work are higher than other reports, which span 3 orders of magnitude. When considering factors that affect  $\alpha$ , we show here that FT has an equal or greater influence on  $\alpha$ . While these studies (Figure 3.4a) have been conducted under several different conditions that make direct comparison difficult, they highlight the significant effect of FT on nanoplastic mobility in model groundwaters.

The predicted particle travel distance can be defined as the depth of packed sand that is required to remove 99.9% of the nanoplastics from the fluid phase and can be used to estimate potential nanoplastic exposures in subsurface environments (Figure 3.4b). Travel distances were calculated using the experimentally determined  $\alpha_{z-avg}$  in Table 3.1 (see Section S3.6 for equation). For the conditions studied, the greatest travel distance was 10 m for bare nanoplastics at 3 mM IS.

We observe a decrease in the travel distance of nanoplastics after exposure to 10 FT cycles at low IS. Following FT, calculated travel distances did not exceed 1 m for any condition. As IS increases, the travel distance for bare nanoplastics exposed to FT and 10 °C converge as the nanoplastics are already destabilized from the high electrolyte concentration. The IS at which this occurs is shifted to higher concentrations in the presence of NOM.

### 3.4 Conclusions

Recent evidence has confirmed the presence of microplastics in groundwater and drinking water from groundwater sources.<sup>59, 60</sup> and the prevalence of nanoplastics, though still unknown, is likely. Meanwhile, the effect of freeze-thaw on the mobility of nanoplastics in the subsurface environment has been largely overlooked. Previous literature looking at warm and cold – though not freezing – temperatures has suggested that drinking water wells in colder climates are at higher risk of nanoplastic and other nanomaterial contamination due to the higher particle mobility observed at lower temperatures.<sup>19, 20, 23, 61</sup> Repeated freeze-thaw cycles are an important weather feature experienced in cold climates with some parts of the world having up to 105 FT cycles annually.<sup>62</sup> Our results, in which exposure of nanoplastics to 10 FT cycles was shown to reduce transport under all conditions, suggest that nanoplastics are more likely to be associated with soils and less likely to undergo long range transport in groundwater in colder climates following freezing temperatures. This has implications in a broader context as emerging research shows that nanoplastics can act as transport vehicles for persistent organic pollutants in saturated porous media.<sup>59</sup> Consequently, this FT-induced change in nanoplastic transport might mitigate the mobility of these organic pollutants. We propose that the increase in deposition following FT observed in this work was driven by the freezing-induced aggregation of nanoplastics in suspension. This was recently observed for TiO<sub>2</sub> nanoparticles where a single FT cycle induced aggregation and reduced transport in otherwise stable suspensions.<sup>30</sup> While the presence of NOM significantly increases nanoplastic mobility, it was not sufficient to counter the impact of FT. Stability tests show that the aggregates formed after FT exposure are not prone to disaggregate even after applying high shear stress, suggesting that they will be stable over longer time scales in the environment. By ignoring the impact of freezing temperatures, transport predictions may overestimate the travel distances of nanoplastics in cold climates. This highlights the need to account for weather patterns when assessing the risks associated with nanoplastic release in aquatic systems.

## Conflicts of interest

There is no conflict of interest.

## Acknowledgements

The authors acknowledge the financial support of the Canada Research Chairs program, the Natural Sciences and Engineering Research Council of Canada (NSERC), the Canada Foundation for Innovation, the Petroleum Technology Development Fund (PTDF) of Nigeria for an award to OSA, McGill University for a MEDA and Eugenie Ulmer-Lamothe award to OSA, and NSERC PURE CREATE for a scholarship to OSA.

## References

1. Pivokonsky, M.; Cermakova, L.; Novotna, K.; Peer, P.; Cajthaml, T.; Janda, V., Occurrence of microplastics in raw and treated drinking water. *Sci. Total Environ.* **2018**, *643*, 1644-1651.
2. Koelmans, A. A.; Mohamed Nor, N. H.; Hermsen, E.; Kooi, M.; Mintenig, S. M.; De France, J., Microplastics in freshwaters and drinking water: Critical review and assessment of data quality. *Water Res.* **2019**, *155*, 410-422.
3. Zubris, K. A. V.; Richards, B. K., Synthetic fibers as an indicator of land application of sludge. *Environ. Pollut.* **2005**, *138* (2), 201-211.
4. Law, K. L.; Moret-Ferguson, S.; Maximenko, N. A.; Proskurowski, G.; Peacock, E. E.; Hafner, J.; Reddy, C. M., Plastic accumulation in the North Atlantic subtropical gyre. *Sci* **2010**, *329* (5996), 1185-8.
5. Panko, J. M.; Chu, J.; Kreider, M. L.; Unice, K. M., Measurement of airborne concentrations of tire and road wear particles in urban and rural areas of France, Japan, and the United States. *Atmos. Environ.* **2013**, *72*, 192-199.
6. Nizzetto, L.; Futter, M.; Langaas, S., Are Agricultural Soils Dumps for Microplastics of Urban Origin? *Environ. Sci. Technol.* **2016**, *50* (20), 10777-10779.
7. Alimi, O. S.; Farner Budarz, J.; Hernandez, L. M.; Tufenkji, N., Microplastics and nanoplastics in aquatic environments: Aggregation, deposition, and enhanced contaminant transport. *Environ. Sci. Technol.* **2018**, *52* (4), 1704-1724.
8. Andrady, A. L., Microplastics in the marine environment. *Mar. Pollut. Bull.* **2011**, *62* (8), 1596-605.
9. Mattsson, K.; Hansson, L. A.; Cedervall, T., Nano-plastics in the aquatic environment. *Environ. Sci. Process Impacts* **2015**, *17* (10), 1712-21.
10. Hernandez, L. M.; Yousefi, N.; Tufenkji, N., Are there nanoplastics in your personal care products? *Environ. Sci. Technol. Lett.* **2017**, *4* (7), 280-285.
11. Hurley, R. R.; Nizzetto, L., Fate and occurrence of micro(nano)plastics in soils: Knowledge gaps and possible risks. *Curr. Opin. in Environ. Sci. Health* **2018**, *1*, 6-11.
12. Duis, K.; Coors, A., Microplastics in the aquatic and terrestrial environment: sources (with a specific focus on personal care products), fate and effects. *Environ. Sci. Eur.* **2016**, *28* (1), 2.
13. Quevedo, I. R.; Tufenkji, N., Mobility of functionalized quantum dots and a model polystyrene nanoparticle in saturated quartz sand and loamy sand. *Environ. Sci. Technol.* **2012**, *46* (8), 4449-57.

14. Petosa, A. R.; Jaisi, D. P.; Quevedo, I. R.; Elimelech, M.; Tufenkji, N., Aggregation and deposition of engineered nanomaterials in aquatic environments: role of physicochemical interactions. *Environ. Sci. Technol.* **2010**, *44* (17), 6532-49.
15. Tufenkji, N.; Elimelech, M., Correlation equation for predicting single-collector efficiency in physicochemical filtration in saturated porous media. *Environ. Sci. Technol.* **2004**, *38* (2), 529-36.
16. Bradford, S. A.; Bettahar, M., Concentration dependent transport of colloids in saturated porous media. *J. Contam. Hydrol.* **2006**, *82* (1-2), 99-117.
17. Bradford, S. A.; Yates, S. R.; Bettahar, M.; Simunek, J., Physical factors affecting the transport and fate of colloids in saturated porous media. *Water Resour. Res.* **2002**, *38* (12), 63-12.
18. Pelley, A. J.; Tufenkji, N., Effect of particle size and natural organic matter on the migration of nano- and microscale latex particles in saturated porous media. *J. Colloid Interface Sci.* **2008**, *321* (1), 74-83.
19. Kim, H. N.; Walker, S. L., *Escherichia coli* transport in porous media: influence of cell strain, solution chemistry, and temperature. *Colloids Surf. B. Biointerfaces* **2009**, *71* (1), 160-7.
20. Sasidharan, S.; Torkzaban, S.; Bradford, S. A.; Cook, P. G.; Gupta, V., Temperature dependency of virus and nanoparticle transport and retention in saturated porous media. *J. Contam. Hydrol.* **2017**, *196*, 10-20.
21. Bense, V.; Kooi, H., Temporal and spatial variations of shallow subsurface temperature as a record of lateral variations in groundwater flow. *J. Geophys. Res. Solid Earth* **2004**, *109* (B4).
22. Yan, Z.; Huang, X.; Yang, C., Deposition of colloidal particles in a microchannel at elevated temperatures. *Microfluid. Nanofluid.* **2014**, *18* (3), 403-414.
23. Wang, M.; Gao, B.; Tang, D.; Yu, C., Concurrent aggregation and transport of graphene oxide in saturated porous media: Roles of temperature, cation type, and electrolyte concentration. *Environ. Pollut.* **2018**, *235*, 350-357.
24. Bales, R. C.; Li, S.; Yeh, T. C. J.; Lenczewski, M. E.; Gerba, C. P., Bacteriophage and microsphere transport in saturated porous media: Forced-gradient experiment at Borden, Ontario. *Water Resour. Res.* **1997**, *33* (4), 639-648.
25. Castro, F. D.; Tufenkji, N., Relevance of nontoxigenic strains as surrogates for *Escherichia coli* O157:H7 in groundwater contamination potential: role of temperature and cell acclimation time. *Environ. Sci. Technol.* **2007**, *41* (12), 4332-8.
26. Asadishad, B.; Ghoshal, S.; Tufenkji, N., Role of cold climate and freeze-thaw on the survival, transport, and virulence of *Yersinia enterocolitica*. *Environ. Sci. Technol.* **2013**, *47* (24), 14169-77.
27. Rocard, J. M.; Asadishad, B.; Samonte, P. R. V.; Ghoshal, S.; Tufenkji, N., Natural freeze-thaw cycles may increase the risk associated with *Salmonella* contamination in surface and groundwater environments. *Water Res. X* **2018**, *1*, 100005.
28. Hakimzadeh, A.; Okshevsky, M.; Maisuria, V.; Deziel, E.; Tufenkji, N., Exposure to Freeze-Thaw Conditions Increases Virulence of *Pseudomonas aeruginosa* to *Drosophila melanogaster*. *Environ. Sci. Technol.* **2018**, *52* (24), 14180-14186.
29. Asadishad, B.; Olsson, A. L.; Dusane, D. H.; Ghoshal, S.; Tufenkji, N., Transport, motility, biofilm forming potential and survival of *Bacillus subtilis* exposed to cold temperature and freeze-thaw. *Water Res.* **2014**, *58*, 239-47.

30. Farner, J. M.; De Tommaso, J.; Mantel, H.; Cheong, R. S.; Tufenkji, N., Effect of freeze/thaw on aggregation and transport of nano-TiO<sub>2</sub> in saturated porous media. *Environ. Sci. Nano* **2020**.
31. Barb, W. G.; Mikucki, W., On the coagulation of polymer latices by freezing and thawing. *J. Polym. Sci.* **1959**, *37* (132), 499-514.
32. Chou, K.-S.; Liu, H.-L.; Kao, L.-H.; Yang, C.-M.; Huang, S.-H., A novel granulation technique using a freeze–thaw method. *Ceram. Int.* **2014**, *40* (6), 8875-8878.
33. Lowry, G. V.; Hill, R. J.; Harper, S.; Rawle, A. F.; Hendren, C. O.; Klaessig, F.; Nobbmann, U.; Sayre, P.; Rumble, J., Guidance to improve the scientific value of zeta-potential measurements in nanoEHS. *Environmental Science: Nano* **2016**, *3* (5), 953-965.
34. Mitzel, M. R.; Sand, S.; Whalen, J. K.; Tufenkji, N., Hydrophobicity of biofilm coatings influences the transport dynamics of polystyrene nanoparticles in biofilm-coated sand. *Water Res.* **2016**, *92* (7), 113-20.
35. Yao, K.-M.; Habibian, M. T.; O'Melia, C. R., Water and waste water filtration. Concepts and applications. *Environ. Sci. Technol.* **1971**, *5* (11), 1105-1112.
36. Domingos, R. F.; Baalousha, M. A.; Ju-Nam, Y.; Reid, M. M.; Tufenkji, N.; Lead, J. R.; Leppard, G. G.; Wilkinson, K. J., Characterizing manufactured nanoparticles in the environment: multimethod determination of particle sizes. *Environ. Sci. Technol.* **2009**, *43* (19), 7277-84.
37. Bhattacharjee, S., DLS and zeta potential - What they are and what they are not? *J. Control Release* **2016**, *235*, 337-351.
38. Farner, J. M.; Cheong, R. S.; Mahé, E.; Anand, H.; Tufenkji, N., Comparing TiO<sub>2</sub> nanoparticle formulations: stability and photoreactivity are key factors in acute toxicity to *Daphnia magna*. *Environ. Sci. Nano* **2019**, *6* (8), 2532-2543.
39. Probes, M., Working With Fluospheres® Fluorescent Microspheres. Technologies, M. P. I. D., Ed. 2004.
40. Malvern *Dynamic Light Scattering - Common Terms Defined*; 2011.
41. Song, Z.; Yang, X.; Chen, F.; Zhao, F.; Zhao, Y.; Ruan, L.; Wang, Y.; Yang, Y., Fate and transport of nanoplastics in complex natural aquifer media: Effect of particle size and surface functionalization. *Sci. Total Environ.* **2019**, *669*, 120-128.
42. Franchi, A.; O'Melia, C. R., Effects of natural organic matter and solution chemistry on the deposition and reentrainment of colloids in porous media. *Environ. Sci. Technol.* **2003**, *37* (6), 1122-9.
43. Saleh, N. B.; Pfefferle, L. D.; Elimelech, M., Influence of biomacromolecules and humic acid on the aggregation kinetics of single-walled carbon nanotubes. *Environ. Sci. Technol.* **2010**, *44* (7), 2412-8.
44. Xiang, H.; Chan, D.; Bates, R., Minimization of Freeze/Thaw-Induced Protein aggregation and optimization of a drug substance formulation matrix. *BioPharm. Int.* **2015**, *28* (8), 30-37.
45. Halde, R., Concentration of impurities by progressive freezing. *Water Res.* **1980**, *14* (6), 575-580.
46. Verwey, E. J. W.; Overbeek, J. T. G.; Nes, K. v., Theory of the stability of lyophobic colloids : the interaction of sol particles having an electric double layer. **1948**.
47. Derjaguin, B.; Landau, L., Theory of the stability of strongly charged lyophobic sols and of the adhesion of strongly charged particles in solutions of electrolytes. *Prog. Surf. Sci.* **1993**, *43* (1-4), 30-59.

48. Liu, D.; Johnson, P. R.; Elimelech, M., Colloid deposition dynamics in flow-through porous media: role of electrolyte concentration. *Environ. Sci. Technol.* **1995**, *29* (12), 2963-73.
49. Petosa, A. R.; Öhl, C.; Rajput, F.; Tufenkji, N., Mobility of nanosized cerium dioxide and polymeric capsules in quartz and loamy sands saturated with model and natural groundwaters. *Water Res.* **2013**, *47* (15), 5889-5900.
50. Busenberg, E.; Plummer, N.; Doughten, M. W.; Widman, P. K.; Bartholomay, R. C. *Chemical and isotopic composition and gas concentrations of ground water and surface water from selected sites at and near the Idaho National Engineering and Environmental Laboratory, Idaho, 1994-97; 2000-81; 2000.*
51. Deshiikan, S. R.; Eschenazi, E.; Papadopoulos, K. D., Transport of colloids through porous beds in the presence of natural organic matter. *Colloids Surf. A. Physicochem Eng. Asp.* **1998**, *145* (1), 93-100.
52. Yu, S.; Shen, M.; Li, S.; Fu, Y.; Zhang, D.; Liu, H.; Liu, J., Aggregation kinetics of different surface-modified polystyrene nanoparticles in monovalent and divalent electrolytes. *Environ. Pollut.* **2019**, *255*, 113302.
53. Wu, J.; Jiang, R.; Lin, W.; Ouyang, G., Effect of salinity and humic acid on the aggregation and toxicity of polystyrene nanoplastics with different functional groups and charges. *Environ. Pollut.* **2019**, *245*, 836-843.
54. Aiken, G. R.; Hsu-Kim, H.; Ryan, J. N., Influence of Dissolved Organic Matter on the Environmental Fate of Metals, Nanoparticles, and Colloids. *Environ. Sci. Technol.* **2011**, *45* (8), 3196-3201.
55. Philippe, A.; Schaumann, G. E., Interactions of Dissolved Organic Matter with Natural and Engineered Inorganic Colloids: A Review. *Environ. Sci. Technol.* **2014**, *48* (16), 8946-8962.
56. Johnson, W. P.; Logan, B. E., Enhanced transport of bacteria in porous media by sediment-phase and aqueous-phase natural organic matter. *Water Res.* **1996**, *30* (4), 923-931.
57. Xu, S.; Gao, B.; Saiers, J. E., Straining of colloidal particles in saturated porous media. *Water Resources Research* **2006**, *42* (12).
58. Tufenkji, N.; Miller, G. F.; Ryan, J. N.; Harvey, R. W.; Elimelech, M., Transport of Cryptosporidium Oocysts in Porous Media: Role of Straining and Physicochemical Filtration. *Environ. Sci. Technol.* **2004**, *38* (22), 5932-5938.
59. Panno, S. V.; Kelly, W. R.; Scott, J.; Zheng, W.; McNeish, R. E.; Holm, N.; Hoellein, T. J.; Baranski, E. L., Microplastic Contamination in Karst Groundwater Systems. *Ground Water* **2019**, *57* (2), 189-196.
60. Mintenig, S. M.; Loder, M. G. J.; Primpke, S.; Gerdt, G., Low numbers of microplastics detected in drinking water from ground water sources. *Sci. Total Environ.* **2019**, *648*, 631-635.
61. Elimelech, M.; Gregory, J.; Jia, X., *Particle deposition and aggregation : Measurement, modelling, and simulation.* Butterworth-Heinemann: Oxford, England, 1995; p 448.
62. NOAA/NCDC, Engineering Weather Data. Air Force Combat Climatology Center (AFCCC) 2000.

### 3.5 Supporting information

#### S3.1: Temperature profile.

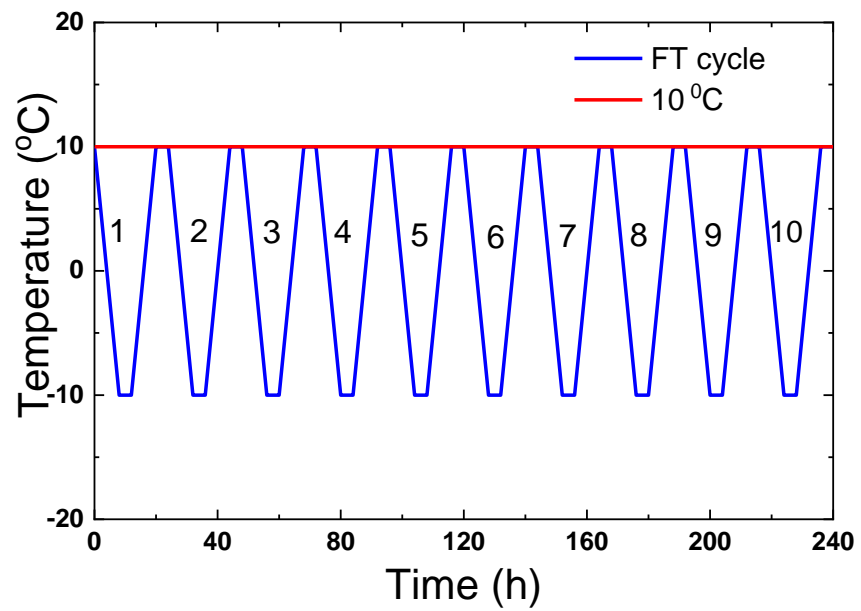
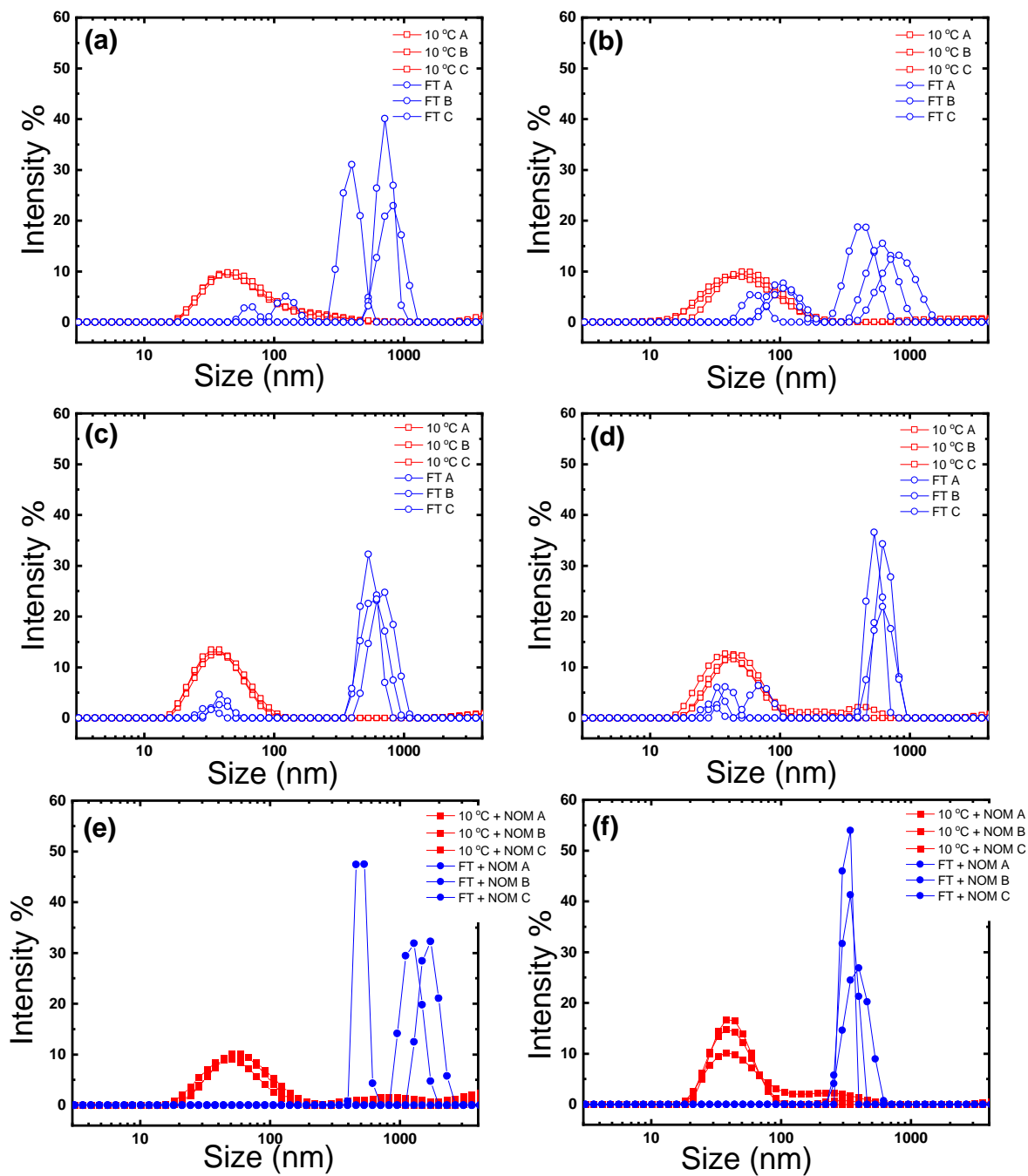


Figure S3.1. Temperature profiles for 10 °C and FT pretreatments.

### S3.2: Representative DLS intensity size distributions



**Figure S3.2.** Representative intensity weighted particle size distribution of 20 nm PS before and after FT treatment (a) 3 mM (b) 10 mM (c) 30 mM (d) 100 mM (e) 30 mM + NOM (f) 100 mM + NOM. Plots indicate triplicate measurements of the same sample suspension.

### S3.3: Particle size distributions

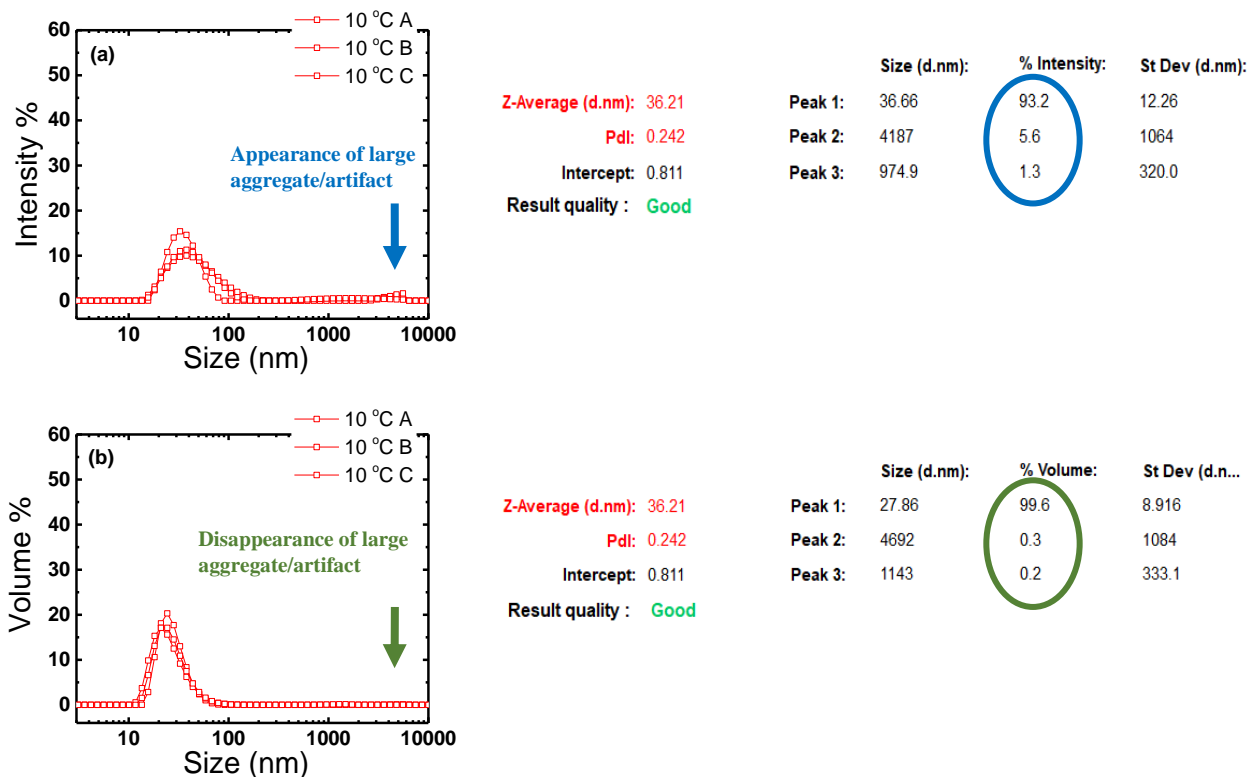


**Figure S3.3.** Representative (a) intensity particle size distribution versus (b) volume particle size distribution in 10 mM IS at 10 °C highlighting the insignificance of large aggregates or artifacts above 2000 nm. Plots indicate triplicate measurements of the same sample suspension.

As stated in the main text, when the intensity weighted PSD indicated the presence of a small sub-population of aggregates at large sizes (e.g. > 2,000 nm) at 10 °C, the peak having up to 90% of the particle population was used as the  $d_{h, \text{intensity}}$ . This peak corresponds to the vast majority of particles in suspension, which is of greatest interest in the column experiments. A very small number of large aggregates will skew the overall intensity weighted average size of the suspension to larger sizes since scattering scales to the 6<sup>th</sup> power<sup>1</sup>. The relative influence of this can be observed if the number or intensity or volume weighted PSD is plotted as a function of size<sup>2</sup>. From Figure S3.3, we clearly see that the contribution of such peaks is very small in terms of concentration. We therefore infer that such peaks may be artifacts.

**S3.4: Breakthrough curve highlighting the effect of natural organic matter (10 °C versus FT)**

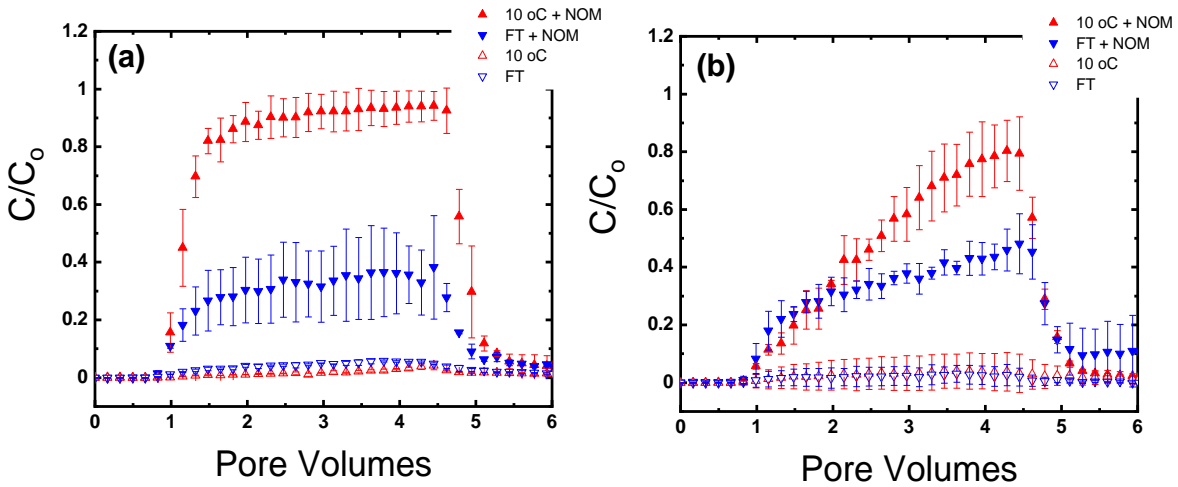


**Figure S3.4.** Breakthrough curve of the NPs in (a) 30 mM and (b) 100 mM NaCl highlighting the effect of FT in the presence of NOM.

**S3.5: Stability curve of nanoplastics using different DLS sizes.**

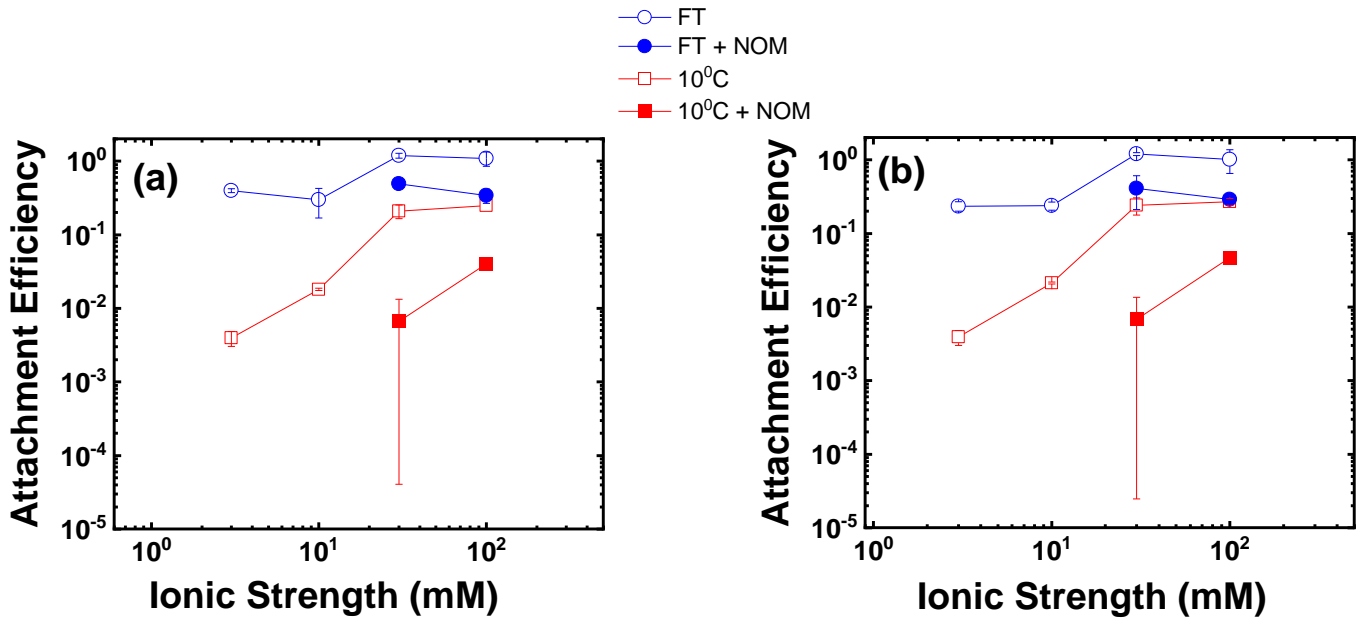


**Figure S3.5.** Attachment efficiency as a function of ionic strength calculated using (a) DLS hydrodynamic Z-average,  $d_{h, Z\text{-avg}}$  and (b) DLS hydrodynamic intensity mean,  $d_{h, intensity}$ .

### S3.6: Predicted travel distance

The predicted travel distance is given as <sup>3</sup>;

$$L_{99} = -\ln\left(\frac{C}{C_0}\right) \left(\frac{2d_c}{3(1-\theta)\alpha\eta_0}\right)$$

- $L_{99}$ : filtration distance required to achieve 99.9% removal  
 $\alpha$ : attachment efficiency  
 $d_c$ : grain size  
 $C/C_0$ : concentration in the effluent (set to 0.001)  
 $\theta$ : porosity  
 $\eta_0$ : single-collector contact efficiency

### S3.7. Parameters used in calculating attachment efficiency.

Porous medium porosity	0.43
Collector diameter	0.256 mm
Fluid approach velocity	$7.5 \times 10^{-5}$ m/sec
Particle density	1055 kg/m <sup>3</sup>
Temperature	283 K
Hamaker constant <sup>4</sup>	$1.0 \times 10^{-20}$ J

### References

1. Domingos, R. F.; Baalousha, M. A.; Ju-Nam, Y.; Reid, M. M.; Tufenkji, N.; Lead, J. R.; Leppard, G. G.; Wilkinson, K. J., Characterizing manufactured nanoparticles in the environment: multimethod determination of particle sizes. *Environ. Sci. Technol.* **2009**, *43* (19), 7277-84.
2. Stetefeld, J.; McKenna, S. A.; Patel, T. R., Dynamic light scattering: a practical guide and applications in biomedical sciences. *Biophys Rev* **2016**, *8* (4), 409-427.
3. Elimelech, M.; Gregory, J.; Jia, X., *Particle deposition and aggregation : Measurement, modelling, and simulation*. Butterworth-Heinemann: Oxford, England, 1995; p 448.
4. Esumi, K., *Polymer interfaces and emulsions*. CRC Press: 1999.

## **Preamble to Chapter 4**

The critical literature review in chapter 2 revealed that the effect of natural organic matter on nanoplastic stability is sparse, which precludes a holistic understanding of nanoplastics transformation in aquatic environments. There are also limited studies investigating the stability of nanoplastics in more complex heterogenous matrices with no quantitative data of their behaviour in these systems. The bulk of the reviewed aggregation literature often relies on using unrealistically high plastic: natural organic matter concentration which may overestimate their true fate in the natural environment. Therefore, the goal of this chapter was to understand the mechanisms by which different environmental organic matter interact with nanoplastics of different sizes at realistic relative plastic to organic matter concentrations. The stability of nanoplastics was also investigated in natural waters with increasing salinity gradients and compared to the synthetic water matrices often used in laboratory studies. Lastly, the interaction of nanoplastics/nanoplastic aggregate with silica which is ubiquitous in the marine environment was examined.

The findings from this chapter has been prepared for submission in *Water Research*.

## **Chapter 4: Mechanistic Understanding of the Aggregation Kinetics of Nanoplastics in Marine Environments**

### **Abstract**

Plastics that existing below the submicron scale have been detected in the oceans and their transformations will control their fate and bioavailability. In this study, the initial aggregation kinetics of two different sizes of polystyrene nanoplastics: 28 nm (NP<sub>28</sub>) and 220 nm (NP<sub>220</sub>), were investigated using time-resolved dynamic light scattering. The stability of the plastics was evaluated in the presence and absence of three natural organic matters (NOM) – the Suwannee River humic acid (HA) and fulvic acid (FA), and the biopolymer alginate (AL) – and in varying concentrations of divalent salt – including in artificial seawater (ASW) and natural surface water (NW) with varying salinities. In the absence of NOM, the critical coagulation concentration (CCC) in CaCl<sub>2</sub> was independent of particle size, however, the addition of HA enhanced aggregation via bridging regardless of the size of the plastics. In contrast, the interaction of the plastics with alginate was size dependent. In CaCl<sub>2</sub>, alginate appeared to enhance aggregation by encapsulation for NP<sub>28</sub> and gel bridging for NP<sub>220</sub>, while FA had little or no effect. In ASW, HA enhanced the aggregation of NP<sub>220</sub> while alginate was seen to stabilize the particle suspension. Generally, the effects of the three NOM were more pronounced for the NP<sub>220</sub> as compared to the NP<sub>28</sub>. While there were no significant differences in the attachment efficiencies of the bare nanoplastics in either CaCl<sub>2</sub> or in ASW, the NP<sub>220</sub> was more stable than NP<sub>28</sub> in the natural seawater matrix. Finally, in CaCl<sub>2</sub>, the interaction of nanoplastic aggregates with a model silica surface was less repulsive in the presence of AL and HA than FA. This study highlights the importance of considering the interplay of different particle sizes and realistic complex water chemistries when assessing the fate of plastics in the marine environment.

## 4.1 Introduction

A recent estimate shows that the marine environment is a large sink for plastics, receiving between 4.8 – 12.7 million metric tons in 2010.<sup>1</sup> Environmental degradation and fragmentation generates microplastics and nanoplastics,<sup>2</sup> that have been documented globally in the marine environment<sup>3</sup> and raised both environmental and public health concerns. Recent studies have detected microplastics in the tissues and intestinal tracts of marine organisms<sup>5</sup> and have reported on their trophic transfer,<sup>6</sup> which can potentially be passed on to humans. In addition to entering the food web, plastic particles have been reported to adversely affect the health of marine biota due to neurotoxicity, oxidative stress,<sup>7</sup> reduced feeding,<sup>8</sup> bioaccumulation of pollutants,<sup>9</sup> and other causes. Several ecotoxicological studies have highlighted that the size of a plastic particle will determine its potential to interact with aquatic biota, including its ability to be taken up and retained by an organism, or to be translocated into organs. Specifically, smaller plastic particles are often reported to be more toxic than larger ones due to easier passage/uptake.<sup>10</sup> A few studies have shown that organisms will take up nanoplastics smaller than their primary food size.<sup>11</sup> Hence, understanding the fate of nanoplastics and microplastics in the marine environment is important for accurate risk assessments.

When nanoplastics and microplastics are released into the aquatic environment, they may undergo several processes and transformations, amongst which is aggregation.<sup>12, 13</sup> Aggregation will change the apparent size of plastics, which in turn determines their mobility, bioavailability and effects. To quantitatively assess the aggregation kinetics of the particles, particle-particle attachment efficiencies ( $\alpha$ ) and the critical coagulation efficiencies (CCC, *i.e.*, the concentration of electrolyte where aggregation transitions from being reaction-limited to diffusion-limited) are often used. These parameters are described by the classical Derjaguin–Landau–Verwey–Overbeek (DLVO) theory.<sup>14</sup> The role of ionic strength, pH, the presence of natural organic matter (NOM), and temperature on the stability of plastic particles have been recently studied in simulated and natural waters.<sup>15-17</sup> However, the impact of size on the CCC of plastic particles remains unclear. A few studies have examined how size affects the aggregation of other nanoparticles in the absence of NOM, however, they have reported contradictory conclusions. For example, two studies observed a decrease of CCC with decreasing particle size,<sup>18, 19</sup> while others reported either an increase in CCC with a decrease in size,<sup>20, 21</sup> or a CCC that independent of size.<sup>22</sup> Furthermore, since different particle compositions will have different Hamaker constants (which governs van

der Waals attractions),<sup>13</sup> the conclusions gained from these nanoparticles may not necessarily be applicable to plastic particles.

The composition of natural organic matter (NOM) in marine systems is complex and location dependent but is comprised of humic substances, and polysaccharides<sup>23</sup> which can play important roles in the fate and persistence of colloidal particles. While several studies have examined the effects of humic and fulvic acids on the behavior of plastic particles in model single cation water matrices, there still exist important knowledge gaps, especially in complex waters. For example, the effect of particle size in the presence of the different kinds of NOM is unknown. NOM molecules are expected to far outnumber plastic particles in marine systems,<sup>24</sup> yet, most microplastic aggregation studies use unrealistically high plastic/NOM ratios. Also, the effect of algal polysaccharides, such as alginate, on the aggregation of plastics is unclear. In complex ion mixtures, as found in the marine environment, it is unknown how plastics of different sizes will interact with polysaccharides, which may be at high concentrations during seasonal algal blooms. Even though alginate have been reported to destabilize nanoparticles when in the presence of divalent ions and stabilize them when in the presence of monovalent ions, the mechanism is unknown, especially with particles of different sizes. Moreover, no study has quantitatively and systematically compared the aggregation kinetics of nanoplastics in synthetic versus natural waters. A few studies<sup>25, 26</sup> have examined the effect of the presence of alginate on single sizes of nanoplastics, however, these studies have been conducted in single cation systems.

Following aggregation, plastic aggregates may come in contact with coastal sediments or suspended colloidal aggregates (*e.g.* during seawater intrusion events). For example, in marine systems, plastic aggregates can interact with silica particles to form larger heteroaggregates. Larger and denser plastic aggregates can also settle in the water column where they can interact with larger SiO<sub>2</sub> sediments.<sup>27</sup> This has been shown for other particulate contaminants<sup>28-30</sup> although how this process might influence the fate of plastics in natural waters is unclear.

Therefore, the main objective of this study was to systematically investigate the effects of NOM on the aggregation of different sized nanoplastics in increasingly complex water matrices (both simulated and natural). A second objective of this work was to examine the impact of NOM on nanoplastic interactions with a model Si surface using an optical NanoTweezer. Low concentrations of carboxylated polystyrene nanobeads (28 and 220 nm) were used as model

nanoplastics<sup>2</sup> to ensure that plastic/NOM ratios were as realistic as possible with respect to marine systems. Carboxylated plastics were chosen as a proxy to reflect the oxidation state of environmental plastics<sup>31</sup> and the uniform, negative surface charge allows a mechanistic insight into the interactions of different types of NOM.

## **4.2 Materials and methods**

### **4.2.1 Preparation of water samples and aqueous suspensions of the plastics**

Stock suspensions of carboxylated polystyrene model nanoplastics called NP<sub>28</sub> (nominally 28 nm, based upon data the manufacturer and confirmed by transmission electron microscopy) and NP<sub>220</sub> (220 nm) were obtained from Thermo Fisher (Lots# 1790453 and 1820029, respectively). Fifty mg/L stock suspensions were prepared by diluting the NP<sub>28</sub> and NP<sub>220</sub> in filtered reverse osmosis water (Biolab Scientific). Prior to each experimental run, the concentrated suspension was vortexed for ~30 seconds and then diluted to the working concentration of 2 mg/L ( $1.65 \times 10^{11}$  and  $3.4 \times 10^8$  particles/mL for NP<sub>28</sub> and NP<sub>220</sub>, respectively; see Table S4.1).

Sodium alginate (AL), extracted from brown algae was purchased from Sigma-Aldrich. Suwannee River humic acid III (HA) and Suwannee River fulvic acid II (FA) were obtained from the International Humic Substances Society. One hundred mg/L stock solutions of all three NOM were prepared, by raising the pH of the stock solution to ~10 (to ensure complete solubilization) prior to their dilution to concentrations that were more representative of natural seawater (i.e. 1 and 10 mg/L).<sup>23</sup> The total organic carbon (TOC) content of the stock solutions was determined using a TOC analyzer (TOC-VCPN, Shimadzu, Japan) as 45, 54, and 28 mg C/L for the HA, FA, and AL, respectively. In the natural environment, [NOM]:[plastic] are expected to be high (up to 10,000).<sup>32</sup> To be environmentally relevant, the working NOM concentration chosen at 10 mg/L ensured a [NOM]:[plastic] ratio of 5 which is far greater than ratios used in the literature.

Aggregation kinetics of the nanoplastics were studied in the presence of divalent salts (CaCl<sub>2</sub>, Sigma-Aldrich), artificial seawater (ASW) and several natural surface waters (NW). Because the same concentration of a divalent salt has a higher impact as compared to a monovalent ion, we focus on Ca<sup>2+</sup> when making comparisons between the ASW and NW. Additionally, Ca<sup>2+</sup> has a unique behavior which can favor aggregation in the presence of HA and alginate via bridging.<sup>33</sup> A stock electrolyte of 500 mM CaCl<sub>2</sub> was used for dilutions. ASW was prepared by diluting 40 g of artificial sea salts (Sigma-Aldrich, Lot #SLBX3050, Table S4.1) in 1 L of filtered reverse

osmosis water (Biolab Scientific). Before use, the pH in each working suspension was adjusted to  $8 \pm 0.5$  (representative of seawater<sup>34</sup>) with 0.1 mM NaOH. Finally, four natural surface water samples were collected in the St. Lawrence River (QC, Canada), between August and September 2020, filtered through 300  $\mu\text{m}$  nylon mesh (McMaster-Carr, USA) then stored at 4°C before use. The sampling locations spanned from Montreal to Cacouna (low/freshwater salinity to high/close to seawater salinity) with sample points (named NW1, NW2, NW3, NW4) having <0.2, 17.1, 34.8 and 34.2 practical salinity units, respectively and 1.9, 0.3, 0.1 and 0.2 mg/L dissolved organic carbon, respectively. Details on the sampling sites and the physicochemical properties of the samples are provided in Table S4.2.

## 4.2.2 Nanoplastic aggregation

### 4.2.2.1 Aggregation experiments

Time-resolved dynamic light scattering (DLS) measurements, which monitored the evolution of the hydrodynamic size of the particles were performed using a Malvern Zetasizer Nano ZS (Malvern Panalytical) with a laser source of 633 nm and a detection angle of 173°. Z-average hydrodynamic ( $D_h$ ) diameters were collected over 30 min at 30 sec intervals. To simulate the release of nanoplastics into the environment, stock solutions of the NOM and salts were premixed into a cuvette, and particles were added as the last item (total volume of 1 mL before each DLS measurement). Prior to use, cuvettes were cleaned with filtered reverse osmosis water. Electrophoretic mobilities (EPM) were measured by laser Doppler velocimetry using the same equipment. Each experimental condition was repeated three times in order to evaluate reproducibility.

### 4.2.2.2 Determination of aggregation rate

The initial increase in  $D_h$ , obtained through a linear least squares regression analysis, was used to compute the aggregation rate constant ( $k$ ),

$$k \propto \frac{1}{N_0} \left( \frac{dD_h(t)}{dt} \right)_{t \rightarrow 0} \quad (4.1)$$

where  $N_0$  is the initial particle concentration. In some cases, the aggregation profile did not capture the initial primary particle sizes (limitations of the instrument) because aggregation was too fast. In these cases of extremely rapid aggregation, the slope of the initial linear part of the data capturing only a few data points was used to calculate  $k$ , as has been widely done previously in the aggregation literature.<sup>15, 26, 35, 36</sup> Particle-particle attachment efficiencies,  $\alpha$ , were then obtained by

normalizing aggregation rates,  $k$ , to the rate at which particles were fully destabilized,  $k_{fast}$  (diffusion limited aggregation; Equation 4.2). Aggregation rates are often reaction-limited (RLA) (i.e.  $\alpha < 1$ ) at low ionic strengths, while diffusion limited aggregation (DLA) occurs more often at high salt concentrations. The transition between these two regimes represents the critical coagulation concentration (CCC).

$$\alpha = \frac{1}{W} = \frac{k}{k_{fast}} = \frac{\frac{1}{N_0} \left( \frac{dD_h(t)}{dt} \right)_{t \rightarrow 0}}{\frac{1}{(N_0)_{fast}} \left( \frac{dD_h(t)}{dt} \right)_{t \rightarrow 0, fast}} \quad (4.2)$$

In Eq 4.2,  $W$  is the stability ratio. In this study,  $N_0$  can be ignored in equations (1) and (2) given that the initial particle number concentration was the same in all experiments, for both particle sizes. For each water type tested,  $k$  was normalized with the  $k_{fast}$  obtained in  $\text{CaCl}_2$  in the absence of NOM.

#### 4.2.2.3 Aggregate microstructure

The size and morphology of  $\text{NP}_{28}$  and  $\text{NP}_{220}$  were determined by transmission electron microscopy (TEM, FEI Technai 120 kV TEM) coupled with a Gatan Ultrascan 4000 4k×4k CCD camera. TEM was performed on suspensions deposited onto thin carbon film grids (Pacific Grid-Tech, 300 mesh, 3.05 mm O.D., hole size). The drop cast suspension was allowed to sit a few min before the excess liquid was wicked away using a Whatman filter paper and the grid was allowed to dry at room temperature.

#### 4.2.3 Probing nanoplastic interactions with silica

To better understand how nanoplastics might interact with a silica surface such as suspended or sedimented silica in a water matrix, an optical tweezer (NanoTweezer, Optofluidics, Philadelphia) was used to determine nanoplastic-Si interaction energy profiles in the presence of the 3 NOM types (see Table S4.3 and Section S4.1 for details on the operation of the optical tweezer). Following methods previously described<sup>37</sup> measurements with the NanoTweezer were taken by flowing the particle suspension through a silica chip (within 30 min of sample preparation).  $\text{NP}_{220}$  were introduced to an already mixed electrolyte (working  $\text{CaCl}_2$  concentration of 0.5 mM) with and without NOM. The  $\text{NP}_{220}$  suspension was introduced into the silica chip at a rate of 0.2  $\mu\text{L}/\text{min}$  and the laser power was increased in 0.5 mW increments, until particle entrapment. Sixty 30 sec videos, were acquired and analyzed using Fiji ImageJ. At least 45 particles were tracked in each

experiment and a minimum of 3000 measurements/particle track were collected. Each experimental condition was repeated three times. With the information obtained from the recorded videos, the parameters  $A$  and  $\lambda_D$  in the electrostatic interaction equation (Eq. S4.1) could be calculated for each plastic-NOM-surface combination. Videos of 1 mg/L NOM and 0.5 mM CaCl<sub>2</sub> (no plastic particles), taken at the maximum laser power (for highest trapping efficiency), were used as negative controls in order to confirm that the scattering of NOM molecules was negligible.

## 4.3 Results and discussions

### 4.3.1 Aggregation kinetics in the absence of organic matter

Both NP<sub>220</sub> and NP<sub>28</sub> formed aggregates in suspension (Figure 4.1a, b). Indeed, for the bare NP<sub>220</sub> and NP<sub>28</sub> in 1–30 mM CaCl<sub>2</sub>, a typical aggregation profile can be seen in Figure 4.1c, in the absence of organic matter. At 1 mM CaCl<sub>2</sub>, both dispersions were quite stable over 30 min. As the electrolyte concentration increased to 5 mM CaCl<sub>2</sub>, a significant increase in aggregation rate was observed for NP<sub>28</sub>. At 30 mM, the mean hydrodynamic diameter of the particles increased further, and the dispersions were completely destabilized. Increasing the salt concentration to 100 mM did not result in any significant increase in hydrodynamic size compared to 30 mM (Figure S4.1), which suggested that aggregation was diffusion limited. As the CaCl<sub>2</sub> concentration increased from 1 to 10 mM, the magnitude of the EPM decreased for both particle sizes and approached 0  $\mu\text{m}\cdot\text{cm}/\text{V}\cdot\text{s}$  (Figure 4.2). This phenomenon can be attributed to a screening of the particle charge, resulting in a compression of the electrical double layer and a corresponding reduction in interparticle repulsive forces. It is worth noting that the EPM for the NP<sub>220</sub> and NP<sub>28</sub> are similar for a given condition. All calculated aggregation rates are presented in Figure S4.2. The higher aggregation rates observed for the NP<sub>28</sub> compared to NP<sub>220</sub> are not surprising because under the same conditions, smaller sized particles are less stable than larger ones due to the higher surface energy of the former.<sup>38</sup> The lower aggregation rate of NP<sub>220</sub> compared to that of NP<sub>28</sub> is somewhat consistent with their particle number concentration. For example, at 10 mM CaCl<sub>2</sub>, there is a 10-fold increase in aggregation rate of NP<sub>220</sub> (0.54 nm/s) compared to NP<sub>28</sub> (0.052 nm/s) while the difference in number concentration is 1000-fold.

From the stability curve (Figure 4.1e), we observe that, in agreement with DLVO theory,  $\alpha$  increases with electrolyte concentration (RLA conditions) until DLA is presumed to occur ( $\alpha=1$ ; CCC=10 mM). The presence of RLA and DLA regimes in the stability curve is consistent with electrostatic interactions being the governing mechanism in the system. The CCC is independent

of the size of the plastic particles. Although, contradictory findings about the influence of size on CCC for other nanomaterials exist in the literature, our results agree with theoretical predictions. Based on the Smoluchowski approximation, which assumes that the double layer thickness was much smaller than the particle size, DLVO predicts that particle size and concentration should have no effect on the CCC.<sup>39</sup> Particles with comparable surface properties in a given solution chemistry are also expected to show similar colloidal stability, independent of size.<sup>40</sup> It is important to note that NP<sub>28</sub> had a lower reported charge density compared to NP<sub>220</sub> (as function of surface area, Table S4.1) which was confirmed by our measurements of the EPM in 10 mM NaCl (-1.5 for the NP<sub>28</sub> vs -3.5  $\mu\text{m}\cdot\text{cm}/\text{V}\cdot\text{s}$  for the NP<sub>220</sub>). However, in the conditions under study, we see that both particles have comparable EPM in CaCl<sub>2</sub> (Figure 4.2a, b; 1 mM: -2 vs -1.8  $\mu\text{m}\cdot\text{cm}/\text{V}\cdot\text{s}$ ; 10 mM: -1 vs -1.1  $\mu\text{m}\cdot\text{cm}/\text{V}\cdot\text{s}$ ). Hence, as ionic strength increases, the effective charge of the particles are similar leading to similar values of CCC for the two plastics (i.e. 10 mM for NP<sub>28</sub> and NP<sub>220</sub>). Note that in the literature, CCC values for polystyrene particles range between 2.95 and 71.28 mM for divalent salt solutions (Table S4.4). When CCCs reported in the literature are compared as a function of particle size (Figure S4.3), there appears to be weak relationship, with no clear trend. This lack of clear trend cannot be generalized to our study since these studies were performed using different pH and particles having different surfaces, surface heterogeneities, charge densities etc. which makes direct comparison difficult. Nonetheless, two studies working with single particle sizes reported CCC that are comparable to our values (i.e. 12 mM CaCl<sub>2</sub><sup>41</sup> and 10 mM CaCl<sub>2</sub><sup>42</sup>). For studies examining two different sizes of polystyrene particles, a size dependency with CCC was reported; namely, 50 and 500 nm particles had CCC of 18 and 250 mM CaCl<sub>2</sub>, respectively,<sup>43</sup> while 20 and 100 nm particles had CCC of 13 and 32 mM CaCl<sub>2</sub>, respectively.<sup>44</sup>

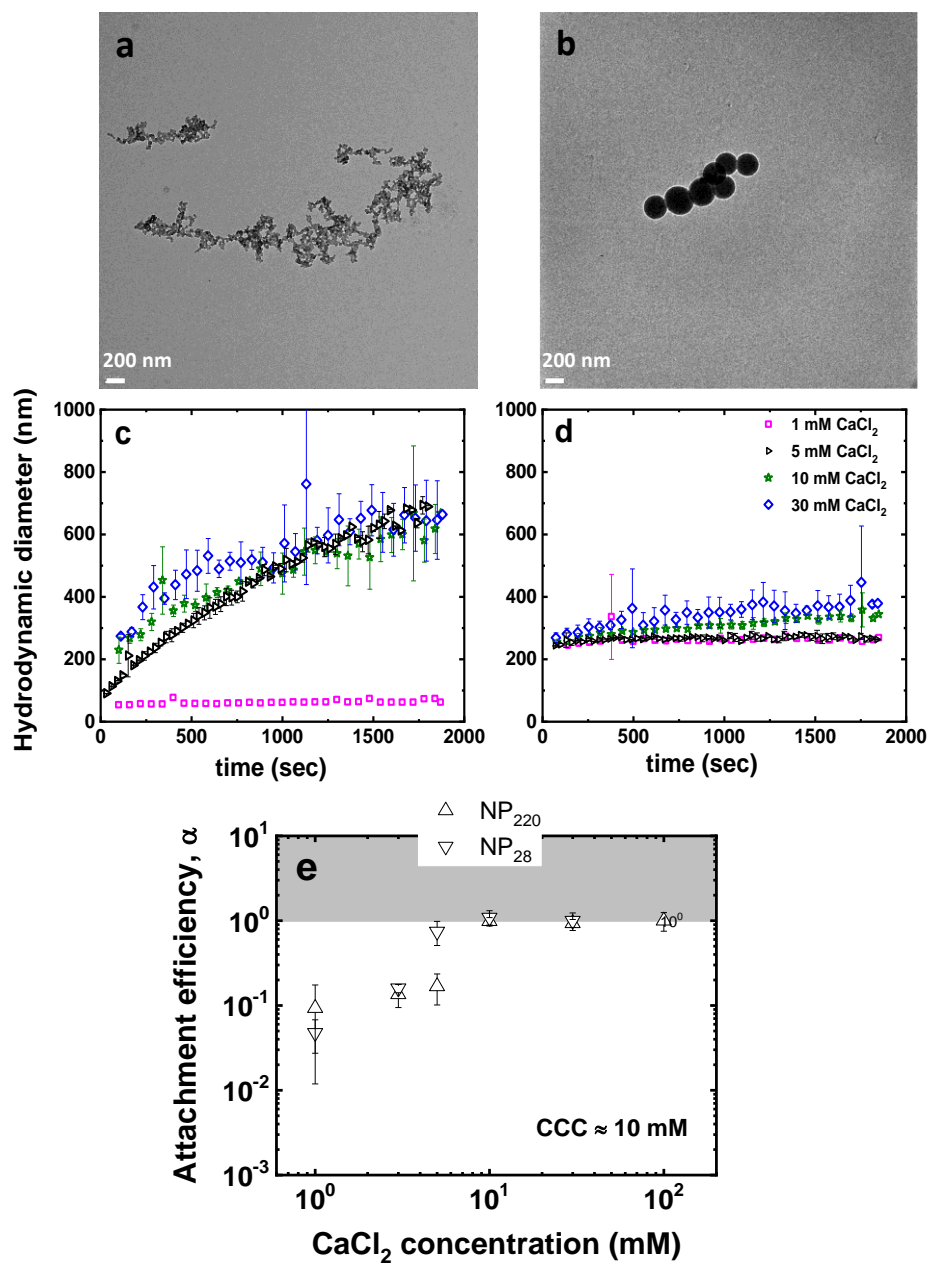


**Figure 4.1.** Transmission electron micrographs of (a) NP<sub>28</sub> and (b) NP<sub>220</sub> in 10 mM CaCl<sub>2</sub>, representative aggregation profiles of (c) NP<sub>28</sub> and (d) NP<sub>220</sub> in CaCl<sub>2</sub>. (e) Attachment efficiency of nanoplastics in CaCl<sub>2</sub>.

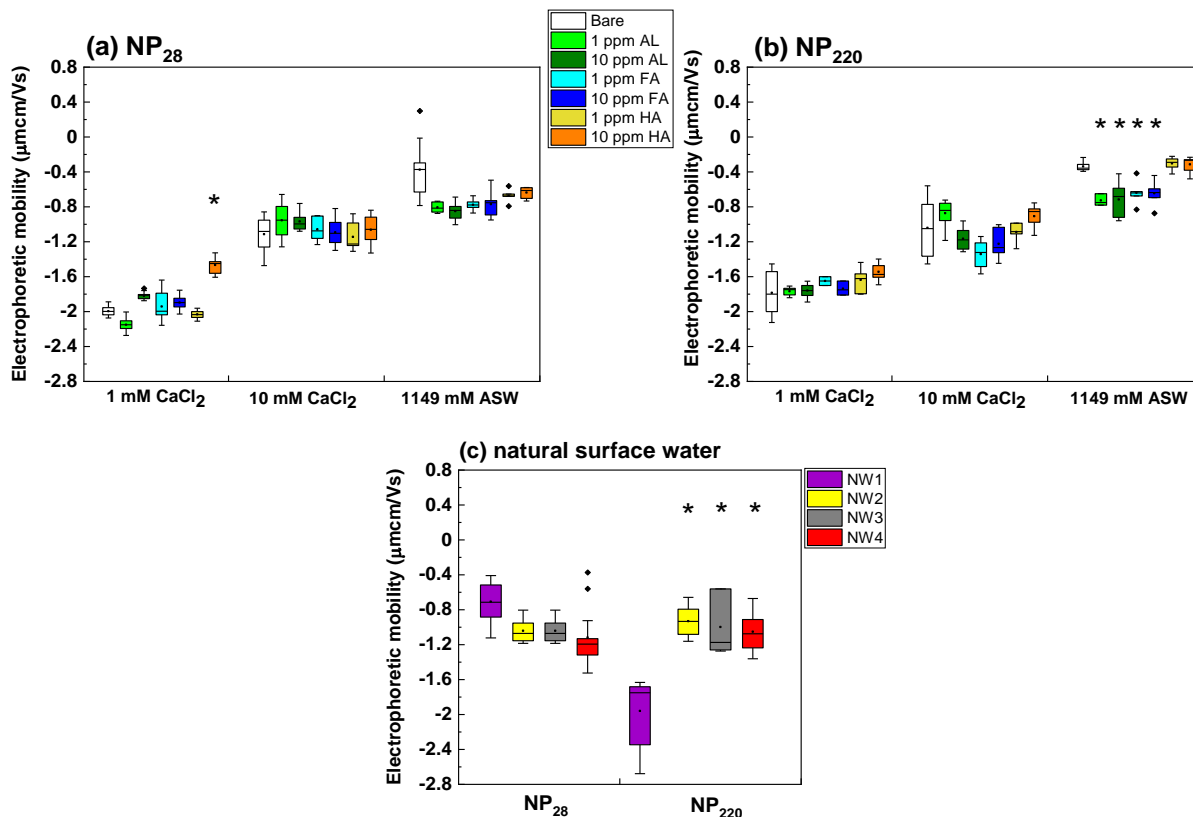


**Figure 4.2.** Electrophoretic mobilities of (a) NP<sub>28</sub> and (b) NP<sub>220</sub> as a function of electrolyte concentration in CaCl<sub>2</sub> and ASW. All experiments were carried out at a pH of  $8 \pm 0.5$ . ASW ionic strength is equivalent to 561 – 714 mM; (c) Electrophoretic mobilities of both plastic sizes in natural surface water (NW) samples. The box plots show mean, 25<sup>th</sup> and 75<sup>th</sup> percentiles, and outliers. \*  $p < 0.05$  when compared to each bare or NW1 sample using One-way ANOVA and Tukey mean comparison.

#### 4.3.2 Size dependent enhanced aggregation in the presence of Ca<sup>2+</sup> and alginate.

The aggregation kinetics of the plastic particles were investigated in the presence of AL (1 and 10 mg/L). The aggregation rates presented in Figure S4.2 show a slight increase in the presence of 10 mg/L AL as compared to 1 mg/L for NP<sub>220</sub>. While  $\alpha$  for the bare plastics is not significantly different in the presence of AL in the RLA regime of the stability curve (Figure 4.3e), at salt concentrations  $\geq$  the CCC (10 mM),  $\alpha$  appears to exceed a value of 1 for the NP<sub>220</sub>. This enhanced aggregation is readily observed in the aggregation profiles of Figure 4.3a, e. For both particle sizes, the EPM did not change significantly in the presence of AL as compared to its absence (Figure 4.2), indicating that factors other than electrostatic forces were likely destabilizing the plastics.

TEM images suggest that the interaction of the particles with the calcium and the AL depended upon particle size. From Figure 4.4a, b, we clearly see that the structures are different

(higher magnification images shown in Figure S4.4 b, c) for NP<sub>28</sub> with respect to NP<sub>220</sub>. For NP<sub>28</sub>, the particles appear to be entrapped/encapsulated, while for NP<sub>220</sub>, a distinct net-like (coil-like) network appears to bridge the particles together. Interestingly, similar fibrillar aggregate structures have been observed for colloidal aggregates isolated from lake<sup>45</sup> or marine systems.<sup>46</sup>

Alginate is a biopolymer consisting of mannuronic (M) and guluronic (G) blocks, known to form strong gel networks or extended coils in the presence of divalent ions, (e.g. Ca<sup>2+</sup>, Mg<sup>2+</sup>).<sup>47</sup> In natural water samples, alginate has been found to be a fairly flexible biopolymer capable of forming fibrillar structures/networks where colloids can be embedded, hence destabilizing them.<sup>45</sup><sup>48</sup> Laboratory studies have reported that in the presence of Ca<sup>2+</sup>, AL may destabilize hematite,<sup>49</sup> boron,<sup>50</sup> and manganese dioxide nanoparticles<sup>51</sup> via bridging. A recent study crosslinked alginate with 10 mM CaCl<sub>2</sub> as a proxy for a biofilm and investigated the diffusion of three different particle sizes through the gel structure.<sup>52</sup> They showed that the alginate gel matrix was heterogenous, and the accessibility of the gel pores was particle size dependent. Hence, we hypothesize that the interaction of the plastic particles and the alginate aggregate/coils depended on the relationship between the polymeric network mesh size ( $\varepsilon$ ) and the size of the plastic particles ( $d_p$ ). In the absence of plastic particles, sheet-like calcium alginate structures can be observed (Figure S4.4a). The  $\varepsilon$  of any alginate aggregate structure depends on the polymer and crosslinker concentrations. Typical  $\varepsilon$  reported for hydrogels ranges from 5 – 100 nm<sup>53</sup> and 5 – 200 nm<sup>54</sup> for calcium alginate gels. When  $\varepsilon > d_p$ , as may be the case for NP<sub>28</sub>, the particles may be able to diffuse more easily through the alginate gel. When  $\varepsilon < d_p$ , as is the case for NP<sub>220</sub>, the particles would be more likely to sorb onto the alginate chains, similar to the ‘pearls on a necklace’ observed by Santchi et al.<sup>46</sup> The bigger particles are not physically trapped inside the gel, rather alginate can acts to bridge the NP<sub>220</sub> during the aggregation process.

There is limited information on the effect of plastic size on aggregation in the presence of calcium alginate. Two studies, each looking at a single particle size, have observed differing types of alginate gel structures in the presence of Ca<sup>2+</sup>.

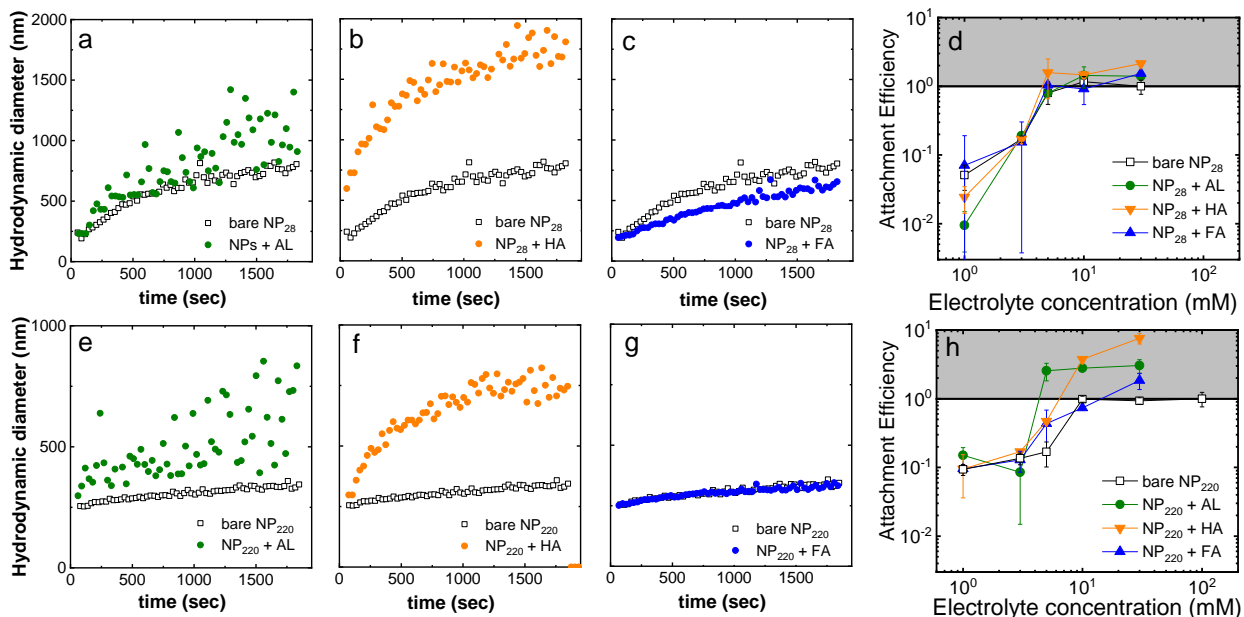


**Figure 4.3.** (top panels = NP<sub>28</sub>. bottom panels = NP<sub>220</sub>) Representative aggregation profile in 10 mM CaCl<sub>2</sub> (CCC) in the presence and absence of 10 mg/L alginate (a & e), 10 mg/L humic acid (b & f) and 10 mg/L fulvic acid (c & g). Stability curves of NP<sub>28</sub> and NP<sub>220</sub> in the absence and presence of all three organic matters at 10 mg/L (d & h). Error bars represent standard deviation for 3 independent experiments. Using One-way ANOVA and Tukey mean comparison, in the diffusion limited regime, attachment efficiencies of particles in AL and HA were significantly different ( $p < 0.05$ ) compared to the bare particles (for NP<sub>220</sub>, panel d) while no significant difference for NP<sub>28</sub>, panel h).

#### 4.3.3 Effect of fulvic acid in the presence of Ca<sup>2+</sup> differs with plastic size.

Representative aggregation profiles in the presence of FA show that FA slightly stabilized the NP<sub>28</sub> (slower aggregation rate in the presence of FA in Figure 3c, but had no impact on the aggregation rate for NP<sub>220</sub> (Figure 3g). No significant difference in EPM was observed when comparing with particles in the presence and absence of FA (Figure 4.1). The similarity in EPM could be explained by the significant electrostatic repulsion of bare carboxylated plastics which was either of similar charge density as the FA or sufficient to cause significant electrostatic repulsion (and thus limited sorption of the FA). The role of NOM on colloidal stability can be attributed to steric hindrance when its adsorption is sufficiently thick that it prevents particle approach and collision.<sup>55</sup> However, FA is a small molecule that is not known to aggregate, even in the presence of Ca<sup>2+</sup>.<sup>56</sup> Under the conditions of this study (NOM concentration of 10 mg/L) the FA is in large excess with respect to the available surface area of the nanoplastic (Table S4.5, assuming 1 nm for FA). Nonetheless, the attachment efficiencies of FA coated particles (Figure 4.3d, h) are generally similar for the bare particles (only small differences observed in a few cases) as the bare particles. This might be attributed to the FA molecules not having sufficiently coated the particles, hence significantly

lower  $\alpha$  values wouldn't necessarily be observed in the early stages of aggregation probed here. The relative weak effect of the FA on nanoplastic stability would suggest that adsorbed FA either insignificant or smaller than the electric double layer thickness (Debye length, Table S6) (precluding mechanisms involving either steric hinderance or bridging flocculation).

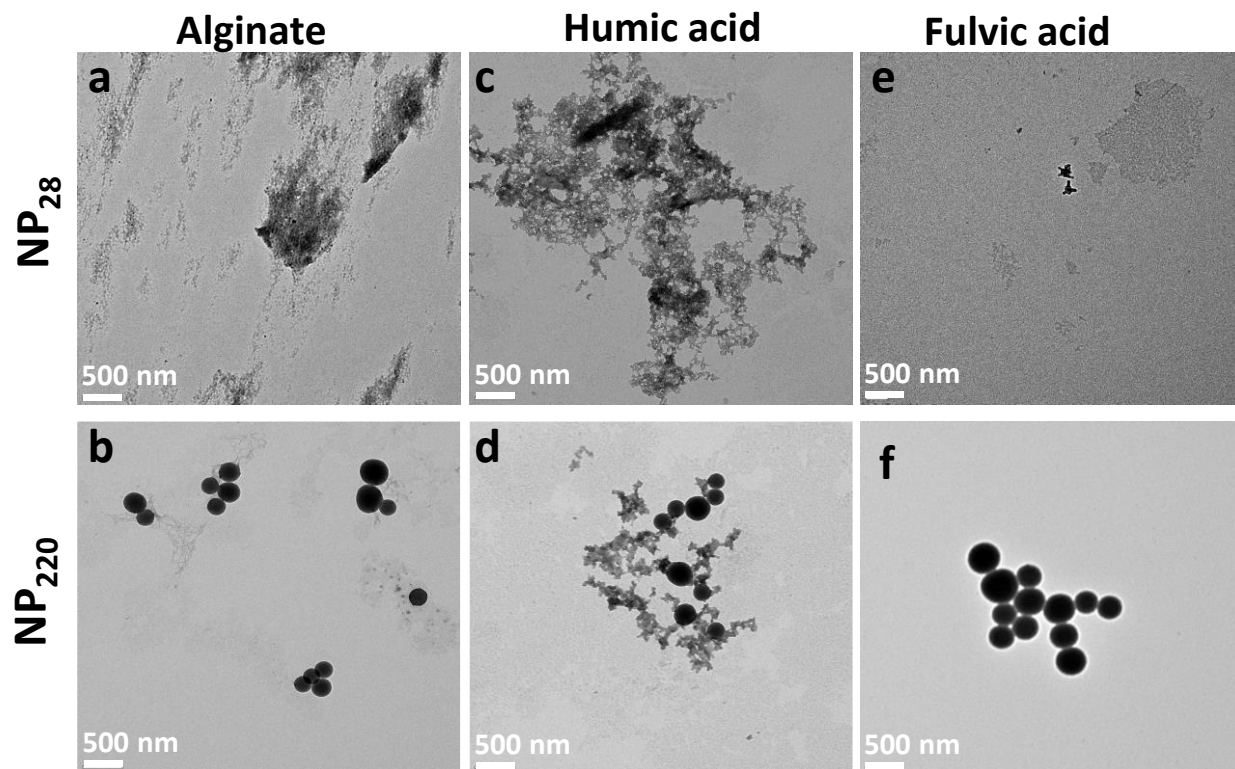


**Figure 4.4.** (Top panel = NP<sub>28</sub>. Bottom panel = NP<sub>220</sub>) Transmission electron micrographs of NP<sub>28</sub> and NP<sub>220</sub> in the presence of alginate (a & b), humic acid (c & d) and fulvic acid (e & h). Salt concentration = 10 mM CaCl<sub>2</sub>, NOM concentration = 10 mg/L. All experiments were carried out at a pH of  $8 \pm 0.5$ .

#### 4.3.4 Enhanced aggregation in the presence of Ca<sup>2+</sup> and humic acid

Higher aggregation rates were observed in the presence of HA with respect to its absence, especially for NP<sub>220</sub> (Figure 4.3b, f). The attachment efficiency also notably increased, generally consistent with the DLA regime for NP<sub>220</sub> but exceeding 1 in some cases. The enhanced aggregation observed in the presence of HA may be explained by a cation bridging mechanism. Indeed, the TEM images suggested that NP<sub>220</sub> monomers/dimers had combined with HA aggregates (Figure 4d). On the other hand, for the NP<sub>28</sub>, nanoplastic aggregates appeared to combine with HA aggregates (cluster-cluster aggregation, Figure 4c). Indeed, while the HA bridge is easily seen for the NP<sub>220</sub> (Figure 4d), it is not clear for NP<sub>28</sub> (Figure 4.4c). This may be because the HA aggregates are similar in size as the primary nanoplastics and their aggregates. Humic acids

have reported nominal sizes of 2.5 – 12.8 nm<sup>56-58</sup> and may form large aggregates in the presence of CaCl<sub>2</sub><sup>33, 59</sup> (see also Figure S4.5). Since in the presence of Ca<sup>2+</sup>, the HA seem to form large aggregates, it is unlikely that the HA molecules could fully cover the nanoplastic - thus a lack of stabilization is not surprising. Such large HA aggregates may be able to adsorb to the nanoplastic surface, exceeding the particle Debye length and leading to particle-particle bridging.<sup>60</sup> High aggregation rates in the presence of Ca<sup>2+</sup> have been shown for fullerene,<sup>59</sup> silica<sup>61</sup> and polystyrene microplastics.<sup>62</sup> Although some studies performed in Ca<sup>2+</sup> and Mg<sup>2+</sup> have reported a stabilizing effect of the HA for fullerene nanoparticles,<sup>59</sup> silica<sup>61</sup> and carbon nanotubes,<sup>63</sup> it occurred mainly at low concentrations of divalent cations where the HA were less likely to form aggregates or be in excess. Generally, when in monovalent salts, nanoparticles are thought to be stabilized by humic substances via steric or electrostatic repulsion,<sup>59</sup> however, in solutions of divalent ions, this does not appear to be the case, especially at high concentrations. This change is ascribed to cation complexation with the functional groups on the humic substance, thereby “caging” the NP<sub>220</sub> into larger aggregates.<sup>59</sup> The destabilization observed for HA as compared to the FA may also be ascribed to the slightly higher molecular weight and hydrophobicity of the former. For high concentrations of divalent cations, high molar mass NOM have been shown to promote aggregation of fullerene nanoparticles to a greater extent than low molar mass NOM.<sup>64</sup> A schematic of the proposed interactions between the different types of organic matters and nanoplastics has been presented in Figure 4.5.

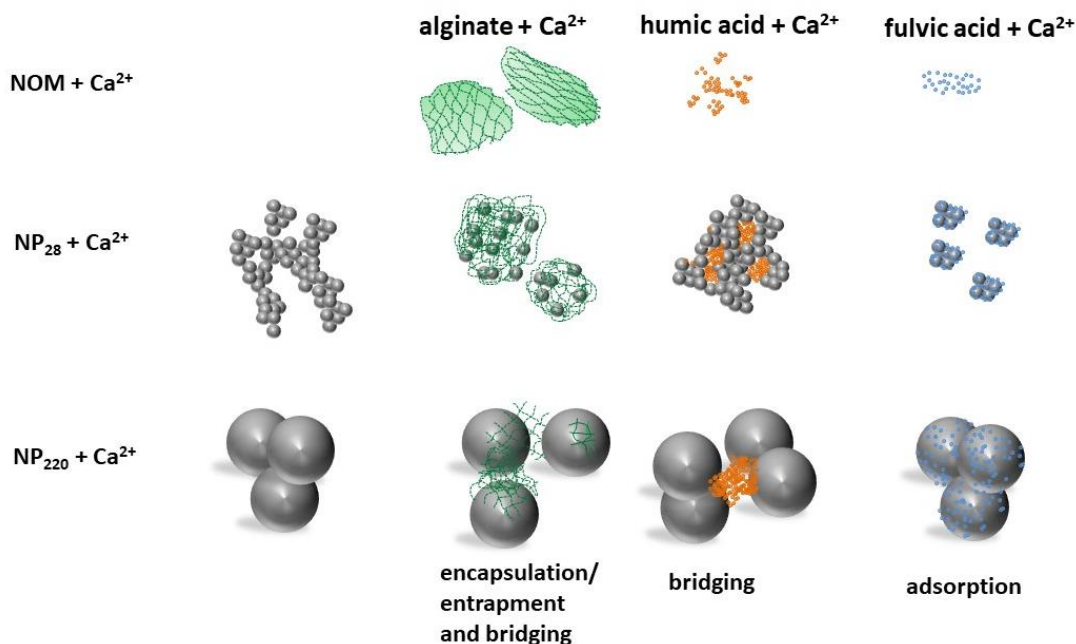


**Figure 4.5.** Schematic showing the proposed/possible mechanisms of interaction between NP<sub>28</sub> and NP<sub>220</sub> with alginate, humic acid and fulvic acid in CaCl<sub>2</sub> in the diffusion limited regime. Schematic is for illustration purposes and not drawn to scale

#### 4.3.5 Aggregation kinetics of the nanoplastics in artificial seawater with and without natural organic matter.

In order to mimic real marine systems, aggregation kinetics of the plastic particles, in the absence and presence of all 3 NOM were investigated in an ASW (Table S4.1). Significant aggregation of the bare NP<sub>28</sub> and NP<sub>220</sub> was seen in the ASW, especially for NP<sub>28</sub> (Figure 4.6a). Interestingly, for the bare plastics, the value of  $\alpha$  determined in the ASW was comparable to the  $\alpha$  in CCC in CaCl<sub>2</sub> (~1, Figure 4.6b). On adding 10 mg/L FA,  $\alpha$  decreased only slightly for NP<sub>220</sub>. In contrast, in the presence of HA,  $\alpha$  was considerably higher than in its absence ( $2.13 \pm 0.43$  vs  $1.13 \pm 0.19$  for NP<sub>220</sub>). It is possible that the enhanced aggregation observed in HA resulted from the presence of Ca<sup>2+</sup> in the ASW. As seen above, in the presence of monovalent salts, the humic acid is likely to stabilize colloidal particles however, de-stabilization may predominate in the presence of the divalent salts. The ASW has a Ca<sup>2+</sup> concentration corresponding to its CCC for CaCl<sub>2</sub> (10 mM) in addition to 470 mM of monovalent ions.

The HA had no statistically significant effect on the early-stage aggregation rates of NP<sub>28</sub> ( $\alpha = 1.24 \pm 0.21$  in the absence and  $1.00 \pm 0.40$  in the presence of HA). On the other hand, for time scales exceeding 30 min, the hydrodynamic diameter of NP<sub>28</sub> was greater in the presence than in the absence of HA (Figure S4.7a). Interestingly, a recent study by Tallec *et al.* showed that the

presence of HA in ASW increased the hydrodynamic diameter of 50 nm carboxylated nanoplastics only slightly after 24 h, but significantly after 48 h.<sup>65</sup> In the presence of the AL, a considerable decrease in  $\alpha$  was observed for NP<sub>220</sub> but no significant difference for NP<sub>28</sub> (Figure 4.6b). In Ca<sup>2+</sup>, AL destabilized the plastic dispersions (Figure 4.3a, e). In the presence of monovalent cations and Mg<sup>2+</sup>, AL is unable to strongly form a gel/coil.<sup>66</sup> Since there are more monovalent ions in the ASW, they might dominate the interactions and the type of AL gel structure that is formed. Indeed, Chen *et al.* showed the detrimental effect of Na<sup>+</sup> when added to the same system during the formation of the AL gel (that could enhance aggregation).<sup>67</sup> Another toxicity study also showed that the presence of 45 mg/L AL stabilized TiO<sub>2</sub> nanoparticle in ASW.<sup>68</sup> These results suggest that when AL is in abundance in marine environments such as occurs during algal blooms, NP<sub>28</sub> and NP<sub>220</sub> may be less likely to aggregate. The significant increase in the magnitude of EPM values in the presence of AL and FA (1 and 10 mg/L, Figure 4.2) suggests that some electrostatic stabilization is occurring, which would be consistent with the small observed reduction in  $\alpha$ .

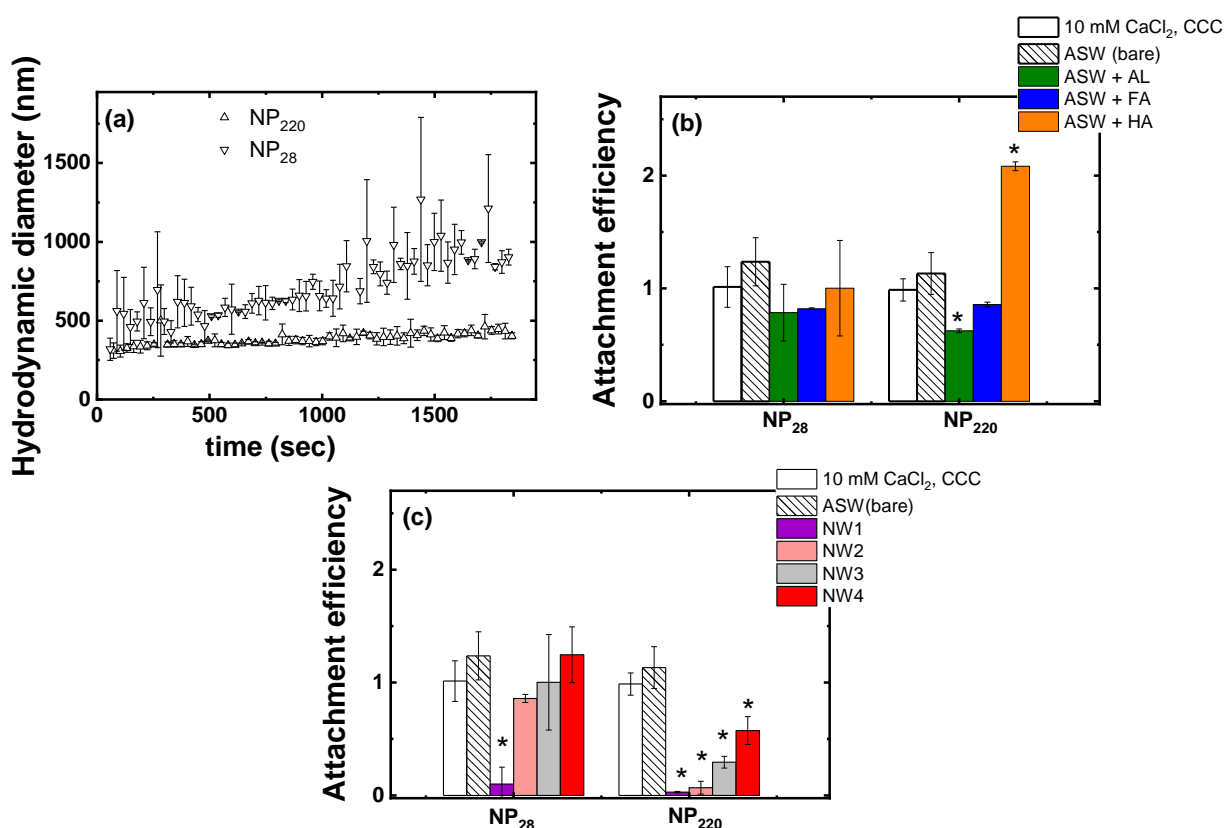
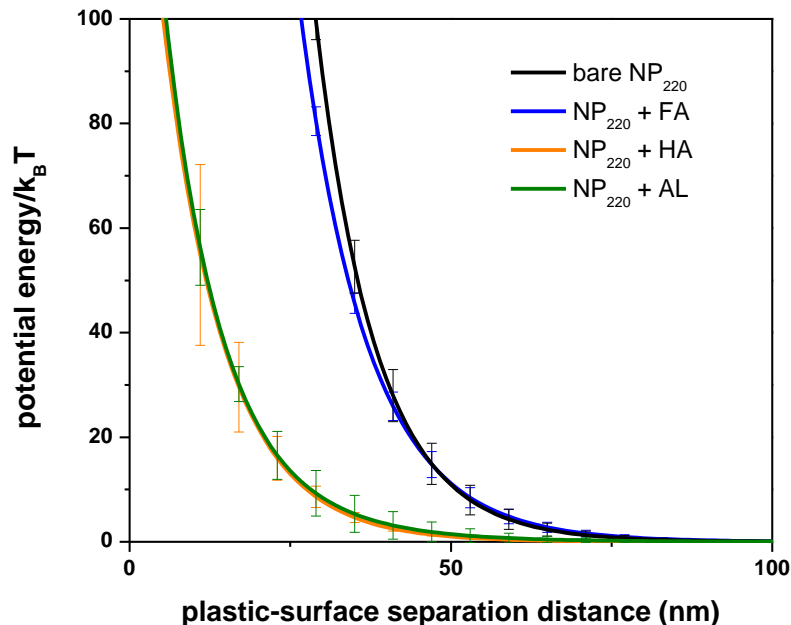


Figure 4.6: (a) Representative aggregation profiles of the bare nanoplastics, NP<sub>28</sub> and NP<sub>220</sub> in ASW and (b) attachment efficiencies in ASW in the presence and absence of humic acid, fulvic acid and alginate, as compared with the attachment efficiency in 10 mM CaCl<sub>2</sub> (i.e CCC). (c) attachment efficiency in natural surface waters as compared with the attachment efficiency at in 10 mM CaCl<sub>2</sub>. Error bars represent standard deviations determined for 3 independent experiments. \*  $p < 0.05$  when compared to 10 mM CaCl<sub>2</sub> or ASW (bare) using One-way ANOVA and Tukey mean comparison.

#### 4.3.6 Aggregation kinetics of the nanoplastics in natural surface water

In order to better understand the behavior of plastics in the natural environment, natural surface water samples were collected with increasing salinities ranging from fresh to seawater (<2 to 35 practical salinity units for NW1 to NW4 sample points respectively) were used. As discussed in section 2.2.2, aggregation rates were normalized with those determined in 10 mM CaCl<sub>2</sub>(CCC). For both nanoplastics,  $\alpha$  was the lowest in the freshwater sample (NW1) and increased with the increase in ionic strength (and decrease in dissolved organic carbon from NW1 to NW4 (Figure 4.6c). For the highest salinity sample, NW4,  $\alpha$  was comparable to that observed in the ASW for NP<sub>28</sub>. In contrast, NP<sub>220</sub> exhibited a much lower  $\alpha$  value as compared to the ASW ( $p < 0.05$ ). The marked difference in  $\alpha$  of NP<sub>220</sub> in ASW ( $1.13 \pm 0.17$ ) versus the natural seawater sample, NW4 ( $0.57 \pm 0.12$ ) demonstrates the importance of assessing the fate of plastics in realistic environments. These results suggest that in the natural environment, NP<sub>220</sub> are more likely to be stable as compared to similar concentration of NP<sub>28</sub>.

#### 4.3.7 Interaction energies between nanoplastics and silica surfaces.



**Figure 4.7.** Interaction energy profiles for the interaction of NP<sub>220</sub> and a silica surface in the presence of 1 mg/L fulvic acid, humic acid and alginate and 0.5 mM CaCl<sub>2</sub>. Error bars indicate standard deviation for  $n = 3$  independent experiments. Details of the fitting parameters are presented in Table S4.8. Note that curves for NP<sub>220</sub> + HA (green) and NP<sub>220</sub> + AL (yellow) largely overlap.

In natural waters, nanoplastics are very likely to interact with natural colloids such as silicates and clays which are generally present in much higher concentrations (e.g. heteroaggregation). It is thus of great interest to examine the interaction of nanoplastics with such surfaces. As a starting point to gain some insight into the complex environmental systems, we measured the interaction energies of NP<sub>220</sub> with a model Si surface in the presence of 1 mg/L organic matter and 0.5 mM CaCl<sub>2</sub> using an optical tweezer (Figure 4.7). According to DLVO theory, electrostatic repulsion will increase as the particles approach a like-charged surface. In the presence of the HA and AL, repulsive forces were similar, while repulsion was greater for the bare NP<sub>220</sub> and the NP<sub>220</sub> in the presence of FA. Thus, interactions between the plastic particles and the silica surface were more favorable in the presence of Ca<sup>2+</sup> and either AL or HA, where some attractive forces (e.g., bridging) may be present (Figure 4.5). Broadly, these results agree with particle-particle aggregation data in Figure 4.3, which indicated that while the aggregation rates of NP<sub>220</sub> and NP<sub>28</sub> in the presence of CaCl<sub>2</sub> increased when either AL (Figure 4.3a, e) or HA (Figure 4.3b, f) were present, this was not the case for FA (Figure 4.3c, g).

#### 4.4 Conclusions

The aggregation behavior of polystyrene NP<sub>28</sub> and NP<sub>220</sub> have been investigated and compared in simple and complex synthetic waters, as well as natural surface water matrices. Using realistic nanoplastic/NOM ratios, we were able to show the specific effects of different kinds of NOM on the aggregation of nanoplastics. At the same mass concentration, in the absence of organic matter, NP<sub>28</sub> aggregated faster than NP<sub>220</sub>, however, the two sizes of nanoplastics had the same CCC. For all conditions, the effect of all NOM was more obvious for NP<sub>220</sub> as compared to NP<sub>28</sub>. While AL and HA destabilized both particles in Ca<sup>2+</sup>, the mechanism of destabilization of AL was dependent on the size of the plastic. The presence of FA in Ca<sup>2+</sup> slightly stabilized NP<sub>28</sub> after 30 min, likely due to increased electrostatic repulsion, but did not appear to affect the NP<sub>220</sub>. HA appeared to destabilize the plastics via a bridging mechanism, while AL destabilized the plastics due to bridging and encapsulation/entrapment. In a simulated seawater, the presence of AL stabilized the particles more (reduced hydrodynamic size) as compared to HA and FA. In the more complex salts and NOM mixture of the natural waters, the plastic particles appeared to be more stable than would have been predicted from experiments performed in synthetic media. This suggests that different organic matter fractions may be playing a role in stabilizing the nanoplastics in natural waters. In the natural environment, NP<sub>28</sub> will be more likely to aggregate compared to NP<sub>220</sub>, a difference

that was underscored when looking at the water with the highest ionic strength (NW4). In this work, we quantitatively showed that while NP<sub>28</sub> behaved similarly in ASW and NW (NW4), NP<sub>220</sub> aggregation in natural waters (NW4) is substantially lower than predicted using ASW (which is often used as a proxy for seawater). Ultimately, this study shows the importance of considering both the size of plastic particles and the different organic matter components that may be present in natural waters, and the need to design experiments with more realistic complex matrices when predicting the fate of plastic particles in the environment.

## Acknowledgments

The authors acknowledge the support of the Canada Research Chairs program, the Natural Sciences and Engineering Research Council of Canada, the Killam Research Fellowship program, and the Petroleum Technology Development Fund of Nigeria and the Eugenie Ulmer Lamothe Fund at McGill for awards to OSA. This project was supported partially by a financial contribution from Fisheries and Oceans Canada. We also thank Sara Hashmi for her helpful comments in the preliminary phase of the project. The surface water samples were collected during the *Lampsilis* campaign (July/August 2019) cofunded by the Réseau Québec Maritime, Merinov and MITACS.

## References

1. Jambeck, J. R.; Geyer, R.; Wilcox, C.; Siegler, T. R.; Perryman, M.; Andrady, A.; Narayan, R.; Law, K. L., Plastic waste inputs from land into the ocean. *Sci* **2015**, *347* (6223), 768-771.
2. Gigault, J.; El Hadri, H.; Nguyen, B.; Grassl, B.; Rowenczyk, L.; Tufenkji, N.; Feng, S.; Wiesner, M., Nanoplastics are neither microplastics nor engineered nanoparticles. *Nat. Nanotechnol.* **2021**.
3. Shim, W. J.; Hong, S. H.; Eo, S., Chapter 1 - Marine microplastics: Abundance, distribution, and composition. In *Microplastic Contamination in Aquatic Environments*, Zeng, E. Y., Ed. Elsevier: 2018; pp 1-26.
4. Browne, M. A.; Crump, P.; Niven, S. J.; Teuten, E.; Tonkin, A.; Galloway, T.; Thompson, R., Accumulation of microplastic on shorelines worldwide: sources and sinks. *Environ. Sci. Technol.* **2011**, *45* (21), 9175-9.
5. Rochman, C. M.; Tahir, A.; Williams, S. L.; Baxa, D. V.; Lam, R.; Miller, J. T.; Teh, F.-C.; Werorilangi, S.; Teh, S. J., Anthropogenic debris in seafood: Plastic debris and fibers from textiles in fish and bivalves sold for human consumption. *Sci. Rep.* **2015**, *5* (1), 14340.
6. Athey, S. N.; Albotra, S. D.; Gordon, C. A.; Monteleone, B.; Seaton, P.; Andrady, A. L.; Taylor, A. R.; Brander, S. M., Trophic transfer of microplastics in an estuarine food chain and the effects of a sorbed legacy pollutant. *Limnol. Oceanogr. Lett.* **2020**, *5* (1), 154-162.
7. Jeong, C.-B.; Kang, H.-M.; Lee, M.-C.; Kim, D.-H.; Han, J.; Hwang, D.-S.; Souissi, S.; Lee, S.-J.; Shin, K.-H.; Park, H. G.; Lee, J.-S., Adverse effects of microplastics and oxidative stress-induced MAPK/Nrf2 pathway-mediated defense mechanisms in the marine copepod *Paracyclopsina nana*. *Sci. Rep.* **2017**, *7* (1), 41323.

8. Carbery, M.; O'Connor, W.; Palanisami, T., Trophic transfer of microplastics and mixed contaminants in the marine food web and implications for human health. *Environ. Int.* **2018**, *115*, 400-409.
9. Tanaka, K.; Takada, H.; Yamashita, R.; Mizukawa, K.; Fukuwaka, M.-a.; Watanuki, Y., Accumulation of plastic-derived chemicals in tissues of seabirds ingesting marine plastics. *Mar. Pollut. Bull.* **2013**, *69* (1-2), 219-222.
10. Gu, W.; Liu, S.; Chen, L.; Liu, Y.; Gu, C.; Ren, H.-q.; Wu, B., Single-cell RNA sequencing reveals size-dependent effects of polystyrene microplastics on immune and secretory cell populations from zebrafish intestines. *Environ. Sci. Technol.* **2020**, *54* (6), 3417-3427.
11. Merzel, R. L.; Purser, L.; Soucy, T. L.; Olszewski, M.; Colón-Bernal, I.; Duhaime, M.; Elgin, A. K.; Banaszak Holl, M. M., Uptake and retention of nanoplastics in *quagga* mussels. *Global Challenges* **2020**, *4* (6), 1800104.
12. Alimi, O. S.; Farner Budarz, J.; Hernandez, L. M.; Tufenkji, N., Microplastics and nanoplastics in aquatic environments: Aggregation, deposition, and enhanced contaminant transport. *Environ. Sci. Technol.* **2018**, *52* (4), 1704-1724.
13. Petosa, A. R.; Jaisi, D. P.; Quevedo, I. R.; Elimelech, M.; Tufenkji, N., Aggregation and deposition of engineered nanomaterials in aquatic environments: role of physicochemical interactions. *Environ. Sci. Technol.* **2010**, *44* (17), 6532-49.
14. Verwey, E. J.; Overbeek, J. T. G., Long distance forces acting between colloidal particles. *J. Chem. Soc. Faraday Trans.* **1946**, *42*, B117-B123.
15. Mao, Y.; Li, H.; Huangfu, X.; Liu, Y.; He, Q., Nanoplastics display strong stability in aqueous environments: Insights from aggregation behaviour and theoretical calculations. *Environ. Pollut.* **2020**, *258*, 113760.
16. Alimi, O. S.; Farner, J. M.; Tufenkji, N., Exposure of nanoplastics to freeze-thaw leads to aggregation and reduced transport in model groundwater environments. *Water Res.* **2020**, 116533.
17. Wang, X.; Bolan, N.; Tsang, D. C. W.; Binoy, S.; Bradney, L.; Li, Y., A review of microplastics aggregation in aquatic environment: Influence factors, analytical methods, and environmental implications. *J. Hazard. Mater.* **2020**, 123496.
18. Zhou, D.; Ji, Z.; Jiang, X.; Dunphy, D. R.; Brinker, J.; Keller, A. A., Influence of material properties on TiO<sub>2</sub> nanoparticle agglomeration. *PloS one* **2013**, *8* (11), e81239.
19. He, Y. T.; Wan, J.; Tokunaga, T., Kinetic stability of hematite nanoparticles: the effect of particle sizes. *J. of Nanopart. Res.* **2008**, *10* (2), 321-332.
20. Mulvihill, M. J.; Habas, S. E.; Jen-La Plante, I.; Wan, J.; Mokari, T., Influence of size, shape, and surface coating on the stability of aqueous suspensions of CdSe nanoparticles. *Chem. Mater.* **2010**, *22* (18), 5251-5257.
21. Ntim, S. A.; Sae-Khow, O.; Desai, C.; Witzmann, F. A.; Mitra, S., Size dependent aqueous dispersibility of carboxylated multiwall carbon nanotubes. *J. Environ. Monit.* **2012**, *14* (10), 2772-2779.
22. Liu, J.; Legros, S.; Ma, G.; Veinot, J. G. C.; von der Kammer, F.; Hofmann, T., Influence of surface functionalization and particle size on the aggregation kinetics of engineered nanoparticles. *Chemosphere* **2012**, *87* (8), 918-924.
23. Thurman, E., Aquatic humic substances. In *Organic geochemistry of natural waters*, Springer: 1985; pp 273-361.
24. Lowry, G. V.; Gregory, K. B.; Apte, S. C.; Lead, J. R., Transformations of nanomaterials in the environment. *Environ. Sci. Technol.* **2012**, *46* (13), 6893-9.

25. Pradel, A.; Ferreres, S.; Veclin, C.; El Hadri, H.; Gautier, M.; Grassl, B.; Gigault, J., Stabilization of fragmental polystyrene nanoplastic by natural organic matter: Insight into mechanisms. *ACS ES&T Water* **2021**, *1* (5), 1198-1208.
26. Oriekhova, O.; Stoll, S., Heteroaggregation of nanoplastic particles in the presence of inorganic colloids and natural organic matter. *Environ. Sci. Nano* **2018**, *5* (3), 792-799.
27. Li, Y.; Wang, X.; Fu, W.; Xia, X.; Liu, C.; Min, J.; Zhang, W.; Crittenden, J. C., Interactions between nano/micro plastics and suspended sediment in water: Implications on aggregation and settling. *Water Res.* **2019**, *161*, 486-495.
28. Praetorius, A.; Labille, J.; Scheringer, M.; Thill, A.; Hungerbühler, K.; Bottero, J. Y., Heteroaggregation of titanium dioxide nanoparticles with model natural colloids under environmentally relevant conditions. *Environ. Sci. Technol.* **2014**, *48* (18), 10690-8.
29. Quik, J. T. K.; Velzeboer, I.; Wouterse, M.; Koelmans, A. A.; Meent, v. d. D., Heteroaggregation and sedimentation rates for nanomaterials in natural waters. *Water Res.* **2014**, *48* (1), 269-279.
30. Maillette, S.; Peyrot, C.; Purkait, T.; Iqbal, M.; Veinot, J. G. C.; Wilkinson, K. J., Heteroagglomeration of nanosilver with colloidal SiO<sub>2</sub> and clay. *Environ. Chem.* **2017**, *14* (1), 1-8.
31. Roweczyk, L.; Dazzi, A.; Deniset-Besseau, A.; Beltran, V.; Goudounèche, D.; Wong-Wah-Chung, P.; Boyron, O.; George, M.; Fabre, P.; Roux, C., Microstructure characterization of oceanic polyethylene debris. *Environ. Sci. Technol.* **2020**, *54* (7), 4102-4109.
32. Koelmans, A. A.; Bakir, A.; Burton, G. A.; Janssen, C. R., Microplastic as a vector for chemicals in the aquatic environment: Critical review and model-supported reinterpretation of empirical studies. *Environ. Sci. Technol.* **2016**, *50* (7), 3315-26.33.
33. Kloster, N.; Brigante, M.; Zanini, G.; Avena, M., Aggregation kinetics of humic acids in the presence of calcium ions. *Colloids Surf. Physicochem. Eng. Aspects* **2013**, *427*, 76-82.
34. Marion, G. M.; Millero, F. J.; Camões, M. F.; Spitzer, P.; Feistel, R.; Chen, C. T. A., pH of seawater. *Mar. Chem.* **2011**, *126* (1), 89-96.
35. Kobayashi, M.; Juillerat, F.; Galletto, P.; Bowen, P.; Borkovec, M., Aggregation and charging of colloidal silica particles: Effect of particle size. *Langmuir* **2005**, *21* (13), 5761-5769.
36. Smith, B.; Wepasnick, K.; Schrote, K. E.; Bertele, A. R.; Ball, W. P.; O'Melia, C.; Fairbrother, D. H., Colloidal properties of aqueous suspensions of acid-treated, multi-walled carbon nanotubes. *Environ. Sci. Technol.* **2009**, *43* (3), 819-825.
37. Akanbi, M. O.; Hernandez, L. M.; Mobarok, M. H.; Veinot, J. G. C.; Tufenkji, N., QCM-D and NanoTweezer measurements to characterize the effect of soil cellulase on the deposition of PEG-coated TiO<sub>2</sub> nanoparticles in model subsurface environments. *Environ. Sci. Nano* **2018**, *5* (9), 2172-2183.
38. Nanda, K. K.; Maisels, A.; Kruis, F. E.; Fissan, H.; Stappert, S., Higher surface energy of free nanoparticles. *Phys. Rev. Lett.* **2003**, *91* (10), 106102.
39. Elimelech, M.; Gregory, J.; Jia, X., *Particle deposition and aggregation : Measurement, modelling, and simulation*. Butterworth-Heinemann: Oxford, England, 1995; p 448.
40. Elimelech, M.; O'Melia, C. R., Effect of particle size on collision efficiency in the deposition of Brownian particles with electrostatic energy barriers. *Langmuir* **1990**, *6* (6), 1153-1163.
41. Wang, J.; Zhao, X.; Wu, A.; Tang, Z.; Niu, L.; Wu, F.; Wang, F.; Zhao, T.; Fu, Z., Aggregation and stability of sulfate-modified polystyrene nanoplastics in synthetic and natural waters. *Environ. Pollut.* **2021**, *268*, 114240.

42. Li, X.; He, E.; Jiang, K.; Peijnenburg, W. J. G. M.; Qiu, H., The crucial role of a protein corona in determining the aggregation kinetics and colloidal stability of polystyrene nanoplastics. *Water Res.* **2021**, *190*, 116742.
43. Liu, L.; Song, J.; Zhang, M.; Jiang, W., Aggregation and deposition kinetics of polystyrene microplastics and nanoplastics in aquatic environment. *Bull. Environ. Contam. Toxicol.* **2021**.
44. Li, X.; He, E.; Xia, B.; Liu, Y.; Zhang, P.; Cao, X.; Zhao, L.; Xu, X.; Qiu, H., Protein corona-induced aggregation of differently sized nanoplastics: impacts of protein type and concentration. *Environ. Sci. Nano* **2021**.
45. Wilkinson, K. J.; Balnois, E.; Leppard, G. G.; Buffle, J., Characteristic features of the major components of freshwater colloidal organic matter revealed by transmission electron and atomic force microscopy. *Colloids Surf. Physicochem. Eng. Aspects* **1999**, *155* (2), 287-310.
46. Santschi, P. H.; Balnois, E.; Wilkinson, K. J.; Zhang, J.; Buffle, J.; Guo, L., Fibrillar polysaccharides in marine macromolecular organic matter as imaged by atomic force microscopy and transmission electron microscopy. *Limnol. Oceanogr.* **1998**, *43* (5), 896-908.
47. Grant, G. T.; Morris, E. R.; Rees, D. A.; Smith, P. J. C.; Thom, D., Biological interactions between polysaccharides and divalent cations: The egg-box model. *FEBS Lett.* **1973**, *32* (1), 195-198.
48. Buffle, J.; Wilkinson, K. J.; Stoll, S.; Filella, M.; Zhang, J., A generalized description of aquatic colloidal interactions: The three-colloidal component approach. *Environ. Sci. Technol.* **1998**, *32* (19), 2887-2899.
49. Chen, K. L.; Mylon, S. E.; Elimelech, M., Enhanced aggregation of alginate-coated iron oxide (hematite) nanoparticles in the presence of calcium, strontium, and barium cations. *Langmuir* **2007**, *23* (11), 5920-5928.
50. Liu, X.; Wazne, M.; Han, Y.; Christodoulatos, C.; Jasinkiewicz, K. L., Effects of natural organic matter on aggregation kinetics of boron nanoparticles in monovalent and divalent electrolytes. *J. Colloid Interf. Sci.* **2010**, *348* (1), 101-107.
51. Huangfu, X.; Jiang, J.; Ma, J.; Liu, Y.; Yang, J., Aggregation kinetics of manganese dioxide colloids in aqueous solution: Influence of humic substances and biomacromolecules. *Environ. Sci. Technol.* **2013**, *47* (18), 10285-10292.
52. Rodríguez-Suárez, J. M.; Butler, C. S.; Gershenson, A.; Lau, B. L. T., Heterogeneous diffusion of polystyrene nanoparticles through an alginate matrix: The role of cross-linking and particle size. *Environ. Sci. Technol.* **2020**, *54* (8), 5159-5166.
53. Li, J.; Mooney, D. J., Designing hydrogels for controlled drug delivery. *Nat. Rev. Mater.* **2016**, *1* (12), 16071.
54. Andresen, I.-L.; Skipnes, O.; SmidsrØD, O.; Ostgaard, K.; Hemmer, P. C., Some biological functions of matrix components in benthic algae in relation to their chemistry and the composition of seawater. In *Cellul. Chem. Technol.*, American Chemical Society: 1977; Vol. 48, pp 361-381.
55. Domingos, R. F.; Tufenkji, N.; Wilkinson, K. J., Aggregation of titanium dioxide nanoparticles: Role of a fulvic acid. *Environ. Sci. Technol.* **2009**, *43* (5), 1282-1286.
56. Lead, J. R.; Wilkinson, K. J.; Starchev, K.; Canonica, S.; Buffle, J., Determination of diffusion coefficients of humic substances by fluorescence correlation spectroscopy: Role of solution conditions. *Environ. Sci. Technol.* **2000**, *34* (7), 1365-1369.
57. Kawahigashi, M.; Sumida, H.; Yamamoto, K., Size and shape of soil humic acids estimated by viscosity and molecular weight. *J. Colloid Interf. Sci.* **2005**, *284* (2), 463-469.

58. Lead, J. R.; Wilkinson, K. J.; Balnois, E.; Cutak, B. J.; Larive, C. K.; Assemi, S.; Beckett, R., Diffusion coefficients and polydispersities of the suwannee river fulvic acid: Comparison of fluorescence correlation spectroscopy, pulsed-field gradient nuclear magnetic resonance, and flow field-flow fractionation. *Environ. Sci. Technol.* **2000**, *34* (16), 3508-3513.
59. Chen, K. L.; Elimelech, M., Influence of humic acid on the aggregation kinetics of fullerene (C<sub>60</sub>) nanoparticles in monovalent and divalent electrolyte solutions. *J. Colloid Interface Sci.* **2007**, *309* (1), 126-134.
60. Wang, H.; Adeleye, A. S.; Huang, Y.; Li, F.; Keller, A. A., Heteroaggregation of nanoparticles with biocolloids and geocolloids. *Adv. Colloid Interface Sci.* **2015**, *226*, 24-36.
61. Abe, T.; Kobayashi, S.; Kobayashi, M., Aggregation of colloidal silica particles in the presence of fulvic acid, humic acid, or alginate: Effects of ionic composition. *Colloids Surf. Physicochem. Eng. Aspects* **2011**, *379* (1), 21-26.
62. Liu, Y.; Huang, Z.; Zhou, J.; Tang, J.; Yang, C.; Chen, C.; Huang, W.; Dang, Z., Influence of environmental and biological macromolecules on aggregation kinetics of nanoplastics in aquatic systems. *Water Res.* **2020**, 116316.
63. Saleh, N. B.; Pfefferle, L. D.; Elimelech, M., Aggregation kinetics of multiwalled carbon nanotubes in aquatic systems: measurements and environmental implications. *Environ. Sci. Technol.* **2008**, *42* (21), 7963-9.
64. Shen, M.-H.; Yin, Y.-G.; Booth, A.; Liu, J.-F., Effects of molecular weight-dependent physicochemical heterogeneity of natural organic matter on the aggregation of fullerene nanoparticles in mono- and di-valent electrolyte solutions. *Water Res.* **2015**, *71*, 11-20.
65. Tallec, K.; Blard, O.; González-Fernández, C.; Brotons, G.; Berchel, M.; Soudant, P.; Huvet, A.; Paul-Pont, I., Surface functionalization determines behavior of nanoplastic solutions in model aquatic environments. *Chemosphere* **2019**, *225*, 639-646.
66. Miao, L.; Wang, C.; Hou, J.; Wang, P.; Ao, Y.; Li, Y.; Lv, B.; Yang, Y.; You, G.; Xu, Y., Effect of alginate on the aggregation kinetics of copper oxide nanoparticles (CuO NPs): bridging interaction and hetero-aggregation induced by Ca<sup>2+</sup>. *Environ. Sci. Pollut. Res.* **2016**, *23* (12), 11611-11619.
67. Chen, K. L.; Mylon, S. E.; Elimelech, M., Aggregation kinetics of alginate-coated hematite nanoparticles in monovalent and divalent electrolytes. *Environ. Sci. Technol.* **2006**, *40* (5), 1516-1523.
68. Callegaro, S.; Minetto, D.; Pojana, G.; Bilanicová, D.; Libralato, G.; Volpi Ghirardini, A.; Hassellöv, M.; Marcomini, A., Effects of alginate on stability and ecotoxicity of nano-TiO<sub>2</sub> in artificial seawater. *Ecotoxicol. Environ. Saf.* **2015**, *117*, 107-114.

## Supporting information

**Table S4.1.** The properties and conditions of plastic and electrolyte used in the study

NP <sub>28</sub> working concentration	2 mg/L (~ 1.66 × 10 <sup>11</sup> particles/mL)
NP <sub>220</sub> working concentration	2 mg/L (~ 3.42 × 10 <sup>8</sup> particles/mL)
NP <sub>28</sub> charge density*	2.5 × 10 <sup>-7</sup> meq/cm <sup>2</sup>
NP <sub>220</sub> charge density*	1.9 × 10 <sup>-6</sup> meq/ cm <sup>2</sup>
Plastic density*	1.05 g/cm <sup>3</sup>
Artificial Seawater Composition (mg/L)*	Chloride: 19000- 20000 Sodium: 10700-11000 Sulfate: 2660 Potassium: 300-400 Calcium: 400 Carbonate: 140-200 Boron: 5.6 Magnesium: 1320 Strontium: 8.8
Artificial seawater ionic strength	561 – 714 mM
Artificial seawater conductivity	~36000 μS/cm

\* provided by the manufacturer.

**Table S4.2.** Properties of the natural surface water

Sample name	Location site GPS coordinates	Temperature (°C)	Conductivity (μS/cm)	pH	DO <sub>2</sub> (%)	Calculated salinity (PSU)	DOC (mg/L)
NW1	Lake Saint-Louis / Beaconsfield 45° 24.181' N 73° 52.556' W	25.04	252	7.96	63.9	<2	1.9
NW2	St Joseph de la Rive 47° 26.755'N 70° 18.022'W	15.98	22897	7.66	129.3	17.1	0.333
NW3	Baie Ste Catherine 47° 58.498' N 69° 42.990' W	11.01	38804	7.77	112.3	34.8	0.133
NW4	Cacouna 47° 55.709'N 69° 32.673'W	11.7	38893	7.83	103.3	34.2	0.167

### S4.1. Mechanism of operation of the optical tweezer

This equipment is based upon total internal reflection microscopy (TRIM) and uses light to capture particles and push them towards the surface.<sup>1</sup> As the optical tweezer confines the light and particles in two dimensions, it increases the signal-to-noise ratio in comparison to TRIM.<sup>1,2</sup> When the particle is captured, an evanescent field will be generated around it which scatters light. The

intensity of scattered light will depend on the position of the particle within the evanescent field.<sup>2</sup> This intensity is then measured by the instrument and is used to generate potential wells of interaction. Potential energy maps are calculated by correlating the scattered light to the particle-surface interaction. Briefly, a Boltzmann inversion is used to calculate the equilibrium state and then all other states are compared to the equilibrium state, therefore generating the map.<sup>1</sup> The principal component of particle-surface interaction is the overlapping of electrical double layers. Using DLVO theory, we calculate the screened electrostatic interaction as:

$$\frac{U}{k_b T} = A e^{\frac{-z}{\lambda_D}} \quad (\text{S4.1})$$

where  $U$  is the interaction energy,  $k_b$  is the Boltzmann constant,  $T$  is the absolute temperature,  $z$  is the distance between the PS nanoparticles and the surface,  $\lambda_D$  is the Debye screening length, and  $A$  is the interaction coefficient for steric repulsion.

**Table S4.3.** Experimental details for aggregation versus plastic-surface interaction experiments.

Parameter	particle-particle experiments	particle-surface experiments
particle concentration (mg/L)	2	10
plastic size	NP <sub>28</sub> , NP <sub>220</sub>	NP <sub>220</sub>
CaCl <sub>2</sub> concentration (mM)	1, 3, 5, 10, 30 and 100	0.5
organic matter concentration (mg/L)	1 and 10	1

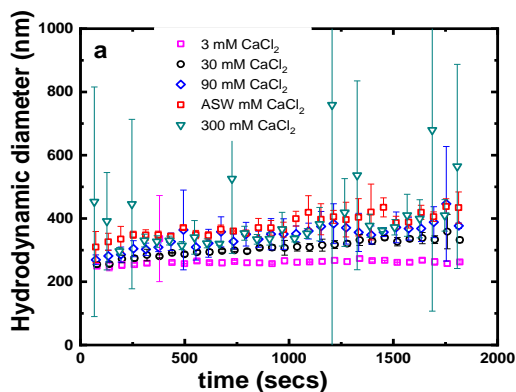


**Figure S4.1.** Representative aggregation profile showing the effect of ionic strength (1, 10, 30, 100 mM CaCl<sub>2</sub> and ASW) on the NP<sub>220</sub>.

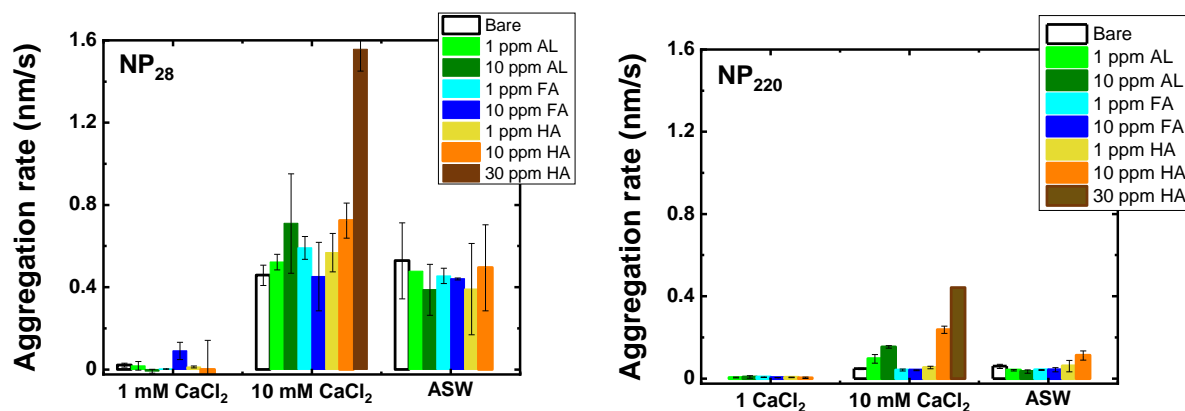


**Figure S4.2.** Aggregation rates of NP28 and NP220 in CaCl<sub>2</sub> and ASW in the presence and absence of different organic matter. AL = Alginate, HA = humic acid, FA = fulvic acid and ASW = artificial seawater. Error bars represent standard deviation of at least 3 measurements. Additional experiments were carried out at 30 ppm HA only to better elucidate its interaction with the smaller NPs since the aggregation rate measured in the presence of 10 ppm HA was not significantly different from 1 ppm HA.

**Table S4.4.** Relationship between CCC in divalent salts and polystyrene plastic size from literature

Reference	Plastic size	CCC (mM)	pH	Concentration (mg/L)	Modification	NOM concentration
this study	20, 200 nm	10 CaCl <sub>2</sub>	8	2	carboxyl	1, 10 mg/L
3	1 μm, 0.53 μm	20 CaCl <sub>2</sub> 30 CaCl <sub>2</sub>	4	4.5	carboxyl, sulfate	-
4	12 ± 3.4 μm	2.95 CaCl <sub>2</sub> 3.20 BaCl <sub>2</sub>	6 6	20	-	15 mg TOC/L
5	100 nm	71.28 CaCl <sub>2</sub> 63.10 BaCl <sub>2</sub>	7.5			-
6	269 nm	12.2 CaCl <sub>2</sub>	6	20	sulfate	1 - 50
7	100 nm	28 CaCl <sub>2</sub>		10	bare, carboxyl	1, 5, 10 C/L NOM
8	120 nm	29 BaCl <sub>2</sub> 33 CaCl <sub>2</sub> 44 MgCl <sub>2</sub>		20	no surface modification	-
9	PS - 900 nm PE - 200 - 750 nm	PS - 10 CaCl <sub>2</sub> PS - 25 MgCl <sub>2</sub> PE - 0.4 CaCl <sub>2</sub> PE - 8 MgCl <sub>2</sub>		20	PE-SDS	-
10	240 nm	25 CaCl <sub>2</sub>		10		-
11	50 nm	-		100	carboxyl, amidine and plain	1, 10, 30 mg/L
12	50 - 100 nm	32 CaCl <sub>2</sub>		10	no surface modification	1, 2 and 5 mg C/L
13	50 and 500 nm	18 and 250 mM CaCl <sub>2</sub>	6 ± 0.2	20	no surface modification	-

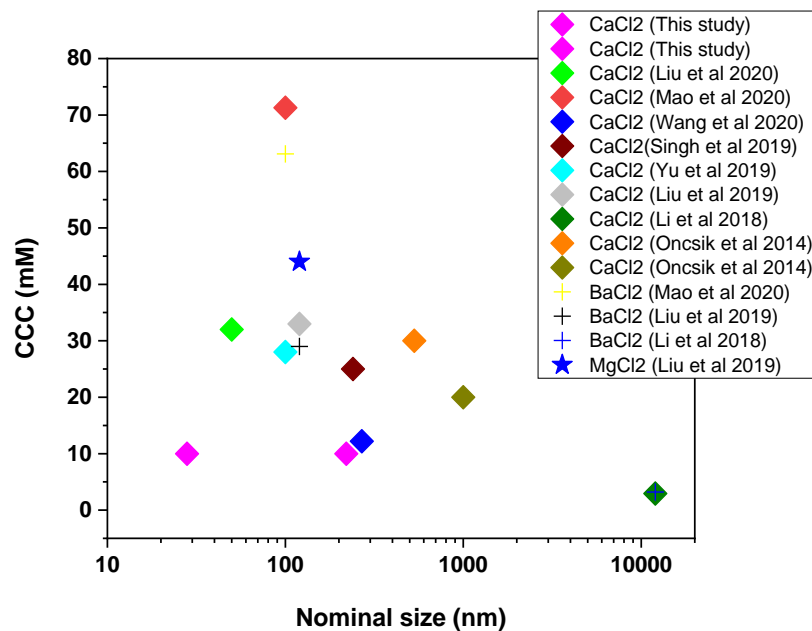


**Figure S4.3.** Comparison of CCC of nanoplastics and microplastics from literature to show the effect of particle size on CCC.

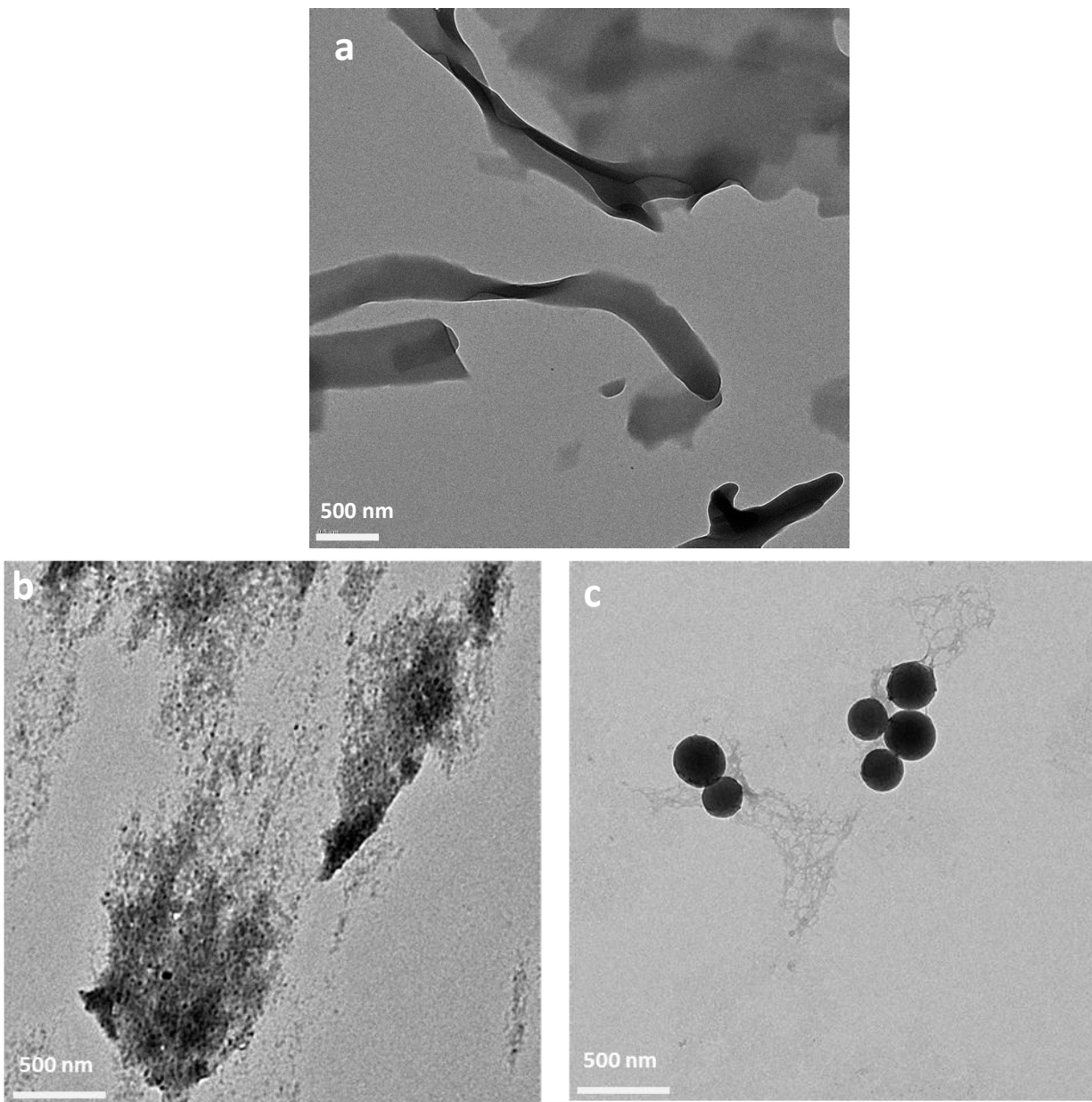


**Figure S4.4.** Transmission electron microscope images of (a) calcium alginate sheets formed in the absence of plastic particles. Close up images of plastic interaction with calcium alginate (b) NP<sub>28</sub> (c) NP<sub>220</sub>

**Table S4.5.** Surface coverage calculation of natural organic matter present in working solution

	<b>Fulvic acid</b>		<b>Humic acid</b>	
	<b>NP<sub>28</sub></b>	<b>NP<sub>220</sub></b>	<b>NP<sub>28</sub></b>	<b>NP<sub>220</sub></b>
Nominal size of plastic ( $\mu\text{m}$ )	0.028	0.22	0.028	0.22
Working concentration of plastic (mg/L)	2	2	2	2
Working concentration (particles/mL)	$1.66 \times 10^{11}$	$3.42 \times 10^8$	$1.66 \times 10^{11}$	$3.42 \times 10^8$
Surface area of working concentration ( $\text{cm}^2/\text{g}$ )	$2 \times 10^6$	$2.6 \times 10^5$	$2 \times 10^6$	$2.6 \times 10^5$
Surface area of 1 plastic ( $\text{nm}^2$ )	$1.26 \times 10^3$	$1.26 \times 10^5$	$1.26 \times 10^3$	$1.26 \times 10^5$
Total surface area of plastic in 1mL	$4.1 \times 10^{14}$	$5.2 \times 10^{13}$	$4.1 \times 10^{14}$	$4.29 \times 10^{13}$
Number of NOM particles needed for 100% coverage	$4.1 \times 10^{14}$	$5.2 \times 10^{13}$	$4.1 \times 10^{13}$	$4.29 \times 10^{12}$
Number of NOM in experiment (particles/mL)	$1.1 \times 10^{16}$	$1.1 \times 10^{16}$	$1.7 \times 10^{13}$	$1.7 \times 10^{13}$
$\theta = \frac{\text{number of NOM in 1 mL}}{\text{number of NOM for 100\% SA coverage}}$	<b>26.89</b>	<b>211.26</b>	<b>0.42</b>	<b>3.27</b>
No of FA particles/mL	$1.097 \times 10^{16}$			
No of HA particles/mL	$1.097 \times 10^{13}$			
Nominal size of fulvic acid assumed	<b>1 nm</b>			
Nominal size of humic acid assumed	<b>10 nm</b>			
Humic acid size (nm)	4.4 and 12.8 nm <sup>14</sup>			
Fulvic acid size (nm)	1.3 - 1.6 <sup>15</sup>			
Suwanee River Fulvic acid (nm)	1.5 - 2.5 <sup>16</sup>			
Natural organic matter (nm)	1.8 - 2 <sup>16</sup>			

NOM = natural organic matter

SA = surface area

$\theta$  = plastic coverage ratio

**Table S4.6.** Debye length in CaCl<sub>2</sub> concentration

1 mM	5.51 nm
5 mM	2.46 nm
10 mM	1.74 nm

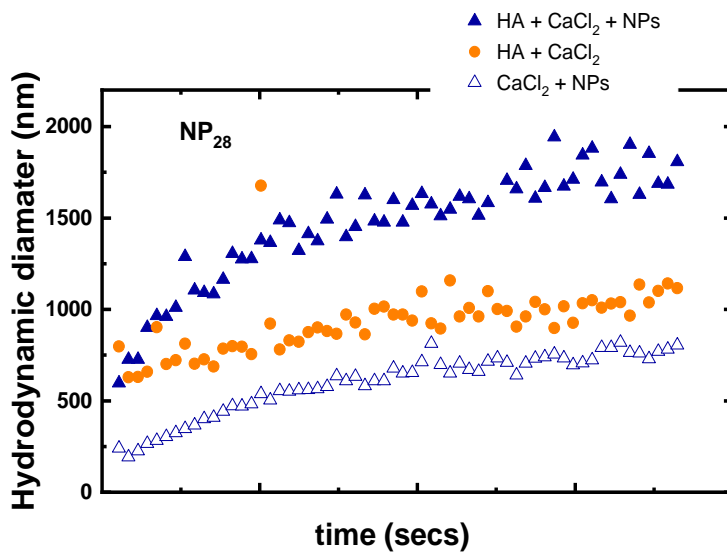


**Figure S4.5.** Representative aggregation profile of NP<sub>28</sub> showing the effect of humic acid at 10 mM CaCl<sub>2</sub> and 10 ppm HA.

**Table S4.7.** Elemental composition of organic matter used as reported by the International Humic Substances Society

Type	Humic Acid	Fulvic acid
Cat No.	3S101H	2S101F
H <sub>2</sub> O	11.9	16.9
Ash	4.62	0.58
C	54.59	52.34
H	3.90	4.36
O	40.03	42.98
N	1.50	0.67
S	0.55	0.46
P	nd	0.0004

**Table S4.8.** Fitting parameters from plastic-surface interaction.

Treatment	Calculated A	Calculated $\lambda_D$ (nm)
Bare plastics	51.99 ± 6.11	9.44 ± 1.62
Plastics + FA	45.79 ± 3.72	10.57 ± 1.32
Plastics + HA	4.86 ± 2.81	9.70 ± 1.27
Plastics + AL	6.18 ± 4.48	11.29 ± 3.37

$\lambda_D$  = Debye screening length, A = parameter related to steric and electrostatic interactions.

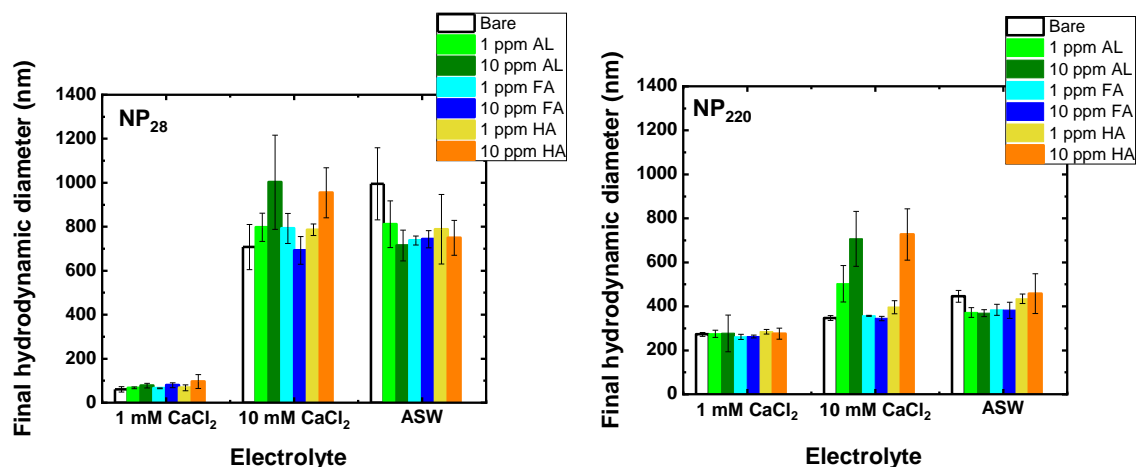


**Figure S4.6.** Hydrodynamic diameter of NP28 and NP220 after 30 minutes in CaCl<sub>2</sub> and ASW in the presence and absence of different organic matter. AL = Alginate, HA = humic acid, FA = fulvic acid and ASW = artificial seawater. Error bars represent standard deviation of at least 3 measurements.

## References

- Schein, P.; Ashcroft, C. K.; O'Dell, D.; Adam, I. S.; DiPaolo, B.; Sabharwal, M.; Shi, C.; Hart, R.; Earhart, C.; Erickson, D., Near-field Light Scattering Techniques for Measuring Nanoparticle-Surface Interaction Energies and Forces. *J Lightwave Technol* **2015**, *33* (16), 3494-3502.
- Erickson, D.; Serey, X.; Chen, Y.-F.; Mandal, S., Nanomanipulation using near field photonics. *LChip* **2011**, *11* (6), 995-1009.
- Oncsik, T.; Trefalt, G.; Csendes, Z.; Szilagyi, I.; Borkovec, M., Aggregation of negatively charged colloidal particles in the presence of multivalent cations. *Langmuir* **2014**, *30* (3), 733-41.
- Li, S.; Liu, H.; Gao, R.; Abdurahman, A.; Dai, J.; Zeng, F., Aggregation kinetics of microplastics in aquatic environment: Complex roles of electrolytes, pH, and natural organic matter. *Environ. Pollut.* **2018**, *237*, 126-132.
- Mao, Y.; Li, H.; Huangfu, X.; Liu, Y.; He, Q., Nanoplastics display strong stability in aqueous environments: Insights from aggregation behaviour and theoretical calculations. *Environ. Pollut.* **2020**, *258*, 113760.
- Wang, J.; Zhao, X.; Wu, A.; Tang, Z.; Niu, L.; Wu, F.; Wang, F.; Zhao, T.; Fu, Z., Aggregation and stability of sulfate-modified polystyrene nanoplastics in synthetic and natural waters. *Environ. Pollut.* **2021**, *268*, 114240.
- Yu, S.; Shen, M.; Li, S.; Fu, Y.; Zhang, D.; Liu, H.; Liu, J., Aggregation kinetics of different surface-modified polystyrene nanoparticles in monovalent and divalent electrolytes. *Environ. Pollut.* **2019**, *255*, 113302.
- Liu, Y.; Hu, Y.; Yang, C.; Chen, C.; Huang, W.; Dang, Z., Aggregation kinetics of UV irradiated nanoplastics in aquatic environments. *Water Res.* **2019**, *163*, 114870.
- Shams, M.; Alam, I.; Chowdhury, I., Aggregation and stability of nanoscale plastics in aquatic environment. *Water Res.* **2020**, *171*, 115401.
- Singh, K.; Raghav, A.; Jha, P. K.; Satapathi, S., Effect of size and charge asymmetry on aggregation kinetics of oppositely charged nanoparticles. *Sci. Rep.* **2019**, *9* (1), 3762.
- Talleg, K.; Blard, O.; González-Fernández, C.; Brotons, G.; Berchel, M.; Soudant, P.; Huvet, A.; Paul-Pont, I., Surface functionalization determines behavior of nanoplastic solutions in model aquatic environments. *Chemosphere* **2019**, *225*, 639-646.

12. Liu, Y.; Huang, Z.; Zhou, J.; Tang, J.; Yang, C.; Chen, C.; Huang, W.; Dang, Z., Influence of environmental and biological macromolecules on aggregation kinetics of nanoplastics in aquatic systems. *Water Res.* **2020**, 116316.
13. Liu, L.; Song, J.; Zhang, M.; Jiang, W., Aggregation and deposition kinetics of polystyrene microplastics and nanoplastics in aquatic environment. *Bull. Environ. Contam. Toxicol.* **2021**.
14. Kawahigashi, M.; Sumida, H.; Yamamoto, K., Size and shape of soil humic acids estimated by viscosity and molecular weight. *J. Colloid Interf. Sci.* **2005**, 284 (2), 463-469.
15. Domingos, R. F.; Tufenkji, N.; Wilkinson, K. J., Aggregation of titanium dioxide nanoparticles: Role of a fulvic acid. *Environ. Sci. Technol.* **2009**, 43 (5), 1282-1286.
16. Lead, J. R.; Wilkinson, K. J.; Starchev, K.; Canonica, S.; Buffle, J., Determination of diffusion coefficients of humic substances by fluorescence correlation spectroscopy: Role of solution conditions. *Environ. Sci. Technol.* **2000**, 34 (7), 1365-1369.

## **Preamble to Chapter 5**

The risks associated with microplastics cannot be fully understood by using pristine particles. Even though an increasing number of studies consider more realistic scenarios with the use of environmentally relevant microplastics, we observed huge variability and disparity in weathering protocols used across these studies. The use of less realistic weathering pathways or protocols that lack rationale may overestimate or trivialize environmental risks. Hence, we present a novel and extensive synthesis of laboratory effect studies in the context of environmentally relevant protocols for weathered microplastics, nanoplastics and leachates while providing a framework for method harmonization. We found that only ten percent of laboratory studies investigating the effects of microplastic pollution in ecosystems used environmentally relevant (aged) particles. This has important implications for realistic risk assessments and for the design of experiments examining the effects of these contaminants and their associated hazards.

The findings from this chapter was published in *Journal of Hazardous Materials* in August 2021.

# **Chapter 5: Weathering Pathways and Protocols for Environmentally Relevant Microplastics and Nanoplastics: What Are We Missing?**

## **Abstract**

To date, most studies of microplastics have been carried out with pristine particles. However, most plastics in the environment will be aged to some extent; hence, understanding the effects of weathering and accurately mimicking weathering processes are crucial. By using microplastics that lack environmental relevance, we are unable to fully assess the risks associated with microplastic pollution in the environment. Emerging studies advocate for harmonization of experimental methods, however, the subject of reliable weathering protocols for realistic assessment has not been addressed. In this work, we critically analysed the current knowledge regarding protocols used for generating environmentally relevant microplastics and leachates for effects studies. We present the expected and overlooked weathering pathways that plastics will undergo throughout their lifecycle. International standard weathering protocols developed for polymers were critically analysed for their appropriateness for use in microplastics research. We show that most studies using weathered microplastics involve sorption experiments followed by toxicity assays. The most frequently reported weathered plastic types in the literature are polystyrene>polyethylene>polypropylene>polyvinyl chloride, which does not reflect the global plastic production and plastic types detected globally. Only ~10% of published effect studies have used aged microplastics and of these, only 12 use aged nanoplastics. This highlights the need to embrace the use of environmentally relevant microplastics and to pay critical attention to the appropriateness of the weathering methods adopted moving forward. We advocate for quality reporting of weathering protocols and characterisation for harmonization and reproducibility across different research efforts.

## **5.1 Introduction**

Plastic pollution in the environment has received considerable attention over the last decade. The projected rate of global plastic production has been estimated to outweigh current and predicted future efforts aimed at reducing plastic pollution<sup>1</sup> and plastic debris already accumulated in the environment are persistent. Hence, the environmental impacts of plastics may not decrease for the next decade even with new legislation and initiatives. The smaller fragments, known as

microplastics and nanoplastics are even more worrisome due to their reported and potential adverse effects.<sup>2-4</sup> Microplastics form as a result of fragmentation of bulk plastics due to environmental weathering, referred to as secondary microplastics, or are intentionally manufactured, known as primary microplastics.<sup>5, 6</sup> A vast majority of plastics in the environment are of secondary origin, while between 15–31% of plastics in the environment is estimated to be primary.<sup>7</sup>

Although some microplastics will be pristine (as manufactured) at the point of release into the environment, those that come from water or wastewater treatment plants would have undergone some degree of weathering before release into the environment. Even though these processes can remove up to 95% of microplastics, the biosolids streams (i.e., dewatered or stabilized sludge) of these facilities can still end up in the environment (via land application). Hence, the contribution of the pathways occurring in these systems to the physicochemical changes of plastics during their lifecycle should not be ignored.

Plastics may undergo various physical, chemical and biological transformations, before release into the environment, some of which lead to the production of micro- or nanoplastics. These include: hydrolysis,<sup>8</sup> photooxidation,<sup>9</sup> chemical oxidation,<sup>10</sup> natural organic matter (NOM) adsorption/attachment and flocculant aggregation,<sup>11, 12</sup> etc. Upon release into the natural environment, plastic particles may further undergo photodegradation, hydrolysis, chemical oxidation, biodegradation, mechanical stress, *etc.*<sup>5, 13, 14</sup> Plastics will encounter one or more of these weathering pathways during their lifecycle either simultaneously or sequentially; however, most microplastics studies only explore a few of these processes in isolation when mimicking environmentally relevant systems. To mimic microplastics that are representative of those found in the environment, weathering studies must consider the processes that occur both before and after release into the environment.

The time it takes to observe noticeable physicochemical changes in weathered plastics may range from a few weeks to several years;<sup>15</sup> hence, the weathering process is commonly accelerated in the laboratory. For accelerated weathering, there exist international standard protocols developed for plastics and other polymeric materials for quality control purposes. These protocols are sometimes already incorporated in commercial weatherometers or can be adapted in custom-made laboratory chambers. The former usually offers more control over the parameters and more comparable results, but it is expensive and not readily available in environmental research

laboratories. The latter offers more flexibility in terms of design and is less costly, but the results are specific to each system. Standard protocols generally recommend using specific lamp types, condensation cycles *etc.* to simulate natural conditions.<sup>16</sup> However, microplastic studies are increasingly using methods to initiate fast degradation without adequate justification which can potentially lead to unrealistic physicochemical changes and conclusions.

The majority of microplastics recovered from various environmental compartments and organisms are weathered and have been well characterized both in the macro- (bulk) and micro-scales.<sup>17-20</sup> In the context of this review, environmentally relevant microplastics are defined as plastics that have properties mimicking microplastics found in the environment and those that have undergone similar processes as would be experienced by plastics in the real environment. Until recently, most laboratory studies have been carried out using pristine microplastics and nanoplastics;<sup>21</sup> hence, the majority of the known risks associated with microplastic pollution were determined under less realistic conditions. Therefore, our understanding of the true risks associated with microplastic pollution may be limited. To advance knowledge in this field, emerging studies now include more environmentally relevant microplastics and the majority show that aged microplastics behave differently from pristine ones under same conditions. By ignoring the impact of key weathering processes, most findings in the current microplastics literature may be inconclusive. Recent reports are calling for standardization of methods across microplastics studies<sup>22</sup> and quality criteria for risk assessment to lay a foundation to increase harmonization and comparability across studies.<sup>23</sup> However, there is a lack of standardized protocols for microplastic weathering.

Therefore, the purpose of this review is to: (i) highlight and discuss the typical and expected weathering pathways (especially those that might have been overlooked in water treatment processes) that microplastics will undergo before and after release into the environment during use and disposal, (ii) discuss the need to mimic weathering pathways in the water cycle where exposure is important, (iii) critically review the current methods used in weathering microplastics in laboratory effects studies to assess their appropriateness, (iv) critically review existing international standard protocols recommended for weathering bulk plastics and assess their applicability for microplastics studies, (v) propose useful weathering guidelines to address some of the identified knowledge gaps.

## **5.2 Key weathering conditions and pathways encountered by plastics throughout their lifecycle**

### **5.2.1 UV photooxidation**

Sunlight is mainly composed of infrared (wavelength  $\lambda$  between 700 nm to 1 mm), visible ( $\lambda = 400\text{-}700$  nm) and ultraviolet light or UV ( $\lambda = 100\text{-}400$  nm).<sup>24</sup> The latter has higher photon energy due to its higher frequency, and is divided into three main subtypes: UVC ( $\lambda = 100\text{-}280$  nm), which is completely absorbed by the ozone layer in the atmosphere, UVB ( $\lambda = 280\text{-}315$  nm), mostly absorbed by the ozone layer, but still reaching the Earth's surface, and UVA ( $\lambda = 315\text{-}400$  nm), which is not affected by the ozone layer and comprises more than 95% of the UV radiation that reaches the Earth's surface.<sup>25</sup> It is believed that photodegradation initiated by UV in the presence of oxygen, or photooxidation, is the most important type of abiotic degradation pathway that plastics undergo in the environment.<sup>26, 27</sup>

The three steps of photooxidation are initiation, propagation and termination. First, the photon needs to be absorbed by a chemical bond leading to chain scission and free radical creation. Cleavage of weaker C-H bonds from tertiary carbons, present in polypropylene and polystyrene for instance, is particularly favourable and forms stable radicals to continue the photooxidation.<sup>28</sup> During propagation, oxygen is quickly added to these radicals to form peroxy radicals, which in turn withdraw hydrogens from vicinal chains and form hydroperoxide groups and new free radicals. The reaction is terminated once radicals combine and form inactive/stable groups. Stabilizers commonly incorporated in plastics act to preferentially absorb UV radiation or to capture and stabilize free radicals. During photooxidation, not only chain scission but crosslinking, branching and the formation of oxidized groups in the polymer chain such as carbonyl, carboxyl and hydroxyl is expected.<sup>26</sup> Yellowing is a typical consequence of photooxidation, creating more chromophores and facilitating further degradation.<sup>29</sup> As the molecular weight of the polymer decreases, the original physical properties are lost and the materials become brittle and more prone to fragmentation.<sup>30</sup> Photooxidation increases roughness and surface area, forming flakes and grooves to a depth of approximately 100  $\mu\text{m}$ , and so the fragmentation easily leads to micro- and nanoplastic release.<sup>31</sup> Mechanical abrasion after photooxidation accelerates the fragmentation process by breaking the brittle degraded surfaces of plastics such as expanded polystyrene.<sup>32</sup>

The extent of photodegradation is also determined by the intensity of the radiation,<sup>30</sup> which depends on the solar irradiance, or the total power per unit area received from the sun. Absorption

and scattering in the atmosphere, reflection on Earth's surface, meteorological conditions, seasons and geographical position alter the value of solar irradiance that reaches plastic fragments in the environment. The UV dose is a product of irradiance ( $I$ ), expressed as energy per unit surface area, and time of exposure ( $t$ ). A long time of exposure in a natural environment leads to a high UV dose, while artificial UV irradiation used during water treatment for pathogen inactivation has a negligible UV dose due to a very short time of exposure (few seconds),<sup>33-35</sup> even considering the high irradiance (typically 40 mJ/cm<sup>2</sup>) used.<sup>36</sup> A UV reactor (e.g., low pressure and high intensity irradiance lamp) with a monochromatic UVC irradiance (254 nm) can provide enough energy to initiate the plastic surface photodegradation, but natural weathering over a long period of time (e.g., several weeks) contributes more significantly to plastic photooxidation. More research is needed in this area, notably for polymer degradation being driven by  $I$  only rather than by  $I \times t$ .

### **5.2.2 Biological weathering**

Biological weathering, or biodegradation, may occur when plastics are exposed to various types of microorganisms. Biodegradation can be simplified as the hydrolysis of polymer into monomers or final mineralization products (CO<sub>2</sub>, CH<sub>4</sub>) by enzymatic activity. This involves extracellular depolymerases to break down polymers into molecules small enough to pass the cell membranes, and intracellular depolymerases in which those small molecules are used for cell metabolism.<sup>14</sup> The proliferation of such microorganisms depends on environmental parameters (e.g., temperature, pH, moisture, salinity) and morphology of the microplastics that enables attachment of microorganisms and formation of biofilm.<sup>37</sup> Biological activity can be measured by monitoring the production of final mineralization products. The degradation of specific organic molecules can be monitored, for example, by using labelled carbon to enable differentiation from the background carbon.<sup>38, 39</sup>

Biological weathering occurs to some extent in most environmental compartments, however, microplastics may be in contact with high concentrations of active microorganisms in soils,<sup>39</sup> anoxic waters and wastewater processes.<sup>33</sup> In wastewater treatment and sludge treatment streams, microplastics are contacted with a wide range of microbial ecosystems, in aerobic, anoxic or anaerobic conditions. These processes often host specific microorganisms such as methanogenic archaea or nitrifying bacteria, with high concentrations of active biomass (e.g., 1500 to 4000 mg/L in conventional activated sludge). It is worth noting the high concentration of biological solids in sludge (60 to 1300 g/L), as most microplastics that transit wastewater treatment plants are captured

in the solids stream.<sup>40</sup> Most wastewater or sludge treatment processes provide partial biodegradation of microplastics.<sup>41</sup> Specific species can degrade different types of plastics.<sup>14</sup>

### 5.2.3 Chemical oxidation and disinfection

Chlorine, chloramines, ozone, potassium permanganate and hydrogen peroxide are widely used in the drinking water industry for oxidation and disinfection. While ozone has a higher oxidative potential ( $E^{\circ}_{\text{red}}$ : 2.08 V), its concentration decreases quickly in full-scale processes and no residual concentration is expected in the distribution system.<sup>42</sup> The chlorine oxidative potential of HOCl is lower ( $E^{\circ}_{\text{red}}$ : 1.48 V),<sup>42</sup> but a residual concentration is usually maintained in the distribution system (> 0.3 mg Cl<sub>2</sub>/L in North America). Consequently, the non-filterable plastics are exposed to chlorine for several hours. In drinking water applications, disinfection is generally performed after granular filtration which removes a fair number of microplastics (87–99 %).<sup>43</sup> However, if implemented before filtration (inter-oxidation), chemical oxidation via ozonation has the potential to fragment larger microplastics into smaller plastic debris. In wastewater treatment, ozone is usually implemented at the end of the water treatment process to reduce ozone consumption caused by non-selective reactions with colloids; thus, the majority of plastics are not exposed to ozone as they are efficiently removed during settling. However, some plastic debris are persistent and remain in settled waters. In wastewater treatment, the ozone concentration is considerably higher compared to the concentration used for drinking water disinfection. This increases the risk of plastic degradation via chemical oxidation pathways. Chemical oxidation was shown to alter the polymer backbone (formation of hydroxyl and carbonyl groups), hence initiating the degradation sequence,<sup>38, 44-46</sup> and to change the surface charge (reduction of the zeta potential by using 0.5–5 mg O<sub>3</sub>/L).<sup>47</sup> The impact of ozone combined with low water flow shearing (25–80 s<sup>-1</sup>) was investigated in a full-scale process and the concentration of 1–5 μm microplastics increased, although it is not clear if the increase was associated with plastic fragmentation or to a better detection due to the cleaner plastic surface after ozonation.<sup>48, 49</sup> To date, no study has clearly explored the combination of chemical oxidation with high-shearing events on plastic degradation/fragmentation. Ozonating/fragmenting plastics into smaller pieces would reduce their settling velocity, as velocity is proportional to the diameter,<sup>2, 50, 51</sup> which will affect their transport into clarifiers and aquatic ecosystems.

#### 5.2.4 Thermal effects

Microplastics are exposed to thermal variation in aquatic environments and urban waters during 1) drinking and wastewater treatment, 2) sludge treatment and 3) distribution and usage of potable water. While many common drinking water and wastewater treatment processes occur between 1 and 30°C, several processes in the sludge treatment line are maintained at higher temperature.<sup>33</sup> For example, anaerobic digestion occurs between 30 and 57°C, composting occurs between 50 to 70°C and incineration occurs between 650 and 820°C.<sup>33</sup> As 90–99% of microplastics in wastewater facilities passes in the sludge treatment line,<sup>52</sup> microplastics are likely to be exposed to a wide range of temperatures. Thermal stress encountered by microplastics in distribution and usage of drinking water occurs via hot water pipelines (50-95°C) and boiling in cooking processes (95°C). Microplastics will also undergo thermal stress at cold and freezing temperatures (e.g. freeze-thaw cycling) in cold climate regions. Stable aggregates of nanoplastics have been observed after exposure to several cycles of freeze-thaw.<sup>53</sup>

Several authors have characterized thermal aging of bulk plastics or microplastics using depletion of antioxidant, depth of carbonyl groups,<sup>54, 55</sup> changes in molecular structure and crystallinity,<sup>55</sup> appearance of fractures,<sup>54-57</sup> changes in surface groups<sup>58</sup> and monitoring of mass loss.<sup>41</sup> Colin *et al* observed an Arrhenius dependency of thermal aging processes of PE pipes between 20 and 105°C.<sup>54</sup> Though fractures have been observed on the surface of plastics, studies that report release of smaller microplastics or nanoplastics following thermal degradation of bulk plastics or microplastics are sparse. Hernandez *et al.* showed that exposure of bulk plastic to 95°C for five min led to leaching of considerable micro- and nanoplastics.<sup>59</sup>

Thermal aging is affected by environmental factors. First, the effect of temperature is affected by the presence of oxidizers. The presence or absence of oxygen in sludge treatment (e.g., aerobic or anaerobic conditions) favors oxidation or hydrolysis, respectively. Oxidation kinetics of commonly used oxidants in drinking water treatment (chlorine, chlorine oxide, ozone, etc.) are faster at higher temperature. Moreover, aging by thermal oxidation is affected by the presence or absence of antioxidant in bulk plastics<sup>57</sup>. Finally, the establishment of microbial communities that support plastic biodegradation is affected by temperature; thus, higher temperatures generally lead to increases in both thermal degradation and biodegradation<sup>56</sup>.

### 5.2.5 Other transformations

Plastic debris are known to be weathered via multiple pathways (e.g., (photo)oxidation, thermal degradation, biodegradation, etc.) causing alteration of the polymer backbone. However, plastic materials could experience other transformations in natural waters and water treatment processes: heteroaggregation with natural colloids, NOM adsorption, binding of salts, biofilm formation, and coagulant/flocculant adsorption. Although these may not be considered as weathering pathways affecting the polymer backbone, such transformations are nonetheless expected to affect the fate, behavior and impacts of plastics in the environment.

In sea waters and surface waters, binding of divalent ions ( $\text{Ca}^{2+}$  or  $\text{Mg}^{2+}$ ), heteroaggregation with natural colloids and adsorption of natural NOM on plastics have been observed by many researchers and were reported to influence the stability of microplastics. Consequently, such pre-coating/corona on plastic surfaces could significantly impact nanoplastics and microplastics transport as some NOM fractions or colloids may act as stabilizers (limiting aggregation) while others (e.g., high molecular weight NOM fractions) promote aggregation via interparticle bridging effects.<sup>11, 60-62</sup> Similar results were observed by Liu et al., where nanoparticle stability and aggregation were considerably modified by organic coatings.<sup>63</sup>

Water treatment was also reported to change plastic surface chemistry. While a large proportion of plastics is expected to be trapped in aggregates and settled sludge, a small proportion is however refractory to treatment and is *de facto* released in aquatic environments.<sup>13, 64, 65</sup> The coagulants (e.g., alum), flocculants (e.g., polyacrylamide) and bioflocculants (extracellular polymeric substances, EPS) present in wastewater<sup>66</sup> are expected to coat the plastic surface, hence modifying its transport and fate once released in aquatic environments. It was reported that metal-based coagulants (e.g., alum; 1–6 mg Al/L)<sup>11, 67, 68</sup> and organic cationic polymers (e.g., polyamines; 0.1–0.6 mg/L)<sup>42, 69</sup> interact with plastic surfaces *via* electrostatic affinities on negatively charged sites (e.g., hydroxyl and carboxyl groups) or via hydrogen bonding.<sup>11</sup> Quartz crystal microbalance with dissipation (QCM-D) experiments showed that positively charged inorganic and organic coagulants deposited more on weathered plastic surfaces, as more anionic functions are available.<sup>11</sup> UV exposure could also have an impact on plastics aggregation and stability. Wang et al. concluded that UV-induced weathering that degrades sulfate and amine groups of plastics reduced the electrostatic repulsion, hence promoting nanoplastic homoaggregation (NaCl solution).<sup>70</sup>

### 5.2.6 Weathering processes in major environmental compartments of the water cycle

Weathering pathways encountered by microplastics in major environmental compartments are summarized in Figure 5.1. We present the mass flux of plastics in major compartments of the water cycle and show the important weathering processes occurring in them (Figure 5.1). Microplastics undergo several weathering pathways at the same time in each environmental compartment, leading to combined effects. For example, the presence of carbonyl groups on UV-degraded microplastic surfaces favors biofilm growth.<sup>28</sup> Conversely, a biofilm covers the surface of the plastic fragments and may also increase their density and make them sink in water.<sup>71</sup> Marine snow can also transport micro- and nanoplastics to ocean sediments regardless of their density.<sup>72</sup> This may explain the presence of buoyant plastics in sediments and a lower-than-expected presence in surface waters.<sup>73</sup> Other combinations of weathering processes accelerate microplastic fragmentation: photooxidation combined with mechanical abrasion<sup>32</sup> or thermal degradation combined with biodegradation.<sup>14</sup>

Weathering pathways are complex even within a single compartment. For example, the impact of photooxidation on plastics depends on the plastic composition and sunlight penetration in water. Buoyant polymers such as PE (density = 0.91-0.97 g/cm<sup>3</sup>) and PP (density 0.90-0.92 g/cm<sup>3</sup>) are more prone to photooxidation in open bodies of water than common polymers that sink, such as polyethylene terephthalate (PET, density = 1.35-1.45 g/cm<sup>3</sup>) and polyvinyl chloride (PVC, density = 1.1-1.45 g/cm<sup>3</sup>). In seawater, where the water density is higher, some grades of PS and expanded PS also float and are subjected to direct solar radiation. Shape is another factor that will contribute to how a particular fragment will be exposed to radiation. Flat fragments in the water surface will tend to expose mainly one side, which will receive more radiation, while more symmetrical cubic fragments will rotate and present a more homogeneous degradation on all sides.<sup>31</sup> The impact of each weathering process is related to both the intensity and duration of exposure. Therefore, typical residence times in the water cycle must be considered when assessing microplastic weathering processes. A water droplet transits for 9 days in the atmosphere, 2 weeks in a river, 10 years in big lakes, 120 years in superficial layers of oceans, and 3000 years in deep oceans.<sup>74</sup> The residence time of water in most drinking water and wastewater treatment processes is less than two days,<sup>33</sup> however, in many cases, the sludge retention time (few days to few months)

may be considered instead of the water retention time because most plastics are trapped in the sludge.

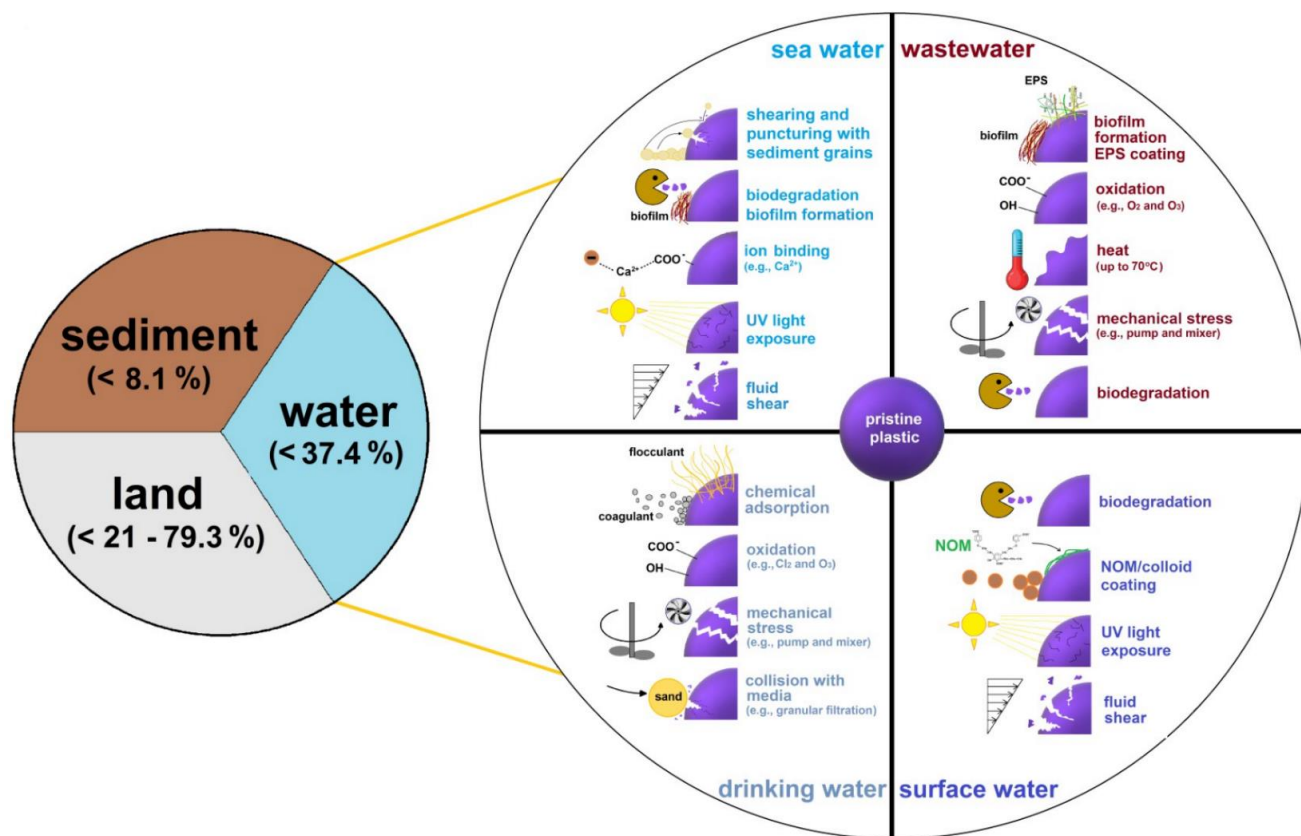


**Figure 5.1.** Major weathering pathways that plastic and its degradation products will encounter throughout its lifecycle before and after entering the environment. Percentages refer to estimated fraction of plastics released into a given compartment after manufacturing and use based on data from <sup>13</sup>.

### 5.3 Effects of weathering on microplastic fate in the environment

In the previous section, we described how weathering can change the properties of plastics. Those physicochemical changes are reported to affect plastic fate in the environment and removal during water treatment.<sup>11</sup> Weathering can also affect how microplastics interact with aquatic organisms.<sup>75</sup> The color, size, attached biofilm and surface charge changes will determine microplastic uptake and potential effects.<sup>76</sup> There is a lack of understanding on how weathering affects microplastic removal during water treatment, transport and aggregation processes, hence, this section will briefly discuss these three processes.

During water treatment, weathered plastics were recently shown to interact better with coagulants and flocculant. 90-99% of weathered plastic removal was systematically measured<sup>11</sup>,

<sup>69, 77, 78</sup> while lower removals were observed with pristine plastics: ~ 80%<sup>11</sup> and <30%.<sup>79</sup> Similarly, on-site measurements systematically reported removals higher than 95% for naturally weathered plastics.<sup>69, 80, 81</sup> Such higher interaction of coagulant, flocculant and bioflocculant (EPS) is attributable to a more heterogeneous plastic surface obtained after weathering (e.g., (photo)oxidation) and/or after other surface modifications (e.g., NOM coating), hence offering new anchoring points for coagulants, while pristine plastic surfaces are relatively homogeneous and less reactive.<sup>11</sup> Consequently, studies designed with pristine plastic materials might underestimate plastic aggregation and removal in full-scale water treatment plants. Considering that pristine plastics are likely inexistent in natural environments, these studies reveal the importance of designing research protocols with realistic weathering conditions. To overcome systematic plastics release, water treatment plants could be designed considering the surface chemistry of weathered and refractory plastics e.g., by adjusting the aggregation conditions such as coagulant types and pH.

Few studies have shown the effect of weathering on the transport of nanoplastics in model groundwaters and their stability in surface waters. One study highlighted the importance of considering weathering conditions in cold climates. Exposure of PS nanoplastics to repeated freeze-thaw cycles led to significant aggregation even in the presence of NOM, resulting in lowered mobility of the particles in saturated quartz sand compared to nanoplastics at constant cold temperature.<sup>53</sup> A different study showed that UV and ozone weathering increased the mobility of nanoplastics and facilitated the transport of contaminants in a loamy sand. The enhanced mobility of the weathered nanoplastics was attributed to the increase in surface oxidation and reduced hydrophobicity.<sup>82</sup> UV weathering also impacts the stability of nanoplastics in simulated natural waters.<sup>83</sup> A combination of new carboxyl functional groups and decreased particle size (from 120 to 80 nm) of the UVA-aged nanoplastics compared to pristine ones enhanced the aggregation of the nanoplastics in calcium chloride solution (ascribed to bridging via oxygen-containing functional groups) but promoted stability in sodium chloride solution.<sup>83</sup> Our understanding of the effects of weathering on other environmental fate processes besides toxicity and sorption is still very limited; hence, more studies are needed for realistic risk assessment.

## **5.4 Current knowledge about weathering protocols used in microplastics effect studies**

A comprehensive literature search was conducted using the Scopus and Google Scholar citation databases (as of May 25, 2021). The search was carried out to identify laboratory-based effect studies that (i) compared weathered/aged plastics with pristine ones in the same study, (ii) used leachate from weathered plastics and, (iii) used pristine microplastic only (detailed criteria in Table S5.1). An effect study in this context is defined as a study that investigates the effect of weathered microplastics or leachate on transport, aggregation, or toxicity of particles, sorption of contaminants, etc. Leachates commonly contain organic/inorganic additives and monomers that are released during the weathering process,<sup>84</sup> and can also contain nano- or microplastics.<sup>85</sup> Studies investigating the fragmentation or biodegradability of microplastics without evaluating the effects of the aged microplastics were excluded from the search.

### **5.4.1 Weathering protocols used in microplastic effect studies.**

Most weathered microplastic effect studies use pristine commercial primary microplastics or nanoplastics and weather them via UV, chemical, thermal or biological degradation. A few studies use microplastics obtained from the environment (mostly beaches) for laboratory studies. A subset of these studies uses degradation products leached from bulk plastic for toxicity studies. Figure 5.2 shows the distribution of the various types of weathering treatments applied to microplastics or their leachates. It is evident that there are fewer studies using leachate compared to the weathered microplastics. As mentioned above, there are more studies investigating the effect of weathering on microplastic sorption/desorption capacity (Figure 5.2, layer 2). Few studies have used microplastics weathered via natural UV radiation (sunlight) with only two of them reporting irradiance.<sup>44, 86</sup>

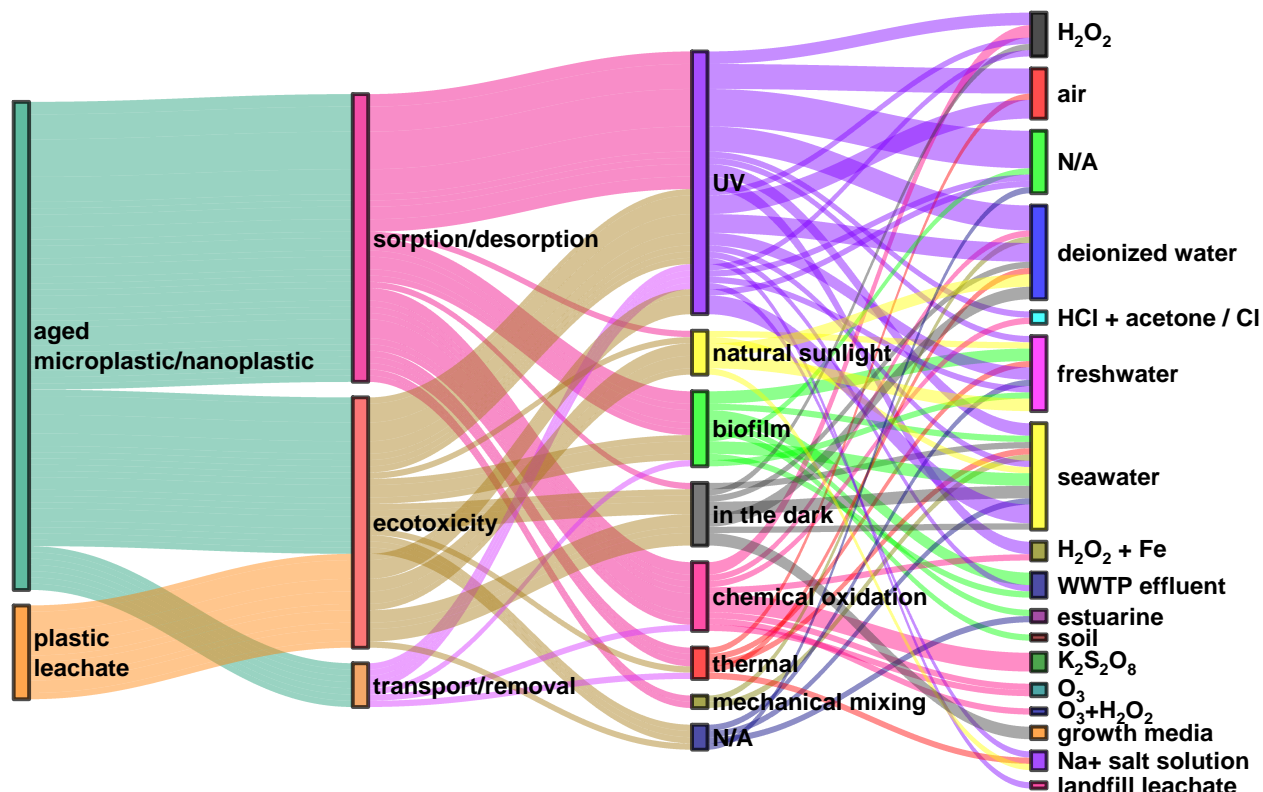


**Figure 5.2.** Distribution of the various types of weathering treatments applied to microplastics and plastic leachates among controlled laboratory effects studies. First layer = plastic state, second layer = study type/effect studied, third layer = weathering pathway/choice, fourth layer = weathering medium. WWTP – Wastewater treatment plant, N/A – Not available. Total of 93 studies identified from 63 articles. Articles reporting more than one weathering media are treated as separate studies. Data references provided in Table S5.2.

For studies using UV radiation, we compared the irradiance versus duration of exposure for microplastics weathered naturally or artificially as well as the type of plastic used (Figure 5.3). The radiation time varies from 24 to 7920 hours in these studies. There is no generalized method of exposure as the irradiance and duration of exposure vary significantly across these studies with PS having the most variation. It is worth noting that 49% of studies (31/63 articles) report the temperature in the weathering setup. The cumulative distribution (Figure S5.1) shows that 70% of these studies use temperatures  $<35^{\circ}\text{C}$  with only two investigating effect of weathering at cold<sup>87</sup> and freezing temperature.<sup>53</sup> The plastics weathered via UV radiation are typically suspended in media that range from deionised water to natural water and chemical oxidants (Figure 5.2, layer 4). Two studies used a combination of UVC light and  $\text{H}_2\text{O}_2$  to weather microplastics for 96 hours.<sup>88, 89</sup> While UVC light is not most representative of the natural environment, it is sometimes used in water treatment disinfection. UVC light exposure in water treatment is usually done at

short contact times (~ 5 sec), hence studies using this approach should mimic the short residence time accordingly. Other studies have used chemical oxidation approaches including Fenton reagent, hydrogen chloride, ozone, potassium permanganate and hydrogen peroxide<sup>90, 91</sup> while some combined  $\text{Fe}^{2+}$  with UV light (photo-Fenton)<sup>91, 92</sup> or high temperature.<sup>90</sup> While these chemicals are sometimes used in water and wastewater treatment, hence relevant, there is variability in the working concentrations used across studies (20–200 mM  $\text{Fe}^{2+}$ , 2 g and 10 mM  $\text{K}_2\text{S}_2\text{O}_8$ ), making comparability and environmental appropriateness difficult to assess. Environmental appropriateness is sometimes questionable as there is a need to justify the choice of high chemical dose and weathering pathway being mimicked. One study used natural sunlight to weather PS and PE, and compared the results to microplastics weathered via Fenton reaction and heat-activated  $\text{K}_2\text{S}_2\text{O}_8$ .<sup>44</sup> Microplastics were suspended in water samples from Yangtze River and Taihu Lake, China and placed on a building rooftop for 11 months. It was argued that the degradation products formed after initiating natural UV radiation yields same products as the advanced oxidation process i.e., free radicals. The oxygen/carbon ratio of the aged microplastics was also quantified and it was shown that it could be used as an alternative parameter to carbonyl index typically used to measure extent of oxidation. These oxidation processes are promising approaches that could shorten the aging time of microplastics for laboratory effect studies but may require further validation.

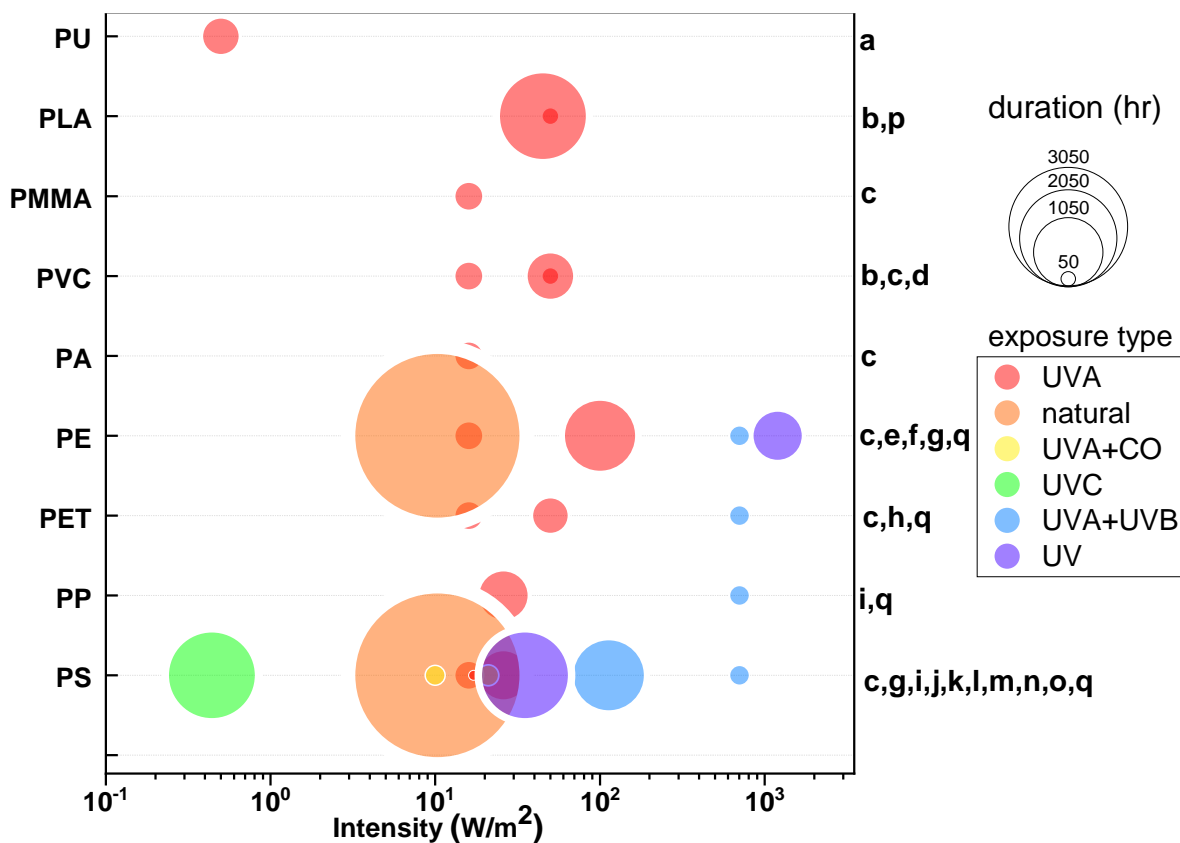


**Figure 5.3.** General trend in irradiance versus duration (hr) and plastic type across different laboratory effect studies reporting these parameters. Here, we see that the type of UV treatment and plastic type varies across studies. CO -chemical oxidation, PS - polystyrene, PE - polyethylene, PP - polypropylene, PVC - polyvinyl chloride, PET - polyethylene terephthalate, PA - polyamide, PC - polycarbonate, PMMA - polymethyl methacrylate, PLA - polylactic acid. References: a - <sup>93</sup>, b - <sup>94</sup>, c - <sup>95</sup>, d - <sup>96</sup>, e - <sup>11</sup>, f - <sup>97</sup>, g - <sup>44</sup>, h - <sup>98</sup>, i - <sup>99</sup>, j - <sup>92</sup>, k - <sup>83</sup>, l - <sup>100</sup>, m - <sup>101</sup>, n - <sup>102</sup>, o - <sup>103</sup>, p - <sup>104</sup>, q - <sup>105</sup>.

Microplastics can be weathered with the aim of growing biofilms on them.<sup>87, 106-108</sup> Wang et al.<sup>108</sup> mimicked weathering in wastewater treatment plants by placing PE microplastics in sewage outlets in Shanghai for 20 days. This resulted in a pore size reduction (from 10 to 3 nm) and an increase in specific surface area (from 0.24-0.78 m<sup>2</sup>/g) of the plastic. When mimicking biofouling in a riverine, estuarine and marine system in Australia, Johansen *et al.* observed that patchy biofilm enriched with Si, Al and O developed on the plastic surface.<sup>109</sup> PS microbeads placed in filtered seawater for 3 weeks in the dark showed that aging enhanced plastics ingestion by zooplankton.<sup>87</sup> However, no characterisation was done to confirm the presence of biofilm on the plastic surface. Even though some studies are designed to produce biofilm-aged microplastics, characterising its presence after weathering is helpful. Schur *et al.* showed this in a recent study where dissolved organic matter rather than the presence of biofilm was suggested as the driving mechanism for the multigenerational effect of wastewater-incubated PS on *Daphnia*.<sup>110</sup> A recent

study revealed that microplastics exposed to freshwater from an artificial pond and seawater from a marine aquarium led to the coating of biomolecules forming an eco-corona, which facilitated their uptake in mouse cells.<sup>111</sup> These non-UV weathering pathways particularly highlight the importance of exploring other weathering processes microplastics will encounter in the environment. For example, while it was shown that UV-aged PA microplastics had limited toxicity to zebrafish larvae,<sup>102</sup> another study reported tissue alterations in mussels exposed to PE microplastics incubated in seawater.<sup>75</sup>

Thermal weathering pathways have also been used to obtain environmentally relevant plastics. One study exposed PS nanoplastics to temperatures typically encountered in cold climate regions<sup>53</sup> for transport experiments in saturated quartz sand. The nanoplastics were suspended in monovalent salt solution (in the presence and absence of natural organic matter) and subjected to several controlled freeze-thaw cycles (from 10°C to -10°C). These temperature ranges closely mimic those encountered during the shoulder periods in southern Quebec, Canada. Another study used a higher temperature of 70°C to weather PS microplastics suspended in sea water and freshwater for sorption experiments.<sup>58</sup> However, it is unclear which environmental compartment was being mimicked or where plastic would normally encounter such high temperatures. Since such high temperatures will not be typically encountered in freshwater and seawater, there is a need to better describe the rationale behind such choices.

Another approach used in obtaining environmentally relevant microplastics is by using leachates obtained during the weathering of bulk plastics. The particles contained in leachates could be more representative of the types of nano- and microplastics found in the environment, therefore, we included some studies using leachates in this review. It is however important to note that some of these studies do not use corresponding reference or control pristine particles for comparison. Nevertheless, we can gain some insights from the weathering methods used. Leachates were obtained either by weathering bulk plastics in the dark or exposure to natural sunlight.<sup>85, 86, 97</sup> The reported leachate studies use background medium ranging from deionised water, tap water and natural/artificial seawater.

Overall, we noted considerable variability in the methods, duration, and medium used for weathering microplastics. While few of the identified laboratory-based studies follow existing international standards, a larger percentage used custom-designed weathering protocols, and some

do not justify the rationale behind the choice of weathering process. There is no notable difference in the protocols used for nanoplastics versus microplastics across studies. In general, the biofilm/biodegradation related effect studies seem to use the most realistic protocols having direct environmental relevance. Some studies have weathered plastics naturally by placing them outdoors but fail to report the irradiation values, making comparison difficult. Effect studies mimicking mechanical abrasion that might occur in sandy beaches or deep bed sediments are sparse. Weathering processes occurring in biosolids streams are also overlooked.

#### **5.4.2 Proportion of microplastic effect studies that use weathered plastics**

Figure 5.4a shows the proportion of effect studies carried out with weathered plastics. Only few microplastics effect studies (~10%) used weathered microplastics, of which a considerable proportion found weathering to have a significant effect (~90%). By focusing on only pristine plastics, current models may be underestimating (or overestimating) the risks associated with microplastic pollution. Figure 5.4c presents the ranking of the top five most frequently reported polymer types across microplastic studies. Across all effect studies, the most frequently weathered plastic type was polystyrene > polyethylene > polypropylene > polyvinyl chloride > others (Figure 5.4b). Comparing the type of plastics detected in various environmental compartments globally as well as the current global plastic demand, there seems to be a mismatch (Figure 5.4c). Indeed, majority of weathering studies use polystyrene whereas it is not the most commonly occurring plastic in environmental samples. Polypropylene which ranks second in most environmental studies,<sup>112-114</sup> is the third most weathered plastic. Polyethylene appears to be the most commonly occurring plastic, hence should be used in more weathering research to understand its effects.

## Overview of microplastic effect studies using weathered microplastics

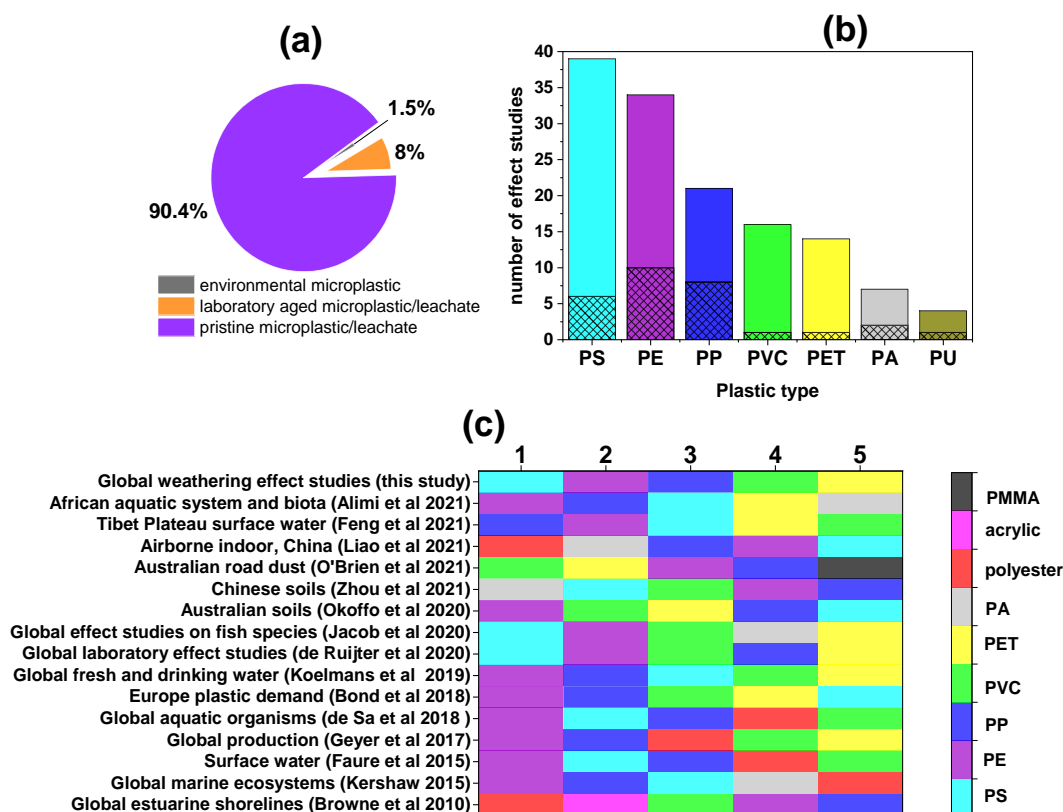


**Figure 5.4.** (a) The distribution of microplastic types used in effect studies highlighting the small proportion using weathered plastics in comparison to pristine ones; (b) The number of effects studies reporting types of polymer weathered in those studies. Dot pattern are polymer types reported in effects studies using microplastics sampled from the environment. Studies reporting both PE and HDPE/LDPE were counted as one PE; (c) A ranking of top 5 plastic types used in weathering effects studies globally. Plastics rank 1 (most common) – 5 (least common) from left to right. PS - polystyrene, PE - polyethylene, PP - polypropylene, PVC – polyvinyl chloride, PET – polyethylene terephthalate, PA – polyamide, PC – polycarbonate, PMMA – polymethyl methacrylate, PU - polyurethane.

### 5.4.3 Microplastics effect studies using environmental samples: comparison with laboratory weathered microplastics.

Few effect studies (<2%) have used microplastics collected in the natural environment (Figure 5.4a, Table S5.3). Again, majority of these studies focus on sorption/desorption and the most frequently used plastics follow PE>PP~PS. Although this approach yields microplastics that are of significant environmental relevance, it makes study reproducibility quite challenging. Zhang *et al.* collected beached microplastics from North China and compared their contaminant sorption capacity to virgin PS foams with similar sizes.<sup>115</sup> The beached microplastics adsorbed contaminants two times as much as the pristine ones (Freundlich isotherm constant = 425 and 894 mg/kg. (l/mg)<sup>1/n</sup> respectively). This was attributed to the higher specific surface area of the aged

microplastic. Using PE pellets collected from beaches in South West England, researchers have shown that higher amount of trace metals adsorb on the beached plastics compared to virgin ones.<sup>116</sup> Waldschlager *et al.* recently used microplastics recovered from a fluvial environment to determine their fate.<sup>117</sup> They showed that the environmentally weathered microplastics had much slower settling and rising velocities compared to pristine plastics used in their previous study.<sup>118</sup> Some of these studies show that the aged microplastics collected in the environment behaved differently than pristine microplastics of the same or similar material while others do not compare with pristine ones. Generally, this approach should be embraced by the microplastic community as it can provide more realistic insights on the effects of microplastic pollution in the environment.

In Figure 5.5 and Table 5.1, we compared the characteristics of microplastics weathered in the laboratory versus those collected from the environment. Interestingly, we observed that only 12 laboratory effect studies have used aged nanoplastics. Additionally, only few studies report the size of plastic retrieved from the environment which prevents an extensive meta-analysis (some report < 5 mm without an actual value or range). The few environmental microplastics with size ranges up to 0.45  $\mu\text{m}$ , were obtained by grinding milli-sized samples.<sup>115, 119, 120</sup> The lack of environmental samples using nanoplastics might be associated with the methodological difficulties associated with separating the nanoplastics from the complex background matrix. The shapes of plastics used are also very different as fragments dominate environmental microplastics whereas aged beads/spheres are more commonly used in the laboratory studies. While most environmental microplastics were collected from agricultural soils and beaches, only one laboratory effect study used landfill and soil as weathering media. Clearly, there exists several gaps between these two types of microplastics used in effect studies.

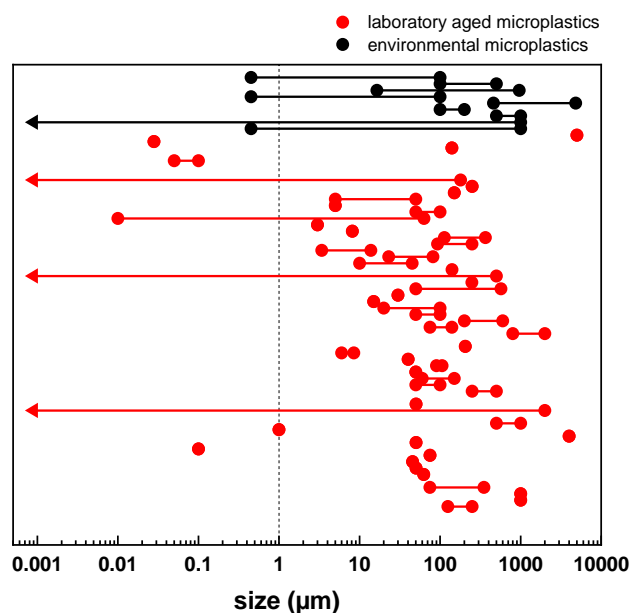


**Figure 5.5.** Size ranges of weathered microplastics used in effect studies. Detailed references provided in Tables S5.2 and S5.3. Arrows indicate that no lower limit was provided for that study.

**Table 5.1.** Comparison of characteristics and weathering conditions of effect studies using microplastics aged in the laboratory or collected in the environment. Detailed references in Tables S5.2 and S5.3

Characteristics	Laboratory weathered microplastics	Microplastics collected from environment
polymer types	PS > PE > PP > PVC > PET > PA > PU > PMMA, PTFE, PLA, PC	PE > PP > PS > PA > PVC, PET
shapes	beads > fragments, films, fibers	fragments > beads, films, fibers
weathering medium/sampling environment	air, deionized water, artificial and natural surface waters, chemical oxidants, landfill/soil, wastewater effluent	beach sediment, farmland soil
physical characterisation	size, density, morphology, specific surface area, crystallinity, color, contact angle, glass transition temperature, melting point	size, density, color, morphology
chemical characterisation	polymer type, surface chemistry (zeta potential, carbonyl index)	polymer type, surface chemistry (zeta potential, functional groups, carbonyl index, point of zero charge)
other conditions reported	plastic source, irradiation, wavelength, temperature, humidity, duration	location

## 5.5 Standardized international weathering protocols in different applications

Long before the onset of microplastics research (Figure 5.6a), standard weathering protocols were developed to assess whether a new plastic product will maintain acceptable properties during its lifecycle. Nonetheless, there has been an increase in the number of publications on microplastics or nanoplastics that mention these protocols (Figure 5.6b). In this section, we review selected active standards from ASTM International and the International Organization for Standardization (ISO) and discuss whether they are appropriate and adaptable for the study of plastic fragmentation into micro- and nanoplastics in the environment. These standards are classified below according to the type of exposure they intend to reproduce: outdoor exposure, marine exposure and solid waste conditions. A list of all standards used in this section, including ASTM/ISO equivalencies is available in Table S5.4.

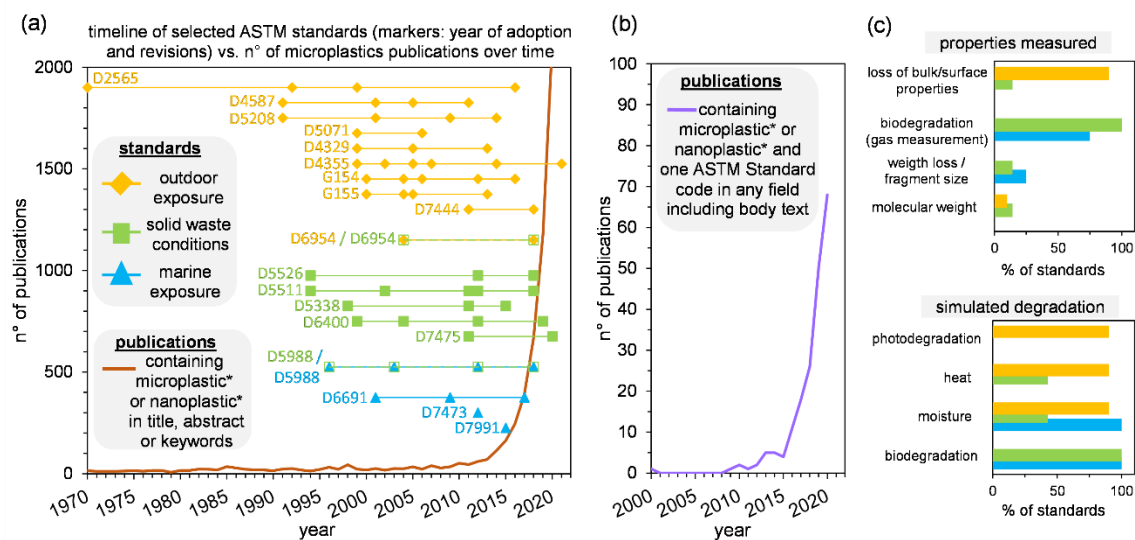


**Figure 5.6.** Selected ASTM standards for simulated weathering, classified as outdoor exposure, marine exposure or solid waste conditions: (a) timeline including the creation and revision of each standard, compared with the surge in scientific publications including microplastic\* or nanoplastic\* in title, abstract or keywords (Scopus, May 4, 2021); (b) publications including microplastic\* or nanoplastic\* and at least one code (e.g., D6400) of the selected ASTM standards in any field, including the body text (Google Scholar, May 4, 2021); (c) simulated degradation pathway and the outcome properties measured within each type of exposure. Standards of natural exposure were not included in this selection.

### 5.5.1 Outdoor exposure

The standards aimed for natural outdoor exposure, such as ASTM D1435/ISO 877.2, ISO 15314, ISO 877, and ASTM D 5272, recommend that specimens should be exposed in several locations, and state that an average result in a given location can only be achieved after several years of repeated exposure.

The standard protocols that simulate outdoor exposure using accelerated weathering are carried out in a chamber in which plastic degradation is induced by light (photodegradation), heat and moisture (Figure 5.6c). These standards do not intend to simulate other degradation pathways such as mechanical abrasion, biodegradation or advanced oxidation processes. To produce photooxidation, most protocols recommend the use of either a fluorescence UV lamp or a xenon arc lamp. ASTM D4329/ISO 4892-3 describe the practice for exposing plastics to UVA lamps, which match the solar irradiance in the UV region to produce the most damaging type of radiation that can occur in the environment. But even though the higher energies of UV-range radiation are more deleterious to plastics, in the environment they are exposed to a wider range of radiation of different energies. Experiments using a narrow frequency band may overlook synergistic effects or overexpose plastics to their UV wavelengths of maximum sensitivity, which are not so abundant in the environment.<sup>30, 121</sup> Xenon arc lamps simulate the sunlight spectrum including UV, visible and infrared light, and therefore are generally preferred if a product is intended for outdoor use, as described by ASTM D2565 (similar to ISO 4892-2).

Weathering chambers allow for irradiance, temperature and humidity control to improve the simulation of natural phenomena. While the majority of the standards specify a temperature suitable for each exposure, some of these temperatures are higher than those encountered in typical natural waters/environments. Condensation cycles can be reproduced in UV chambers by an increase of chamber temperature and relative humidity followed by a temperature decrease. Alternatively, chambers equipped with xenon arc lamps use a water spray cycle to simulate rain and fast temperature changes. The presence of water on the surface of plastics can accelerate the reactions involved in the degradation process, while fast temperature changes cause contraction and expansion of the specimens. Different cycles with small variations in these parameters are also proposed, but in all cases, the cycle is repeated every few hours with the same parameters.

The test time depends on the materials and can be defined by the stakeholders involved, but it is recommended that the minimum test time should produce a substantial performance difference between the specimen and the control. Some standards recommend the use of two controls: one with known superior durability and another with known inferior durability. Appearance and mechanical properties of the bulk plastic parts are common properties evaluated by the users.

### **5.5.2 Marine exposure**

In the marine environment, plastic specimens are in constant contact with water and microorganisms, and exposed to different levels of UV radiation depending on their buoyancy. ISO 15314 is one of the few standards aimed at natural exposure of plastics in marine environments. It provides three exposure scenarios: plastic floating on the surface, partial immersion of plastic and complete immersion to assess the persistence of marine litter. ISO 15314 is suitable for different types of specimens commonly found in consumer products such as plastic films, sheets, fibers and ropes. This standard recommends exposure at different locations to account for variability in radiation, temperature, microorganism populations, *etc.* The accelerated weathering standards that simulate marine exposure account for the fact that material degradation in natural waters is mainly dependent on the presence of microorganisms<sup>122</sup>, giving emphasis to biodegradation and often omitting other processes such as photodegradation and temperature variations (Figure 5.6c). ASTM 7473 simulates marine exposure in open system aquarium incubations with natural flowing seawater, but without sunlight as the test is aimed for non-buoyant plastics. The protocol uses marine sediments, which contain several orders of magnitude more bacteria than seawater, to guarantee the presence of microorganisms. The standard recommends evaluating the specimen visually and measuring the weight loss over time to obtain some insight on the fragmentation rate. ASTM D6691 and D7991 describe methods to assess the aerobic biodegradation of plastics in controlled laboratory conditions, in which the amount of CO<sub>2</sub> produced by the biodegradation of the specimen is measured over time. In ASTM D6691, a well-defined population of microorganisms present in the marine environment is used, while the method described in ASTM D7991 reproduces the tidal environment with specimens buried in natural sandy marine sediment. But just as the protocols aimed for outdoor exposure, the ones that mimic the marine environment are only concerned with the degradation of the bulk plastic specimens, which are easier to separate and recover for analysis.

### **5.5.3 Solid waste conditions**

In the standards that simulate weathering in solid waste conditions, biodegradation is also the main degradation pathway, in combination with heat and moisture (Figure 5.6c), in different types of media. ASTM D5988 (equivalent to ISO 17556) aims to simulate biodegradation of plastics when disposed in aerobic soil environment. A biometer flask is used and the specimen is buried in equal parts of soil, sand and manure. The CO<sub>2</sub> produced by the system is trapped in the flask and

measured periodically. Control flasks with no specimens are important since the soil will naturally produce CO<sub>2</sub>. The standard does not specify the type of polymer to be tested and recommends that the results should not be used to classify the material as biodegradable or not. Depending on the type of plastic, signs of biodegradation that can be captured by this method can take a long time to appear. Natural polymers more susceptible to biodegradation produce CO<sub>2</sub> faster than polypropylene, for instance, and are better suited for the method.<sup>123</sup> The aerobic biodegradation of plastics is also evaluated in controlled composting conditions at thermophilic temperatures (ASTM D5338, equivalent to ISO 14835). ASTM D5338 is often used together with ASTM D6400 (equivalent to ISO 17088), which determines the requirements needed to label a given plastic as compostable in aerobic municipal or industrial composting facilities. Based on this standard, a compostable plastic will have 90% or more of its fragments passing a 2 mm sieve after 12 weeks in composting conditions. At 180 days, 90% of the carbon present in the plastic must be converted to CO<sub>2</sub>. ASTM D6400 mentions that the rate of degradation in the specified timeframe is thickness dependent, and each material that aims to be labeled as compostable must specify the maximum thickness at which the requirements above are met.

Anaerobic biodegradation can be simulated by the ASTM D5511 (equivalent to ISO 15985) in high-solids anaerobic-digestion conditions (wastewater sludge) or by ASTM D5526 in accelerated landfill conditions, both using sealed vessels to measure the gas residues (CO<sub>2</sub> + methane) over time. Both standards recommend the use of methanogenic inoculum derived from anaerobic digester as the medium to reproduce anaerobic conditions. ASTM D5526 is also designed to produce a mixture of household and plastic waste in different stages of degradation that can be used for ecotoxicological assessment.

The protocol described by ASTM D7475 combines both aerobic and anaerobic biodegradation in simulated biologically active landfills. In the aerobic phase, plastic specimens are mixed with pretreated household waste and changes in mass, molecular weight and selected physical properties should be measured before and after as indications of biodegradation. The anaerobic phase of the protocol is analogous to ASTM D5526.

#### **5.5.4 Appropriateness of standard protocols for micro/nanoplastics research**

Standard protocols for accelerated weathering explicitly state the claims that can be made with the measured results and highlight that the proposed exposure conditions of each protocol cannot be

used to predict/extrapolate the absolute degradation rates of plastics. Their main advantage is to produce faster degradation and reproducible conditions compared to natural degradation,<sup>124</sup> which is sought after in micro/nanoplastics research while the drawback is creating conditions that do not match natural weathering.

The standards for outdoor exposure focus on accelerated photodegradation (Figure 5.5b) and are used to monitor the loss of bulk or surface properties after weathering (Figure 5.5c). These standards are not concerned with the generation of small fragments or leachates produced by the degradation. If a strip of textile made of plastic fibers maintains an acceptable color variation and mechanical properties after a standardized weathering test, for example, the product is approved even though it may produce microplastics during its common use. Furthermore, condensation and water spray cycles inside the weathering chambers can wash away these by-products. In microplastic research, the most mentioned outdoor exposure standards are the guides on how to operate either a fluorescent UV lamp or a Xenon arc lamp and water apparatus (ASTM G154 and G155),<sup>125</sup> which can be used in non-commercial weathering chambers commonly built in research laboratories. The most typical adaptation that is made in microplastic research is the use of a water-filled container containing the plastic to be weathered, to retain micro/nanoplastics and leachates during the process. This type of sample exposure is not covered by the international standard protocols, which were designed to expose plastic parts attached to a panel to produce homogeneous exposure. In some commercial weathering chambers that comply with the standards, the samples are exposed at an angle and even vertically, which makes it difficult to adapt for the exposure of open water-filled containers containing plastic to be weathered. This gap could be bridged with new standards on how to expose this type of sample aimed for leachate/micro and nanoplastic retention.

The standards for marine exposure and solid waste conditions are mainly used to evaluate biodegradable, compostable or oxo-biodegradable plastics by the biodegradation gases produced under different weathering conditions (Figure 5.5c). These types of plastic are often presented as a sustainable alternative to conventional plastics, but the standards used to evaluate biodegradability or compostability are also not concerned with the generation of micro- and nanoplastics in soil or compost. A plastic classified as biodegradable according to ASTM D6691, for instance, may not completely biodegrade in the natural marine environment, since the test conditions described by the standard may overestimate the natural biodegradation rate<sup>122</sup> while

ASTM D6400 allows the presence of microplastics (fragments  $\leq 2$  mm) in the final compost after fragmentation for a plastic to be labelled as compostable.<sup>126</sup> This apparent contradiction has made ASTM D6400 one of the most cited international standard protocols in microplastics research. Adapting these standards as a weathering method to study plastic fragmentation is challenging due to the complexity of the remaining medium, often a mixture of waste/soil/sediment and plastic fragments. As different methods to separate micro- and nanoplastics from complex samples are being developed,<sup>52</sup> new international protocols designed specifically for the separation and analysis of micro- and nanoplastics could be created and used in conjunction with existing weathering standards.

A combination of protocols is also a potential future direction to create conditions that are closer to natural weathering. ASTM D6954 is a guide that combines different degradation pathways: thermal or photooxidation (outdoor exposure standards) followed by biodegradation in soil or solid waste. This guide also recommends the assessment of the ecological impact of degradation by-products. Each weathering step is analyzed separately and consecutively. More characterization data to compare artificially and naturally weathered samples (as described in Table 5.1) is needed to verify if this approach can produce realistic samples, since natural weathering pathways often occur concurrently.

The size, thickness and shape of the specimens is rarely specified in most weathering standards. The recommendation is that they should fit inside the sample holders and be appropriate for the before/after properties measurements. But the rate of fragmentation into micro- and nanoplastics is highly dependent on these characteristics. As mentioned earlier, degradation pathways start on the surface, so samples with high surface area are more susceptible to faster deterioration and fragmentation. This partly explains the ubiquity of microfibers in the environment.<sup>127</sup>

## **5.6 Overview of the current state of research on environmentally relevant microplastics and proposed weathering guidelines for future research.**

This review outlined several important aspects related to protocols for obtaining environmentally relevant microplastics and nanoplastics:

- Most of the studies reviewed show that weathering largely has an effect on the behavior of microplastics in the environment, however, many studies (~90%) are still using pristine plastics.
- There is a lack of effect studies using aged nanoplastics from accelerated laboratory weathering or environmental samples.
- Environmental microplastics are dominated by fragments while those aged in the laboratory are mostly beads/spherical.
- Reported weathering studies are focused on polystyrene > polyethylene > polypropylene > polyvinyl chloride, while the most produced/detected plastics include polyethylene > polypropylene. Polystyrene has been overrepresented in microplastics research and more efforts should be dedicated to other plastic types, especially microfibers.
- Current plastic standard weathering protocols, developed before the increased concern about plastic pollution, may not be fully suited for microplastic studies as they aim to monitor durability and understand bulk plastic behavior, with little concern about fragments or leachates produced during degradation. Combining different protocols and creating new sampling protocols for micro- and nanoplastics could increase the use of international standards and improve reproducibility in microplastics research. To achieve this objective, more characterization data comparing naturally and artificially weathered samples is needed.
- Important weathering pathways are not well represented in microplastics research. Many microplastics will undergo biodegradation or biological coating under various temperature ranges, due to their predominance in biosolids streams or in land. Chemical oxidation encountered in the water treatment cycle is also overlooked.
- The combined impacts of several weathering pathways on polymer backbone alteration (e.g., mechanical stress combined with (photo)oxidation) and other surface modifications (e.g., NOM coating) are currently neglected, although such combinations are likely to drastically change interactions with surfaces and to synergistically contribute to plastic fragmentation.
- The characterization of leached plastics has particularly been overlooked. While we focus on the weathering of microplastics, we may miss an essential component: are smaller

microplastics or nanoplastics being leached from primary microplastics and/or bulk plastics<sup>4?</sup>

As the microplastic scientific community is now moving towards plastics and microplastics of greater environmental significance, it is important that protocols used for weathering effect studies be standardized for the sake of harmonization. Without documenting the actual conditions used and appropriate metrics, comparison across studies becomes challenging. Overall, there is a lack of justification of the choice for some weathering pathways. A selected method or protocol should attempt to mimic a weathering pathway encountered in the environment. As a way of harmonizing methods, we recommend that future weathering effect studies follow some of the guidelines presented in Table 5.2. In this table, important parameters related to materials and protocols are listed. Currently, only few microplastics research studies describe all these materials and parameters. Notably, too much focus has been given to the primary materials without considering the initial microplastics, leached chemicals and leached plastics as a whole.

**Table 5.2.** Proposed reporting guidelines for studies on effects of weathered microplastics

	<b>Parameter/property</b>	<b>Guidance to improve comparability and reproducibility</b>
<b>Materials</b>	Polymer type	Characterise polymer type before and after weathering
	Polymer source	Specify source: purchased or collected in the environment
	Physical and mechanical characterisation	Indicate the properties of the plastics before and after weathering. <i>e.g.</i> , color, size, shape, morphology, roughness, melting point, tensile strength, hardness, etc.
	Chemical characterisation	Report chemical changes before and after weathering. <i>e.g.</i> , surface functionalization, crystallinity, surface charge, molecular weight
	Leached chemicals	For plastic leachates, report organic and inorganic products generated during weathering
	Leached plastics	Monitor the formation of secondary microplastics and nanoplastics during weathering
<b>Methods/Protocols</b>	Irradiance	For samples exposed to UV, report the total irradiance measured in the sample compartment and wavelength of light
	Weathering exposure time	Report the duration of each weathering exposure
	Weathering pathway	Justify the weathering pathway being mimicked in the environment
	Medium	Describe the background medium in which plastic is weathered. <i>e.g.</i> , air, activated sludge, seawater, saline solution, presence of organic matter, river water
	Oxidation	Report the dosage of oxidants (type, concentration, contact time)
	Temperature	Indicate the temperature in the weathering setup
	Humidity	Report the relative humidity in the weathering setup, especially for samples exposed to air
	Location	In the case of microplastics collected from the field, the location and environmental compartment as well as extraction procedure should be outlined
	Control	Control of same microplastic type and/or procedural blanks should be used to elucidate the effect of weathering
	Replicates	Characterise variability by replication

## Acknowledgements

The authors acknowledge the support of the Canada Research Chairs program, the Natural Sciences and Engineering Research Council of Canada, the Killam Research Fellowship program, the Petroleum Technology Development Fund of Nigeria for an award to OSA, an NSERC Banting Fellowship to DCM, an NSERC postdoctoral fellowship to RSK, and Mitacs Canada and Kemira for a postdoctoral fellowship to ML. This project was supported partially by a financial contribution from Fisheries and Oceans Canada. We also thank Laura Rowencyk for her helpful comments.

### **CRedit authorship contribution statement**

**Olubukola S. Alimi:** Conceptualization, Writing – original draft, Data Curation, Formal Analysis, Visualization, Methodology. **Dominique Claveau-Mallet:** Conceptualization, Writing – original draft, Visualization, Supervision. **Rafael Kusuru:** Writing – original draft, Visualization, Data Curation. **Mathieu Lapointe:** Writing – original draft, Visualization. **Stéphane Bayen:** Writing – review & editing, Supervision. **Nathalie Tufenkji:** Writing – review & editing, Supervision.

## References

1. Borrelle, S. B.; Ringma, J.; Law, K. L.; Monnahan, C. C.; Lebreton, L.; McGivern, A.; Murphy, E.; Jambeck, J.; Leonard, G. H.; Hilleary, M. A., Predicted growth in plastic waste exceeds efforts to mitigate plastic pollution. *Sci* **2020**, *369* (6510), 1515-1518.
2. Jeong, C.-B.; Kang, H.-M.; Lee, M.-C.; Kim, D.-H.; Han, J.; Hwang, D.-S.; Souissi, S.; Lee, S.-J.; Shin, K.-H.; Park, H. G.; Lee, J.-S., Adverse effects of microplastics and oxidative stress-induced MAPK/Nrf2 pathway-mediated defense mechanisms in the marine copepod *Paracyclops nana*. *Sci. Rep.* **2017**, *7* (1), 41323.
3. Carbery, M.; O'Connor, W.; Palanisami, T., Trophic transfer of microplastics and mixed contaminants in the marine food web and implications for human health. *Environ. Int.* **2018**, *115*, 400-409.
4. Gigault, J.; El Hadri, H.; Nguyen, B.; Grassl, B.; Rowenczyk, L.; Tufenkji, N.; Feng, S.; Wiesner, M., Nanoplastics are neither microplastics nor engineered nanoparticles. *Nat. Nanotechnol.* **2021**.
5. Andrady, A. L., Microplastics in the marine environment. *Mar. Pollut. Bull.* **2011**, *62* (8), 1596-605.
6. Cole, M.; Lindeque, P.; Halsband, C.; Galloway, T. S., Microplastics as contaminants in the marine environment: a review. *Mar. Pollut. Bull.* **2011**, *62* (12), 2588-97.
7. Boucher, J.; Friot, D., *Primary microplastics in the oceans: a global evaluation of sources*. IUCN Gland, Switzerland: 2017.
8. Sarno, A.; Olafsen, K.; Kubowicz, S.; Karimov, F.; Sait, S. T. L.; Sørensen, L.; Booth, A. M., Accelerated Hydrolysis Method for Producing Partially Degraded Polyester Microplastic Fiber Reference Materials. *Environ. Sci. Technol. Lett.* **2020**.
9. Cai, L.; Wang, J.; Peng, J.; Wu, Z.; Tan, X., Observation of the degradation of three types of plastic pellets exposed to UV irradiation in three different environments. *Sci. Total Environ.* **2018**, *628-629*, 740-747.
10. Bianchetti, G. O.; Devlin, C. L.; Seddon, K. R., Bleaching systems in domestic laundry detergents: a review. *Rsc Advances* **2015**, *5* (80), 65365-65384.
11. Lapointe, M.; Farner, J. M.; Hernandez, L. M.; Tufenkji, N., Understanding and improving microplastic removal during water treatment: Impact of coagulation and flocculation. *Environ. Sci. Technol.* **2020**, *54* (14), 8719-8727.
12. Lowry, G. V.; Gregory, K. B.; Apte, S. C.; Lead, J. R., Transformations of nanomaterials in the environment. *Environ. Sci. Technol.* **2012**, *46* (13), 6893-9.
13. Alimi, O. S.; Farner Budarz, J.; Hernandez, L. M.; Tufenkji, N., Microplastics and nanoplastics in aquatic environments: Aggregation, deposition, and enhanced contaminant transport. *Environ. Sci. Technol.* **2018**, *52* (4), 1704-1724.
14. Shah, A. A.; Hasan, F.; Hameed, A.; Ahmed, S., Biological degradation of plastics: A comprehensive review. *Biotechnol. Adv.* **2008**, *26* (3), 246-265.
15. Chamas, A.; Moon, H.; Zheng, J.; Qiu, Y.; Tabassum, T.; Jang, J. H.; Abu-Omar, M.; Scott, S. L.; Suh, S., Degradation Rates of Plastics in the Environment. *ACS Sustain. Chem. Eng.* **2020**, *8* (9), 3494-3511.
16. ASTM. In *Annual Book of ASTM Standards, 1990: Subject Index; Alphanumeric List*, American Society for Testing & Materials: 1990.
17. McGivney, E.; Cederholm, L.; Barth, A.; Hakkarainen, M.; Hamacher-Barth, E.; Ogonowski, M.; Gorokhova, E., Rapid Physicochemical Changes in Microplastic Induced by Biofilm Formation. *Front. bioeng. biotechnol.* **2020**, *8*, 205.
18. Garvey, C. J.; Impéror-Clerc, M.; Rouzière, S.; Gouadec, G.; Boyron, O.; Rowenczyk, L.; Mingotaud, A. F.; ter Halle, A., Molecular-Scale Understanding of the Embrittlement in Polyethylene Ocean Debris. *Environ. Sci. Technol.* **2020**, *54* (18), 11173-11181.

19. Rowenczyk, L.; Dazzi, A.; Deniset-Besseau, A.; Beltran, V.; Goudounèche, D.; Wong-Wah-Chung, P.; Boyron, O.; George, M.; Fabre, P.; Roux, C., Microstructure characterization of oceanic polyethylene debris. *Environ. Sci. Technol.* **2020**, *54* (7), 4102-4109.
20. Krause, S.; Molari, M.; Gorb, E. V.; Gorb, S. N.; Kossel, E.; Haeckel, M., Persistence of plastic debris and its colonization by bacterial communities after two decades on the abyssal seafloor. *Sci. Rep.* **2020**, *10* (1), 9484.
21. Waldman, W. R.; Rillig, M. C., Microplastic Research Should Embrace the Complexity of Secondary Particles. *Environ. Sci. Technol.* **2020**, *54* (13), 7751-7753.
22. Cowger, W.; Booth, A.; Hamilton, B.; Primpke, S.; Munno, K.; Lusher, A.; Dehaut, A.; Vaz, V. P.; Liboiron, M.; Devriese, L. I., EXPRESS: Reporting Guidelines to Increase the Reproducibility and Comparability of Research on Microplastics. *Appl. Spectrosc.* **2020**, 0003702820930292.
23. de Ruijter, V. N.; Redondo Hasselerharm, P. E.; Gouin, T.; Koelmans, A. A., Quality criteria for microplastic effect studies in the context of risk assessment: A critical review. *Environ. Sci. Technol.* **2020**.
24. Tobiska, W.; Nusinov, A., ISO 21348-Process for determining solar irradiances. *cosp* **2006**, *36*, 2621.
25. D'Orazio, J.; Jarrett, S.; Amaro-Ortiz, A.; Scott, T., UV radiation and the skin. *Int. J. Mol. Sci.* **2013**, *14* (6), 12222-12248.
26. Gewert, B.; Plassmann, M. M.; MacLeod, M., Pathways for degradation of plastic polymers floating in the marine environment. *Environmental Science: Processes & Impacts* **2015**, *17* (9), 1513-1521.
27. Gijssman, P.; Meijers, G.; Vitarelli, G., Comparison of the UV-degradation chemistry of polypropylene, polyethylene, polyamide 6 and polybutylene terephthalate. *Polym. Degrad. Stabil.* **1999**, *65* (3), 433-441.
28. Min, K.; Cuiffi, J. D.; Mathers, R. T., Ranking environmental degradation trends of plastic marine debris based on physical properties and molecular structure. *Nat. commun.* **2020**, *11* (1), 1-11.
29. Andradý, A. L.; Hamid, S. H.; Hu, X.; Torikai, A., Effects of increased solar ultraviolet radiation on materials. *J. Photochem. Photobiol. B: Biol.* **1998**, *46* (1), 96-103.
30. Feldman, D., Polymer weathering: photo-oxidation. *J. Polym. Environ.* **2002**, *10* (4), 163-173.
31. Ter Halle, A.; Ladirat, L.; Gendre, X.; Goudounèche, D.; Pusineri, C.; Routaboul, C.; Tenailleau, C.; Duployer, B.; Perez, E., Understanding the fragmentation pattern of marine plastic debris. *Environ. Sci. Technol.* **2016**, *50* (11), 5668-5675.
32. Song, Y. K.; Hong, S. H.; Jang, M.; Han, G. M.; Jung, S. W.; Shim, W. J., Combined Effects of UV Exposure Duration and Mechanical Abrasion on Microplastic Fragmentation by Polymer Type. *Environ. Sci. Technol.* **2017**, *51* (8), 4368-4376.
33. Metcalf; Eddy; Tchobanoglous, G.; Stensel, H. D.; Tsuchihashi, R.; Burton, F. L.; Abu-Orf, M.; Bowden, G.; Pfrang, W., *Wastewater engineering : treatment and resource recovery*. Fifth edition / ed.; McGraw-Hill Education: New York, NY, 2014.
34. Oram, B., UV Disinfection Drinking Water. *Water Research Center, Dallas, PA, USA. <https://www.water-research.net/index.php/water-treatment/water-disinfection/uv-disinfection> (accessed 23 February 2018)* **2014**.
35. Wolfe, R. L., Ultraviolet disinfection of potable water. *Environ. Sci. Technol.* **1990**, *24* (6), 768-773.
36. United States Environmental Protection Agency, *Alternative disinfectants and oxidants guidance manual*. US Environmental Protection Agency, Office of Water: 1999.
37. Sun, Y.; Yuan, J.; Zhou, T.; Zhao, Y.; Yu, F.; Ma, J., Laboratory simulation of microplastics weathering and its adsorption behaviors in an aqueous environment: A systematic review. *Environ. Pollut.* **2020**, *265*, 114864.
38. Tian, L.; Kolvenbach, B.; Corvini, N.; Wang, S.; Tavanaie, N.; Wang, L.; Ma, Y.; Scheu, S.; Corvini, P. F.-X.; Ji, R., Mineralisation of <sup>14</sup>C-labelled polystyrene plastics by *Penicillium variable* after ozonation pre-treatment. *New Biotechnology* **2017**, *38*, 101-105.

39. Sander, M., Biodegradation of Polymeric Mulch Films in Agricultural Soils: Concepts, Knowledge Gaps, and Future Research Directions. *Environ. Sci. Technol.* **2019**, *53* (5), 2304-2315.
40. Carr, S. A.; Liu, J.; Tesoro, A. G., Transport and fate of microplastic particles in wastewater treatment plants. *Water Res.* **2016**, *91*, 174-82.
41. Rom, M.; Fabia, J.; Grübel, K.; Sarna, E.; Graczyk, T.; Janicki, J., Study of the biodegradability of polylactide fibers in wastewater treatment processes. *Polimery* **2017**, *62*.
42. American Water Works Association, *Water quality and treatment : a handbook of community water supplies*. 5th ed. ed.; McGraw-Hill: New York, 1999.
43. Zhang, Y.; Diehl, A.; Lewandowski, A.; Gopalakrishnan, K.; Baker, T., Removal efficiency of micro-and nanoplastics (180 nm–125 µm) during drinking water treatment. *Sci. Total Environ.* **2020**, *720*, 137383.
44. Liu, P.; Qian, L.; Wang, H.; Zhan, X.; Lu, K.; Gu, C.; Gao, S., New insights into the aging behavior of microplastics accelerated by advanced oxidation processes. *Environ. Sci. Technol.* **2019**, *53* (7), 3579-3588.
45. Razumovskii, S. D.; Karpukhin, O. N.; Kefeli, A. A.; Pokholok, T. V.; Zaikov, G. Y., The reaction of ozone with solid polystyrene. *Polymer Science U.S.S.R.* **1971**, *13* (4), 880-890.
46. Jia, Y.; Chen, J.; Asahara, H.; Asoh, T.-A.; Uyama, H., Polymer Surface Oxidation by Light-Activated Chlorine Dioxide Radical for Metal–Plastics Adhesion. *ACS Appl. Polym. Mat.* **2019**, *1* (12), 3452-3458.
47. Pulido-Reyes, G.; Mitrano, D. M.; Kägi, R.; von Gunten, U. In *The Effect of Drinking Water Ozonation on Different Types of Submicron Plastic Particles*, Cham, Springer International Publishing: Cham, 2020; pp 152-157.
48. Wang, Z.; Lin, T.; Chen, W., Occurrence and removal of microplastics in an advanced drinking water treatment plant (ADWTP). *Sci. Total Environ.* **2020**, *700*, 134520.
49. Horton, A. A.; Walton, A.; Spurgeon, D. J.; Lahive, E.; Svendsen, C., Microplastics in freshwater and terrestrial environments: Evaluating the current understanding to identify the knowledge gaps and future research priorities. *Sci. Total Environ.* **2017**, *586*, 127-141.
50. Johnson, C. P.; Li, X.; Logan, B. E., Settling Velocities of Fractal Aggregates. *Environ. Sci. Technol.* **1996**, *30* (6), 1911-1918.
51. Lapointe, M.; Barbeau, B., Characterization of ballasted flocs in water treatment using microscopy. *Water Res.* **2016**, *90*, 119-127.
52. Nguyen, B.; Claveau-Mallet, D.; Hernandez, L. M.; Xu, E. G.; Farner, J. M.; Tufenkji, N., Separation and Analysis of Microplastics and Nanoplastics in Complex Environmental Samples. *Acc. Chem. Res.* **2019**, *52* (4), 858-866.
53. Alimi, O. S.; Farner, J. M.; Tufenkji, N., Exposure of nanoplastics to freeze-thaw leads to aggregation and reduced transport in model groundwater environments. *Water Res.* **2020**, 116533.
54. Colin, X.; Audouin, L.; Verdu, J.; Rozental-Evesque, M.; Rabaud, B.; Martin, F.; Bourguine, F., Aging of polyethylene pipes transporting drinking water disinfected by chlorine dioxide. Part II—Lifetime prediction. *Polym. Eng. Sci.* **2009**, *49* (8), 1642-1652.
55. Viebke, J.; Gedde, U. W., Assessment of lifetime of hot-water polyethylene pipes based on oxidation induction time data. *Polym. Eng. Sci.* **1998**, *38* (8), 1244-1250.
56. Chen, Z.; Zhao, W.; Xing, R.; Xie, S.; Yang, X.; Cui, P.; Lü, J.; Liao, H.; Yu, Z.; Wang, S.; Zhou, S., Enhanced in situ biodegradation of microplastics in sewage sludge using hyperthermophilic composting technology. *J. Hazard. Mater.* **2020**, *384*, 121271.
57. Viebke, J.; Elble, E.; Ifwarson, M.; Gedde, U. W., Degradation of unstabilized medium-density polyethylene pipes in hot-water applications. *Polym. Eng. Sci.* **1994**, *34* (17), 1354-1361.
58. Ding, L.; Mao, R.; Ma, S.; Guo, X.; Zhu, L., High temperature depended on the ageing mechanism of microplastics under different environmental conditions and its effect on the distribution of organic pollutants. *Water Res.* **2020**, *174*, 115634.

59. Hernandez, L. M.; Xu, E. G.; Larsson, H. C. E.; Tahara, R.; Maisuria, V. B.; Tufenkji, N., Plastic teabags release billions of microparticles and nanoparticles into tea. *Environ. Sci. Technol.* **2019**, *53* (21), 12300-12310.
60. Shams, M.; Alam, I.; Chowdhury, I., Aggregation and stability of nanoscale plastics in aquatic environment. *Water Res.* **2020**, *171*, 115401.
61. Liu, P.; Zhan, X.; Wu, X.; Li, J.; Wang, H.; Gao, S., Effect of weathering on environmental behavior of microplastics: Properties, sorption and potential risks. *Chemosphere* **2020**, *242*, 125193.
62. Wu, J.; Jiang, R.; Liu, Q.; Ouyang, G., Impact of different modes of adsorption of natural organic matter on the environmental fate of nanoplastics. *Chemosphere* *263*, 127967.
63. Liu, J.; Dai, C.; Hu, Y., Aqueous aggregation behavior of citric acid coated magnetite nanoparticles: Effects of pH, cations, anions, and humic acid. *Environ. Res.* **2018**, *161*, 49-60.
64. Mason, S. A.; Garneau, D.; Sutton, R.; Chu, Y.; Ehmann, K.; Barnes, J.; Fink, P.; Papazissimos, D.; Rogers, D. L., Microplastic pollution is widely detected in US municipal wastewater treatment plant effluent. *Environ. Pollut.* **2016**, *218*, 1045-1054.
65. Talvitie, J.; Mikola, A.; Koistinen, A.; Setälä, O., Solutions to microplastic pollution - Removal of microplastics from wastewater effluent with advanced wastewater treatment technologies. *Water Res.* **2017**, *123*, 401-407.
66. Sheng, G.-P.; Yu, H.-Q.; Li, X.-Y., Extracellular polymeric substances (EPS) of microbial aggregates in biological wastewater treatment systems: A review. *Biotechnol. Adv.* **2010**, *28* (6), 882-894.
67. Cai, L.; Hu, L.; Shi, H.; Ye, J.; Zhang, Y.; Kim, H., Effects of inorganic ions and natural organic matter on the aggregation of nanoplastics. *Chemosphere* **2018**, *197*, 142-151.
68. Kawamura, S., *Integrated design and operation of water treatment facilities*. 2nd ed. ed.; John Wiley & Sons: New York, 2000.
69. Rajala, K.; Grönfors, O.; Hesampour, M.; Mikola, A., Removal of microplastics from secondary wastewater treatment plant effluent by coagulation/flocculation with iron, aluminum and polyamine-based chemicals. *Water Res.* **2020**, *183*, 116045.
70. Wang, X.; Li, Y.; Zhao, J.; Xia, X.; Shi, X.; Duan, J.; Zhang, W., UV-induced aggregation of polystyrene nanoplastics: effects of radicals, surface functional groups and electrolyte. *Environmental Science: Nano* **2020**, *7* (12), 3914-3926.
71. Fazey, F. M.; Ryan, P. G., Biofouling on buoyant marine plastics: An experimental study into the effect of size on surface longevity. *Environ. Pollut.* **2016**, *210*, 354-360.
72. Porter, A.; Lyons, B. P.; Galloway, T. S.; Lewis, C., Role of marine snows in microplastic fate and bioavailability. *Environ. Sci. Technol.* **2018**, *52* (12), 7111-7119.
73. Karlsson, T. M.; Hassellöv, M.; Jakubowicz, I., Influence of thermooxidative degradation on the in situ fate of polyethylene in temperate coastal waters. *Mar. Pollut. Bull.* **2018**, *135*, 187-194.
74. Nazaroff, W. W.; Alvarez-Cohen, L., *Environmental engineering science*. Wiley: New York, 2001.
75. Bråte, I. L. N.; Blázquez, M.; Brooks, S. J.; Thomas, K. V., Weathering impacts the uptake of polyethylene microparticles from toothpaste in Mediterranean mussels (*M. galloprovincialis*). *Sci. Total Environ.* **2018**, *626*, 1310-1318.
76. Chen, Q.; Li, Y.; Li, B., Is color a matter of concern during microplastic exposure to *Scenedesmus obliquus* and *Daphnia magna*? *J. Hazard. Mater.* **2020**, *383*, 121224.
77. Perren, W.; Wojtasik, A.; Cai, Q., Removal of Microbeads from Wastewater Using Electrocoagulation. *ACS Omega* **2018**, *3* (3), 3357-3364.
78. Hidayaturrehman, H.; Lee, T.-G., A study on characteristics of microplastic in wastewater of South Korea: Identification, quantification, and fate of microplastics during treatment process. *Mar. Pollut. Bull.* **2019**, *146*, 696-702.
79. Ma, B.; Xue, W.; Hu, C.; Liu, H.; Qu, J.; Li, L., Characteristics of microplastic removal via coagulation and ultrafiltration during drinking water treatment. *Chem. Eng. J.* **2019**, *359*, 159-167.

80. Bilgin, M.; Yurtsever, M.; Karadagli, F., Microplastic removal by aerated grit chambers versus settling tanks of a municipal wastewater treatment plant. *J. of Water Process Eng.* **2020**, *38*, 101604.
81. Sun, J.; Dai, X.; Wang, Q.; van Loosdrecht, M. C. M.; Ni, B.-J., Microplastics in wastewater treatment plants: Detection, occurrence and removal. *Water Res.* **2019**, *152*, 21-37.
82. Liu, J.; Zhang, T.; Tian, L.; Liu, X.; Qi, Z.; Ma, Y.; Ji, R.; Chen, W., Aging significantly affects mobility and contaminant-mobilizing ability of nanoplastics in saturated loamy sand. *Environ. Sci. Technol.* **2019**, *53* (10), 5805-5815.
83. Liu, Y.; Hu, Y.; Yang, C.; Chen, C.; Huang, W.; Dang, Z., Aggregation kinetics of UV irradiated nanoplastics in aquatic environments. *Water Res.* **2019**, *163*, 114870.
84. Gunaalan, K.; Fabbri, E.; Capolupo, M., The hidden threat of plastic leachates: A critical review on their impacts on aquatic organisms. *Water Res.* **2020**, *184*, 116170.
85. Xu, E. G.; Cheong, R. S.; Liu, L.; Hernandez, L. M.; Azimzada, A.; Bayen, S.; Tufenkji, N., Primary and secondary plastic particles exhibit limited acute toxicity but chronic effects on *Daphnia magna*. *Environ. Sci. Technol.* **2020**, *54* (11), 6859-6868.
86. Luo, H.; Xiang, Y.; He, D.; Li, Y.; Zhao, Y.; Wang, S.; Pan, X., Leaching behavior of fluorescent additives from microplastics and the toxicity of leachate to *Chlorella vulgaris*. *Sci. Total Environ.* **2019**, *678*, 1-9.
87. Vroom, R. J. E.; Koelmans, A. A.; Besseling, E.; Halsband, C., Aging of microplastics promotes their ingestion by marine zooplankton. *Environ. Pollut.* **2017**, *231*, 987-996.
88. Hüffer, T.; Weniger, A.-K.; Hofmann, T., Sorption of organic compounds by aged polystyrene microplastic particles. *Environ. Pollut.* **2018**, *236*, 218-225.
89. Mao, Y.; Li, H.; Huangfu, X.; Liu, Y.; He, Q., Nanoplastics display strong stability in aqueous environments: Insights from aggregation behaviour and theoretical calculations. *Environ. Pollut.* **2020**, *258*, 113760.
90. Wu, X.; Liu, P.; Huang, H.; Gao, S., Adsorption of triclosan onto different aged polypropylene microplastics: Critical effect of cations. *Sci. Total Environ.* **2020**, *717*, 137033.
91. Liu, P.; Wu, X.; Liu, H.; Wang, H.; Lu, K.; Gao, S., Desorption of pharmaceuticals from pristine and aged polystyrene microplastics under simulated gastrointestinal conditions. *J. Hazard. Mater.* **2020**, *392*, 122346.
92. Liu, P.; Lu, K.; Li, J.; Wu, X.; Qian, L.; Wang, M.; Gao, S., Effect of aging on adsorption behavior of polystyrene microplastics for pharmaceuticals: Adsorption mechanism and role of aging intermediates. *J. Hazard. Mater.* **2020**, *384*, 121193.
93. Černá, T.; Pražanová, K.; Beneš, H.; Titov, I.; Klubalová, K.; Filipová, A.; Klusoň, P.; Cajthaml, T., Polycyclic aromatic hydrocarbon accumulation in aged and unaged polyurethane microplastics in contaminated soil. *Sci. Total Environ.* **2021**, *770*, 145254.
94. Fan, X.; Zou, Y.; Geng, N.; Liu, J.; Hou, J.; Li, D.; Yang, C.; Li, Y., Investigation on the adsorption and desorption behaviors of antibiotics by degradable MPs with or without UV ageing process. *J. Hazard. Mater.* **2021**, *401*, 123363.
95. Yang, J.; Cang, L.; Sun, Q.; Dong, G.; Ata-Ul-Karim, S. T.; Zhou, D., Effects of soil environmental factors and UV aging on Cu<sup>2+</sup> adsorption on microplastics. *Environ. Sci. Pollut. Res.* **2019**, *26* (22), 23027-23036.
96. Wang, Q.; Wangjin, X.; Zhang, Y.; Wang, N.; Wang, Y.; Meng, G.; Chen, Y., The toxicity of virgin and UV-aged PVC microplastics on the growth of freshwater algae *Chlamydomonas reinhardtii*. *Sci. Total Environ.* **2020**, *749*, 141603.
97. Luo, H.; Li, Y.; Zhao, Y.; Xiang, Y.; He, D.; Pan, X., Effects of accelerated aging on characteristics, leaching, and toxicity of commercial lead chromate pigmented microplastics. *Environ. Pollut.* **2020**, *257*, 113475.
98. Wang, Q.; Zhang, Y.; Wangjin, X.; Wang, Y.; Meng, G.; Chen, Y., The adsorption behavior of metals in aqueous solution by microplastics effected by UV radiation. *JEnvS* **2020**, *87*, 272-280.

99. Müller, A.; Becker, R.; Dorgerloh, U.; Simon, F. G.; Braun, U., The effect of polymer aging on the uptake of fuel aromatics and ethers by microplastics. *Environ. Pollut.* **2018**, *240*, 639-646.
100. Wu, J.; Xu, P.; Chen, Q.; Ma, D.; Ge, W.; Jiang, T.; Chai, C., Effects of polymer aging on sorption of 2,2',4,4'-tetrabromodiphenyl ether by polystyrene microplastics. *Chemosphere* **2020**, *253*, 126706.
101. Wang, X.; Zheng, H.; Zhao, J.; Luo, X.; Wang, Z.; Xing, B., Photodegradation Elevated the Toxicity of Polystyrene Microplastics to Grouper (*Epinephelus moara*) through Disrupting Hepatic Lipid Homeostasis. *Environ. Sci. Technol.* **2020**, *54* (10), 6202-6212.
102. Zou, W.; Xia, M.; Jiang, K.; Cao, Z.; Zhang, X.; Hu, X., Photo-Oxidative Degradation Mitigated the Developmental Toxicity of Polyamide Microplastics to Zebrafish Larvae by Modulating Macrophage-Triggered Proinflammatory Responses and Apoptosis. *Environ. Sci. Technol.* **2020**, *54* (21), 13888-13898.
103. Liu, X.; Sun, P.; Qu, G.; Jing, J.; Zhang, T.; Shi, H.; Zhao, Y., Insight into the characteristics and sorption behaviors of aged polystyrene microplastics through three type of accelerated oxidation processes. *J. Hazard. Mater.* **2021**, *407*, 124836.
104. Zhang, X.; Xia, M.; Su, X.; Yuan, P.; Li, X.; Zhou, C.; Wan, Z.; Zou, W., Photolytic degradation elevated the toxicity of polylactic acid microplastics to developing zebrafish by triggering mitochondrial dysfunction and apoptosis. *J. Hazard. Mater.* **2021**, *413*, 125321.
105. Rummel, C. D.; Escher, B. I.; Sandblom, O.; Plassmann, M. M.; Arp, H. P. H.; MacLeod, M.; Jahnke, A., Effects of Leachates from UV-Weathered Microplastic in Cell-Based Bioassays. *Environ. Sci. Technol.* **2019**, *53* (15), 9214-9223.
106. Kalčíková, G.; Skalar, T.; Marolt, G.; Jemec Kokalj, A., An environmental concentration of aged microplastics with adsorbed silver significantly affects aquatic organisms. *Water Res.* **2020**, *175*, 115644.
107. Kaposi, K. L.; Mos, B.; Kelaher, B. P.; Dworjanyn, S. A., Ingestion of Microplastic Has Limited Impact on a Marine Larva. *Environ. Sci. Technol.* **2014**, *48* (3), 1638-1645.
108. Wang, Y.; Wang, X.; Li, Y.; Li, J.; Wang, F.; Xia, S.; Zhao, J., Biofilm alters tetracycline and copper adsorption behaviors onto polyethylene microplastics. *Chem. Eng. J.* **2020**, *392*, 123808.
109. Johansen, M. P.; Cresswell, T.; Davis, J.; Howard, D. L.; Howell, N. R.; Prentice, E., Biofilm-enhanced adsorption of strong and weak cations onto different microplastic sample types: Use of spectroscopy, microscopy and radiotracer methods. *Water Res.* **2019**, *158*, 392-400.
110. Schür, C.; Weil, C.; Baum, M.; Wallraff, J.; Schreier, M.; Oehlmann, J.; Wagner, M., Incubation in Wastewater Reduces the Multigenerational Effects of Microplastics in *Daphnia magna*. *Environ. Sci. Technol.* **2021**, *55* (4), 2491-2499.
111. Ramsperger, A. F. R. M.; Narayana, V. K. B.; Gross, W.; Mohanraj, J.; Thelakkat, M.; Greiner, A.; Schmalz, H.; Kress, H.; Laforsch, C., Environmental exposure enhances the internalization of microplastic particles into cells. *Sci. Adv.* **2020**, *6* (50), eabd1211.
112. Alimi, O. S.; Fadare, O. O.; Okoffo, E. D., Microplastics in African ecosystems: Current knowledge, abundance, associated contaminants, techniques, and research needs. *Sci. Total Environ.* **2021**, *755*, 142422.
113. Koelmans, A. A.; Mohamed Nor, N. H.; Hermesen, E.; Kooi, M.; Mintenig, S. M.; De France, J., Microplastics in freshwaters and drinking water: Critical review and assessment of data quality. *Water Res.* **2019**, *155*, 410-422.
114. Geyer, R.; Jambeck, J. R.; Law, K. L., Production, use, and fate of all plastics ever made. *Sci. Adv.* **2017**, *3* (7), e1700782.
115. Zhang, H.; Wang, J.; Zhou, B.; Zhou, Y.; Dai, Z.; Zhou, Q.; Christie, P.; Luo, Y., Enhanced adsorption of oxytetracycline to weathered microplastic polystyrene: kinetics, isotherms and influencing factors. *Environ. Pollut.* **2018**, *243*, 1550-1557.
116. Holmes, L. A.; Turner, A.; Thompson, R. C., Adsorption of trace metals to plastic resin pellets in the marine environment. *Environ. Pollut.* **2012**, *160* (1), 42-8.
117. Waldschläger, K.; Born, M.; Cowger, W.; Gray, A.; Schüttrumpf, H., Settling and rising velocities of environmentally weathered micro-and macroplastic particles. *Environ. Res.* **2020**, 110192.

118. Waldschläger, K.; Schüttrumpf, H., Effects of particle properties on the settling and rise velocities of microplastics in freshwater under laboratory conditions. *Environ. Sci. Technol.* **2019**, *53* (4), 1958-1966.
119. Missawi, O.; Bousserhine, N.; Zitouni, N.; Maisano, M.; Boughattas, I.; De Marco, G.; Cappello, T.; Belbekhouche, S.; Guerrouache, M.; Alphonse, V.; Banni, M., Uptake, accumulation and associated cellular alterations of environmental samples of microplastics in the seaworm *Hediste diversicolor*. *J. Hazard. Mater.* **2021**, *406*, 124287.
120. Zitouni, N.; Bousserhine, N.; Missawi, O.; Boughattas, I.; Chèvre, N.; Santos, R.; Belbekhouche, S.; Alphonse, V.; Tisserand, F.; Balmassiere, L.; Dos Santos, S. P.; Mokni, M.; Guerbej, H.; Banni, M., Uptake, tissue distribution and toxicological effects of environmental microplastics in early juvenile fish *Dicentrarchus labrax*. *J. Hazard. Mater.* **2021**, *403*, 124055.
121. Andrady, A. L., Wavelength sensitivity in polymer photodegradation. In *Polymer Analysis Polymer Physics*, Springer: 1997; pp 47-94.
122. Viera, J. S. C.; Marques, M. R. C.; Nazareth, M. C.; Jimenez, P. C.; Sanz-Lázaro, C.; Castro, Í. B., Are biodegradable plastics an environmental rip off? *J. Hazard. Mater.* **2021**, *416*, 125957.
123. Sadi, R. K.; Fechine, G. J.; Demarquette, N. R., Effect of prior photodegradation on the biodegradation of polypropylene/poly (3-hydroxybutyrate) blends. *Polym. Eng. Sci.* **2013**, *53* (10), 2109-2122.
124. Gewert, B.; Plassmann, M.; Sandblom, O.; MacLeod, M., Identification of chain scission products released to water by plastic exposed to ultraviolet light. *Environ. Sci. Technol. Lett.* **2018**, *5* (5), 272-276.
125. González-López, M. E.; Martín del Campo, A. S.; Robledo-Ortíz, J. R.; Arellano, M.; Pérez-Fonseca, A. A., Accelerated weathering of poly(lactic acid) and its biocomposites: A review. *Polymer Degradation and Stability* **2020**, *179*, 109290.
126. Brodhagen, M.; Goldberger, J. R.; Hayes, D. G.; Inglis, D. A.; Marsh, T. L.; Miles, C., Policy considerations for limiting unintended residual plastic in agricultural soils. *Environ. Sci. Policy* **2017**, *69*, 81-84.
127. Henry, B.; Laitala, K.; Klepp, I. G., Microfibres from apparel and home textiles: Prospects for including microplastics in environmental sustainability assessment. *Sci. Total Environ.* **2019**, *652*, 483-494.

## 5.7 Supporting information

### S5.1: Search criteria for literature review.

A systematic and extensive literature search was carried using the Scopus search engine to retrieve all research papers reporting the effect of microplastics up until May 2021. The criteria followed during the search is presented in Table S5.1. The abstract and titles of the retrieved articles were further reviewed for relevance to include only studies that investigated the effect or transformation of either pristine or weathered microplastics. All review articles, book chapters, opinion papers, etc. were removed from the search. A total of 785 articles were obtained from this search after removing articles that do not meet the criteria presented in Table S5.1.

**Table S5.1.** Literature search criteria

Search strings	Exempted words	Exempted study themes
(“microplastic” OR “nanoplastic” OR “plastic leachate” OR “tiny plastic” OR “microfiber” OR “microfibre” OR “microbead”)  AND  different combinations of these keywords:  (“effect” OR “aggregation” OR “deposition” OR “adsorption” OR “toxicity” OR “leaching” OR “desorption” OR “transport” OR “removal”)	“detection”, “abundance”, “review”, “distribution”, “beach”, “occurrence”, “quantification”, “techniques”, “methods”	<ul style="list-style-type: none"> <li>• Detection/abundance/occurrence of microplastic in food, water, sediment, biota, environment, wastewater etc.</li> <li>• Weathering of plastics or microplastics without investigating at least one effect.</li> <li>• Detection/sampling/identification techniques</li> <li>• Human microplastic consumption</li> </ul>

**Table S5.2.** Summary of laboratory studies investigating the effect of weathered microplastics, nanoplastics and leachates

Reference	Plastic	Size	Weathering conditions
1	PS	125 - 250 $\mu\text{m}$	UVC light with 10% $\text{H}_2\text{O}_2$ 96 hours
2	PS, PP	L - 3.5mm. W - 2.2 mm	UVA light. 26 $\text{W}/\text{m}^2$ 60 $^\circ\text{C}$ , 4 weeks
3	PET	1 x 1 mm	UVA light, 50 $\text{W}/\text{m}^2$ , $\lambda = 313$ nm 200 - 500 hours
4	PET, PVC, PMMA, PE, PS, PA	74.76 - 350.8 $\mu\text{m}$	UVA light, $\lambda = 340$ nm humidity = 60%, temperature = 30 $^\circ\text{C}$
5	PS		Mercury UV light ( $\lambda = 365$ nm) in water, $\text{H}_2\text{O}_2$ (10%) and Cl (25 mg/L) 96 hours
6	PP	62.6 $\mu\text{m}$	2.5g/100 mL $\text{K}_2\text{S}_2\text{O}_8$ with high temperature, pH 7, 40 days 70 $^\circ\text{C}$
7	PS + PE	50.4 $\pm$ 11.9 $\mu\text{m}$ 45.5 $\pm$ 12.9 $\mu\text{m}$	Natural sunlight (0.12 - 2.26 $\text{mW}/\text{cm}^2$ ) in filtered freshwater from Yangtze and Tihu Lake for 5 and 11 months, -4 to 38 $^\circ\text{C}$ Fenton reaction (30% $\text{H}_2\text{O}_2$ + 200 mM $\text{Fe}^{2+}$ ) for 1,5,10,20 and 30 days, pH 4 $\text{K}_2\text{S}_2\text{O}_8$ oxidation (100 mM $\text{K}_2\text{S}_2\text{O}_8$ ) with high temperature for 1,5,10,20 and 30 days, 70 $^\circ\text{C}$ , pH 7
8	PS + PVC	75 $\mu\text{m}$	UVC light, $\lambda = 254$ nm, 96 hours
9	PS	0.1 $\mu\text{m}$	UVA light in air, pure water and seawater, $\lambda = 340$ nm, 1, 2 and 3 months 25 $^\circ\text{C}$
10	PS	50.4 $\pm$ 11.9 $\mu\text{m}$	Photo-Fenton (30% $\text{H}_2\text{O}_2$ + 20 mM $\text{Fe}^{2+}$ ), $\lambda = 365$ nm, 2.1 $\text{mW}/\text{cm}^2$ 0, 6, 12, 24, 48, 72, 108 hours 25 $^\circ\text{C}$
11	PS	4 mm	UV ( $\lambda = 340$ nm), 44 $\mu\text{W}/\text{cm}^2$ , seawater, 90 days
12	PS	1 $\mu\text{m}$	high temperature (75 $^\circ\text{C}$ ) in air, pure water and seawater 1, 2 and 3 months
13	PE	0.5 - 1 mm	UV (in water) and mechanical, $\lambda = 254$ nm 10 and 4 months 40 $^\circ\text{C}$
14	PE, PS	-	UV
15	PA	< 2 mm	HCl (15%) + Acetone (20%), 24 hours
16	PS	50.4 $\pm$ 11.9 $\mu\text{m}$	Photo-Fenton (30% $\text{H}_2\text{O}_2$ + 20 mM $\text{Fe}^{2+}$ ), $\lambda = 365$ nm, 1 $\text{mW}/\text{cm}^2$ , 120 hours 30 $^\circ\text{C}$ , pH 3
17	PS	-	Fenton reaction (1.5% $\text{H}_2\text{O}_2$ + Fe) and $\text{H}_2\text{O}_2$ (1.5%) 1, 3, 5 and 7 days for each treatment
18	PLA, PVC	250 - 500 $\mu\text{m}$ 50 - 100 $\mu\text{m}$	UVA bulb, $\lambda = 313$ nm, 50 $\text{W}/\text{m}^2$ , Milli Q water, 3 - 72 hours

19	PE	60 - 150 $\mu\text{m}$	sewage effluent in Shanghai 20 days
20	HDPE, PP	50, 90 - 106 $\mu\text{m}$	Biofilm formation in Georges River, estuarine and marine water samples with gamma irradiation (1.17 MeV, $^{60}\text{Co}$ source), 19 days
21	PS	40.1 $\pm$ 9.1 nm	UVA bulb, 120 hours, air
22	PE	6 - 8.5 $\mu\text{m}$	Mixing in synthetic seawater 7, 14, 21, 28, 42 and 56 days
23	PS	205.4 $\pm$ 72.2 nm	UV light exposure in ultrapure water and activated sludge for biofilm formation (18/6 light-dark cycle, UVA+UVB: 15280 – 15460 $\mu\text{W}/\text{cm}^2$ , UVC: 108 – 112 $\mu\text{W}/\text{cm}^2$ ) 120 and 720 hours 32 - 36 $^{\circ}\text{C}$
24	PE, TWP	-	200 mg/L $\text{K}_2\text{S}_2\text{O}_8$ oxidation with high temperature, 15 days 70 $^{\circ}\text{C}$ , 60 rpm
25	PU	0.8 - 2 mm	UVA bulb, 0.5 $\text{W}/\text{m}^2$ (360 nm), 240 hours Black body temperature = 60 $^{\circ}\text{C}$ Dry bulb temperature = 30 $^{\circ}\text{C}$ , RH = 5%
26	PE	75 - 140 $\mu\text{m}$	incubation in soil and river (Shanghai), 20 days each exposure to air with UVC bulb ( $\lambda = 254$ nm), 4 days
27	PE, PS, PP	200 - 600 $\mu\text{m}$	$\text{O}_3$ (88 mg/L) $\text{O}_3 + \text{H}_2\text{O}_2$ ( $\text{O}_3 : \text{H}_2\text{O}_2$ ratio of 0.5)
28	PU	50 – 100 mesh	UVC (5 $\text{mW}/\text{cm}^2$ , $\lambda = 254$ nm)
29	PS	45 $\mu\text{m}$	biofilm colonization in unfiltered seawater, 168 hours
30	PS	20 - 100 $\mu\text{m}$	UVA + UVB, 113 $\pm$ 45 $\text{W}/\text{m}^2$ , natural filtered seawater, 60 days 25 $\pm$ 3 $^{\circ}\text{C}$
31	PS	15 & 30 $\mu\text{m}$	in the dark in filtered seawater (for biofilm formation), 3 weeks 6.4 $^{\circ}\text{C}$
32	PE	50 – 570 $\mu\text{m}$ , 247.7 $\pm$ 95.1 $\mu\text{m}$	natural weathering in seawater (using outdoor wave simulator basin), 21 days
33	PE	< 500 $\mu\text{m}$	UV (Xenon), 1200 $\text{W}/\text{m}^2$ , 1 – 8 weeks 60 $^{\circ}\text{C}$ , RH = 50%
34	PE	140.6 $\pm$ 80.0 $\mu\text{m}$	incubation in river, WWTP and landfill leachate samples with daylight fluorescent lamps - 16/8 h (light/dark), 3 weeks 23 $\pm$ 2 $^{\circ}\text{C}$
35	PE	10 - 45 $\mu\text{m}$	natural sunlight in unfiltered seawater, 216 hours 15 - 25 $^{\circ}\text{C}$
36		-	biofilm colonization
37	PE, PP, PET, PA	Leachate 0.3 – 17 $\mu\text{m}$ 0.01 – 0.8 $\mu\text{m}$	natural sunlight, deionised water 20 days
38	PU	3 $\times$ 3 $\times$ 3 mm leachate	natural sunlight in deionised water, natural water, tap water and sodium chloride solution. 8640 hours 25 $^{\circ}\text{C}$
39	PE	leachate	UV (Xenon), 1200 $\text{W}/\text{m}^2$ , 672 hours 60 $^{\circ}\text{C}$
40	HDPE, PVC	leachate	some light, seawater, 120 hours 22 $^{\circ}\text{C}$
41	PET, PS, PP, PVC, CTR	leachate	In the dark, seawater, freshwater and seawater algae growth media, 336 hours 25 $^{\circ}\text{C}$
42	PET, HDPE, PVC, LDPE, PP, PS, PC	leachate	N/A, 24 hours 28 $^{\circ}\text{C}$
43	PVC	leachate	In the dark, aged seawater sample, 24 hours 20 $^{\circ}\text{C}$
44	PP, HDPE, PVC, ABS, epoxy	leachate	In the dark, deionized water, 72 hours 20-50 $^{\circ}\text{C}$
45	PC, PVC, PU, PE, PS, LDPE, HDPE, PET, PMMA, PTFE, ABS, PP, MDPE,	leachate	In the dark, deionized water, 72 hours 20 $^{\circ}\text{C}$
46	PET, Nylon	leachate 52.3 $\pm$ 29.3 $\mu\text{m}$ 8.6 $\pm$ 5.2 $\mu\text{m}$ 171 $\pm$ 78 nm 229 $\pm$ 116 nm	thermal degradation in deionised water, 95 $^{\circ}\text{C}$ <1 hour

47	PE, PET, PP, PS	leachate	UVA + UVB lamp (702.8 W/m <sup>2</sup> ), artificial seawater 96 hours, 20 - 30 °C
48	PA	8.13 ± 2.27 μm	In the dark, UV light, UV bulb + 7.5 μM H <sub>2</sub> O <sub>2</sub> , 35 W/m <sup>2</sup> , 2160 hours, λ < 420
49	PS	3 μm	incubation in freshwater and seawater, 336 hours
50	PS	≤ 63 μm	Incubation in wastewater sample, 216 hours
51	PVC	50 - 100 μm	UVA, 50 W/m <sup>2</sup> , λ = 313 nm, 600 hours
52	PS	5 μm	UVC bulb, λ = 254 nm, 240 hours
53	PLA, PVC	5 - 50 μm	deionised water, λ > 310 nm, 45W/m <sup>2</sup> , 2160 hours
54	PS, PVC	150 and 250 μm	UVA light for 3 months, λ > 340 nm
55	PS, PVC, PP, PET, PE	leachate	19.1 ± 2.3 W/m <sup>2</sup> (UVC, 2.3 ± 0.3 W/m <sup>2</sup> (UVA; including 0.25 W/m <sup>2</sup> of UVB) 23.1 - 45.2 °C ultrapure water
56	PA	0 - 180 μm	UVC light exposure with tap water
57	PS, PVC, PP, PET, PE	leachate	UV light and dark exposure in brackish water (7% salinity, pH = 7.9), 1 rpm mixing 700 W/m <sup>2</sup>
58	PS	-	UVC with 10% H <sub>2</sub> O <sub>2</sub> , λ = 254 nm, 120 hours
59	PS	0.05 - 0.1	UVA, λ > 365 nm, 1.71 mW/cm <sup>2</sup> , 24 hours
60	PS	-	UV bulb with 5 mM NaNO <sub>3</sub> and ozone, 12 hours
61	PE	140 μm	UVA bulb, surface water (St Lawrence river), λ = 365 nm, 10 mW/cm <sup>2</sup> , 1440 hours
62	PS	28 nm	cold and fluctuating freezing temperature (-10 to 10 °C) in sodium chloride (3 - 300 mM) solution and in the presence and absence of natural organic matter (5 mg/L), 10 days
63	PVC, PP, PET	5 x 5 mm square	biofilm colonization in freshwater samples (Niushoushan River, Qinhuai River and East lake, China), 1056 hours

PS = polystyrene, PE = polyethylene, PP = polypropylene, PA= polyamide, PEVA = polyethylene vinyl acetate, PVC = polyvinyl chloride, PLA = polylactic acid, PU = polyurethane, CTR = car tire rubber, PET = polyethylene terephthalate, PC = polycarbonate, ABS = acrylonitrile butadiene styrene, TWP = tire wear particles

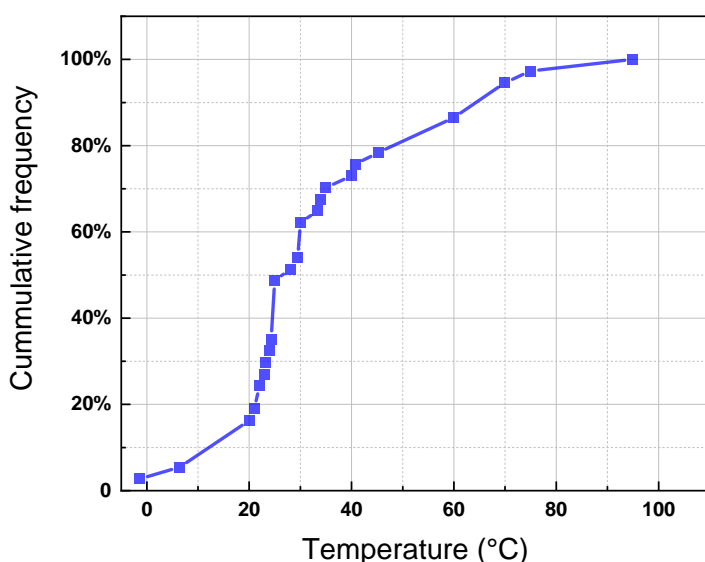


Figure S5.1. Cumulative frequency distribution for average temperatures used in weathering protocols for effect studies.

**Table S5.3.** Summary of effect studies using microplastics collected from the environment

Reference	Plastic	Size	Sampling location
64	PS	0.45 – 1 mm	North China
65	PE	< 1 mm	Southwest England
66	PS, PE	0.5 – 1 mm 0.1 – 0.2 mm	East China Sea and Yellow Sea
67	PE, PP, PS, PVC, PET, EPS	460 – 4830* $\mu\text{m}$	Southern California
68	PP		Shenyang city
69	PP, PE, HDPE, PEVA, PP, PA	0.45 – 100 $\mu\text{m}$	Gabes beach, Tunisia
70	PE, PP, PS	16.4 – 962.2 $\mu\text{m}$	Easter Island, Guam and Hawaii
71	PE		Beijing, China
72	PE, PP	100 – 500 $\mu\text{m}$	Lake Ontario shoreline
73	PE, PP	leachates	sandy beaches, Guadeloupe archipelago, France
74	PE, PP, PA, PEVA	0.45 – 100 $\mu\text{m}$	sea surface and sandy beach in Bizerte, northern Tunisia
75	PE, PC, PP, PS, PU, HDPE,	leachates	North Pacific Gyre

\* = equivalent sphere diameter. PS = polystyrene, PE = polyethylene, PP = polypropylene, PA= polyamide, PEVA = polyethylene vinyl acetate, PVC = polyvinyl chloride, EPS = expanded polystyrene

**Table S5.4.** Summary of international standard weathering protocols developed for plastics and other polymers

reference	Type of exposure	Summary	simulated degradation / parameters	controlled parameters	Outcome / Report	ISO or ASTM equivalence or technical similarity
ISO 15314	natural marine	Three methods for natural exposure of plastics in a marine environment: floating, partially immersed and completely immersed	natural degradation (photodegradation, heat and moisture) variations	duration of exposure, exposure raft and rack; specimen mounting, water depth, climate	bulk/surface properties loss	-
ASTM D1435	natural outdoor	Procedures for natural outdoor exposure of plastic materials	natural degradation (photodegradation, heat and moisture)	angle and duration of exposure, climate	bulk/surface properties loss	ISO 877.2
ASTM D5272-08	natural outdoor	Method for natural exposure of photodegradable plastics	natural degradation (photodegradation, heat and moisture)	angle and duration of exposure, climate	bulk/surface properties loss	-
ASTM D4364	natural/accelerated outdoor	How to perform a weathering test using sunlight concentrated with Fresnel reflectors	natural degradation (accelerated photodegradation, heat and moisture)	duration of exposure, climate, duration of spray cycle	n/a (no report generated - operation only)	ISO 877-3
ASTM D7444	accelerated outdoor	Method to induce degradation of oxidatively degradable plastics under atmospheric pressure and thermal and humidity variations	heat and moisture	temperature, relative humidity, specimen thickness	bulk/surface properties loss	-
ASTM G154-0	accelerated outdoor	How to operate a fluorescent UV lamp and water apparatus	photodegradation	type of UV lamp, specimen mounting	n/a (no report generated)	ISO 4892-3 and ISO 16474-3
ASTM D 4329	accelerated outdoor	Test conditions to perform accelerated weathering of plastics using UV fluorescent lamps	photodegradation; heat; moisture (condensation)	duration of exposure and condensation cycle, irradiance, black panel temperature	bulk/surface properties loss	ISO 4892-3
ASTM D 4587	accelerated outdoor	Test conditions to perform accelerated weathering of paints and coating using UV fluorescent lamps	photodegradation; heat; moisture (condensation)	duration of exposure and condensation cycle, irradiance, black panel temperature	bulk/surface properties loss	ISO 11507
ASTM D5208-14	accelerated outdoor	Test conditions to perform accelerated weathering of degradable plastics using UV fluorescent lamps; Simulate conditions that might be experienced when the material is discarded as litter	photodegradation; heat; moisture (condensation)	duration of exposure and condensation cycle, irradiance, black panel temperature	bulk/surface properties loss	-

ASTM G155	accelerated outdoor	How to operate a xenon arc light and water apparatus	photodegradation	type of xenon arc lamp, filters, specimen mounting	n/a (no report generated)	ISO 4892-2, ISO 11341, ISO 105 B02, ISO 105 B04, ISO 105 B05, and ISO 105 B06
ASTM D2565	accelerated outdoor	Practice for the exposure of plastics to xenon-arc lamps	photodegradation; heat; moisture (spray)	duration of exposure and spray cycle, irradiance, black panel and air temperature, relative humidity	bulk/surface properties loss	ISO 4892-2
ASTM D5071	accelerated outdoor	Test conditions to perform accelerated weathering of degradable plastics using xenon arc lamps;	photodegradation; heat; moisture (spray)	duration of exposure and spray cycle, irradiance, black panel and air temperature, relative humidity	bulk/surface properties loss	ISO 4892-2
ASTM D4355	accelerated outdoor	Test description to evaluate the tensile strength of weathered geotextiles over time	photodegradation; heat; moisture (spray or relative humidity)	duration of exposure and spray cycle, irradiance, black panel and air temperature, relative humidity	bulk/surface properties loss	-
ISO 19679	accelerated outdoor/marine	Method to determine the degree and level of aerobic biodegradation of plastics when settled in marine sediment at the interface between seawater and seafloor	photodegradation / aerobic biodegradation; moisture	microorganism's population	biodegradation gases	-
ASTM D7473-12	accelerated marine	Method to determine the weight loss of non-floating plastic materials when exposed to open marine aquarium conditions	aerobic biodegradation; moisture	duration of exposure, film thickness, source of natural sea water and surface marine sediment	weight loss	-
ASTD D6691	accelerated marine	Respirometry flask test to evaluate the degree and rate of aerobic biodegradation of plastics exposed to a defined microbial population in controlled laboratory conditions	aerobic biodegradation; moisture	microorganism's population	biodegradation gases	-
ASTM D7991	accelerated marine	Test to evaluate the level of aerobic biodegradation of plastics exposed to conditions that simulate the environment of sandy tidal zones	aerobic biodegradation; moisture	marine sediment type	biodegradation gases	-
ASTM D5988	accelerated marine / solid waste	Test to evaluate the degree and rate of aerobic biodegradation of plastics and formulation additives in contact with soil	aerobic biodegradation; moisture	soil source	biodegradation gases	ISO 17556

ISO 14851	accelerated marine / solid waste	Respirometry flask test to measure the oxygen demand to evaluate the degree of aerobic biodegradation of plastics in an aqueous medium • an inoculum from activated sludge may be used	aerobic biodegradation; moisture	microorganism's population	biodegradation gases (oxygen demand)	-
ASTM D5338	solid waste	Method to determine the degree and level of aerobic biodegradation of plastics in controlled composting conditions at thermophilic temperatures	aerobic biodegradation; heat; moisture	test duration, temperature, inoculum to be used	biodegradation gases/ visual aspect after biodegradation	ISO 14855
ASTM D6400	solid waste	It established the requirements to label a plastic as compostable when exposed to aerobic municipal or industrial composting facilities • the criteria are related to final fragment size, biodegradation and potential hazard to plant growth	aerobic biodegradation	sieving, biodegradation results, ability	biodegradation gases; fragment size; effect on plant growth	ISO 17088
ISO 14852	solid waste	Method to determine the degree of aerobic biodegradation of plastics exposed to an inoculum from activated sludge, mature compost or soil in aerobic mesophilic conditions	aerobic biodegradation; heat; moisture	test duration, temperature, type of sludge or soil used	biodegradation gases	-
ASTM D5526	solid waste	Method to determine the degree and level of anaerobic biodegradation of plastics in accelerated landfill conditions The test also produces a mixture of plastics and household waste that can be used to assess environmental and health risks using other standards	anaerobic biodegradation	test duration, choice of solid waste and inoculum to be used	biodegradation gases	-
ASTM D5511	solid waste	Method to determine the degree and level of anaerobic biodegradation of plastics in high-solids anaerobic digestion conditions	anaerobic biodegradation; heat	test duration, temperature, inoculum to be used	biodegradation gases	ISO 15985
ISO 14853	solid waste	Method to determine the degree of anaerobic biodegradation of plastics exposed to digested sludge	anaerobic biodegradation; heat	test duration, temperature, inoculum to be used	biodegradation gases	-
ASTM D7475	solid waste	Protocol to measure biodegradation changing from aerobic to anaerobic environment, simulating what occurs in landfills as the depth is increased	aerobic and anaerobic biodegradation; moisture	test duration, temperature, specimen shape, household waste characteristics	bulk/surface properties loss; biodegradation gases; molecular weight	-

ASTM D6954	accelerated outdoor / solid waste	A guide that establishes a method to expose plastics first to oxidation (UV or heat) and then to biodegradation, combining other standards in a given order • Toxicity may also be employed with the residue from biodegradation	photodegradation; aerobic and anaerobic biodegradation; heat; moisture (spray or humidity control)	Tier 1: duration of exposure, temperature, humidity or spray or condensation; Tier 2: test duration, inoculum used, temperature;	bulk/surface properties loss; biodegradation gases; weight loss; fragment size; molecular weight; toxicity results	-
------------	-----------------------------------	--	--	--	--	---

## References

1. Hüffer, T.; Weniger, A.-K.; Hofmann, T., Sorption of organic compounds by aged polystyrene microplastic particles. *Environ. Pollut.* **2018**, *236*, 218-225.
2. Müller, A.; Becker, R.; Dorgerloh, U.; Simon, F. G.; Braun, U., The effect of polymer aging on the uptake of fuel aromatics and ethers by microplastics. *Environ. Pollut.* **2018**, *240*, 639-646.
3. Wang, Q.; Zhang, Y.; Wangjin, X.; Wang, Y.; Meng, G.; Chen, Y., The adsorption behavior of metals in aqueous solution by microplastics effected by UV radiation. *JEnvS* **2020**, *87*, 272-280.
4. Yang, J.; Cang, L.; Sun, Q.; Dong, G.; Ata-Ul-Karim, S. T.; Zhou, D., Effects of soil environmental factors and UV aging on Cu<sup>2+</sup> adsorption on microplastics. *Environ. Sci. Pollut. Res.* **2019**, *26* (22), 23027-23036.
5. Liu, X.; Sun, P.; Qu, G.; Jing, J.; Zhang, T.; Shi, H.; Zhao, Y., Insight into the characteristics and sorption behaviors of aged polystyrene microplastics through three type of accelerated oxidation processes. *J. Hazard. Mater.* **2021**, *407*, 124836.
6. Wu, X.; Liu, P.; Huang, H.; Gao, S., Adsorption of triclosan onto different aged polypropylene microplastics: Critical effect of cations. *Sci. Total Environ.* **2020**, *717*, 137033.
7. Liu, P.; Qian, L.; Wang, H.; Zhan, X.; Lu, K.; Gu, C.; Gao, S., New insights into the aging behavior of microplastics accelerated by advanced oxidation processes. *Environ. Sci. Technol.* **2019**, *53* (7), 3579-3588.
8. Liu, G.; Zhu, Z.; Yang, Y.; Sun, Y.; Yu, F.; Ma, J., Sorption behavior and mechanism of hydrophilic organic chemicals to virgin and aged microplastics in freshwater and seawater. *Environ. Pollut.* **2019**, *246*, 26-33.
9. Mao, R.; Lang, M.; Yu, X.; Wu, R.; Yang, X.; Guo, X., Aging mechanism of microplastics with UV irradiation and its effects on the adsorption of heavy metals. *J. Hazard. Mater.* **2020**, 122515.
10. Liu, P.; Lu, K.; Li, J.; Wu, X.; Qian, L.; Wang, M.; Gao, S., Effect of aging on adsorption behavior of polystyrene microplastics for pharmaceuticals: Adsorption mechanism and role of aging intermediates. *J. Hazard. Mater.* **2020**, *384*, 121193.
11. Wu, J.; Xu, P.; Chen, Q.; Ma, D.; Ge, W.; Jiang, T.; Chai, C., Effects of polymer aging on sorption of 2,2',4,4'-tetrabromodiphenyl ether by polystyrene microplastics. *Chemosphere* **2020**, *253*, 126706.
12. Ding, L.; Mao, R.; Ma, S.; Guo, X.; Zhu, L., High temperature depended on the ageing mechanism of microplastics under different environmental conditions and its effect on the distribution of organic pollutants. *Water Res.* **2020**, *174*, 115634.
13. Vockenber, T.; Wichard, T.; Ueberschaar, N.; Franke, M.; Stelter, M.; Braeutigam, P., The sorption behaviour of amine micropollutants on polyethylene microplastics – impact of aging and interactions with green seaweed. *Environmental Science: Processes & Impacts* **2020**, *22* (8), 1678-1687.
14. Xu, P. C.; Guo, J.; Ma, D.; Ge, W.; Zhou, Z. F.; Chai, C., [Sorption of Polybrominated Diphenyl Ethers by Virgin and Aged Microplastics]. *Huan Jing Ke Xue* **2020**, *41* (3), 1329-1337.
15. Goedecke, C.; Mülrow-Stollin, U.; Hering, S.; Richter, J.; Piechotta, C.; Paul, A.; Braun, U., A first pilot study on the sorption of environmental pollutants on various microplastic materials. **2017**.

16. Liu, P.; Wu, X.; Liu, H.; Wang, H.; Lu, K.; Gao, S., Desorption of pharmaceuticals from pristine and aged polystyrene microplastics under simulated gastrointestinal conditions. *J. Hazard. Mater.* **2020**, *392*, 122346.
17. Lang, M.; Yu, X.; Liu, J.; Xia, T.; Wang, T.; Jia, H.; Guo, X., Fenton aging significantly affects the heavy metal adsorption capacity of polystyrene microplastics. *Sci. Total Environ.* **2020**, 137762.
18. Fan, X.; Zou, Y.; Geng, N.; Liu, J.; Hou, J.; Li, D.; Yang, C.; Li, Y., Investigation on the adsorption and desorption behaviors of antibiotics by degradable MPs with or without UV ageing process. *J. Hazard. Mater.* **2021**, *401*, 123363.
19. Wang, Y.; Wang, X.; Li, Y.; Li, J.; Wang, F.; Xia, S.; Zhao, J., Biofilm alters tetracycline and copper adsorption behaviors onto polyethylene microplastics. *Chem. Eng. J.* **2020**, *392*, 123808.
20. Johansen, M. P.; Cresswell, T.; Davis, J.; Howard, D. L.; Howell, N. R.; Prentice, E., Biofilm-enhanced adsorption of strong and weak cations onto different microplastic sample types: Use of spectroscopy, microscopy and radiotracer methods. *Water Res.* **2019**, *158*, 392-400.
21. Xiong, Y.; Zhao, J.; Li, L.; Wang, Y.; Dai, X.; Yu, F.; Ma, J., Interfacial interaction between micro/nanoplastics and typical PPCPs and nanoplastics removal via electrosorption from an aqueous solution. *Water Res.* **2020**, 116100.
22. Yang, M.; Chen, B.; Xin, X.; Song, X.; Liu, J.; Dong, G.; Lee, K.; Zhang, B., Interactions between microplastics and oil dispersion in the marine environment. *J. Hazard. Mater.* **2021**, *403*, 123944.
23. Ho, W.-K.; Law, J. C.-F.; Zhang, T.; Leung, K. S.-Y., Effects of Weathering on the Sorption Behavior and Toxicity of Polystyrene Microplastics in Multi-solute Systems. *Water Res.* **2020**, *187*, 116419.
24. Fan, X.; Gan, R.; Liu, J.; Xie, Y.; Xu, D.; Xiang, Y.; Su, J.; Teng, Z.; Hou, J., Adsorption and desorption behaviors of antibiotics by tire wear particles and polyethylene microplastics with or without aging processes. *Sci. Total Environ.* **2021**, *771*, 145451.
25. Černá, T.; Pražanová, K.; Beneš, H.; Titov, I.; Klubalová, K.; Filipová, A.; Klusoň, P.; Cajthaml, T., Polycyclic aromatic hydrocarbon accumulation in aged and unaged polyurethane microplastics in contaminated soil. *Sci. Total Environ.* **2021**, *770*, 145254.
26. Wang, Y.; Wang, X.; Li, Y.; Li, J.; Liu, Y.; Xia, S.; Zhao, J., Effects of exposure of polyethylene microplastics to air, water and soil on their adsorption behaviors for copper and tetracycline. *Chem. Eng. J.* **2021**, *404*, 126412.
27. Gomes de Aragão Belé, T.; F. Neves, T.; Cristale, J.; Prediger, P.; Constapel, M.; F. Dantas, R., Oxidation of microplastics by O<sub>3</sub> and O<sub>3</sub>/H<sub>2</sub>O<sub>2</sub>: Surface modification and adsorption capacity. *Journal of Water Process Engineering* **2021**, *41*, 102072.
28. Xue, X.-D.; Fang, C.-R.; Zhuang, H.-F., Adsorption behaviors of the pristine and aged thermoplastic polyurethane microplastics in Cu(II)-OTC coexisting system. *J. Hazard. Mater.* **2021**, *407*, 124835.
29. Murano, C.; Donnarumma, V.; Corsi, I.; Casotti, R.; Palumbo, A., Impact of Microbial Colonization of Polystyrene Microbeads on the Toxicological Responses in the Sea Urchin *Paracentrotus lividus*. *Environ. Sci. Technol.* **2021**.
30. Wang, X.; Zheng, H.; Zhao, J.; Luo, X.; Wang, Z.; Xing, B., Photodegradation Elevated the Toxicity of Polystyrene Microplastics to Grouper (*Epinephelus moara*) through Disrupting Hepatic Lipid Homeostasis. *Environ. Sci. Technol.* **2020**, *54* (10), 6202-6212.

31. Vroom, R. J. E.; Koelmans, A. A.; Besseling, E.; Halsband, C., Aging of microplastics promotes their ingestion by marine zooplankton. *Environ. Pollut.* **2017**, *231*, 987-996.
32. Bråte, I. L. N.; Blázquez, M.; Brooks, S. J.; Thomas, K. V., Weathering impacts the uptake of polyethylene microparticles from toothpaste in Mediterranean mussels (*M. galloprovincialis*). *Sci. Total Environ.* **2018**, *626*, 1310-1318.
33. Luo, H.; Zhao, Y.; Li, Y.; Xiang, Y.; He, D.; Pan, X., Aging of microplastics affects their surface properties, thermal decomposition, additives leaching and interactions in simulated fluids. *Sci. Total Environ.* **2020**, *714*, 136862.
34. Jemec Kokalj, A.; Kuehnel, D.; Puntar, B.; Žgajnar Gotvajn, A.; Kalčíkova, G., An exploratory ecotoxicity study of primary microplastics versus aged in natural waters and wastewaters. *Environ. Pollut.* **2019**, *254*, 112980.
35. Kaposi, K. L.; Mos, B.; Kelaher, B. P.; Dworjanyn, S. A., Ingestion of Microplastic Has Limited Impact on a Marine Larva. *Environ. Sci. Technol.* **2014**, *48* (3), 1638-1645.
36. Kalčíková, G.; Skalar, T.; Marolt, G.; Kokalj, A. J., An environmental concentration of aged microplastics with adsorbed silver significantly affects aquatic organisms. *Water Res.* **2020**, 115644.
37. Xu, E. G.; Cheong, R. S.; Liu, L.; Hernandez, L. M.; Azimzada, A.; Bayen, S.; Tufenkji, N., Primary and secondary plastic particles exhibit limited acute toxicity but chronic effects on *Daphnia magna*. *Environ. Sci. Technol.* **2020**, *54* (11), 6859-6868.
38. Luo, H.; Xiang, Y.; He, D.; Li, Y.; Zhao, Y.; Wang, S.; Pan, X., Leaching behavior of fluorescent additives from microplastics and the toxicity of leachate to *Chlorella vulgaris*. *Sci. Total Environ.* **2019**, *678*, 1-9.
39. Luo, H.; Li, Y.; Zhao, Y.; Xiang, Y.; He, D.; Pan, X., Effects of accelerated aging on characteristics, leaching, and toxicity of commercial lead chromate pigmented microplastics. *Environ. Pollut.* **2020**, *257*, 113475.
40. Tetu, S. G.; Sarker, I.; Schrameyer, V.; Pickford, R.; Elbourne, L. D. H.; Moore, L. R.; Paulsen, I. T., Plastic leachates impair growth and oxygen production in *Prochlorococcus*, the ocean's most abundant photosynthetic bacteria. *Communications Biology* **2019**, *2* (1), 184.
41. Capolupo, M.; Sørensen, L.; Jayasena, K. D. R.; Booth, A. M.; Fabbri, E., Chemical composition and ecotoxicity of plastic and car tire rubber leachates to aquatic organisms. *Water Res.* **2020**, *169*, 115270.
42. Li, H.-X.; Getzinger, G. J.; Ferguson, P. L.; Orihuela, B.; Zhu, M.; Rittschof, D., Effects of Toxic Leachate from Commercial Plastics on Larval Survival and Settlement of the Barnacle *Amphibalanus amphitrite*. *Environ. Sci. Technol.* **2016**, *50* (2), 924-931.
43. Oliviero, M.; Tato, T.; Schiavo, S.; Fernández, V.; Manzo, S.; Beiras, R., Leachates of micronized plastic toys provoke embryotoxic effects upon sea urchin *Paracentrotus lividus*. *Environ. Pollut.* **2019**, *247*, 706-715.
44. Lithner, D.; Nordensvan, I.; Dave, G., Comparative acute toxicity of leachates from plastic products made of polypropylene, polyethylene, PVC, acrylonitrile-butadiene-styrene, and epoxy to *Daphnia magna*. *Environ Sci Pollut Res Int* **2012**, *19* (5), 1763-72.
45. Lithner, D.; Damberg, J.; Dave, G.; Larsson, Å., Leachates from plastic consumer products – Screening for toxicity with *Daphnia magna*. *Chemosphere* **2009**, *74* (9), 1195-1200.
46. Hernandez, L. M.; Xu, E. G.; Larsson, H. C. E.; Tahara, R.; Maisuria, V. B.; Tufenkji, N., Plastic teabags release billions of microparticles and nanoparticles into tea. *Environ. Sci. Technol.* **2019**, *53* (21), 12300-12310.

47. Rummel, C. D.; Escher, B. I.; Sandblom, O.; Plassmann, M. M.; Arp, H. P. H.; MacLeod, M.; Jahnke, A., Effects of Leachates from UV-Weathered Microplastic in Cell-Based Bioassays. *Environ. Sci. Technol.* **2019**, *53* (15), 9214-9223.
48. Zou, W.; Xia, M.; Jiang, K.; Cao, Z.; Zhang, X.; Hu, X., Photo-Oxidative Degradation Mitigated the Developmental Toxicity of Polyamide Microplastics to Zebrafish Larvae by Modulating Macrophage-Triggered Proinflammatory Responses and Apoptosis. *Environ. Sci. Technol.* **2020**, *54* (21), 13888-13898.
49. Ramsperger, A. F. R. M.; Narayana, V. K. B.; Gross, W.; Mohanraj, J.; Thelakkat, M.; Greiner, A.; Schmalz, H.; Kress, H.; Laforsch, C., Environmental exposure enhances the internalization of microplastic particles into cells. *Sci. Adv.* **2020**, *6* (50), eabd1211.
50. Schür, C.; Weil, C.; Baum, M.; Wallraff, J.; Schreier, M.; Oehlmann, J.; Wagner, M., Incubation in Wastewater Reduces the Multigenerational Effects of Microplastics in *Daphnia magna*. *Environ. Sci. Technol.* **2021**, *55* (4), 2491-2499.
51. Wang, Q.; Wangjin, X.; Zhang, Y.; Wang, N.; Wang, Y.; Meng, G.; Chen, Y., The toxicity of virgin and UV-aged PVC microplastics on the growth of freshwater algae *Chlamydomonas reinhardtii*. *Sci. Total Environ.* **2020**, *749*, 141603.
52. Huang, Y.; Ding, J.; Zhang, G.; Liu, S.; Zou, H.; Wang, Z.; Zhu, W.; Geng, J., Interactive effects of microplastics and selected pharmaceuticals on red tilapia: Role of microplastic aging. *Sci. Total Environ.* **2021**, *752*, 142256.
53. Zhang, X.; Xia, M.; Su, X.; Yuan, P.; Li, X.; Zhou, C.; Wan, Z.; Zou, W., Photolytic degradation elevated the toxicity of polylactic acid microplastics to developing zebrafish by triggering mitochondrial dysfunction and apoptosis. *J. Hazard. Mater.* **2021**, *413*, 125321.
54. Wang, Z.; Fu, D.; Gao, L.; Qi, H.; Su, Y.; Peng, L., Aged microplastics decrease the bioavailability of coexisting heavy metals to microalga *Chlorella vulgaris*. *Ecotoxicol. Environ. Saf.* **2021**, *217*, 112199.
55. Klein, K.; Hof, D.; Dombrowski, A.; Schweyen, P.; Dierkes, G.; Ternes, T.; Schulte-Oehlmann, U.; Oehlmann, J., Enhanced in vitro toxicity of plastic leachates after UV irradiation. *Water Res.* **2021**, *199*, 117203.
56. Khosrovyan, A.; Kahru, A., Evaluation of the potential toxicity of UV-weathered virgin polyamide microplastics to non-biting midge *Chironomus riparius*. *Environ. Pollut.* **2021**, *287*, 117334.
57. Gewert, B.; MacLeod, M.; Breitholtz, M., Variability in Toxicity of Plastic Leachates as a Function of Weathering and Polymer Type: A Screening Study with the Copepod *Nitocra spinipes*. *The Biological Bulletin* **2021**, *0* (0), 000-000.
58. Mao, Y.; Li, H.; Huangfu, X.; Liu, Y.; He, Q., Nanoplastics display strong stability in aqueous environments: Insights from aggregation behaviour and theoretical calculations. *Environ. Pollut.* **2020**, *258*, 113760.
59. Liu, Y.; Hu, Y.; Yang, C.; Chen, C.; Huang, W.; Dang, Z., Aggregation kinetics of UV irradiated nanoplastics in aquatic environments. *Water Res.* **2019**, *163*, 114870.
60. Liu, J.; Zhang, T.; Tian, L.; Liu, X.; Qi, Z.; Ma, Y.; Ji, R.; Chen, W., Aging significantly affects mobility and contaminant-mobilizing ability of nanoplastics in saturated loamy sand. *Environ. Sci. Technol.* **2019**, *53* (10), 5805-5815.
61. Lapointe, M.; Farner, J. M.; Hernandez, L. M.; Tufenkji, N., Understanding and improving microplastic removal during water treatment: Impact of coagulation and flocculation. *Environ. Sci. Technol.* **2020**, *54* (14), 8719-8727.

62. Alimi, O. S.; Farner, J. M.; Tufenkji, N., Exposure of nanoplastics to freeze-thaw leads to aggregation and reduced transport in model groundwater environments. *Water Res.* **2020**, 116533.
63. Miao, L.; Gao, Y.; Adyel, T. M.; Huo, Z.; Liu, Z.; Wu, J.; Hou, J., Effects of biofilm colonization on the sinking of microplastics in three freshwater environments. *J. Hazard. Mater.* **2021**, *413*, 125370.
64. Zhang, H.; Wang, J.; Zhou, B.; Zhou, Y.; Dai, Z.; Zhou, Q.; Christie, P.; Luo, Y., Enhanced adsorption of oxytetracycline to weathered microplastic polystyrene: kinetics, isotherms and influencing factors. *Environ. Pollut.* **2018**, *243*, 1550-1557.
65. Holmes, L. A.; Turner, A.; Thompson, R. C., Adsorption of trace metals to plastic resin pellets in the marine environment. *Environ. Pollut.* **2012**, *160* (1), 42-8.
66. Guo, X.; Wang, J., Sorption of antibiotics onto aged microplastics in freshwater and seawater. *Mar Pollut Bull* **2019**, *149*, 110511.
67. Waldschläger, K.; Born, M.; Cowger, W.; Gray, A.; Schüttrumpf, H., Settling and Rising Velocities of Environmentally Weathered Micro-and Macroplastic Particles. *Environ. Res.* **2020**, 110192.
68. Yan, X.; Yang, X.; Tang, Z.; Fu, J.; Chen, F.; Zhao, Y.; Ruan, L.; Yang, Y., Downward transport of naturally-aged light microplastics in natural loamy sand and the implication to the dissemination of antibiotic resistance genes. *Environ. Pollut.* **2020**, *262*, 114270.
69. Missawi, O.; Bousserhine, N.; Zitouni, N.; Maisano, M.; Boughattas, I.; De Marco, G.; Cappello, T.; Belbekhouche, S.; Guerrouache, M.; Alphonse, V.; Banni, M., Uptake, accumulation and associated cellular alterations of environmental samples of microplastics in the seaworm *Hediste diversicolor*. *J. Hazard. Mater.* **2021**, *406*, 124287.
70. Pannetier, P.; Morin, B.; Le Bihanic, F.; Dubreil, L.; Clérandeau, C.; Chouvellon, F.; Van Arkel, K.; Danion, M.; Cachot, J., Environmental samples of microplastics induce significant toxic effects in fish larvae. *Environ. Int.* **2020**, *134*, 105047.
71. Lan, T.; Wang, T.; Cao, F.; Yu, C.; Chu, Q.; Wang, F., A comparative study on the adsorption behavior of pesticides by pristine and aged microplastics from agricultural polyethylene soil films. *Ecotoxicol Environ Saf* **2021**, *209*, 111781.
72. Bucci, K.; Bikker, J.; Stevack, K.; Watson-Leung, T.; Rochman, C., Impacts to Larval Fathead Minnows Vary between Preconsumer and Environmental Microplastics. *Environ. Toxicol. Chem.* **2021**, *n/a* (n/a).
73. Cormier, B.; Gambardella, C.; Tato, T.; Perdriat, Q.; Costa, E.; Veclin, C.; Le Bihanic, F.; Grassl, B.; Dubocq, F.; Kärrman, A.; Van Arkel, K.; Lemoine, S.; Lagarde, F.; Morin, B.; Garaventa, F.; Faimali, M.; Cousin, X.; Bégout, M.-L.; Beiras, R.; Cachot, J., Chemicals sorbed to environmental microplastics are toxic to early life stages of aquatic organisms. *Ecotoxicol. Environ. Saf.* **2021**, *208*, 111665.
74. Zitouni, N.; Bousserhine, N.; Missawi, O.; Boughattas, I.; Chèvre, N.; Santos, R.; Belbekhouche, S.; Alphonse, V.; Tisserand, F.; Balmassiere, L.; Dos Santos, S. P.; Mokni, M.; Guerbej, H.; Banni, M., Uptake, tissue distribution and toxicological effects of environmental microplastics in early juvenile fish *Dicentrarchus labrax*. *J. Hazard. Mater.* **2021**, *403*, 124055.
75. Coffin, S.; Dudley, S.; Taylor, A.; Wolf, D.; Wang, J.; Lee, I.; Schlenk, D., Comparisons of analytical chemistry and biological activities of extracts from North Pacific gyre plastics with UV-treated and untreated plastics using in vitro and in vivo models. *Environ. Int.* **2018**, *121*, 942-954.

## **Preamble to Chapter 6**

The critical literature reviews in chapters 2 and 5 provided the basis for this chapter. Our findings in chapter 5 revealed that only 10% of studies examining the effect of microplastic in the environment were carried out with environmentally relevant microplastics. More so, studies that use plastics originating from secondary sources, which are more prevalent in the environment, are sparse. The transport behavior of environmentally relevant microplastics is also scanty. Hence, the goal of this chapter was to understand how environmental UV weathering changes the physicochemical properties of microplastics from a single-use plastic cup. Thereafter, we aimed to understand how these property changes affect their mobility, transport, and interaction with other contaminants in freshwater.

The findings from this chapter are being prepared for submission to a peer-reviewed journal.

## **Chapter 6: Effects of Weathering on the Properties and Fate of Secondary Microplastics from a Disposable Cup**

### **Abstract**

Our current understanding of the fate and transport of environmentally relevant microplastics originating from real plastic debris is limited. In this work, we probed the changes to the physicochemical properties of polystyrene microplastics (4.5 mm) generated from a disposable cup as a result of UV-weathering, using a range of spectroscopy, microscopy and profilometry techniques. Thereafter, we aimed to understand how these physicochemical changes affect the microplastic contaminant sorption ability and transport potential in the aquatic environment. UV exposure led to measured changes in microplastic hydrophobicity (20-23% decrease), density (3% increase), surface oxidation, and microscale roughness (24-86% increase). The settling velocity of the microplastics increased by 53% after weathering which translates to a settling time that is ~1 hour faster for the aged microplastics to reach the sediment bed in a simulated deep freshwater system of 80 m. Our work suggests that UV aging, rather than just biofouling (as often predicted), can increase microplastic deposition to sediments, while the impact of UV weathering was greater than the predicted effect of the water temperature. Weathered microplastics exhibited reduced sorption capacity (up to 52% decrease) to a model hydrophobic contaminant (triclosan) compared to pristine ones. The adsorption of triclosan to pristine and aged microplastics was slightly reversible with significant desorption hysteresis. These combined effects of weathering could potentially limit the long-range transport and contaminant transport abilities of microplastics. As the first study to investigate the effect of UV aging on the sorption capacity and mobility of a secondary polystyrene microplastic, this work advances our knowledge about the risks associated with microplastics in natural aquatic environments and the need to use environmentally relevant microplastics.

### **6.1 Introduction**

There is growing concern about the true environmental risks posed by microplastic pollution to ecosystems. Microplastics (< ~5 mm) are often classified as either having primary (intentionally produced pellets/beads) or secondary origin (tiny fragments from real plastic debris). Secondary microplastics are thought to be found in larger quantities in the environment compared to primary ones,<sup>1</sup> yet, the majority (~90%) of studies<sup>1</sup> aimed at understanding the risks associated with

microplastic pollution have been carried out with primary (mostly pristine) microplastics.<sup>2</sup> The few effect studies that attempt to mimic environmentally relevant microplastics focused on weathering virgin plastics from primary sources rather than those originating from plastic debris (secondary source). A recent estimate shows that 46% of global plastic debris originates from single-use plastic packaging material,<sup>3</sup> most of which become film fragments in the environment. Numerous field studies also detect microplastic films in the environment and biota, yet, few effect studies use microplastic films (i.e., flattened microplastics) when investigating risks. Although, there are several governmental and institutional legislations and movements to reduce the global plastic footprint (especially with respect to single-use plastics), these measures are still in their infancy. Hence, the burden of plastic pollution will continue in the foreseeable future. In fact, two recent studies predict that plastic emissions and exposure to the environment will increase even with the current rate of intervention strategies.<sup>4,5</sup>

Throughout the lifecycle of microplastics, they experience multiple forms of weathering such as photodegradation, thermal degradation, biofouling etc., either simultaneously or sequentially.<sup>6-8</sup> These processes will impact microplastics properties and buoyancy, and hence their settling behavior which will either lead to long-range transport or accumulation near the source of release in aquatic environments. Understanding the sinking behavior of microplastics is particularly important in designing remediation strategies,<sup>9</sup> predicting the concentration of microplastics in the water column, deposition rates in the seabed, identifying pollution hotspots within the water column,<sup>10</sup> etc. However, in the current literature, there is a lack of understanding about the effect of weathering on the sinking behavior and residence time of microplastics, especially microplastic films/sheets. Although the effect of biofouling on the vertical transport of microplastics has been theoretically modelled,<sup>11</sup> only few experimental studies have attempted to investigate the impact of weathering (no studies on photodegradation) on the settling behavior of microplastics, with contrasting findings. Waldschlager et al. showed that microplastics collected from a fluvial environment settled slower compared to pristine microplastic samples.<sup>12,13</sup> Nguyen et al. also reported that microbe-associated polyurethane microplastics have sinking rates two times slower than pristine ones.<sup>14</sup> On the contrary, two studies show that biofouled microplastics exhibit higher settling velocities than pristine ones.<sup>15,16</sup> Clearly, there is a need to better understand the crucial role of other weathering processes (other than biofouling) in altering the physicochemical properties, and hence the settling behavior of microplastics.

Moreover, despite the substantial number of effect studies that have investigated the sorption/desorption capacity of pristine primary microplastics, our understanding of the interaction of other contaminants with microplastics from secondary sources (both pristine and aged) is still limited. Even though the environmental effects of polystyrene particles are widely studied in the literature,<sup>2, 17</sup> the sorption or desorption capacity of contaminants on secondary polystyrene microplastics derived from single-use plastic is not well understood. The effect of UV weathering on the interaction of this plastic type with other contaminants is also not well known. Indeed, our understanding of the potential effects of weathering on the settling behavior and fate of environmentally relevant microplastics from secondary sources is still limited.

Therefore, to address some of these gaps, the objective of this work is to systematically investigate how UV weathering alters the properties of secondary microplastics (4.5 mm) sourced from a single-use disposable product, and how these changes subsequently affect particle fate and behavior in a simulated freshwater system. For this purpose, microscopy, spectroscopy and profilometry techniques were used to characterize the surface and bulk properties of the microplastics before and after exposure to UV radiation. The adsorption and desorption of the model contaminant, triclosan to the aged and pristine microplastics were also measured. Experimentally determined settling velocities were coupled with a model to simulate the vertical transport and contaminant-facilitated transport potential of microplastics in freshwater systems. Model simulations on the effects of weathering on the transport of microplastics of different shapes are presented for a 220  $\mu\text{m}$  microplastic sizes.

## **6.2 Materials and methods**

### **6.2.1 Plastic source and UV weathering treatment**

Single-use plastic cups (Cogan, #13-3001859) were purchased from a Dollarama store in Montreal, Canada in 2019. A heavy-duty revolving leather punch (SE 7924LP) was used to generate circular microplastic disks with 4.5 mm diameter from the disposable cups. Afterwards, the microplastics were rinsed thoroughly with reverse osmosis water (Biolab Scientific). Some samples were kept at room temperature in the dark and used as pristine microplastics while a separate batch of samples were placed in a glass plate containing 10 mM NaCl solution at pH ~6 (to mimic freshwater) and exposed to UV radiation in a weathering chamber for 8 months. The weathering chamber was kept at a temperature of 27 °C. The UV light consisted of both UVA and UVB bulbs (306 nm; Topbulb G15T8E, 350 nm; Topbulb, Eiko F15T8/BL and 365 nm; Hikari

Lamps) with total intensity of  $\sim 35 \text{ W/m}^2$ . During weathering, the microplastics were gently stirred at 35 rpm which ensured proper exposure of the samples to the UV radiation. After weathering, the microplastics were thoroughly rinsed with reverse osmosis water, air-dried and stored in the dark at room temperature in a desiccator for further use.

### 6.2.2 Characterization of microplastics

The change in microplastic mass after weathering was quantified using an ultra-micro analytical balance (S4, Sartorius) having a weighing accuracy/sensitivity of 0.0001 mg. The density of the microplastic before and after weathering was quantified using the titration method described in ISO 1183-1. Briefly, the microplastics were placed in a glass beaker with 50 mL reverse osmosis water. Then, small droplets of concentrated zinc chloride (#MKCG2036, Sigma Aldrich) solution were added to the beaker while the liquid was stirred. This process was repeated until the microplastic floated to the surface of the liquid. 1 mL of the final solution was then weighed on an analytical balance (MS104TS/00, Mettler Toledo) to determine the density. The thickness of each microplastic was measured using a digital caliper (Mastercraft, Digimatic) with 0.02 mm accuracy. The crystallinity of the microplastic was determined using the conventional density measurement method by estimating the weight fraction crystallinity of the microplastic (equation S1) as described in section S1.

The surface functional groups of the pristine and aged microplastics were characterized using a Fourier-transform infrared spectrometer (FT-IR, Spectrum II, PerkinElmer) in attenuated total reflectance (ATR) mode with a single bounce-diamond. Microplastic disks were analyzed in the region  $400 - 4000 \text{ cm}^{-1}$  with 32 scans at  $4 \text{ cm}^{-1}$  resolution. The specified area under band method<sup>18</sup> was adopted to calculate the ratio of the integrated band under the carbonyl region ( $1650-1800 \text{ cm}^{-1}$ ) and a reference absorption peak band (C-H) because it did not change after weathering ( $640-720 \text{ cm}^{-1}$  centered at  $696 \text{ cm}^{-1}$ ).<sup>19</sup> Spectragryph software (v1.2.15) was used for peak analysis and normalization. X-ray photoelectron spectroscopy (XPS) with etching was used to analyze the oxidation profile of the aged and pristine microplastics. Briefly, the spot size was set to  $200 \mu\text{m}$ , the etching parameters set to 500 eV with a low current (etching rate of  $0.21 \text{ nm/s}$  in  $\text{Ta}_2\text{O}_5$ ), and three levels of etching were measured (0 s, 3 s, and 6 s). Spectra of the C1 and O1 peaks were collected.

The surface hydrophobicity of the microplastics was measured using the sessile water contact angle method on an OCA 20 Goniometer (DataPhysics Instruments). The instrument is

equipped with an automated microliter syringe and digital camera. For both aged and pristine microplastics, a total of 12 disks (6 each for inner and outer surface of the original cup) were used. Briefly, 3  $\mu\text{L}$  of water was dispensed on each sample surface and measurement was carried out within 3 s. Measurement on each sample was repeated twenty times.

The surface morphology of the microplastics was characterized using scanning electron microscopy (FEI Inspect F50). Sample surfaces showing the inner and outer parts of the cup were coated with a 3 nm layer of platinum before measurement (Leica Microsystems EM ACE600 Sputter Coater). A complimentary optical profilometry technique was used to quantitatively characterize the surface roughness of the plastics (Zygo NexView 3D) with Mx software. The Coherence Scanning Interferometry (CSI) mode with high z-resolution, signal oversampling and 20  $\mu\text{m}$  scanning length were adopted. All data were analyzed and extracted from the Mx software to obtain the profile parameters. Briefly, at least 12 microplastics (6 each for the inner and outer surface of the original cup) for each weathering condition were mounted on a glass slide with a double-sided tape before each measurement. The Brunauer–Emmett–Teller (BET) specific surface area was measured using the nitrogen adsorption method (Tristar II Plus, Micromeritics). Prior to the analysis, microplastic samples were degassed to remove any contaminants at 120 °C vacuum overnight. The mass of the microplastic samples after degassing was used for analysis.

The tensile strength of the microplastic was estimated with a Shimadzu EZ Universal Tensile tester. For tensile strength measurements, ASTM D638 (Standard Test Method for Tensile Properties of Plastics) and D882 (Standard Test Method for Tensile Properties of Thin Plastic Sheeting) were used with slight modifications to the sample size. Rectangular plastic strips (70 $\times$ 10 mm) from the disposable cups were used for all measurements and these strips underwent the same weathering procedure as the 4.5 mm disks. Each strip was placed between the parallel plates of the instrument and allowed to stretch until it broke.

### **6.2.3 Settling experiment**

The settling velocity of the microplastics was measured using a cylindrical column (50 cm height and 10 cm diameter) following the procedures described in previous studies.<sup>9, 13</sup> Microplastics were placed at the center of the column, approximately 1 cm below the water surface using stainless steel tweezers and released to fall freely. The time each particle took to travel to a depth of 29 cm was recorded with a stopwatch. This 29 cm depth is between two upper and lower

excluded sections of the water column and was selected because the particles reached terminal velocity at this distance. The fluid in the settling column contained 10 mM NaCl at pH 6 to mimic freshwater. Microplastics were pre-wetted by immersing in the same fluid at least 2 days before each experiment. The temperature of the fluid for all experiments was kept at 20-21 °C and 1 °C. All experiments at 1 °C were carried out in a cold chiller (Danby, DWC032A2BDB) to maintain the temperature during the experiments. To validate the measured settling velocities, the settling velocity of standard polystyrene spheres of a similar order of magnitude in size as the microplastics used in this study was investigated. The polystyrene spheres (Cospheric LLC, Lot # 30199318-07) have a mean diameter of  $4.7 \pm 0.05$  mm and a density of  $1.05 \text{ kg/m}^3$ . The theoretical Stokes settling velocity of the model spheres (calculated as 7.4 cm/s) was compared with the measured settling velocity ( $7.0 \pm 0.0$  cm/s). Since the average measured settling velocity deviated by only 5% from the theoretical value, the protocol used for measuring the microplastic settling velocity was deemed valid and reliable.

#### **6.2.4 Adsorption kinetics and isotherm experiment**

Triclosan was used as the model hydrophobic contaminant ( $\log K_{ow} = 4.76$ ) in this study as it is often detected in freshwater and treated wastewater.<sup>20</sup> Batch kinetic adsorption experiments were conducted at low and high concentrations of 20 and 100  $\mu\text{g/L}$  triclosan, respectively. Isotherm experiments included two additional concentrations of 50 and 150  $\mu\text{g/L}$  triclosan. Preliminary experiments showed that the time needed to reach equilibrium is approximately 21 days, hence all experiments were conducted for at least 21 days. For each condition, 7 disks of either pristine or aged plastic (~30 mg total) were added to 40 mL triclosan solution in amber glass vials (Sigma Aldrich) and shaken in an end-to-end rotator (Boekel Scientific) at 60 rpm. All triclosan solutions were prepared in background electrolyte of 10 mM NaCl. At each sampling time point, each vial was spiked with 50  $\mu\text{g/L}$  of internal standard (triclosan- $\text{d}_3$  from CDN Isotopes), filtered through a 0.22  $\mu\text{m}$  membrane filter (PTFE syringe filter, Canadian Life Science) and stored in a freezer (-4 °C) before analysis. Control samples with triclosan in background electrolyte solution without microplastics were also shaken in the rotator during all experiments to monitor contaminant loss. All experiments were performed at room temperature (~20-22 °C). Solution pH was at  $6 \pm 0.2$  throughout all experiments.

### 6.2.5 Desorption experiment

Triclosan desorption kinetics and isotherm were measured immediately after each respective adsorption phase. Briefly, the microplastic disks were transferred from each adsorption vial using tweezers into 40 mL triclosan-free 10 mM NaCl solution in amber vials. The liquid phase triclosan concentration in each vial was monitored for 21 days to ensure that equilibrium was reached. At each sampling time point, each vial was spiked with 50 µg/L of internal standard (triclosan-d<sub>3</sub>), filtered through a 0.22 µm membrane filter (PTFE syringe filter, Canadian Life Science) and stored in a freezer (-4 °C) before analysis.

### 6.2.6 Analytical instrumentation

The triclosan concentration in all adsorption experiments was measured by an Agilent 1290 Infinity II LC system coupled to a 6545 Q-TOF-MS (Agilent Technologies, Santa Clara, USA). The LC separation was done with a Poreshell120 EC-C18 analytical column (3 mm×100 mm, 2.7 µm; Agilent Technologies) connected with a Poreshell120 EC-C18 guard column (3 mm×5 mm, 2.7 µm; Agilent Technologies). The mobile phase A was HPLC water and the mobile phase B was acetonitrile/methanol mixture (50:50 v/v). Ammonium acetate (5 mM) was added to both mobile phases A and B to improve the electrospray ionization (ESI) efficiency. Samples were kept at 4 °C in the multisampler compartment. Details of HPLC and MS parameters are presented in Table S6.1. During sample run, reference ions (112.9856 and 1033.9881 for ESI in negative mode) were used for automatic mass recalibration of each acquired spectrum.

### 6.2.7 Transport distance simulation

Here, we aim to simulate the effect of aging on microplastic transport and contaminant co-transport potential. To predict the transport of smaller microplastic disks ( $\leq 220$  µm), an equation for the theoretical settling velocity was developed based on Newton's law (balance of forces acting on a single particle falling in a fluid) by assuming the shape of a disk (detailed derivation is provided in equations S6.2-S6.4, supplementary information, section S6.2). This equation is given as;

$$V_p = \sqrt{\frac{2gh(\rho_p - \rho_l)}{C_D\rho_l}} \quad (6.1)$$

where  $V_p$  = terminal settling velocity,  $C_D$  is the drag coefficient which is a function of the Reynolds number ( $Re$ ),  $\rho_l$  = density of the fluid,  $\rho_p$  = density of the particle,  $h$  = thickness of the microplastic disk.

When  $R_e < 1$ , equation 6.2 was obtained while  $C_D$  was calculated using the Stokes equations (see eq S3 in SI). A correction factor ( $C_f$ ) was applied to the  $C_D$  of the aged microplastics to account for any effects of aging on the material surface properties (e.g., diameter, wettability, roughness, etc.). This correction factor allows the simulation of the effect of aging on the settling velocities and travel distance of microplastics. Equation 6.2 was used for simulations presented in section 6.3.2.

$$V_p = \frac{2ghd_e(\rho_p - \rho_l)}{20.4C_f\eta} \quad (6.2)$$

where  $\eta$  = dynamic viscosity,  $d_e$  is the disk equivalent diameter.

### 6.2.8 Data and statistical analysis

All adsorption experimental data were fitted using the linear, Langmuir and Freundlich isotherms. The kinetics were modelled using the pseudo-first and second-order kinetic models. The Solver Add-in Excel tool was used for all curve fitting. All adsorption equations used are summarized in Table S6.1 and the non-linear forms of these models were used in fitting all experimental data for comparison. Where necessary, statistical significance was evaluated using one-way ANOVA and Tukey HSD mean comparison. All statistical analysis was performed using OriginPro software (version 9.8.0.200).

## 6.3 Results and discussion

### 6.3.1 Changes to physical and chemical properties of microplastics after weathering

After aging, we observe that the microplastic disk color changes from white translucent to yellow opaque (Figure 6.1a, b). The yellowing of polystyrene is often observed as a result of the free radicals generated by the chromophore during photooxidation.<sup>21</sup> It is important to note that the bulk plastic cup has a glossy outer layer. This outer layer glossiness was still preserved after aging for all disk samples (Figure S6.1). SEM images show slight changes on the surface of the aged microplastics (Figure 6.1c, d). From observation, the outer side of the aged cup seems to show higher pitting in comparison to the pristine surface, however, this was not comprehensively quantified. The inner side of the cup appeared more irregular than the outer side, however, when comparing the aged sample with the pristine there were no obvious changes (Figure S6.3). To quantitatively characterize and compare the surface roughness of the pristine and aged disks, an optical profiler was used. The results of surface topography characterization are shown in Figure 6.1e, f (2D profile), Figure S6.4 (3D isometric view) and Figure 6.1i, j (roughness parameters of

interest,  $S_a$  the average surface roughness and  $S_z$  the peak to valley height). By inspecting the 2D and 3D scans, we observe deeper valleys and higher peaks (blue and red regions, respectively) on the surface of the aged microplastics compared to the pristine ones. For both cases, the outer side of the cup is considerably smoother. This was confirmed in the measured  $S_a$  and  $S_z$  parameters on  $167 \times 167 \mu\text{m}^2$  areas (Figure 6.1i, j). For all conditions,  $S_a$  and  $S_z$  were lower for the outer side compared to the inner side. After aging, we observe a slight increase in  $S_a$  (for the inside surface) and a larger increase in  $S_z$  (both  $p < 0.05$ ). This shows that weathering increased the microscale roughness of the microplastics which complements the increase in Brunauer–Emmett–Teller specific surface area measured ( $0.34$  and  $0.95 \text{ cm}^2/\text{g}$  for pristine and aged plastics, respectively).

The wettability of the microplastics was measured to understand the effect of aging on the material surface hydrophobicity. The outer surface of the pristine microplastics had the highest contact angle. After weathering, the contact angle of the microplastics decreased indicating an increase in hydrophilicity of the material, as seen in Figure 6.1g, h. When comparing the outer and inner surfaces of the microplastics, we observe that the outer surface was more hydrophobic ( $99 \pm 4.9$  and  $80 \pm 5.3$  vs  $91 \pm 4.6$  and  $70 \pm 4.3$  for both pristine and aged microplastics, respectively,  $p < 0.05$ ). This translates to a decrease in the contact angle of 23% for the inner surface and 20% for the outer surface after weathering. Leaching of additives from the plastic material may also have contributed to the increased hydrophilicity of the material. Similar trends of decreased water contact angle of aged polystyrene microplastics compared to pristine plastics were recently reported.<sup>9, 22</sup>

The mass changes after weathering (Figure 6.1k) showed a slight decrease (14%) in the average mass after weathering, however, this change was not statistically significant ( $p > 0.05$ ). The average diameter also did not significantly change after weathering ( $0.45$  to  $0.44 \pm 0.034 \text{ mm}$ ). This shows how long it may take plastic debris to completely break down in the environment. Interestingly, we observed an increase in the density of the aged microplastics, by 3% (from  $1.04 \pm 0.004$  to  $1.07 \pm 0.004 \text{ g/cm}^3$ ,  $p < 0.05$ ). In polymers, density changes are typically associated with either changes in crystallinity, changes in mass or volume (diameter and thickness), loss of plasticizers, biofouling, etc. UV radiation has been shown to increase crystallinity due to the close and regular packing of the polymer chains.<sup>23</sup> Compared to amorphous areas, the crystalline part of a polymer is more densely packed,<sup>24</sup> hence, increase in crystallinity could lead to increased density (decreased

specific volume). It was previously observed that UV exposure led to increase in nylon density.<sup>25</sup> From the weight fraction crystallinity calculated for pristine and aged microplastics (equation S6.1), the crystallinity of the microplastics increases from 0 to 37%. In addition to increased crystallinity and based on the slight decreases observed in the diameter, thickness ( $0.25 \pm 0.048$  to  $0.24 \pm 0.045$  mm) and mass ( $4.4 \pm 0.78$  to  $3.8 \pm 0.54$  mg), a simulation is presented and discussed in Figure S6.2 and Table S6.3 to show how particle density may change when these parameters change. At constant mass, a decrease in either thickness, diameter or both will lead to between 3–7% increase in densities (Table S6.3). A conservative estimate of slight decrease (1%) each in mass, thickness or diameter can lead to an increase in density of 3%. Therefore, the increase in density can be attributed to either an increase in crystallinity and/or slight decrease in volume.

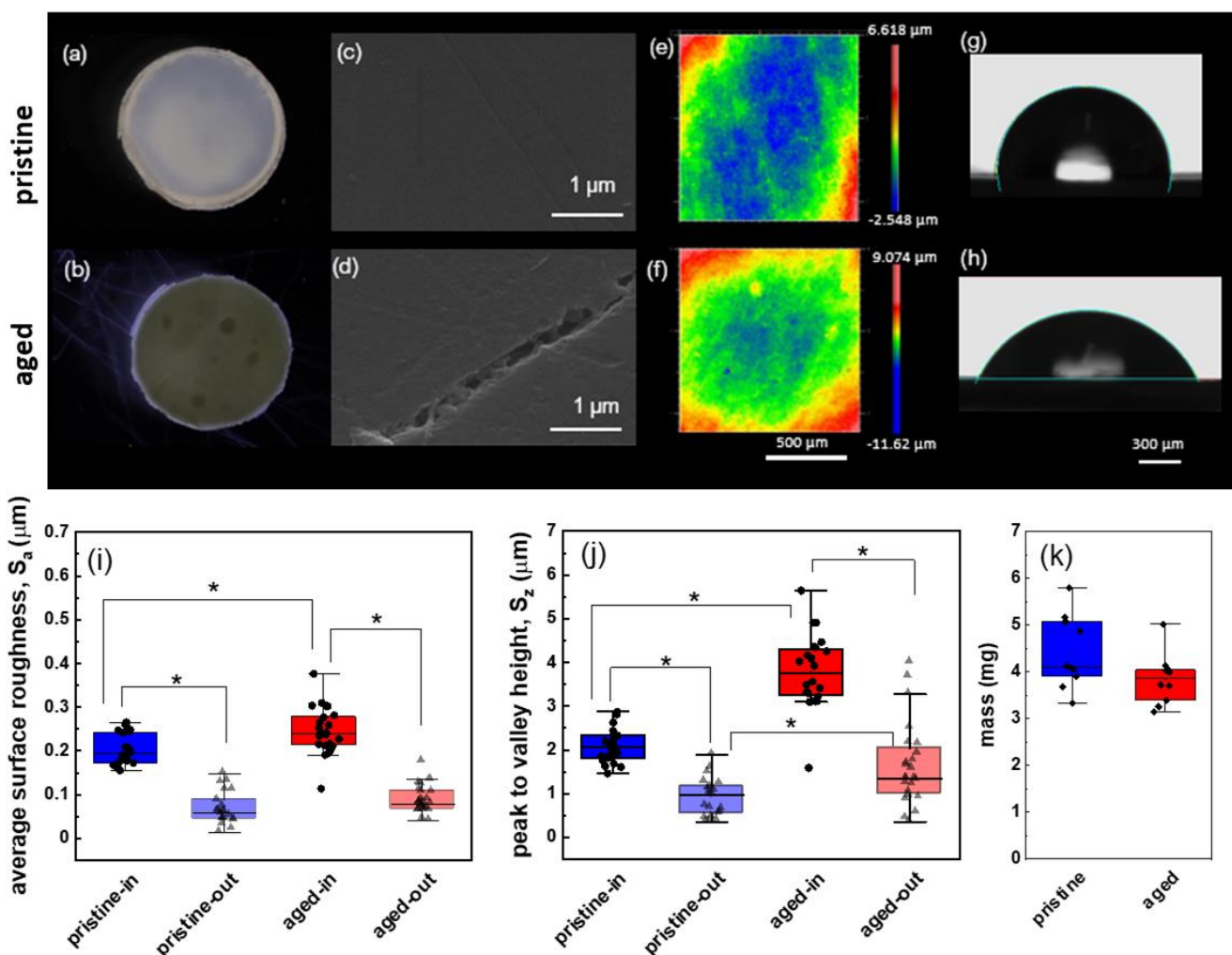


**Figure 6.1.** Physical characterization of the pristine and aged microplastics (a, b) colour changes of the microplastic, (c, d) surface morphology of microplastics (outer side) using SEM, (e, f) roughness profile of the microplastics (inner side) using a profilometer, (g, h) representative image of water droplet for contact angle measurement on pristine and aged microplastics (inner

side), (i, j) roughness parameters,  $S_a$  and  $S_z$  at 50× magnification, (k) mass change of microplastic disks before and after weathering. Pristine-in and aged-in refer to the inner surface of the original cup, while pristine-out and aged-out refer to the outer surface of the cup.

**Table 6.1.** Summary of parameters related to changes in physical, chemical and mechanical properties of the microplastics after aging

Property	pristine-in	pristine-out	aged-in	aged-out
Contact angle (°)	91 ± 4.6	99 ± 4.9	70 ± 4.3	80 ± 5.3
Carbonyl index	0.024 ± 0.012	0.0031 ± 0.0051	0.068 ± 0.042	0.022 ± 0.012
	pristine	aged		
Young's modulus (MPa)	496 ± 54	597 ± 178		
Ultimate elongation	0.074 ± 0.0076	0.023 ± 0.0019		
Thickness (mm)	0.25 ± 0.048	0.24 ± 0.045		
BET specific surface area (cm <sup>2</sup> /g)	0.34	0.96		
Density (g/cm <sup>3</sup> )	1.04 ± 0.004	1.07 ± 0.005		

The pristine microplastics were confirmed as polystyrene using the built-in PerkinElmer software library (99% match). The changes to the functional groups of the inner and outer surfaces of the microplastic disks are compared in Figure 6.2a. The peak characteristic of the carbonyl band (~1742 cm<sup>-1</sup>) is more pronounced for the aged microplastics. This suggests some degree of oxidation on the aged plastics. Indeed, the carbonyl index of the surface of the disks significantly increased after aging from 0.024±0.012 to 0.068±0.042 for the inner surface and from 0.0031±0.0051 to 0.022±0.012 for the outer surface. XPS analysis was used to complement the FTIR measurements and three different depths (depth 0 corresponding to the surface 0 nm, depth 1 corresponding to ~0.63 nm and depth 2 corresponding to ~1.26 nm) were scanned on each side of both pristine and aged microplastics. Figures 6.2b-e and S6.5 show the O1s and C1s spectra. In the C1s spectra (Figure 6.2b, c), we observe an additional peak due to oxidation at the surface (depth 0) at ~288.5 eV which correspond to O=C-OH, while the peak at ~286 eV (binding energy of C=O) increased. This change is consistent on both inner and outer sides (Figure S6c, d). From Figure 6.2d, we observe that the oxygen content at the surface (depth 0) increased after aging. The oxygen content is consistently higher for the aged microplastic, even at greater etching depth into the material (Figure 6.2e). Nonetheless, the extent of oxidation is greatest at the surface of the aged microplastic, and these observations are consistent on both the inner and outer surfaces of the disks (dotted and solid lines respectively, Figure 6.2d, e). These FTIR and XPS results confirm changes in the oxidation state and increase in hydrophilicity of the microplastics after UV treatment which is consistent with the decrease in water contact angles (discussed in the preceding 2 paragraphs)

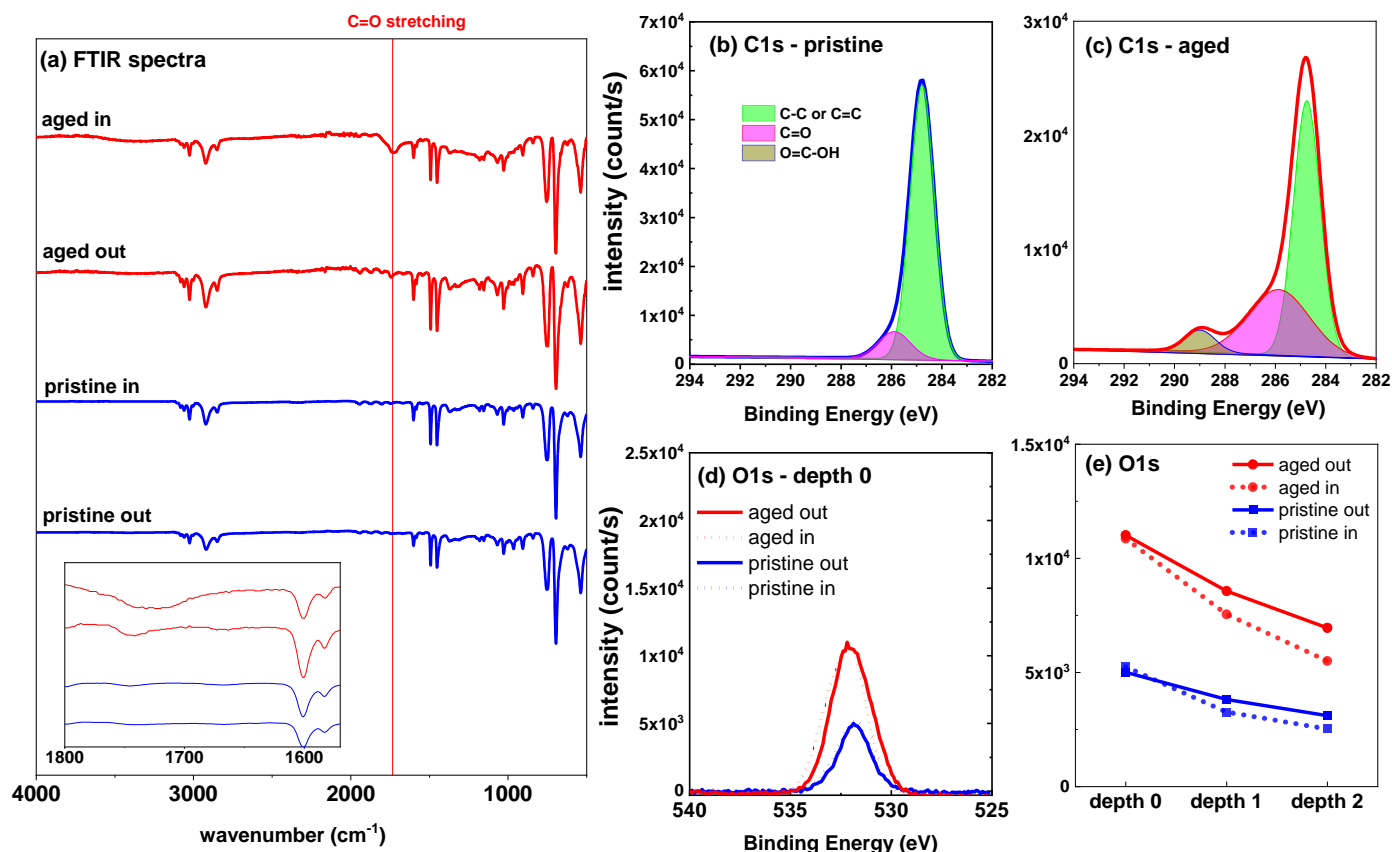


**Figure 6.2.** Surface composition characterization of microplastics. (a) representative FTIR spectra of pristine versus aged microplastics. Inset: zoom-in of FTIR spectra; (b) representative deconvoluted XPS spectra of C1s for pristine disk at depth 0; (c) representative deconvoluted XPS spectra of C1s for aged disk at depth 0; (d) XPS analysis of O1s at depth 0; (e) difference in oxygen content at depths 0, 1 and 2 for inner and outer surfaces. XPS etching done at 400 eV at 0.21 nm/s; depth 0 = outermost surface = 0 s of etching, depth 1 = 3 s, depth 2 = 6 s.

Changes in the mechanical properties of the plastic due to weathering were investigated using tensile strength tests. The experimentally measured stress versus strain curve is presented in Figure S6.7 while the calculated ultimate elongation and Young's modulus are reported in Table 6.1. The shape of the stress-strain curve of the pristine plastic is characteristic of a tough and strong plastic while that of the aged plastic is typical of a brittle polymer.<sup>26</sup> Calculated Young's modulus did not change significantly after weathering, while the ultimate elongation decreased by 69% (Table 6.1). The reduced ultimate elongation of the aged plastics is an indication of increased brittleness, which is often associated with an increase in crystallinity.<sup>27</sup> Indeed, our aged plastic samples were fragile and easy to break. Other studies also report a decrease in ultimate elongation of plastics after UV

weathering.<sup>27, 28</sup> To summarize, we show that weathering affected the surface chemistry, tensile strength, morphology, crystallinity, surface area and density of the plastics. While the inner and outer sides of the disks were exposed to the same weathering conditions, the two sides were not affected the same way. We also noted that the topography of the glossy outer surface of the microplastics seems to be more resistant to UV-weathering.

### **6.3.2 UV weathering increases the settling rate of polystyrene microplastics**

Figure 6.3a shows the settling rate of the pristine versus aged microplastics. Clearly, we see an increase in the settling rate of the disks after weathering, from  $0.87 \pm 0.08$  cm/s to  $1.3 \pm 0.22$  cm/s (~53% increase) at 21 °C, and from  $0.77 \pm 0.11$  cm/s to  $1.2 \pm 0.11$  cm/s (~54% increase) at 1 °C. The mobility of particles in cold temperatures is expected to be slower compared to room temperature (due to changes in fluid viscosity). Interestingly, while the percentage increase in settling velocity after weathering is similar at both temperatures, the impact of weathering is more important than that of the fluid temperature (Figure 6.3a). The measured increase (3%) in plastic density after weathering likely contributes to the observed increased settling rate of the disks. In addition to this change, the surface roughness and hydrophobicity of a particle could affect its drag, and hence, sinking velocity. Our surface roughness measurements show that the microplastics became slightly rougher after weathering which would favor a reduction in settling velocity rather than an increase i.e., higher fluid-solid interactions at the plastic-water interface generate shearing and an additional drag effect. However, the contact angle measurements imply that the microplastics became more hydrophilic with aging which could possibly play a role in decreasing the drag of the microplastics. There are no studies investigating the effect of UV weathering on the sinking velocity of microplastic disks, but we can obtain some insights from biofouling studies. The increased settling velocity of biofouled microplastic films/sheets versus pristine microplastics has been ascribed to increased density as a result of biofilm formation on the plastic surface.<sup>15, 29</sup> A different study shows that microplastic films from municipal plastic waste had settling velocities ranging from 0.45 – 10.47 cm/s which is in the range of our reported values.<sup>9</sup> Others also reported biofouled microplastics having increased settling velocity compared to pristine ones as a result of increased density when using spherical microplastics<sup>16</sup> or irregularly shaped fragments.<sup>30</sup>

To simulate the effect of weathering on the vertical transport of the microplastics, we need to consider that weathering affects the density and other material properties such as hydrophilicity, crystallinity, thickness, diameter, etc. which are expected to affect the drag coefficient of the aged

disks. Hence, a correction factor ( $C_f$ ) is applied to  $C_D$  for the aged microplastics. As described in section 6.2.7, equations 1 and 2 were used to simulate the settling velocity of different microplastic disks and spheres with similar equivalent diameters at different water temperatures. For the smaller-sized disk/sphere ( $\leq 220 \mu\text{m}$ ), the particles were assumed to be in the laminar regime (where  $Re < 1$ ). A lake depth of 80 m is assumed which is representative of lake depths in Quebec, Canada.<sup>31</sup> Figure 6.3b-f shows the results of the transport simulations. For the large microplastic disks (4.5 mm), the particles will settle out of the water column in approximately 3 and 2 hours for pristine and aged microplastics, respectively, at 21 °C. For the smaller disks (220  $\mu\text{m}$ ), we show that they cover the same depth in 18 and 8 days for pristine and aged microplastics, respectively. We also show in all cases (Figure 6.3b-f) that the pristine microplastics will travel slower at both 1 and 21 °C compared to aged microplastics at 1 °C. When the 220  $\mu\text{m}$  disk is compared to spherical plastics of similar equivalent diameter (100  $\mu\text{m}$ ), our transport simulation revealed that microplastic disks will remain in the water column for a longer period before sinking. This is not surprising as a particle of same diameter but that departs from a spherical shape will experience higher drag.

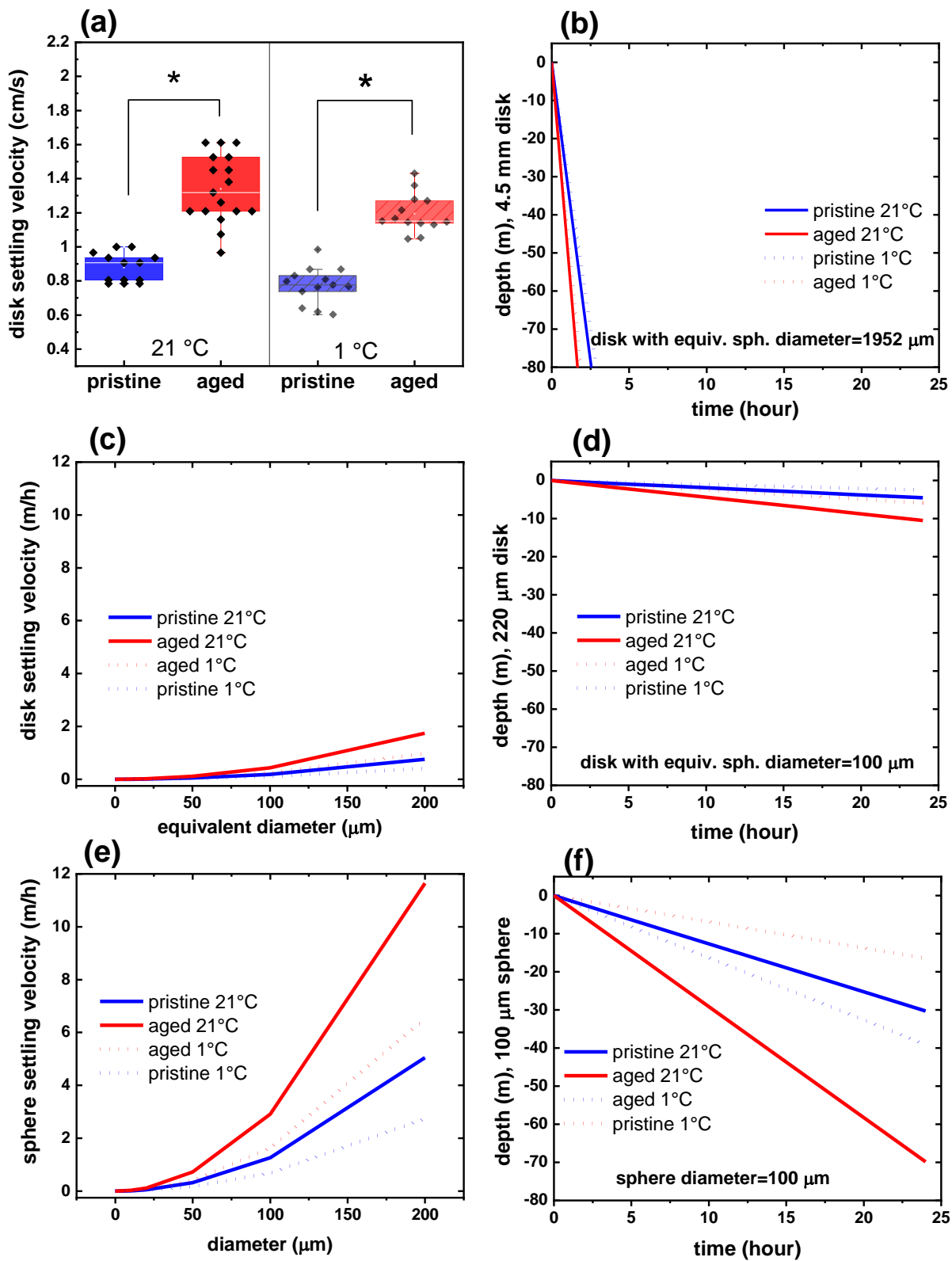


**Figure 6.3.** (a) experimental settling velocity of microplastic disks in 10 mM NaCl ( $d_e = 1952 \mu\text{m}$ ), and (b) simulated transport distance of microplastic disks in a freshwater system ( $d_e = 1952 \mu\text{m}$ ). (c, e) calculated settling velocity of polystyrene disk and spheres, (d, f) simulated transport depth of 100  $\mu\text{m}$  polystyrene disk and sphere.

### 6.3.3 Effect of weathering on adsorption capacity of triclosan on microplastics

The effect of weathering on the affinity of triclosan to the microplastics was investigated in batch sorption experiments. The adsorption kinetics of triclosan on microplastics at two concentrations (low,  $C_0 = 20 \mu\text{g/l}$  and high,  $C_0 = 100 \mu\text{g/l}$ ) are shown in Figure 6.4a, b, while a summary of the parameters obtained from the kinetic models is presented in Table 6.2. Sorption equilibrium was reached for both concentrations at  $\sim 20$  days. This time is considerably higher than equilibrium times typically reported in laboratory studies investigating sorption of contaminants to primary polystyrene microplastics which range from 16 h to 17 days.<sup>32, 33</sup> We observed higher adsorption capacity of the pristine microplastics compared to the aged ones, only at  $C_0 = 100 \mu\text{g/L}$  ( $p < 0.05$ ). Both sets of kinetic experimental data fitted the pseudo second-order model better than the first-order model, which suggests a chemisorption mechanism. The adsorption of several contaminants to microplastics has been shown to follow pseudo second-order kinetics.<sup>32</sup> After aging, the triclosan load ( $q_e$ ) on the microplastics did not change significantly when  $C_0 = 20 \mu\text{g/l}$  ( $13 \pm 0.4$  to  $13 \pm 0.51 \mu\text{g/g}$ ) but decreased when  $C_0 = 100 \mu\text{g/l}$  ( $51 \pm 2.5$  to  $44 \pm 3.1 \mu\text{g/g}$ ,  $p < 0.05$ ). The average adsorption rate,  $k_2$ , also slightly decreased for the aged microplastics suggesting less available adsorption sites. The sorption of hydrophobic contaminants on virgin polystyrene microplastics is often attributed to several mechanisms depending on the water chemistry, contaminant and polymer nature.<sup>34</sup> In our study, we hypothesize that triclosan will interact favorably with the polystyrene via hydrophobic and  $\pi$ - $\pi$  interactions (due to the presence of benzene rings in triclosan and polystyrene). Electrostatic interaction is unlikely since triclosan is neutral at the working pH of 6. Since aging led to reduced hydrophobicity, this might explain the lower adsorption capacity of the aged microplastics. Indeed, in agreement with our study, reduced sorption was reported after aging of polystyrene microplastics for atorvastatin,<sup>35</sup> bisphenol A,<sup>36</sup> and four fuel aromatics and ethers.<sup>37</sup> In marked contrast to our work, some studies found aged polystyrene microplastics to exhibit higher sorption capacity than pristine particles for hydrophobic contaminants. For example, Xiong et al. reported that UV-aged polystyrene nanoplastics have higher sorption capacity than pristine particles for bisphenol A.<sup>38</sup> Higher sorption capacities were also reported for a range of contaminants (with  $\log K_{ow}$  ranging from 0.5 to 5) to thermally-aged microplastics compared to pristine ones.<sup>39</sup> Even though the hydrophobicity of the plastic surface decreased after aging, the increased sorption to aged microplastics was attributed to the higher specific surface area.<sup>39</sup> While we did observe higher surface roughness and surface area of the aged microplastic disks, this did

not translate to higher sorption capacities of triclosan. Interestingly, the sorption capacity of the microplastics in this study at  $C_0 = 100 \mu\text{g/L}$  is higher than some studies using primary polystyrene microplastics with higher specific surface area (Figure 6.4d). With the starting concentration of contaminant and specific surface area of microplastics used by Hai et al ( $C_0=100 \mu\text{g/L}$ ) and Liu et al ( $C_0=50 \mu\text{g/L}$ ),<sup>36, 40</sup> our microplastics still have a higher sorption capacity than these studies (even at  $C_0=20 \mu\text{g/L}$ , Figure 6.4d).

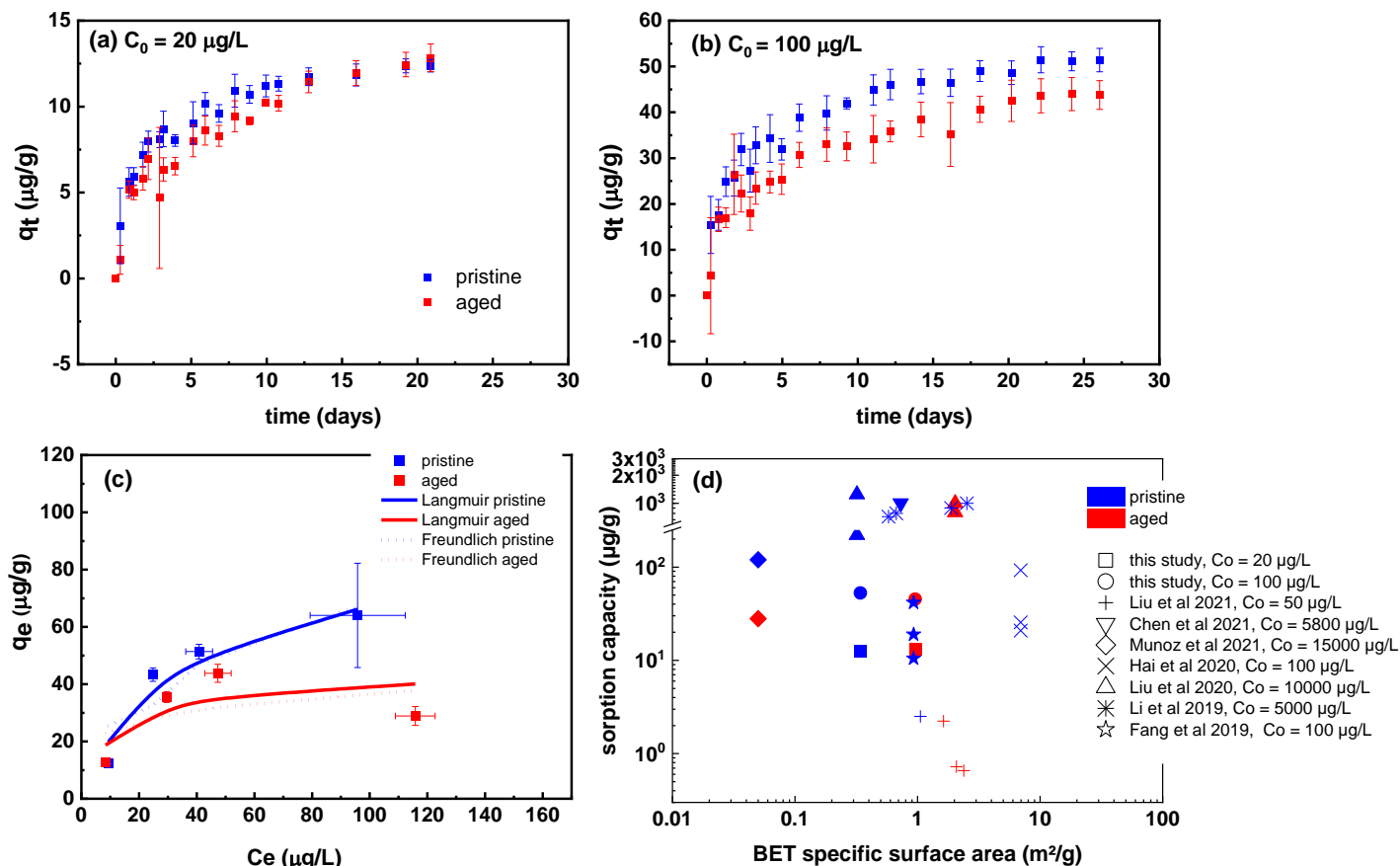


**Figure 6.4.** Effect of weathering on the (a) contaminant adsorption kinetics at  $20 \mu\text{g/L}$  triclosan; (b) at  $100 \mu\text{g/L}$  triclosan; (c) adsorption isotherm at pH 6; (d) comparison of hydrophobic contaminant ( $\log K_{ow}$  3.09 – 4.76) equilibrium adsorption capacity between different polystyrene microplastics in literature. Error bars denote standard deviations between triplicate runs.

From the isotherm in Figure 6.4c, we observe that the pristine microplastics have more affinity for triclosan at high concentration compared to the aged microplastic (that is, at  $C_0 = 50, 100$  and  $150 \mu\text{g/L}$ ,  $p < 0.05$ ). By inspection, both curves follow a non-linear isotherm. Glassy polymers such as polystyrene tend to exhibit both linear and non-linear isotherms while rubbery ones such as polyethylene have linear isotherms.<sup>41</sup> We can also infer from the non-linearity of the isotherm that adsorption rather than absorption is dominant which is in general agreement with previous

observations.<sup>41</sup> Generally, contaminants have more affinity for the amorphous region of a polymer than the crystalline region. Polystyrene is amorphous and at room temperature, it exists in a glassy state. After aging, the crystallinity increased, making the amorphous region less accessible which may contribute to the reduced sorption capacity of the aged microplastics. By fitting the experimental data to the three isotherm models, we show that the data for pristine and aged particles fits the Langmuir model better ( $R^2 = 0.94$  and  $0.95$ , respectively, Table S6.3). This suggests a monolayer coverage of triclosan on the microplastic surface.

**Table 6.2.** Kinetic model fitting parameters for triclosan adsorption and desorption on microplastics

model	parameter	pristine	aged		
<b>Adsorption, <math>C_0 = 20 \mu\text{g/L}</math></b>	$q_{e, \text{exp}}$ ( $\mu\text{g/g}$ )	$12 \pm 0.36$	$13 \pm 0.81$		
	Pseudo-first order	$k_1$ ( $\text{day}^{-1}$ )	$0.53 \pm 0.11$	$0.25 \pm 0.044$	
		$q_e$ ( $\mu\text{g/g}$ )	$11 \pm 0.38$	$12 \pm 1.07$	
		$R^2$	$0.89 \pm 0.04$	$0.86 \pm 0.057$	
	Pseudo-second order	$k_2$ ( $\text{g}(\mu\text{g}\cdot\text{day})^{-1}$ )	$0.058 \pm 0.017$	$0.029 \pm 0.0065$	
		$q_e$ ( $\mu\text{g/g}$ )	$13 \pm 0.39$	$13 \pm 0.51$	
		$R^2$	$0.95 \pm 0.023$	$0.93 \pm 0.0098$	
	<b>Adsorption, <math>C_0 = 100 \mu\text{g/L}</math></b>	$q_{e, \text{exp}}$ ( $\mu\text{g/g}$ )	$51 \pm 2.6$	$44 \pm 3.1$	
		Pseudo-first order	$k_1$ ( $\text{day}^{-1}$ )	$0.39 \pm 0.105$	$0.31 \pm 0.015$
			$q_e$ ( $\mu\text{g/g}$ )	$47 \pm 2.3$	$39 \pm 4.7$
$R^2$			$0.87 \pm 0.05$	$0.81 \pm 0.095$	
Pseudo-second order		$k_2$ ( $\text{g}(\mu\text{g}\cdot\text{day})^{-1}$ )	$0.011 \pm 0.004$	$0.0084 \pm 0.0010$	
		$q_e$ ( $\mu\text{g/g}$ )	$53 \pm 2.5$	$45 \pm 3.5$	
		$R^2$	$0.93 \pm 0.03$	$0.87 \pm 0.069$	
<b>Desorption, <math>C_0 = 100 \mu\text{g/L}</math></b>		$q_{e, \text{exp}}$ ( $\mu\text{g/g}$ )	$42 \pm 2.8$	$38 \pm 3.3$	
		Pseudo-first order	$k_1$ ( $\text{day}^{-1}$ )	$0.49 \pm 0.069$	$0.60 \pm 0.14$
			$q_e$ ( $\mu\text{g/g}$ )	$42 \pm 3.7$	$38 \pm 3.3$
	$R^2$		$0.71 \pm 0.041$	$0.97 \pm 0.008$	
	Pseudo-second order	$k_2$ ( $\text{g}(\mu\text{g}\cdot\text{day})^{-1}$ )	$0.081 \pm 0.0081$	$0.13 \pm 0.04$	
		$q_e$ ( $\mu\text{g/g}$ )	$43 \pm 2.70$	$38 \pm 3.3$	
		$R^2$	$0.98 \pm 0.0046$	$0.98 \pm 0.0079$	

$q_{e, \text{exp}}$  = experimental adsorption capacity at equilibrium

### 6.3.4 Effect of weathering on desorption of triclosan from microplastics and potential for facilitated transport

To understand the potential for release of contaminants in freshwater systems, the desorption kinetics of triclosan from the microplastic disks was monitored in 10 mM NaCl solutions at  $C_0 = 100 \mu\text{g/L}$ . Desorption kinetics as well as adsorption and desorption isotherms are shown in Figure 6.5a, b and c, respectively. First, we observe that the aged and pristine microplastics reach desorption equilibrium at 5 days (Figure 6.5a), which is fast compared to the adsorption time of  $\sim 20$  days. The desorption kinetic data was well fitted to the pseudo second-order model (Table 6.1). Interestingly, more triclosan,  $C_e$ , desorbed from the pristine microplastics compared to the aged ones at equilibrium ( $7.9 \pm 0.10$  vs  $5.1 \pm 0.33 \mu\text{g/L}$  respectively,  $p < 0.05$ ) even though the pristine microplastics have a slightly lower rate of desorption ( $0.081 \pm 0.008$  vs  $0.13 \pm 0.04 \text{ g}/\mu\text{g}\cdot\text{day}$ , respectively). On a mass basis, pristine microplastics desorb more triclosan than the aged sample ( $q_e = \sim 10$  vs  $\sim 7.5 \mu\text{g/g}$  microplastics). The higher  $C_e$  observed for pristine versus aged disks is consistent across a range of starting concentrations (Figure S6.8). Perhaps the aged microplastics did not release more triclosan because of its low initial adsorption capacity,  $q_e$  compared to the pristine microplastics. In the isotherm plot, adsorption and desorption hysteresis is observed for both pristine (Figure 6.5b) and aged microplastics (Figure 6.5c) implying that the adsorption of triclosan by the microplastics is not fully reversible for the tested conditions. This is consistent with the calculated hysteresis indices (HI, Figure 6.5b, c). When HI is  $\leq 0$ , desorption hysteresis is not obvious while the greater the HI value, the higher the degree of hysteresis.<sup>42</sup> The calculated hysteresis indices are generally  $> 0$  except for one value for aged microplastics (Figure 6.5c) which is slightly negative/neutral. The glassy domains in polymeric structures (e.g., polystyrene and geocolloids) have been reported to be favorable for adsorption but energetically unfavorable for desorption of non-polar hydrophobic molecules.<sup>42,43</sup> Liu et al. showed how pyrene was irreversibly adsorbed to polystyrene compared to a rubbery polymer, polyethylene.<sup>42</sup> This may explain the hysteresis observed during desorption. We also observe from the desorption isotherm that generally, the pristine microplastics retain more triclosan than the aged ones (Figure 6.5b, c, Table S6.3).

Triclosan desorption kinetics of pristine and aged disks (Figure 6.5a) were combined with the measured settling rates (Figure 6.3a) to quantify the amount of triclosan released as function of time and depth in natural waters (simulated for lake of 80 m depth where the horizontal flow

was assumed to be negligible). Because of their higher settling rate, aged disks would release triclosan deeper in the water column compared to pristine disks. To account for the microplastic shape, simulations were also performed on a 220  $\mu\text{m}$  disk (having equivalent sphere diameter of 100  $\mu\text{m}$ ) and spherical microplastic (100  $\mu\text{m}$ ). Assuming that the desorption kinetics presented in Figure 6.5a are conserved for a microplastic with an equivalent diameter of 100  $\mu\text{m}$  it is more likely that aged disks and spherical microplastics would release triclosan at the bottom of a lake (i.e., in sediments), while pristine and non-spherical microplastics are more likely to release triclosan in the water column (Figure S6.9).

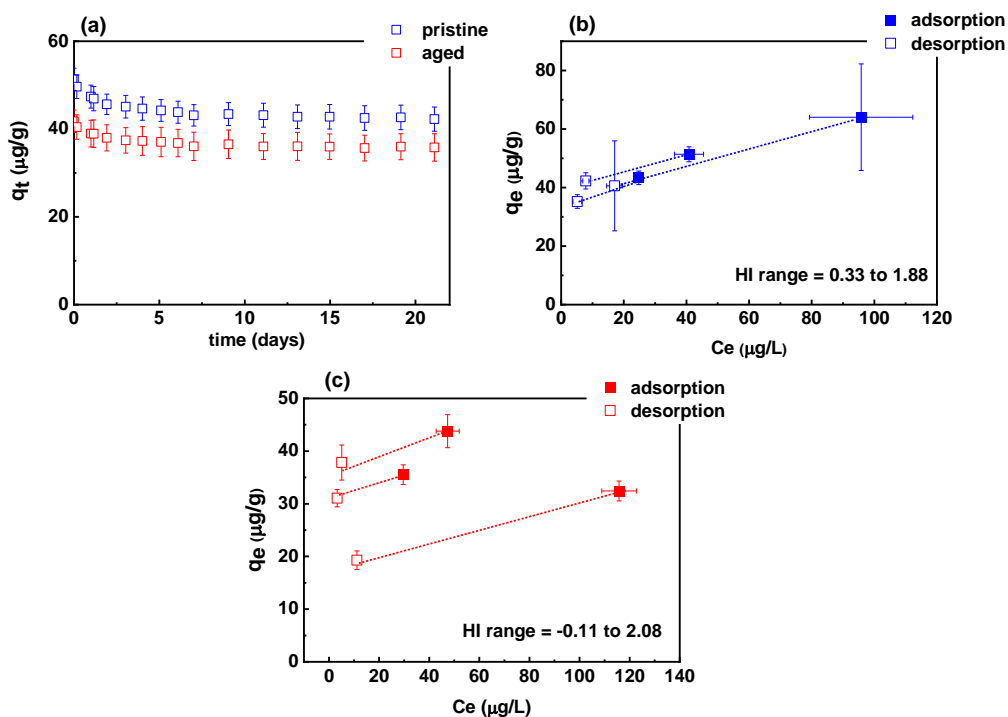


**Figure 6.5.** Desorption data for triclosan in 10 mM NaCl. (a) desorption kinetics at  $C_0 = 100 \mu\text{g/L}$ , (b) desorption isotherm of pristine microplastics, (c) desorption isotherm of aged microplastics. Dotted line drawn to connect each adsorption data with its desorption data. Error bars denote standard deviations of 3 experimental runs. HI = hysteresis index.

## 6.4 Environmental implications

The effect of weathering on the transport and contaminant facilitated transport of microplastics in surface waters is largely underexplored. While some efforts have been made to understand the transport potential of microplastics in the aquatic environment, the use of pristine plastics limits our understanding of the risks associated with environmentally relevant microplastics. This is the first study to investigate the effect of UV-weathering on the settling velocity of secondary

polystyrene microplastics and their interaction with an organic contaminant. We show that weathering will transform some physicochemical and mechanical properties of microplastic disks obtained from a single-use cup which includes the surface roughness, density, surface chemistry, wettability, crystallinity, and tensile strength. These transformations affected the fate, transport and interactions of the microplastics with triclosan in a model aquatic environment.

Specifically, our transport simulations reveal that the impact of weathering of the microplastics outweighs the effect of water temperature. Considering a lake in Quebec as a case study and based on the settling velocities measured, simulations show that weathering will reduce the residence time of a microplastic disk from 3 to 2 hours and 18 to 8 days (for 4.5 mm and 0.220 mm sizes, respectively). Two recent studies reported increased settling rate of aged (biofouled) microplastic films/sheets in natural water samples. While the weathering design in our study (simple water matrix, 10 mM NaCl) was not aimed at producing biofouled microplastics or grow biofilms on microplastics, we show that other transformations (which may include slight reduction in volume/thickness/diameter/polarity and increase in crystallinity of the microplastics) as a result of UV degradation could increase the sinking rates and transport of microplastics. The settling velocity and transport reported in our work for aged microplastics is expected to be even higher when natural colloids or biofilms are attached to the aged microplastics.

Our results also show that aged polystyrene microplastics can have lower affinity for a model hydrophobic contaminant, triclosan and that this contaminant is partially desorbed from pristine polystyrene compared to the aged material. These results suggest that microplastics from bulk plastic debris may act as vectors for hydrophobic contaminants when in a “cleaner” water body or potentially to an organism when ingested. As one of the first studies investigating the sorption capacity of secondary microplastics from bulk products, we show that despite the low working contaminant concentration (ppb range) and low specific surface area of the microplastic disks, we still observe higher adsorption of a hydrophobic contaminant than some primary microplastic types with higher specific surface areas in literature.<sup>36, 40, 44</sup> Indeed, there is need for more studies using microplastics of environmental relevance rather than pristine primary polymers.

The observed higher contaminant sorption and desorption potential as well as the slower settling rates of pristine polystyrene microplastics compared to aged ones, suggests that the pristine

plastics may facilitate the mobility of hydrophobic contaminants (such as triclosan) in surface waters.

### **Acknowledgments**

The authors acknowledge the support of the Canada Research Chairs program, the Natural Sciences and Engineering Research Council of Canada, the Killam Research Fellowship program, the Canada Foundation for Innovation/John R. Evans Leaders Fund grant (Project #35318 of S. Bayen), the Petroleum Technology Development Fund of Nigeria, the Fonds Québécois de la recherche sur la nature et les technologies (FQRNT), and the Eugenie Ulmer Lamothe Fund at McGill for awards to OSA. This project was supported partially by a financial contribution from Fisheries and Oceans Canada. The authors would like to acknowledge M. Sander at ETH Zurich for his helpful insights and comments during the design of the adsorption experiments. We thank R. Leask for access to the tensile testing instrument. We also thank L. Roweczyk and R. Salles Kurusu for helpful discussions about plastic characterization.

## References

1. Boucher, J.; Friot, D., *Primary microplastics in the oceans: a global evaluation of sources*. IUCN Gland, Switzerland: 2017.
2. Alimi, O. S.; Claveau-Mallet, D.; Kurusu, R. S.; Lapointe, M.; Bayen, S.; Tufenkji, N., Weathering pathways and protocols for environmentally relevant microplastics and nanoplastics: What are we missing? *J. Hazard. Mater.* **2022**, *423*, 126955.
3. Geyer, R., Chapter 2 - Production, use, and fate of synthetic polymers. In *Plastic Waste and Recycling*, Letcher, T. M., Ed. Academic Press: 2020; pp 13-32.
4. Borrelle, S. B.; Ringma, J.; Law, K. L.; Monnahan, C. C.; Lebreton, L.; McGivern, A.; Murphy, E.; Jambeck, J.; Leonard, G. H.; Hilleary, M. A., Predicted growth in plastic waste exceeds efforts to mitigate plastic pollution. *Sci* **2020**, *369* (6510), 1515-1518.
5. Lau, W. W. Y.; Shiran, Y.; Bailey, R. M.; Cook, E.; Stuchtey, M. R.; Koskella, J.; Velis, C. A.; Godfrey, L.; Boucher, J.; Murphy, M. B.; Thompson, R. C.; Jankowska, E.; Castillo Castillo, A.; Pilditch, T. D.; Dixon, B.; Koerselman, L.; Kosior, E.; Favoino, E.; Gutberlet, J.; Baulch, S.; Atreya, M. E.; Fischer, D.; He, K. K.; Petit, M. M.; Sumaila, U. R.; Neil, E.; Bernhofen, M. V.; Lawrence, K.; Palardy, J. E., Evaluating scenarios toward zero plastic pollution. *Sci* **2020**, *369* (6510), 1455-1461.
6. Andrady, A. L., Microplastics in the marine environment. *Mar. Pollut. Bull.* **2011**, *62* (8), 1596-605.
7. Jahnke, A.; Arp, H. P. H.; Escher, B. I.; Gewert, B.; Gorokhova, E.; Kühnel, D.; Ogonowski, M.; Potthoff, A.; Rummel, C.; Schmitt-Jansen, M.; Toorman, E.; MacLeod, M., Reducing uncertainty and confronting ignorance about the possible impacts of weathering plastic in the marine environment. *Environ. Sci. Technol. Letters* **2017**, *4* (3), 85-90.
8. Alimi, O. S.; Farner, J. M.; Tufenkji, N., Exposure of nanoplastics to freeze-thaw leads to aggregation and reduced transport in model groundwater environments. *Water Res.* **2020**, 116533.
9. Van Melkebeke, M.; Janssen, C.; De Meester, S., Characteristics and sinking behavior of typical microplastics including the potential effect of biofouling: Implications for remediation. *Environ. Sci. Technol.* **2020**, *54* (14), 8668-8680.
10. Lobelle, D.; Kooi, M.; Koelmans, A. A.; Laufkötter, C.; Jongedijk, C. E.; Kehl, C.; van Sebille, E., Global modeled sinking characteristics of biofouled microplastic. *Journal of Geophysical Research: Oceans* **2021**, *126* (4), e2020JC017098.
11. Kooi, M.; Nes, E. H. v.; Scheffer, M.; Koelmans, A. A., Ups and Downs in the Ocean: Effects of Biofouling on Vertical Transport of Microplastics. *Environ. Sci. Technol.* **2017**, *51* (14), 7963-7971.
12. Waldschläger, K.; Born, M.; Cowger, W.; Gray, A.; Schüttrumpf, H., Settling and rising velocities of environmentally weathered micro-and macroplastic particles. *Environ. Res.* **2020**, 110192.
13. Waldschläger, K.; Schüttrumpf, H., Effects of particle properties on the settling and rise velocities of microplastics in freshwater under laboratory conditions. *Environ. Sci. Technol.* **2019**, *53* (4), 1958-1966.
14. Nguyen, T. H.; Tang, F. H. M.; Maggi, F., Sinking of microbial-associated microplastics in natural waters. *PLOS ONE* **2020**, *15* (2), e0228209.
15. Miao, L.; Gao, Y.; Adyel, T. M.; Huo, Z.; Liu, Z.; Wu, J.; Hou, J., Effects of biofilm colonization on the sinking of microplastics in three freshwater environments. *J. Hazard. Mater.* **2021**, *413*, 125370.

16. Kaiser, D.; Kowalski, N.; Waniek, J. J., Effects of biofouling on the sinking behavior of microplastics. *Environ. Res. Lett.* **2017**, *12* (12), 124003.
17. de Ruijter, V. N.; Redondo Hasselerharm, P. E.; Gouin, T.; Koelmans, A. A., Quality criteria for microplastic effect studies in the context of risk assessment: A critical review. *Environ. Sci. Technol.* **2020**.
18. Almond, J.; Sugumaar, P.; Wenzel, M. N.; Hill, G.; Wallis, C., Determination of the carbonyl index of polyethylene and polypropylene using specified area under band methodology with ATR-FTIR spectroscopy. *e-Polymers* **2020**, *20* (1), 369-381.
19. Brandon, J.; Goldstein, M.; Ohman, M. D., Long-term aging and degradation of microplastic particles: Comparing in situ oceanic and experimental weathering patterns. *Mar Pollut Bull* **2016**, *110* (1), 299-308.
20. Lindström, A.; Buerge, I. J.; Poiger, T.; Bergqvist, P.-A.; Müller, M. D.; Buser, H.-R., Occurrence and Environmental Behavior of the Bactericide Triclosan and Its Methyl Derivative in Surface Waters and in Wastewater. *Environ. Sci. Technol.* **2002**, *36* (11), 2322-2329.
21. Andrady, A. L.; Hamid, S. H.; Hu, X.; Torikai, A., Effects of increased solar ultraviolet radiation on materials. *J. Photochem. Photobiol. B: Biol.* **1998**, *46* (1), 96-103.
22. Krause, S.; Molari, M.; Gorb, E. V.; Gorb, S. N.; Kossel, E.; Haeckel, M., Persistence of plastic debris and its colonization by bacterial communities after two decades on the abyssal seafloor. *Sci. Rep.* **2020**, *10* (1), 9484.
23. Rowenczyk, L.; Dazzi, A.; Deniset-Besseau, A.; Beltran, V.; Goudounèche, D.; Wong-Wah-Chung, P.; Boyron, O.; George, M.; Fabre, P.; Roux, C., Microstructure characterization of oceanic polyethylene debris. *Environ. Sci. Technol.* **2020**, *54* (7), 4102-4109.
24. Rudin, A.; Choi, P., Mechanical properties of polymer solids and liquids. *The Elements of Polymer Science & Engineering* **2013**, *3*.
25. Stowe, B. S.; Salvin, V.; Fornes, R.; Gilbert, R., The effect of near-ultraviolet radiation on the morphology of nylon 66. *Textile research journal* **1973**, *43* (12), 704-714.
26. Meyers, M. A.; Chawla, K. K., *Mechanical behavior of materials*. Cambridge university press: 2008.
27. Jabarin, S. A.; Lofgren, E. A., Photooxidative effects on properties and structure of high-density polyethylene. *J. Appl. Polym. Sci.* **1994**, *53* (4), 411-423.
28. Kalogerakis, N.; Karkanorachaki, K.; Kalogerakis, G. C.; Triantafyllidi, E. I.; Gotsis, A. D.; Partsinevelos, P.; Fava, F., Microplastics generation: Onset of fragmentation of polyethylene films in marine environment mesocosms. *Frontiers in Marine Science* **2017**, *4* (84).
29. Karkanorachaki, K.; Syranidou, E.; Kalogerakis, N., Sinking characteristics of microplastics in the marine environment. *Sci. Total Environ.* **2021**, *793*, 148526.
30. Semcesen, P. O.; Wells, M. G., Biofilm growth on buoyant microplastics leads to changes in settling rates: Implications for microplastic retention in the Great Lakes. *Mar. Pollut. Bull.* **2021**, *170*, 112573.
31. Lakelubbers Quebec deep lakes in Quebec. (accessed 2021-08-10).
32. Santos, L. H. M. L. M.; Rodríguez-Mozaz, S.; Barceló, D., Microplastics as vectors of pharmaceuticals in aquatic organisms – An overview of their environmental implications. *Case Studies in Chemical and Environmental Engineering* **2021**, *3*, 100079.
33. Guo, X.; Wang, J., The chemical behaviors of microplastics in marine environment: A review. *Mar. Pollut. Bull.* **2019**, *142*, 1-14.

34. Alimi, O. S.; Farner Budarz, J.; Hernandez, L. M.; Tufenkji, N., Microplastics and nanoplastics in aquatic environments: Aggregation, deposition, and enhanced contaminant transport. *Environ. Sci. Technol.* **2018**, *52* (4), 1704-1724.
35. Liu, P.; Lu, K.; Li, J.; Wu, X.; Qian, L.; Wang, M.; Gao, S., Effect of aging on adsorption behavior of polystyrene microplastics for pharmaceuticals: Adsorption mechanism and role of aging intermediates. *J. Hazard. Mater.* **2020**, *384*, 121193.
36. Liu, X.; Sun, P.; Qu, G.; Jing, J.; Zhang, T.; Shi, H.; Zhao, Y., Insight into the characteristics and sorption behaviors of aged polystyrene microplastics through three type of accelerated oxidation processes. *J. Hazard. Mater.* **2021**, *407*, 124836.
37. Müller, A.; Becker, R.; Dorgerloh, U.; Simon, F. G.; Braun, U., The effect of polymer aging on the uptake of fuel aromatics and ethers by microplastics. *Environ. Pollut.* **2018**, *240*, 639-646.
38. Xiong, Y.; Zhao, J.; Li, L.; Wang, Y.; Dai, X.; Yu, F.; Ma, J., Interfacial interaction between micro/nanoplastics and typical PPCPs and nanoplastics removal via electrosorption from an aqueous solution. *Water Res.* **2020**, 116100.
39. Ding, L.; Mao, R.; Ma, S.; Guo, X.; Zhu, L., High temperature depended on the ageing mechanism of microplastics under different environmental conditions and its effect on the distribution of organic pollutants. *Water Res.* **2020**, *174*, 115634.
40. Hai, N.; Liu, X.; Li, Y.; Kong, F.; Zhang, Y.; Fang, S., Effects of microplastics on the adsorption and bioavailability of three strobilurin fungicides. *ACS Omega* **2020**, *5* (47), 30679-30686.
41. Hüffer, T.; Hofmann, T., Sorption of non-polar organic compounds by micro-sized plastic particles in aqueous solution. *Environ. Pollut.* **2016**, *214* (17), 194-201.
42. Liu, J.; Ma, Y.; Zhu, D.; Xia, T.; Qi, Y.; Yao, Y.; Guo, X.; Ji, R.; Chen, W., Polystyrene nanoplastics-enhanced contaminant transport: Role of irreversible adsorption in glassy polymeric domain. *Environ. Sci. Technol.* **2018**, *52* (5), 2677-2685.
43. Luthy, R. G.; Aiken, G. R.; Brusseau, M. L.; Cunningham, S. D.; Gschwend, P. M.; Pignatello, J. J.; Reinhard, M.; Traina, S. J.; Weber, W. J.; Westall, J. C., Sequestration of hydrophobic organic contaminants by geosorbents. *Environ. Sci. Technol.* **1997**, *31* (12), 3341-3347.
44. Fang, S.; Yu, W. S.; Li, C. L.; Liu, Y. D.; Qiu, J.; Kong, F. Y., Adsorption behavior of three triazole fungicides on polystyrene microplastics. *Sci. Total Environ.* **2019**, *691*, 1119.

## 6.5 Supporting information

### S6.1. Weight fraction crystallinity calculation

The weight fraction crystallinity can be calculated using density measurements as follows <sup>1</sup>:

$$\chi_c = \frac{\rho_c (\rho - \rho_a)}{\rho (\rho_c - \rho_a)} \quad (\text{S6.1})$$

where  $\rho$  is the density of the sample,  $\rho_a$  is the density of 100% amorphous polystyrene = 1.04 g/cm<sup>3</sup>,  $\rho_c$  = density of 100% crystalline polystyrene = 1.12 g/cm<sup>3</sup><sup>2</sup>. Using the measured densities of 1.04 and 1.07 cm<sup>3</sup>/g for pristine and aged microplastics, the weight fraction crystallinity becomes 0% and 37%, respectively.

**Table S6.1.** LC-MS measurement parameters

<b>Parameter</b>	<b>LC-MS (ESI in negative mode)</b>
Injection volume	4 $\mu$ L
LC eluent program	Mobile A: 5 mM ammonium acetate in water Mobile B: AcN/MeOH 1:1 with 5 mM ammonium acetate 0 to 0.5 min: 5% B 0.5 to 3 min: ramp to 100% B 3 to 7 min: 100% B 7 to 7.01min: back to 5% B 7.01 to 9 min: 5% B
LC flow rate	0.3 mL/min
Post-column run	1 min
LC column temperature	30 °C
MS condition	Gas temperature: 175 °C Drying gas: 10 mL/min Nebulizer: 30 psi Sheath gas temperature: 375 °C Sheath gas flow: 12 mL/min Capillary: 4000 V Nozzle voltage: 2000 V Fragmentor: 125 V Skimmer: 50 V

**Table S6.2.** List of kinetic, isotherm models and other adsorption models used in this study.

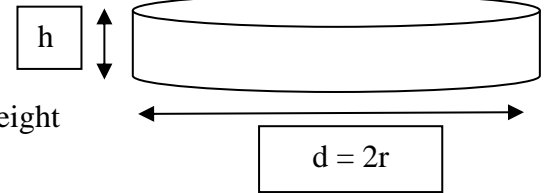
Kinetics model	Equation	Reference
Pseudo-first order	$\frac{dq_t}{dt} = k_1(q_e - q_t)$	3
Pseudo-second order	$\frac{dq_t}{dt} = k_2(q_e - q_t)^2$	4
<b>Isotherm model</b>		
Langmuir	$q_e = \frac{q_m b C_e}{1 + b C_e}$	5
Freundlich	$q_e = k_F C_e^{1/n}$	6
<b>Adsorption capacity</b>		
	$q_t = \frac{(C_0 - C_e)V}{m}$	
<b>Desorption hysteresis index (HI)</b>	$HI = \frac{q_{de} - q_{ad}}{q_{ad}}   T, C_e$	7

$C_e$  = equilibrium concentration,  $C_0$  = initial concentration,  $q_e$  = adsorbed phase concentration at equilibrium,  $q_t$  = adsorbed phase concentration at time  $t$ ,  $q_{de}$  = adsorbed phase concentration during desorption,  $q_{ad}$  = adsorbed phase concentration calculated from  $C_e$  assuming desorption is reversible,  $V$  = liquid volume,  $m$  = microplastic mass,  $k$  = kinetic rate constant

## S6.2. Transport simulation equation and assumptions

Assumption 1: the disk is horizontally aligned during settling

Assumption 2: we assume that  $\frac{dv_p}{dt} = 0$  for the entire column height



$$F_r: \text{residual force} = \rho_p b \frac{dv_p}{dt}$$

$$F_g: \text{gravity force} = (\rho_p - \rho_l)gh$$

$$F_d: \text{drag force} = \frac{C_D A_p V_p^2 \rho_l}{2}$$

$$\text{Also, } Fr = F_g - F_d$$

At terminal velocity,  $\frac{dv_p}{dt} = 0$ . By substituting  $F_d$  and  $F_g$  into  $F_r$ , we obtain;

$$V_p = \sqrt{\frac{2gh(\rho_p - \rho_l)}{C_D \rho_l}} \quad (\text{S6.2})$$

$b$  = particle volume, which is  $\pi r^2 h$  for a disk or  $(4/3)\pi r^3$  for a sphere,  $A_p$  = particle cross sectional area ( $\pi r^2$ ),  $V_p$  = terminal settling velocity,  $C_D$  = drag coefficient,  $\rho_l$  = density of fluid,  $\rho_p$  = density of particle,  $h$  = thickness of the microplastic disk,  $Re$ : Reynolds number.

When  $Re < 1$ , using the simplification for  $C_D$  (equation S3), we calculate this modified Stokes equation (S4) adapted for a disk:

$$C_D = \frac{20.4\eta}{\rho_l V_p d_e} \quad (\text{S6.3})$$

$$V_p = \frac{2ghd_e(\rho_p - \rho_l)}{20.4\eta C_f} \quad (\text{S6.4})$$

where  $\eta$  = dynamic viscosity,  $d_e$  = disk equivalent diameter, 20.4 = shape factor for a disk (24 used for a spherical microplastic) <sup>8</sup>. A correction factor ( $C_f$ ) was applied to the  $C_D$  of the aged microplastics to account for any effects of aging on the material surface properties (e.g., wettability, roughness). Using eq. S4,  $C_f$  at 21 °C was obtained as follows:

$$\frac{V_{p \text{ pristine}}}{V_{p \text{ aged}}} = \frac{31.25 \text{ m/h}}{47.95 \text{ m/h}} = \sqrt{\frac{\frac{0.04}{C_D}}{\frac{0.07}{C_D C_f}}}, C_f = 0.743$$

$\rho_p - \rho_l = 0.04$ , for a pristine microplastic,  $\rho_p - \rho_l = 0.07$ , for an aged microplastic,  $V_p$  of aged and pristine disks were obtained experimentally. The  $C_f$  at 1 °C was calculated as 0.734.

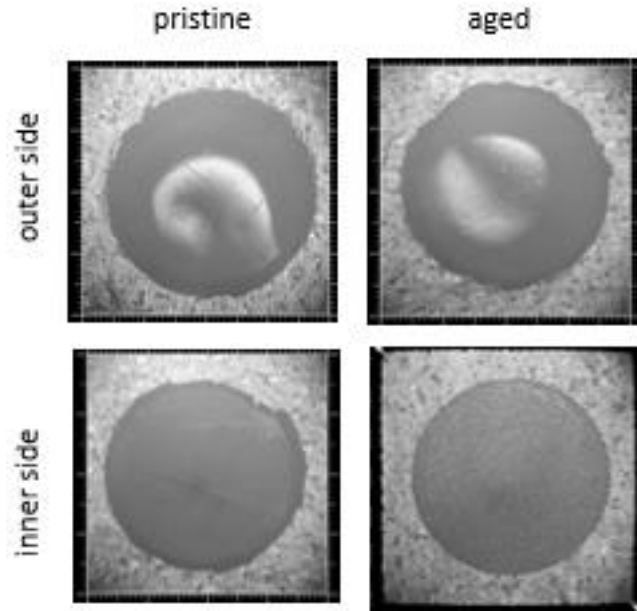


**Figure S6.1.** Surface topography of the microplastics showing the glossy outer surface versus the non-glossy inner side.

**Table S6.3.** Calculated changes to density after aging. Below is a description of different scenarios that may lead to increased density. All values used are approximate average values measured: mass (from 4.4 – 3.8 mg), thickness (from 0.25 to 0.24 mm), and diameter (from 4.5 – 4.44 mm) for pristine and aged microplastics, respectively.

<b>case</b>	<b>description</b>	<b>density increase</b>
A	constant mass + constant thickness + decrease in diameter	3%, Figure S6.2a
B	constant mass + decrease in thickness + constant thickness	4%, Figure S6.2b
C	constant mass + decrease in thickness + decrease in diameter (case A + B)	7%, Figure S6.2c
D	decrease in mass + constant thickness + decrease in diameter	11% decrease, Figure S6.2d
E	decrease in mass + decrease in thickness + constant diameter	10% decrease, Figure S6.2e
F	decrease in mass + decrease in thickness + decrease in diameter (case D + E)	8% decrease, Figure S6.2f
D'	slight decrease in mass + constant thickness + decrease in diameter	2%, Figure S6.2d
E'	slight decrease in mass + decrease in thickness + constant diameter	0%, Figure S6.2e
F'	slight decrease in mass + decrease in thickness + decrease in diameter (case D' + E')	5%, Figure S6.2f

Cases A-F were simulated using average values of mass, thickness and diameter measured. At constant mass, a decrease in thickness, diameter or both as measured during experiments, will lead to density increase (cases A-B). At constant volume, a decrease in mass will not translate to an increase in density, however, decreasing mass and either thickness, diameter or both may lead to density increase or decrease. Cases D-F are for large mass decreases (i.e. 14%, as observed after aging), while D'-F' are for slight mass decreases (2%). Finally, a slight decrease each in mass, thickness and diameter by 1% each can cause density to increase by 3%. This is a conservative estimate by taking into account all measured changes estimated after weathering.

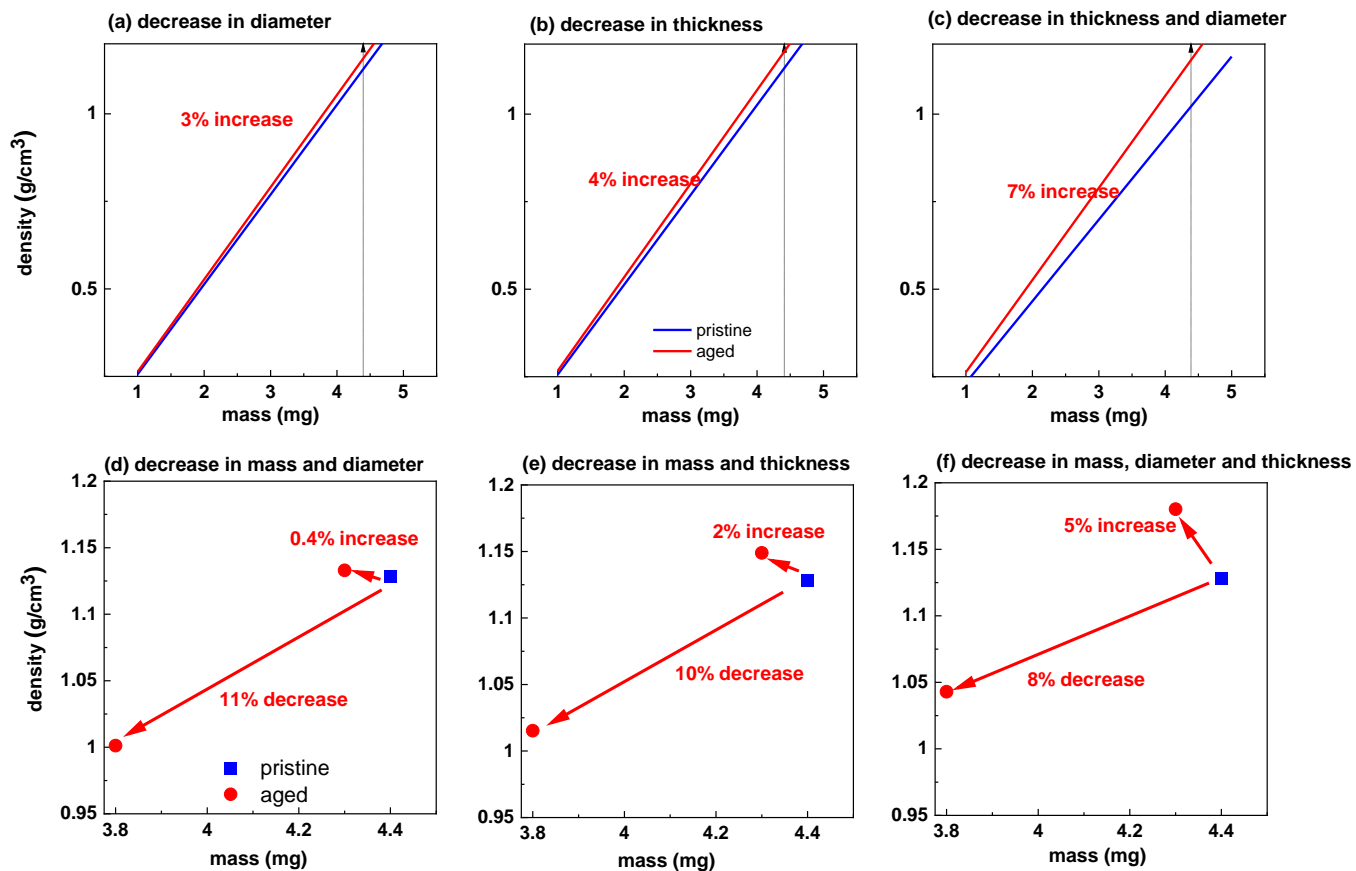


**Figure S6.2.** Different scenarios where changes to mass, diameter, thickness or different combinations of all parameters will impact the density of the microplastic disk.

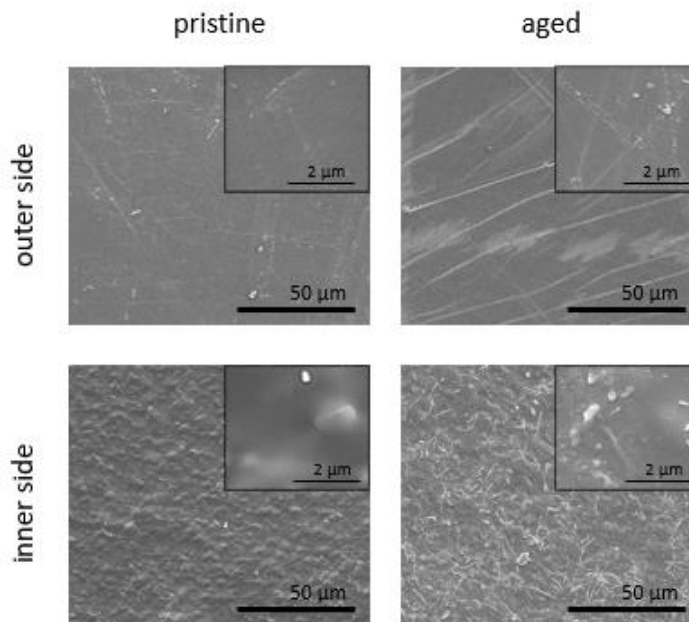


**Figure S6.3.** Representative SEM images showing the morphology of the inner and outer surfaces of the pristine versus aged microplastic disks.

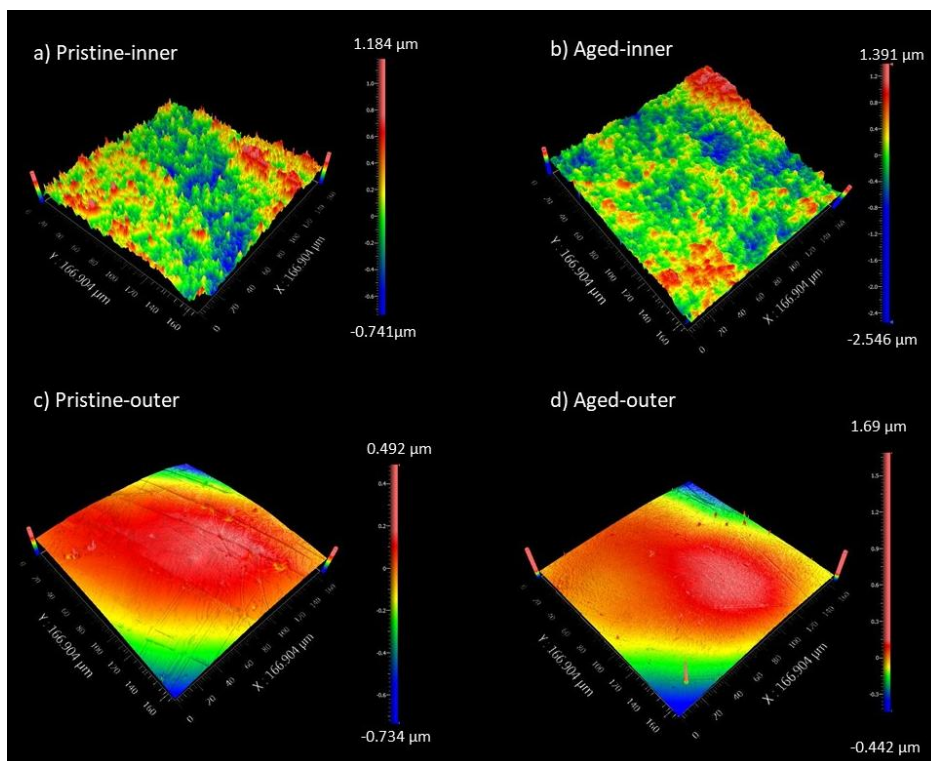


**Figure S6.4.** Representative 3D structures showing the surface topography of the microplastic disks.

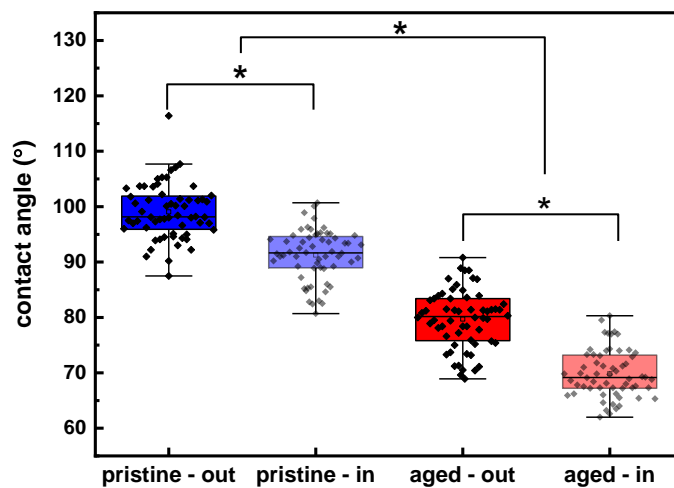


**Figure S6.5.** Contact angle measurements of pristine versus aged microplastics. out and in refer to inner and outer parts of the single-use cup. N = 60 measurements from 3 independent samples (n = 20 each) for each condition. Asterisks represent significant difference at  $p < 0.05$ .

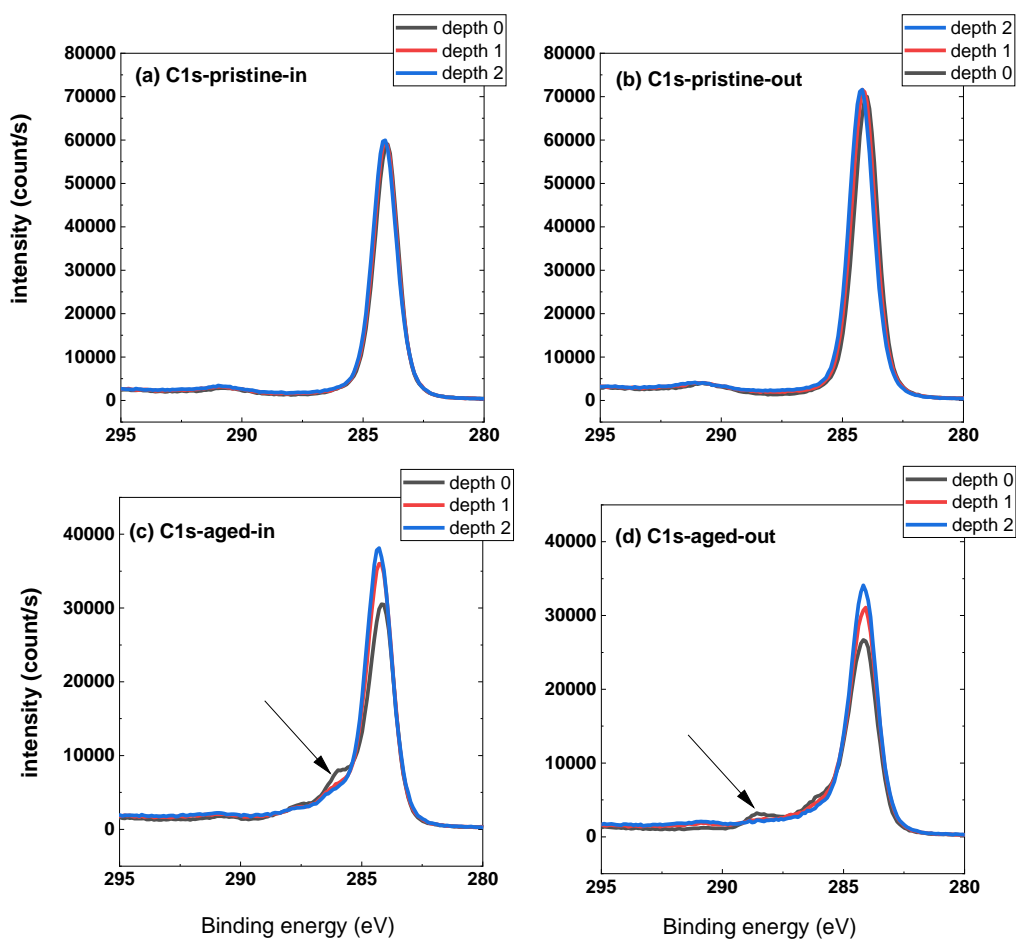


**Figure S6.6.** XPS spectra of pristine versus aged microplastics for C1s and O1s. a-d indicates that additional peaks are observed at depth 0 (surface) for both inner and outer sides.

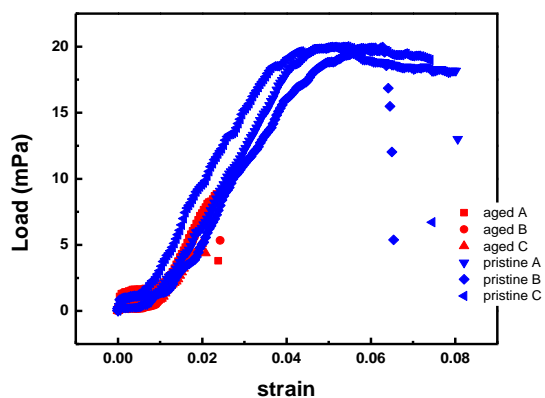


**Figure S6.7.** Stress-strain curves. Samples A, B, C are three independent samples for each treatment. The parameters were calculated as described in <sup>9</sup>. The Young's modulus was calculated as the slope of the stress-strain curve while ignoring the first few flat data points. The ultimate elongation is the plastic strain value where the plastic broke.<sup>9</sup>

**Table S6.3.** Isotherm model fitting parameters for triclosan adsorption on microplastics

model	parameter	pristine	aged
Linear	$K_d$ (L/g)	0.61	0.15
	$R^2$	0.73	0.072
Langmuir	$K_L$ (L/g)	0.31	0.10
	$q_{max}$ ( $\mu\text{g/g}$ )	88.41	41.29
	$R^2$	0.94	0.95
Freundlich	$K_F$ (L/g)	9.98	15.10
	$n$	2.39	5.17
	$R^2$	0.78	0.30

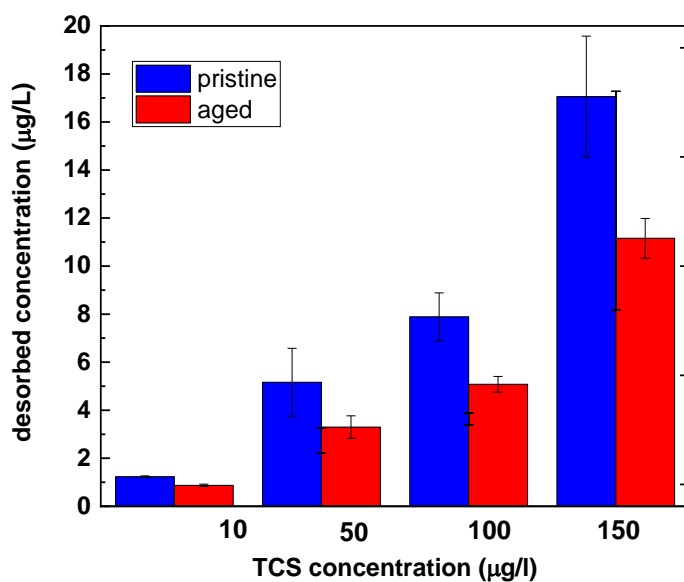


**Figure S6.8.** Effect of weathering on the amount of triclosan released from microplastics (approx. 30 mg) in 10 mM NaCl solution (40 mL). Values on x-axis are the approximate initial starting concentrations during the sorption phase. Error bars represent standard deviation of 3 independent measurements from three separate vials.

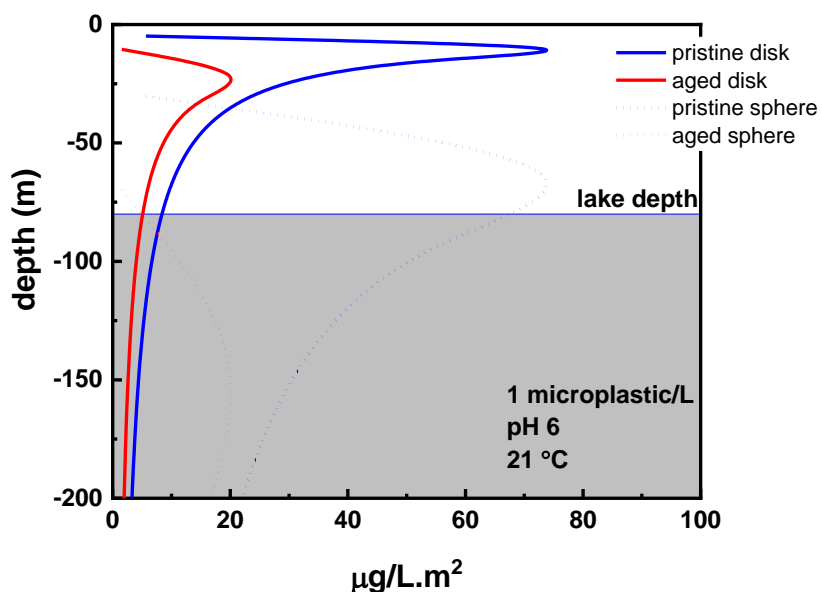


**Figure S6.9.** Effect of weathering on the desorption of triclosan as function of depth for a smaller microplastic disk (diameter of 220  $\mu\text{m}$ ) and sphere both having equivalent diameters of 100  $\mu\text{m}$ .

## References

1. Rudin, A.; Choi, P., Mechanical properties of polymer solids and liquids. *The Elements of Polymer Science & Engineering* **2013**, *3*.
2. Natta, G.; Corradini, P.; Bassi, I. W., Crystal structure of isotactic polystyrene. *Il Nuovo Cimento (1955-1965)* **1960**, *15* (1), 68-82.
3. Lagergren, S., Zur theorie der sogenannten adsorption geloster stoffe. **1898**.
4. Ho, Y. S.; McKay, G., Pseudo-second order model for sorption processes. *Process Biochem.* **1999**, *34* (5), 451-465.
5. Langmuir, I., The constitution and fundamental properties of solids and liquids. Part I. Solids. *J. Am. Chem. Soc.* **1916**, *38* (11), 2221-2295.
6. Skopp, J., Derivation of the Freundlich Adsorption Isotherm from Kinetics. *Journal of Chemical Education* **2009**, *86* (11), 1341.
7. Huang, W.; Yu, H.; Weber, W. J., Hysteresis in the sorption and desorption of hydrophobic organic contaminants by soils and sediments: 1. A comparative analysis of experimental protocols. *J. Contam. Hydrol.* **1998**, *31* (1), 129-148.
8. Gerhart, A. L.; Hochstein, J. I.; Gerhart, P. M., *Munson, Young and Okiishi's Fundamentals of Fluid Mechanics*. John Wiley & Sons: 2020.
9. Kalogerakis, N.; Karkanorachaki, K.; Kalogerakis, G. C.; Triantafyllidi, E. I.; Gotsis, A. D.; Partsiavelos, P.; Fava, F., Microplastics generation: Onset of fragmentation of polyethylene films in marine environment mesocosms. *Frontiers in Marine Science* **2017**, *4* (84).

## **Chapter 7: Conclusions and Future Directions**

### **7.1 Conclusion and implications**

The overall goal of this thesis was to better understand the factors that influence the fate and transformations of nanoplastics and microplastics in aquatic environments. Specifically, the contributions of environmentally relevant factors to nanoplastics and microplastics stability, transport and interaction with other contaminants were investigated.

The effect of environmental physical weathering on the mobility of nanoplastics was examined in water saturated porous media using laboratory scale quartz sand packed columns. The effect of repeated freeze-thaw cycles on the stability and mobility of nanoplastics was investigated while exploring the coupled effect of the presence of natural organic matter (NOM). Exposure of nanoplastics to 10 freeze-thaw cycles led to aggregation and reduced transport of nanoplastics in saturated porous media. Although the presence of NOM significantly increased nanoplastic mobility, the impact of freeze-thaw outweighed its effect. At all ionic strengths examined, the calculated transport distance needed to remove 99% of the freeze-thaw induced aggregates from the liquid phase did not exceed 1 m. Disaggregation experiments on the freeze-thaw induced aggregates suspension suggests that the aggregation was irreversible after 5 days, hence, the aggregates may remain stable over longer time scales in the environment. These findings suggest that previous conclusions on the effect of cold temperature on particle mobility, where particle transport was investigated in warm versus cold but not freezing temperatures, may be overestimated without accounting for temperature cycling. These findings also have significant implications since some parts of the world experience up to 105 FT cycles annually, which further highlights the need to account for climate and temperature changes when assessing the risks associated with nanoplastic release in aquatic systems.

The stability of two different-sized nanoplastics in the presence of three different NOM types was investigated and compared in simple and complex synthetic waters, as well as natural surface water matrices. The interaction of the nanoplastic aggregates with a model silica surface was also examined using an optical tweezer. Realistic nanoplastic/NOM concentration ratios were used to understand the specific interaction mechanism of different types of NOM with the nanoplastics. The minimum concentration of  $\text{CaCl}_2$  required to destabilize the nanoplastic suspension was not size-dependent. The effect of NOM on the attachment efficiency was more evident for the larger

nanoplastic compared to the smaller plastic. In both simple and complex water matrices, humic acid generally enhanced the aggregation of both nanoplastics. On the other hand, the presence of alginate destabilized the nanoplastic in simple divalent salt but stabilized/had no effect on the nanoplastic aggregation in a complex water matrix. The presence of fulvic acid generally had no significant effect on the aggregation behaviour of the nanoplastic suspension. While the smaller nanoplastics behaved similarly in both the highest salinity natural water and synthetic water matrices (aggregated), the larger nanoplastics was shown to behave differently (twice more stable in natural water). The lower attachment efficiency of the larger nanoplastics compared to the smaller ones in natural water highlights the need for using more realistic water matrices when examining the behaviour of nanoplastics in the environment. In a ternary system, the interaction of the nanoplastic aggregates with a model silica surface in the presence of  $\text{CaCl}_2$  was found to be less repulsive in the presence of alginate and humic acid compared to fulvic acid.

The effect of photodegradation on the transport and contaminant facilitated transport of environmentally relevant microplastics in freshwater was also examined. The changes to the physical, chemical and mechanical properties of secondary microplastics was probed before and after UV weathering using a range of techniques. After weathering, changes to microplastic hydrophobicity (20-23% decrease), density (3% increase), surface oxidation, and microscale roughness (24-86% increase) were observed. Exposure of microplastics to UV weathering significantly increased their settling velocity by 53% and 54% at 21°C and 1°C respectively. The impact of weathering on the settling velocity was shown to outweigh the impact of the water column temperature. Based on the measured rates, weathering will reduce the residence time of microplastics in the water column (80 m deep lake) from ~3 to 2 hours and 16 to 7 days for 4.5- and 0.22-mm particles, respectively. The settling velocity and transport reported for aged microplastics is expected to be even higher when natural colloids or biofilms are attached to the aged microplastics. The aged polystyrene microplastics also have a lower affinity for a hydrophobic contaminant, triclosan. This contaminant is partially desorbed from both plastics while the pristine microplastics retain more. The observed higher contaminant sorption and desorption potential as well as the higher residence time of pristine polystyrene microplastics compared to aged ones, suggests that the former may facilitate the mobility of hydrophobic contaminants (such as triclosan) in surface waters. Aged microplastics on the other hand will limit the long-range transport of microplastics and associated contaminants. Ultimately, the weathering

state of a microplastic will determine if a contaminant would be more released in the water column or in sediments. Since most microplastics found in the environment will be secondary and aged to an extent, weathering might reduce the risk of microplastics being available to pelagic organisms while increasing their exposure risk to deposit feeders residing in the water floor.

## **7.1 Future directions**

The current work has addressed important research questions on the factors affecting the behaviour of nanoplastics and microplastics in aquatic environments which has generated additional questions towards mitigating microplastic pollution. In addition to the important knowledge gaps highlighted in the literature review chapters, some research questions include:

### **7.1.1 What is the competitive interaction between microplastics and multiple contaminants and organic matter?**

There is a cocktail of persistent and emerging contaminants in the presence of different organic matter in the environment, thus, microplastics will not interact with only one contaminant in isolation. Different contaminants may interact with microplastics sequentially or simultaneously, perhaps in an antagonistic manner thereby affecting their transport potential. The role of the presence of biofilm in either enhancing or mitigating the sorption/desorption of contaminants with microplastics is also poorly understood. Addressing these gaps will improve the ability to accurately predict the risks associated with microplastic pollution.

### **7.1.2 What is the behaviour of fragmented microplastics and different polymer types?**

The critical literature review presented in this work revealed that 90% of laboratory effect studies have used pristine microplastics while plastics with environmental relevance are rarely used. It was also shown that microplastics collected from the environment for effect studies are dominated by fragments while microplastics aged in the laboratory are mostly beads/spherical. Overall, polystyrene is widely studied while we have limited understanding about the risks posed by other plastics with different properties. Understanding the differences in behavior between polystyrene and other microplastic types is crucial for accurate risk assessment and to drive policy. There is also need for more studies to better understand how aged microplastic fragments from secondary sources of other plastic types behave under realistic environmental conditions in terms of their mobility and stability. Nanoplastics are hypothesized to be equally or more toxic compared to microplastics, yet, effect studies that use plastics in the nanoscale having environmental relevance

are very scarce. The contribution of natural colloids to the stability of nanoplastics also requires further investigation.

Ultimately, this thesis advances our understanding of how different environmental conditions will influence plastic fate and transport and would contribute towards improved microplastic transport and exposure models for accurate predictions.